

# Lateral Load Response of Cikarang Brick Wall Structures – An Experimental Study

Essy Arijoeni Basoenondo

A thesis submitted for the degree of  
Doctor of Philosophy

Centre for Built Environment and Engineering Research  
Queensland University of Technology

March, 2008



## Abstract

---

Despite their poor performance, non-standard clay bricks are commonly used in construction of low-rise buildings and rural houses in Indonesia. These clay bricks are produced traditionally in home industries. Indonesia is located in an active seismic region and many masonry buildings were badly damaged or collapsed during recent earthquakes. Such buildings are classified as non-engineered structures as they are built without using any proper design standard.

Lateral load response of un-reinforced masonry walls is investigated in this research project, with the aim of better understanding the behaviour of these masonry walls using low quality local bricks. A comprehensive experimental program was undertaken with masonry wall elements of 600 mm x 600 mm x 110 mm constructed from local bricks from Cikarang in West Java - Indonesia.

Wall specimens were constructed and tested under a combination of constant vertical compression load and increasing horizontal or lateral in-plane loads, of monotonic, repeated and cyclical nature. The vertical compressive loading was limited to 4% of maximum brick compressive strength. Masonry mortar mix used to construct the specimens was prepared according to Indonesian National Standard. Three different types of masonry wall panels were considered, (i) (normal) brick masonry walls, (ii) surface mortared brick masonry walls and (iii) comforted surface mortared brick masonry walls.

The results indicated that the lateral load bearing capacity of masonry wall is usually lower than that of mortared and comforted walls. Despite this, the lateral load capacity under cyclic loads decreased 50 % of the average capacity of the walls under monotonic and repeated lateral loads.

Using the results from the experimental program, a simplified model for the equivalent diagonal spring stiffness of local clay brick walls was developed. This stiffness model derived from experimental results in then used to simplify the structural analysis of clay brick wall panels in Indonesia. The design guideline for brick masonry houses and low-rise buildings in six Indonesian seismic zones was developed, as a contribution towards the development of design guidance for constructing brick masonry houses in Indonesia.

## Keywords

---

Masonry, Clay Brick, Wall, Cikarang, Indonesia, Lateral load, Experimental, Wall Stiffness.

## Publications

---

**Basoenondo EA**, Giles RS, Thambiratnam DP, Purnomo H. *Response of Unreinforced Brick Masonry Wall Structures to Lateral Loads*, Proceedings of the International Conference on Structural Engineering, Mechanics and Computation, Vol 1, p.419-426, Cape Town, South Africa, April 2-4, 2001.

**Basoenondo EA**, Thambiratnam DP, Purnomo H. *Load-Displacement Response of Non-standardised Clay Brick Masonry Wall Panels to Lateral Loading*, PIC Post Graduate Conference, December 2001, QUT, Australia

**Basoenondo EA**, Thambiratnam DP, Purnomo H. *Load Displacement Response of Non Standardised Clay Brick Masonry Columns Under Compressive Loading*, 6<sup>th</sup> International Masonry Conference, London, UK, November 12 – 15, 2002

**Basoenondo EA**, *Compressive Strength of Cikarang Clay Bricks based on SNI 15 – 2094 – 1991*, International Workshop on Confined Masonry Behaviour and Its Relation to Housing Structure Issues in Indonesia, ITB – Bandung, January 29 – 30, 2003.

**Basoenondo EA**, Thambiratnam DP, Purnomo H. *Study on the Effect of Surface Mortared Confinement to the Improvement of Lateral Stiffness of Masonry Wall Panels Under Lateral Loading*, Proceedings of 9<sup>th</sup> North American Masonry Conference, p.370–380, Clemson, South Caroline, USA, June 1–4, 2003

Purnomo H, **Basoenondo E.A.** and Thambiratnam D.P. *Behaviour of Non Standardised Clay Brick Masonry Wall Panels to Lateral Loading*, 3<sup>rd</sup> APRU/AEARU Research Symposium on Earthquake Hazards around the Pacific Rim, Jakarta, Indonesia, June 21-22, 2007

**Basoenondo EA**, Thambiratnam DP, Purnomo H. *Experimental Study on the Response of Local Clay Brick Wall Panels to the Lateral In-plane Loads*, International Conference on Structural Engineering, Mechanics and Computation, Cape Town, South Africa, September 10-12, 2007.

# Table of Contents

---

<b>Abstract</b>	i
<b>Keywords</b>	i
<b>Publications</b>	ii
<b>Table of Contents</b>	iii
<b>List of Figures</b>	vii
<b>List of Tables</b>	xv
<b>Symbols</b>	xviii
<b>Acronyms</b>	xxi
<b>Statement of Original Authorship</b>	xxii
<b>Acknowledgement</b>	xxiii
<b>Chapter 1. Introduction</b>	<b>1</b>
1.1 Background to the study	1
1.2 Research problem	2
1.3 Research aims and objectives	3
1.4 Research method	3
1.5 Outline of the thesis	4
<b>Chapter 2. Literature Review</b>	<b>7</b>
2.1 Introduction	7
2.2 Seismically active region of Indonesia	9
2.3 The construction of masonry houses in Indonesia	13
2.4 Production of local bricks in Cikarang – Indonesia	15
2.4.1 Process of brick production	17
2.5 The review of previous research on masonry	22
2.5.1 Research Prior to 2000	22
2.5.2 Research Beyond 2000	34

2.5.3	Research Done at QUT	44
2.6	Code provisions for masonry wall structures in resisting lateral loads	47
2.6.1	Australian Standard	47
2.6.2	American Standard	49
2.6.3	British Standard	51
2.6.4	Indonesian Standard	53
2.6.5	Indonesian seismic zones	53
2.7	Conclusion	55
<b>Chapter 3. Experimental Investigation on Physical Characteristics of Brick Assemblages</b>		<b>57</b>
3.1	Introduction	57
3.2	Research scope and limitations	59
3.3	Physical characteristic of bricks based on Indonesian National Standard, SNI 15. 1328 – 1989	59
3.3.1	Mortar compressive strength	61
3.3.2	Brick compressive strength	65
3.3.3	Modulus of elasticity and Poisson's ratio of bricks	69
3.3.4	Modulus of rupture	72
3.4	Brick-mortar bond shear strength	74
3.5	Brick column under compression load	78
3.5.1	Columns SBC	80
3.5.2	Columns BC, MC and CC	82
3.6	Wall panels subjected to vertical compression load	89
3.6.1	Experimental set-up	89
3.6.2	Test procedure	90
3.6.3	Test specimens	91
3.6.4	Test results	91
3.7	Conclusion	102
<b>Chapter 4. Experimental Investigation of Walls under Lateral In-plane Loads</b>		<b>105</b>
4.1	Introduction	105

4.2	Experimental scheme	107
4.2.1	Wall under compression and lateral in-plane load	107
4.2.2	Loading pattern	108
4.2.3	Test set-up and instrumentation	110
4.3	General response of walls under monotonic, repeated and cyclic lateral in-plane loads	111
4.3.1	Walls BW	111
4.3.2	Walls MW	118
4.3.3	Walls CW	126
4.3.4	Walls MWA	135
4.3.5	Walls CWA	141
4.3.6	Walls MWE	146
4.4	Wall capacity in retaining lateral load	150
4.4.1	Wall capacity under monotonic lateral load PH	152
4.4.2	Walls capacity under repeated lateral load PH	153
4.4.3	Wall capacity under cyclic lateral load PH	154
4.4.4	Capacity of wall BW	155
4.4.5	Capacity of walls MW and wall CW	156
4.4.6	Capacity of walls MWA and CWA	156
4.5	Lateral stiffness of wall panels under compression and monotonic lateral in-plane loads	158
4.5.1	Load-displacement response to monotonic lateral loads based on types of walls	158
4.6	The principal stress of walls approaching failure	165
4.6.1	Maximum shear stress of wall BW	166
4.6.2	Maximum shear stress of wall MW and CW	167
4.6.3	Maximum shear stress of walls MWA and CWA	168
4.6.4	Maximum shear stress of wall MWE	169
4.7	Shear modulus of walls	170
4.7.1	Shear stress strain of walls BW	171
4.7.2	Shear stress strain of walls MW and CW	171
4.7.3	Shear stress strain of walls MWA and CWA	172
4.7.4	Shear stress strain of walls MWE	173
4.7.5	Shear modulus of wall panel	174
4.8	Application of results to prototype walls	176

4.9	Conclusion	177
4.10	Further application	179
<b>Chapter 5. Contribution to the Indonesian Guidelines for Un-reinforced Brick Masonry Houses and Low Rise Buildings</b>		181
5.1	Introduction	181
5.2	The characteristics of clay brick masonry	182
5.3	Simplified design approach for unreinforced masonry structures	182
5.3.1	Estimation of load applied to the structures	182
5.3.2	Axial stiffness of wall panels	184
5.3.3	The generalised lateral stiffness of walls	189
5.3.4	Stiffness verification using dimensional analysis	205
5.4	Simplified model for diagonal stiffness of wall panels	209
5.5	Wall capacity based on Indonesian seismic zones	216
5.6	Conclusion	218
<b>Chapter 6. Conclusion</b>		221
<b>References</b>		225
<b>Appendix A</b>		233
<b>Appendix B</b>		239



## List of Figures

---

Figure 1.1	General research in masonry	2
Figure 2.1	Traditional houses in Indonesia	8
Figure 2.2	Brick house in Bali	8
Figure 2.3	The location of seismically active region “Indonesia”	9
Figure 2.4	Earthquakes in Indonesia during 2006	10
Figure 2.5	The red dots show places with severe earthquake damage	10
Figure 2.6	Brick wall for public elementary school building and houses	11
Figure 2.7	Damage on masonry houses during Yogya Earthquake, May 2006	12
Figure 2.8	Damage on masonry houses during Nias Earthquake, March 2005	12
Figure 2.9	Damage on masonry houses during Majalengka Earthquake, April 2001	12
Figure 2.10	Collapse of the local industrial storage buildings during the earthquake	13
Figure 2.11	Masonry wall and brick deposit (Bandung)	14
Figure 2.12	Masonry house without tie beam, during construction (Depok – 2005)	14
Figure 2.13	Masonry house without tie beam and column, viewed from front (Porong – 2006)	15
Figure 2.14	Masonry house viewed from corner direction (Porong - 2006)	15
Figure 2.15	The location of Jakarta, Cikarang and Bandung	16
Figure 2.16	Clay brick factory in Cikarang – Jakarta	16
Figure 2.17	Place of brick storage for drying process called “lio”	17
Figure 2.18	Place of clay extraction	18
Figure 2.19	Process of mixing brick ingredients	18
Figure 2.20	Machinery apparatus for pressing the brick paste	19
Figure 2.21	Moulding process	19
Figure 2.22	Wet brick cutting process	20
Figure 2.23	Treatment for natural air drying process	20
Figure 2.24	General scheme of the oven	21

Figure 2.25	The traditional wood-fired oven	21
Figure 2.26	Well done ready to use solid clay bricks	21
Figure 2.27	Brick samples used for experimental laboratory work	22
Figure 2.28	Test configuration by McNary and Abrams (1985)	25
Figure 2.29	Stress-strain relation measured from experimental test by McNary and Abrams (1985)	26
Figure 2.30	Masonry wall section without tension and with tension.	49
Figure 2.31	Seismic zone in Indonesia with bed stone acceleration within 500 years return period	54
Figure 3.1	Size measurement in mm	59
Figure 3.2	Vernier Caliper	60
Figure 3.3	Weighing balance instruments	60
Figure 3.4	Test scheme for water absorption	60
Figure 3.5	Compressive crushing machine	62
Figure 3.6	50mm × 50mm × 50 mm mortar specimens	63
Figure 3.7	Moulding apparatus for 50 mm × 50 mm × 50 mm mortar cubes	63
Figure 3.8	Mortar compressive strength	64
Figure 3.9	Exponential and logarithmic model of mortar compressive strength	65
Figure 3.10	One unit brick cut into two pieces and connected together with mortar	65
Figure 3.11	(a) Cutting Machine, (b) Half part of unit brick, (c) Cross section area of brick, (d) Cross section area of over burnt brick	66
Figure 3.12	Compressive brick specimens before capping	67
Figure 3.13	Compressive brick specimens after capping	67
Figure 3.14	Compression test on brick specimen without and with LVDT configuration	67
Figure 3.15	Brick and mortar compressive strength	69
Figure 3.16	Stress-strain curves of bricks using different type of mortars	71
Figure 3.17	General stress-strain curve for bricks	71
Figure 3.18	Poisson's ratio of brick	72
Figure 3.19	The scheme of one point and two point load test for bending	73
Figure 3.20	Tests set up for determining the modulus of ruptures	73
Figure 3.21	Triplet bricks under constant $P_V$ and increasing $P_H$ monotonically	74
Figure 3.22	Triplet brick specimens	75

Figure 3.23	Shear test acted on triplet bricks	75
Figure 3.24	Bond-shear test without pressure	76
Figure 3.25	Bond shear strength of triplet bricks	77
Figure 3.26	Triplet specimens after testing with slip failure pattern	78
Figure 3.27	Short Brick Column	78
Figure 3.28	(a) Brick Column, (b) Mortared and Comforted Column	79
Figure 3.29	Failure type of short brick column specimens	80
Figure 3.30	Stress-strain curves of column SBC	81
Figure 3.31	General stress-strain curves of column SBC	82
Figure 3.32	(a) Stress-strain curves of brick column BC, (b) Generalised stress-strain curves of brick column BC	84
Figure 3.33	(a) Stress-strain curves of mortared column MC, (b) Generalised stress-strain curves of mortared column MC	85
Figure 3.34	(a) Stress-strain curves of comforted column CC, (b) Generalised stress-strain curves of comforted column CC	86
Figure 3.35	Stress-strain curves of columns SBC, Brick, BC, MC and CC	87
Figure 3.36	Generalised stress-strain behaviour of bricks and columns	87
Figure 3.37	(a) Column specimen before testing, (b) to (f) Brittle failure of column specimens	88
Figure 3.38	Compressive pressure parallel to brick layers	90
Figure 3.39	Compressive pressure perpendicular to brick layers	90
Figure 3.40	Stress-strain behaviour of compressive wall panel	92
Figure 3.41	Failure patterns of compressive walls, loaded parallel to brick layers	93
Figure 3.42	(a) to (c) Failure pattern of compressive wall MWA and CWA	94
Figure 3.43	Stress-strain curves of wall BW	95
Figure 3.44	Stress-strain curves of wall BW $\perp$	95
Figure 3.45	Stress-strain curves of wall MW	96
Figure 3.46	Stress-strain curves of wall MW $\perp$	97
Figure 3.47	Stress-strain curves of wall MW//	97
Figure 3.48	Stress-strain curves of wall CW	98
Figure 3.49	Stress-strain curves of wall CW//	99
Figure 3.50	Stress-strain curves of wall CW $\perp$	99
Figure 3.51	Stress-strain curves of wall MWA	100
Figure 3.52	Stress-strain curves of wall CWA	101

Figure 3.53	Stress-strain behaviour of compressive walls	101
Figure 4.1	Wall under compression load $P_V$ and increasing lateral in-plane load $P_H$	107
Figure 4.2	Test configuration of wall panel	107
Figure 4.3	Type of horizontal load applied to specimens	108
Figure 4.4	Storage of wall specimens	109
Figure 4.5	Test configuration of walls with diagonal LVDT	110
Figure 4.6	Wall failure pattern caused by lateral loads	111
Figure 4.7	Failure pattern and load-displacement of wall BW04	112
Figure 4.8	Failure pattern and load-displacement of wall BW06	112
Figure 4.9	Failure pattern and load-displacement of wall BW17	112
Figure 4.10	Failure pattern and load-displacement of wall BW03	113
Figure 4.11	Failure pattern and load-displacement of wall BW09	113
Figure 4.12	Failure pattern of wall BW09	114
Figure 4.13	Failure pattern and load-displacement of wall BW18	114
Figure 4.14	Failure pattern and load-displacement of wall BW05	115
Figure 4.15	Failure pattern and Load-displacement of wall BW07	115
Figure 4.16	Failure pattern and load-displacement of wall BW08	116
Figure 4.17	Failure pattern of wall BW08	116
Figure 4.18	Failure pattern and load-displacement of wall BW19	116
Figure 4.19	Failure pattern and load-displacement of wall BW21	117
Figure 4.20	Wall BW 21 before and after testing	117
Figure 4.21	Failure pattern and load-displacement of wall BW10	118
Figure 4.22	Failure pattern and load-displacement of wall BW20	118
Figure 4.23	Failure pattern and load-displacement of wall MW20	119
Figure 4.24	Failure pattern and load-displacement of wall MW21	119
Figure 4.25	Failure type of wall MW21	120
Figure 4.26	Failure pattern and load-displacement of wall MW08	121
Figure 4.27	Failure pattern and load-displacement of wall MW02	121
Figure 4.28	Failure pattern and load-displacement of wall MW22	121
Figure 4.29	Failure pattern and load-displacement of wall MW16	122
Figure 4.30	Failure pattern and load-displacement of wall MW07	122
Figure 4.31	Failure pattern and load-displacement of wall MW03	123
Figure 4.32	Failure pattern and load-displacement of wall MW17	123

Figure 4.33	Failure pattern and load-displacement of wall MW01	124
Figure 4.34	Failure pattern and load-displacement of wall MW04	124
Figure 4.35	Failure pattern and load-displacement of wall MW18	124
Figure 4.36	Failure pattern and load-displacement of wall MW06	125
Figure 4.37	Failure pattern and load-displacement of wall MW05	125
Figure 4.38	Failure pattern and load-displacement of wall MW19	126
Figure 4.39	Failure pattern and load-displacement of wall CW19	126
Figure 4.40	Failure pattern and load-displacement of wall CW20	127
Figure 4.41	Failure type of Wall CW07	127
Figure 4.42	Failure pattern and load-displacement of wall CW07	128
Figure 4.43	Failure pattern and load-displacement of wall CW02	128
Figure 4.44	Failure pattern and load-displacement of wall CW15	128
Figure 4.45	Failure pattern and load-displacement of wall CW21	129
Figure 4.46	Failure pattern and load-displacement of wall CW08	129
Figure 4.47	Failure pattern and load-displacement of wall CW03	130
Figure 4.48	Failure pattern and load-displacement of wall CW22	130
Figure 4.49	Failure pattern and load-displacement of wall CW16	130
Figure 4.50	Failure pattern and load-displacement of wall CW01	131
Figure 4.51	Failure pattern and load-displacement of wall CW05	131
Figure 4.52	Failure pattern and load-displacement of wall CW17	132
Figure 4.53	Failure pattern and load-displacement of wall CW23	132
Figure 4.54	Failure pattern and load-displacement of wall CW06	133
Figure 4.55	Failure pattern and load-displacement of wall CW04	133
Figure 4.56	Failure pattern and load-displacement of wall CW18	134
Figure 4.57	Failure pattern and load-displacement of wall CW24	134
Figure 4.58	Failure pattern of wall CW24	134
Figure 4.59	Failure pattern and load-displacement of wall MWA01	135
Figure 4.60	Failure pattern and load-displacement of wall MWA05	136
Figure 4.61	Failure pattern and load-displacement of wall MWA09	136
Figure 4.62	Failure pattern and load-displacement of wall MWA02	137
Figure 4.63	Failure pattern and load-displacement of wall MWA06	137
Figure 4.64	Failure pattern and load-displacement of wall MWA10	137
Figure 4.65	Failure pattern and load-displacement of wall MWA03	138
Figure 4.66	Failure pattern and load-displacement of wall MWA07	138

Figure 4.67	Failure pattern and load-displacement of wall MWA11	139
Figure 4.68	Failure pattern and load-displacement of wall MWA04	139
Figure 4.69	Failure pattern and load-displacement of wall MWA04	140
Figure 4.70	Failure pattern and load-displacement of wall MWA08	140
Figure 4.71	Failure pattern and load-displacement of wall MWA12	140
Figure 4.72	Failure pattern and load-displacement of wall CWA01	141
Figure 4.73	Failure pattern and load-displacement of wall CWA05	141
Figure 4.74	Failure pattern and load-displacement of wall CWA09	142
Figure 4.75	Failure pattern and load-displacement of wall CWA02	142
Figure 4.76	Failure pattern and load-displacement of wall CWA02	143
Figure 4.77	Failure pattern and load-displacement of wall CWA06	143
Figure 4.78	Failure pattern and load-displacement of wall CWA10	143
Figure 4.79	Failure pattern and load-displacement of wall CWA03	144
Figure 4.80	Failure pattern and load-displacement of wall CWA07	144
Figure 4.81	Failure pattern and load-displacement of wall CWA11	145
Figure 4.82	Failure pattern and load-displacement of wall CWA04	145
Figure 4.83	Failure pattern and load-displacement of wall CWA08	146
Figure 4.84	Failure pattern and load-displacement of wall CWA12	146
Figure 4.85	Failure pattern and load-displacement of wall MWE01	147
Figure 4.86	Failure pattern and load-displacement of wall MWE02	147
Figure 4.87	Failure pattern and load-displacement of wall MWE03	147
Figure 4.88	Failure pattern of wall MWE03	148
Figure 4.89	Failure pattern and load-displacement of wall MWE04	148
Figure 4.90	Failure pattern and load-displacement of wall MWE05	148
Figure 4.91	Failure pattern of walls MWA and CWA	149
Figure 4.92	Cross sections of failure patterns of single walls	149
Figure 4.93	Capacity of wall panels in retaining lateral load	151
Figure 4.94	Capacity of wall panels in retaining monotonic lateral load	152
Figure 4.95	Capacity of wall panels in retaining repeated lateral load	153
Figure 4.96	Capacity of wall panels in retaining cyclic lateral load	154
Figure 4.97	Maximum capacity of walls BW	155
Figure 4.98	Maximum capacity of walls MW	156
Figure 4.99	Maximum capacity of walls CW	157
Figure 4.100	Maximum capacity of walls MWA	157

Figure 4.101	Maximum capacity of walls CWA	158
Figure 4.102	Load-displacement of walls BW under monotonic loads	159
Figure 4.103	Load-displacement of walls MW under monotonic loads	160
Figure 4.104	Load-displacement of walls CW under monotonic loads	161
Figure 4.105	Load-displacement of walls MWA under monotonic loads	162
Figure 4.106	Load-displacement of walls CWA under monotonic loads	162
Figure 4.107	Load-displacement of walls MWE under monotonic loads	163
Figure 4.108	Lateral stiffness of walls	164
Figure 4.109	Generalised lateral stiffness of walls	164
Figure 4.110	Mohr circle for principal stress	165
Figure 4.111	Maximum shear stress of walls BW	167
Figure 4.112	Maximum shear stress of walls MW	167
Figure 4.113	Maximum shear stress of walls CW	168
Figure 4.114	Maximum shear stress of walls MWA	168
Figure 4.115	Maximum shear stress of walls CWA	169
Figure 4.116	Maximum shear stress of walls MWE	169
Figure 4.117	Shear stress - shear strain of walls BW	171
Figure 4.118	Shear stress - shear strain of walls MW	172
Figure 4.119	Shear stress - shear strain of walls CW	172
Figure 4.120	Shear stress - shear strain of walls MWA	173
Figure 4.121	Shear stress - shear strain of walls CWA	173
Figure 4.122	Shear stress - shear strain of walls MWE	174
Figure 4.123	Shear modulus of walls BW, MW, CW, MWA, CWA, MWE	175
Figure 5.1	A simple structural layout of rural masonry house	184
Figure 5.2	Axial stiffness of wall BW	186
Figure 5.3	Axial stiffness of wall MW	186
Figure 5.4	Axial stiffness of wall CW	187
Figure 5.5	Axial stiffness of wall MWA	187
Figure 5.6	Axial stiffness of wall CWA	188
Figure 5.7	Axial stiffness of wall MWE	188
Figure 5.8	Wall panel under compressive pressure and lateral load	189
Figure 5.9	Ratio of cross section area to the height of the walls, based on span size	191

Figure 5.10	Ratio of cross section area to the height of the walls, based on height size	191
Figure 5.11	Shear stiffness of wall BW	196
Figure 5.12	Shear stiffness of wall MW	196
Figure 5.13	Shear stiffness of wall CW	197
Figure 5.14	Shear stiffness of wall MWA	197
Figure 5.15	Shear stiffness of wall CWA	198
Figure 5.16	Shear stiffness of wall MWE	198
Figure 5.17	Flexural stiffness of wall BW	199
Figure 5.18	Flexural stiffness of wall MW	199
Figure 5.19	Flexural stiffness of wall CW	200
Figure 5.20	Flexural stiffness of wall MWA	200
Figure 5.21	Flexural stiffness of wall CWA	201
Figure 5.22	Flexural stiffness of wall MWE	201
Figure 5.23	Lateral stiffness of wall BW	202
Figure 5.24	Lateral stiffness of wall MW	202
Figure 5.25	Lateral stiffness of wall CW	203
Figure 5.26	Lateral stiffness of wall MWA	203
Figure 5.27	Lateral stiffness of wall CWA	204
Figure 5.28	Lateral stiffness of wall MWE	204
Figure 5.29	Spring model for determining the diagonal stiffness of walls	209
Figure 5.30	Diagonal stiffness of wall BW	213
Figure 5.31	Diagonal stiffness of wall MW	213
Figure 5.32	Diagonal stiffness of wall CW	214
Figure 5.33	Diagonal stiffness of wall MWA	214
Figure 5.34	Diagonal stiffness of wall CWA	215
Figure 5.35	Diagonal stiffness of wall MWE	215



## List of Tables

---

Table 2.1	Brick Property in Australia (Brisbane)	47
Table 2.2	The characteristics of clay brick masonry	53
Table 2.3	Coefficient of earthquake response $C_i$	54
Table 3.1	Number and types of specimens	58
Table 3.2	Research limitation	58
Table 3.3	Physical characteristic of Cikarang bricks	61
Table 3.4	Types and categories of mortars	62
Table 3.5	Mortar compressive strength	63
Table 3.6	Number of compressive brick specimens	66
Table 3.7	Ratios of brick to mortar strength	68
Table 3.8	Modulus of elasticity of bricks at each range of compressive stress	70
Table 3.9	Modulus of elasticity of brick	72
Table 3.10	Modulus of rupture of Cikarang bricks	74
Table 3.11	Number and type of test of triplet brick specimens.	75
Table 3.12	Bond-shear strength between mortar and brick surface	76
Table 3.13	Trend-lines of bond shear strength between brick and mortar	77
Table 3.14	The number of column specimens	79
Table 3.15	Modulus of elasticity of SBC, Brick, BC, MC, CC	83
Table 3.16	Axial stiffness ratio of columns to bricks	88
Table 3.17	Description of wall specimens, types and coding	89
Table 3.18	Total number of compressive wall specimens	89
Table 3.19	Compressive wall specimens under monotonic and repeated compression loads	91
Table 3.20	Modulus of elasticity of walls under compression load (MPa)	92
Table 3.21	Axial stiffness of wall panels	102
Table 4.1	Compressive pressure acted on wall specimens	106
Table 4.2	Type and number of wall panels tested under $P_V$ and $P_H$	106
Table 4.3	Wall specimens under compression Load $P_V$ and horizontal load $P_H$	109
Table 4.4	Capacity of wall panels in retaining horizontal loads (kN)	151

Table 4.5	Capacity of wall panels in retaining horizontal monotonic loads (kN)	152
Table 4.6	Capacity of wall panels in retaining horizontal repeated loads (kN)	153
Table 4.7	Capacity of wall panels in retaining horizontal repeated loads (kN)	154
Table 4.8	Lateral stiffness of walls under different types of compressive pressures (kN/mm)	163
Table 4.9	Wall lateral stiffness	163
Table 4.10	The principal stress of walls (MPa)	170
Table 4.11	Trend-line equations of shear modulus	175
Table 4.12	The average value of shear modulus of walls	176
Table 4.13	Summary of Scale Factors for Masonry	177
Table 5.1	Physical characteristics of Cikarang clay bricks	182
Table 5.2	Mechanical characteristics of Cikarang clay bricks	182
Table 5.3	Axial stiffness of wall panels	185
Table 5.4	The ratio of shear cross section area to the height of wall panels	192
Table 5.5	The average value of shear modulus of wall panels	192
Table 5.6	Shear stiffness of walls	193
Table 5.7	Flexural stiffness of walls	194
Table 5.8	Lateral stiffness of walls	195
Table 5.9	Scale factor for length and height of walls	205
Table 5.10	Stiffness of wall BW based on dimensional analysis	206
Table 5.11	Stiffness of wall MW based on dimensional analysis	206
Table 5.12	Stiffness of wall CW based on dimensional analysis	207
Table 5.13	Stiffness of wall MWA based on dimensional analysis	207
Table 5.14	Stiffness of wall CWA based on dimensional analysis	208
Table 5.15	Stiffness of wall MWE based on dimensional analysis	208
Table 5.16	The ratio of axial strain to shear strain of walls	211
Table 5.17	Diagonal stiffness of walls	212
Table 5.18	Capacity of 1 meter wall to retain base static shear force	216
Table 5.19	Static equivalent lateral earthquake load V (kN) for wall of 1 meter length	217
Table 5.20	Dynamic earthquake load (kN)	217

Table 5.21	Type of wall that can be built in Indonesian seismic zone	218
Table 5.22	The permissible construction of houses and low-rise buildings on soft soil	219
Table 5.23	The permissible construction of houses and low-rise buildings on moderate soil	219
Table 5.24	The permissible construction of houses and low-rise buildings on hard soil	220

## Symbols

---

A	Cross section area in $\text{mm}^2$ , $\text{m}^2$
$A_b$	bond shear contact area between mortar and brick surface in $\text{mm}^2$
$A_{dw}$	Bedded area
$A_n$	Cross-sectional area of masonry in $\text{in}^2$
B	Width of section in inch
$C_i$	Earthquake response factor based on earthquake response spectrum.
$c_w$	Non dimensional strain coefficient of wall
d	Distance from extreme compression fibre to centroid of tension reinforcement
E	Modulus of Elasticity in MPa or $\text{N}/\text{mm}^2$
$E_{br}$	Modulus of Elasticity of brick
$f_m$	masonry compressive strength in psi
$f'_m$	Compressive strength of concrete masonry prisms
$f'_{ms}$	Characteristic shear strength of the masonry
$f_{de}$	Design compressive stress on the bed joist under gravity load
$f_{fb}$	Flexural bond strength
G	Shear Modulus in MPa or $\text{N}/\text{mm}^2$
H	Height in mm, m
I	Importancy factor
I	Moment of inertia of masonry in $\text{in}^4$
j	Ratio of distance between centroid of flexural compressive forces and centroid of tensile forces to depth d.
k	Stiffness
kN	Kilo Newton
$k_v$	Shear factor (0.3 for bed joints in clay masonry).
$k_{wd}$	Diagonal stiffness of wall
$k_{wh}$	Lateral stiffness of wall
$k_{wv}$	Axial stiffness of wall
L	Length of wall in mm, m
m	Meter

mm	Milli-meter
M	maximum moment occurring simultaneously with design shear force V at the section under consideration in lb-in
MPa	Mega Pascal
N	Newton
$N_v$	Force acting normal to shear surface in lb
$P_H$	Horizontal or lateral load
$P_v$	Vertical load
$P_v$	Compressive pressure in MPa or $N/mm^2$
$p_v$	Pressure, Compressive pressure in MPa, $N/mm^2$
Q	First moment about the neutral axis of a section in $in^3$
R	Earthquake reduction factor
$S_A$	Scale factor of shear or compressive cross section area
$S_E$	Scale factor of the Modulus of Elasticity
$S_G$	Scale factor of the Shear Modulus
$S_h$	Scale factor of height of walls
$S_L$	Scale factor for the length dimension
$S_t$	Scale factor for the wall thickness
$S_\sigma$	Scale factor for the stress or pressure
t	Thickness of wall in mm
ton-f	Ton-force
V	Seismic base shear force in kN, ton-f
V	Design shear force or horizontal design force
v	Stress due to design loads
$V_0$	The shear bond strength
$V_{le}$	The shear friction strength
W	Weight
$\gamma$	Shear strain
$\gamma_{mv}$	Shear factor for masonry based on British Standard
$\nu$	Poisson's Ratio
$\sigma$	Normal Stress in MPa or $N/mm^2$
$\sigma_{max}$	Maximum principal stress in MPa or $N/mm^2$
$\sigma_{min}$	Minimum principal stress in MPa or $N/mm^2$
$\sigma_x$	Normal stress in x direction in MPa or $N/mm^2$

$\sigma_y$	Normal stress in y direction in MPa or N/mm <sup>2</sup>
$\tau$	Shear stress in MPa or N/mm <sup>2</sup>
$\tau_{xy}, \tau_{yx}$	Shear stress in x-y plane in MPa or N/mm <sup>2</sup>
$\phi$	Capacity reduction factor (0.6 for shear in un-reinforced masonry)

## Acronyms

---

AS3700	Australian Standard 3700
ASCE	American Society of Civil Engineers
ASTM	American Society for Testing and Materials
BS	British Standard
BW	Brick Wall
CW	Comforted Wall
CWA	Comforted Wall using mortar plaster type A
DRAIN-2D	Dynamic Response Analysis of Inelastic 2-Dimensional
FEMA 356	Federal Emergency Management Agency – ASCE provisions
FTUI	Fakultas Teknik Universitas Indonesia
IDARC2D	A Computer Program for Seismic Inelastic Structural Analysis
IRA	Initial Rate of Absorption
JABODETABEK	Jakarta-Bogor-Depok-Tangerang-Bekasi
LVDT	Linear Variable Displacement Transducer
MW	Mortared Wall
MWA	Mortared Wall using mortar plaster type A
MWE	Mortared Wall Extra
PUSKIM	Pusat Penelitian dan Pengembangan Teknologi Permukiman
QUT	Queensland University of Technology
RM	Reinforced Masonry wall
SNI	Standar Nasional Indonesia
UBM	Un-reinforced Brick Masonry wall
URM	Un-reinforced Masonry wall

## Statement of Original Authorship

---

The work contained in this thesis has not been previously submitted to meet requirements for a degree or diploma at this or any other higher education institution. To the best of my knowledge and belief, the thesis contains no material previously published or written by another person except where due reference is made.

Signature:



Date: 10 March, 2008



## Acknowledgement

---

I am extremely grateful and deeply indebted to my principal supervisor Prof. David P. Thambiratnam, for his scholarly guidance, constructive suggestions, endless encouragements and continuous supports given throughout my research. He has been more than an academic supervisor. I thank him for his directing me towards the goals of this research project and for always helping and inspiring me to overcome the difficulties encountered during the candidature. Without such assistance this study would not have been what it is. His immense patience and availability for comments and assistances whenever approached, even amidst his heavy pressure at work, deserves grateful appreciation. Also, I wish to thank A/Prof. Dr. Heru Purnomo, for kindly being my associate supervisor and always directing and supporting my study.

I would like to thank the Department of Civil Engineering, Faculty of Engineering, University of Indonesia through QUE Project funded by the World Bank; the General Directorate of Higher Education, the Republic of Indonesia, for providing Scholarship to carry out my research. I would also like to thank the Structural and Material Laboratory at the Civil Engineering Department FTUI, the Structural Laboratory at PUSKIM Bandung, Lembaga Teknologi FTUI, and the companies PT. Pembangunan Perumahan (Persero) and Clay Brick Factory “HAJI SUGIH” at Cikarang; and also to the Physical Infrastructure Centre and the Faculty of Built Environment & Engineering at QUT for providing financial, materials and necessary facility supports. Many thanks also expressed to Dr. Adriana Bodnarova for her comments, suggestions and corrections to the manuscript.

It is pleasure to thank my colleagues, staffs and friends at DTS-FTUI, School of UD-QUT for their help, encouragements and sharing their ideas. Finally, a deepest and special appreciation is expressed to my lovely husband Centos B. Santoso (In Memoriam, 2004), kids Mayang and Bonang, housemate Yu Sogi for their great understanding, patience and meaningful spiritual support.



# Chapter 1. Introduction

---

## 1.1 Background to the study

Masonry is a well known composite building material all around the world. Generally, depending on the availability of materials in the region, masonry bricks are made of clay, calcium silicate, limestone or natural stone, concrete, fibre composites or artificial materials. In Indonesia, traditional clay bricks are produced locally without following any technical inspection or standard and the quality varies from region to region. These bricks are used for houses and simple buildings, not only in village areas but also in the JAKarta-BOgor-DEpok-TANgerang-BEKasi (*JABODETABEK*) region. The houses made of traditional clay bricks are categorised as non-engineered, un-reinforced masonry (URM) structures.

In general, masonry structures are very good in resisting gravity loads, but do not perform well when subjected to lateral in-plane loading, such as seismic loads caused by an earthquake. As Indonesia is located in a high risk seismic region, many masonry houses experienced severe damage during past earthquakes that caused many injuries and deaths. The houses collapsed gradually in brittle failure without ductility. The performance characteristics of wall material in the houses of this region have never been investigated nor studied. Local builders have always followed a traditional way to construct their houses, with very poor knowledge on construction of masonry houses.

Based on the above mentioned findings, there is an urgent need for research and investigation on the behaviour of brick masonry wall found in Indonesia especially in JABODETABEK region.

## 1.2 Research problem

Masonry structures have been progressively studied since the early of 1960's. Based on the research done all over the world, masonry research can be classified into four major categories, as shown in Figure 1.1.

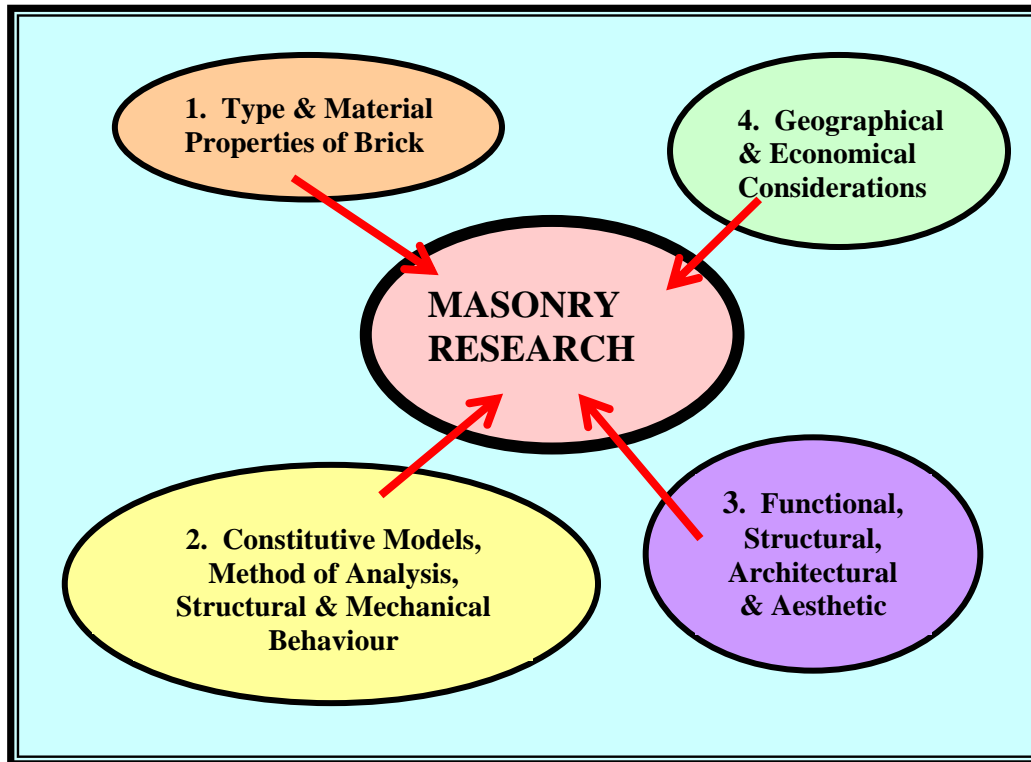


*Figure 1.1 General research in masonry*

Although masonry research started since 40 years ago, it is still considered to have a very limited number of research activities and publications, compared to other civil-structural engineering research areas. Also, there have been very limited investigations and publications in the masonry area in Indonesia.

Therefore, the research presented in this thesis aims to undertake a comprehensive study on the performance characteristics of masonry walls subjected to lateral loading, which are built using clay bricks produced in Indonesian local home industry. It supports the policy for contribution to the development of the Indonesian National Standard for masonry rural houses and low rise buildings by the Ministry of Public Works - The Republic of Indonesia. Previous research in masonry wall carried out at QUT indicated that the proper design of masonry structures can enhance their safety and efficiency under seismic loading.

### 1.3 Research aims and objectives

The research significance of this thesis lies in addressing the problem of efficient and safe design of masonry houses and low-rise buildings in Indonesia. It aims to obtain the performance characteristics of masonry wall panels, built using local clay bricks from Cikarang – Indonesia, under lateral in-plane loading, by experimental testing. The following objectives will be used to achieve the research aim:

- development of stress-strain model for Cikarang brick masonry,
- study of the effect of surface mortar plaster and comforted plaster, on the lateral load response,
- study of the effect of vertical pressure on wall panel under in-plane lateral load,
- determination of peak loads and failure patterns of the wall panels, and
- research information to facilitate the development of guidelines for design and construction of low-rise masonry buildings and houses.

The expected outcomes of this research are a simple model for predicting diagonal stiffness of wall panel and recommendations for more efficient and safer masonry houses in Indonesia.

### 1.4 Research method

The research investigations of this work were supported by experimental work, which consisted of two stages. In the first stage, the physical characteristics and the behaviour of brick assemblages under compression loads were investigated. In the second stage, the responses of wall panels under compressive pressure and lateral in-plane loading were determined.

The experimental results then provided the generalised stress strain behaviour, as the performance characteristic and a simplified diagonal stiffness formula for clay brick masonry wall, as a contribution towards the development of guidelines for masonry houses in Indonesia.

## 1.5 Outline of the thesis

### **Chapter 1: Introduction**

Presents the background and introduction to the topic, defines research problem, states the aim and objectives and outlines the method of investigation used in the research project.

### **Chapter 2: Literature Review**

This chapter refers to the experience of damage of masonry houses during the earthquakes in Indonesia. It reviews the previous published literature in the field of masonry wall structures and highlights the necessity and the scope of the current research.

### **Chapter 3: Experimental Work on Physical and Mechanical**

#### **Characteristic of Brick Assemblage**

This chapter presents the experimental work of stage 1, where stress-strain behaviour of brick assemblages and wall panel under compressive load were determined. The laboratory tests were performed on specimens of individual brick assemblages, brick columns and brick walls and the results obtained were used for development of stiffness formula of brick wall.

### **Chapter 4: Experimental Work on Wall Panels Subjected to Vertical**

#### **Compression and Horizontal In-plane Load**

This chapter presents the experimental work of stage 2. It investigates the effect of surface mortared confinement on masonry wall element under vertical and horizontal in-plane loads. It examines the effect of the surface plaster confinement on the improvement of the stiffness and homogeneity of the wall structure and significant improvement in resisting both gravity and lateral loading, with some improvement on the ductility.

**Chapter 5: Contribution to the Indonesian Guidelines for Un-reinforced Brick Masonry Houses and Low Rise Buildings**

In this chapter, the results from Chapter 3 and 4 were used to derive a simplified formula for wall stiffness. This was the main contribution in developing a design guideline for safer and more efficient masonry structures in Indonesia.

**Chapter 6: Conclusion**

This chapter highlights the main contributions and outcomes of this research. The recommendations for further research are also proposed.





## Chapter 2. Literature Review

---

### 2.1 Introduction

Clay brick masonry houses and low rise buildings have been built in Indonesia for many hundred years by the Dutch in some cities, mostly in Java. The walls were usually thick and strong, and constructed in double layers. These houses and buildings were built under Dutch technical supervision and categorised as historical or heritage buildings.

After the Second World War, Indonesia became an independence country and started to build government and private public houses. These houses were still constructed under Dutch Technical Guidelines and they were also strong and durable. At that time, most village or rural houses were built in traditional style, using local material found in nearby places.

As the changes to modern culture evolved, the type of rural and village housing also changed, to better looking houses made of clay brick walls. However, most of the houses and public buildings were built neither by following a proper technical guideline, nor using good quality clay bricks. Some of the types of traditional and brick houses are shown in Figures 2.1 and 2.2.

Due to many natural disasters like earthquakes, most rural houses lacking in the proper building structure, were damaged in brittle collapse. Consequently, the need for research in material behaviour of local clay brick masonry, especially for masonry structures in Indonesia, became evident. As a result, the literature review of past research done by others in different institutions was undertaken. It was classified into three different categories: first being the study of physical and mechanical behaviour of clay brick masonry; second, the effect of in-plane lateral force to the masonry wall elements; and the third, the design method for un-reinforced masonry buildings, especially with reference to the Indonesian and Australian Standards.

However, since these categories overlap, no such distinction will be made in this chapter.



*Figure 2.1 Traditional houses in Indonesia  
(a) Central Java, (b) South Sulawesi (c) South Sumatera, (d) Yogyakarta*



*Figure 2.2 Brick house in Bali*

## 2.2 Seismically active region of Indonesia

A masonry structure is constructed as the assemblage of bricks or masonry units, properly bonded with an appropriate mortar and commonly used for domestic houses and low-rise buildings. In Indonesia, masonry structures are very popular and can be found anywhere, in small villages or in big cities. Most rural houses and low rise buildings are built without any technical supervision and inspection, using low quality local clay bricks. The reason for using local clay brick materials is because the materials are easily accessible and less expensive, despite the low quality of individual bricks, which can cause severe damage during earthquakes. A brief description of traditional brick making in Indonesia is presented in Section 2.3.

Geographically, Indonesia is located in a seismically active region and this can be seen on the world seismic map in Figure 2.3. Detail of some recent earthquakes in Indonesia in 2006 is shown in Figure 2.4. The map of Indonesia showing places with severe earthquake damage for past 50 years is given in Figure 2.5.

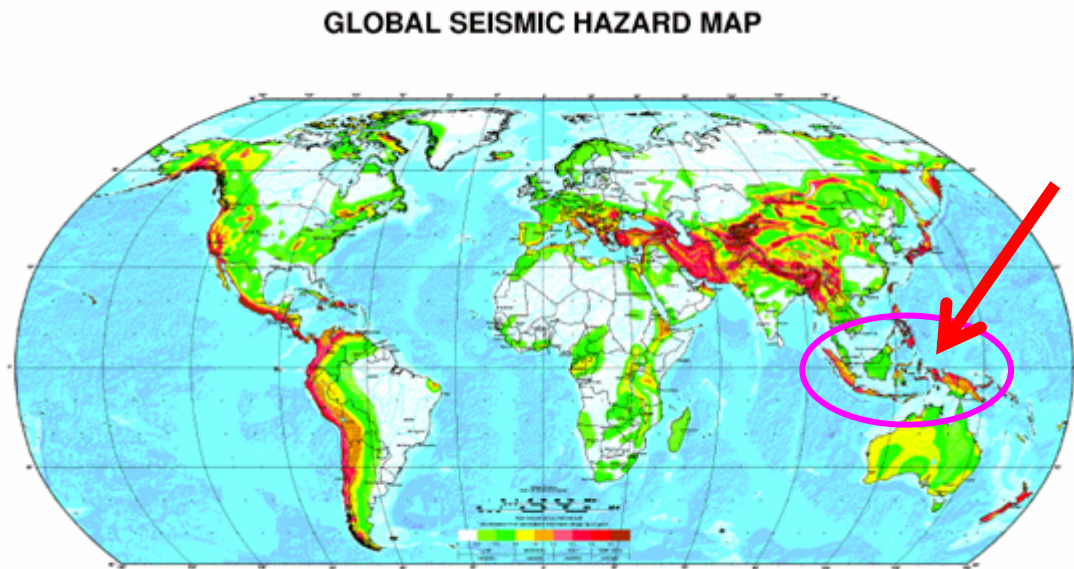


*Figure 2.3 The location of seismically active region “Indonesia”*

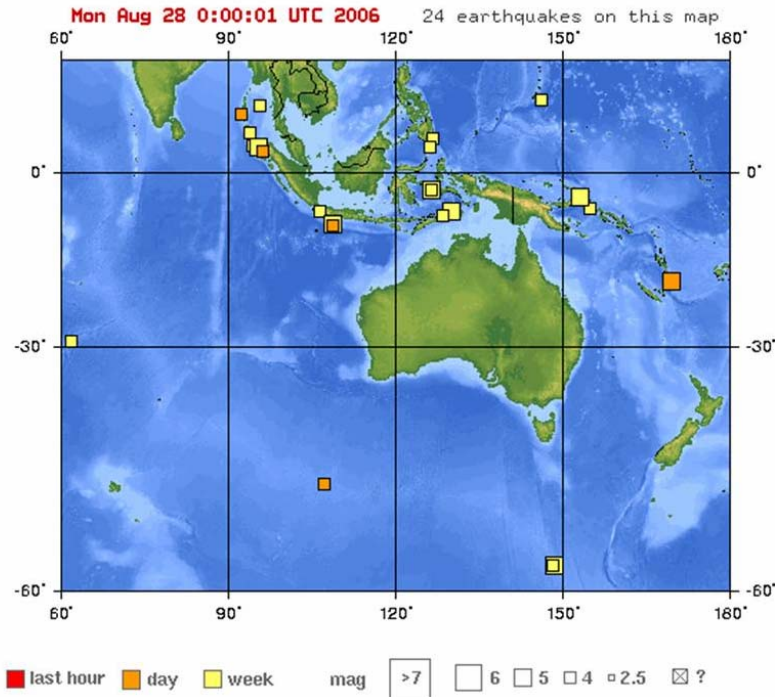


*Figure 2.4 Earthquakes in Indonesia during 2006*

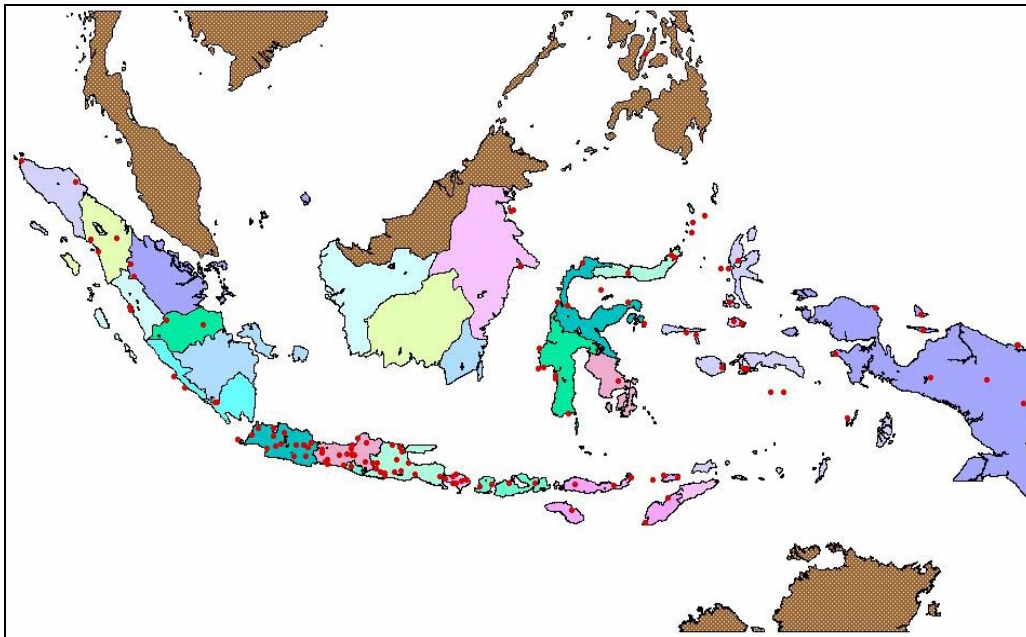


*Figure 2.5 The red dots show places with severe earthquake damage*

In most masonry houses in Indonesia, it is a common practice to confine the walls by using surface mortar plaster. The purpose for applying surface mortar or surface plaster over the surface of the wall is not only to make these walls architecturally more aesthetic, but also to improve their performance. As seen in Figure 2.6, the



public building is constructed by adding a layer of surface mortar plaster to strengthen it and to make the building look better.

Severe damage and in many cases a total collapse resulted in the most non engineered houses and public buildings during the earthquakes, such as the one in Yogya - Central Java in May 2006, the earthquake in Nias - North Sumatra in March 2005 and also in the earthquake in Majalengka – West Java in April 2001. The damage is shown in Figures 2.6, 2.7, 2.8 and 2.9. From examining these figures, it is noticed that severe damage of rural houses was caused by the use of improper construction method with very limited or no technical supervision. It can also be observed that in the opening part of the wall, there is no column and tie beam to strengthen the wall structures in retaining lateral load.



*Figure 2.6 Brick wall for public elementary school building and houses  
(a) Without surface mortar, (b) Plastered with surface mortar  
(c) Plastered with comforted mortar, (d) Process on wall plastering*



*Figure 2.7 Damage on masonry houses during Yogya Earthquake, May 2006  
(a) Severe damage, (b) Partial damage on mortared walls*



*Figure 2.8 Damage on masonry houses during Nias Earthquake, March 2005  
(a) Severe damage, (b) Total collapse*



*Figure 2.9 Damage on masonry houses during Majalengka Earthquake, April 2001  
(a) Severe damage, (b) Partial damage*

Experiencing the structural damage during the recent earthquake in Yogya (May 2006), most non engineered masonry houses collapsed in brittle failure mechanism. The technical guidelines developed by the Department of Public Work of Indonesia have not been implemented in real construction sites. The guidelines are not easily understandable by ordinary people and are mainly proposed for constructing double



brick walls and single wall for main structures and partitions respectively. This type of masonry structures is more expensive and difficult to construct. As people in rural area cannot afford to build double brick wall structures in their houses, single brick wall structures are being chosen and built in most seismically hazard areas. Unfortunately, the construction procedures do not follow any proper technical guidelines and supervision.



*Figure 2.10 Collapse of the local industrial storage buildings during the earthquake*

As seen in Figure 2.10, a storage building was constructed improperly. Neither concrete tie beam nor columns were installed to strengthened brick masonry wall. Although surface mortar plaster was added to wall surface, the wall collapsed during the earthquake.

### **2.3 The construction of masonry houses in Indonesia**

According to the structural detail provided by Indonesian guidelines, some mistakes are often found in many masonry houses or simple structures. In Figure 2.11, fence wall built on the second storey was not properly connected to the supporting beam. This wall was constructed without any column or tie beam. Such brick wall will collapse during earthquake because there is no lateral in-plane stiffener in wall structures.



*Figure 2.11 Masonry wall and brick deposit (Bandung)*

A masonry house shown in Figure 2.12 is considered to be a semi engineered structure, since the structural column and tie beam were not properly installed. There is no closed tie beam constructed at the upper part of the wall to confine the whole structure. It can be expected that some partial damages will occur during earthquake. The wall panels are about 3 m wide and 3.6 m high.

In Figures 2.13 and 2.14, a simple reinforced concrete frame is located in the corner of masonry house. The beam, which is retaining part of the wall structure, is not correctly connected with anchorage to end support. There are also no closed tie beam and column found in this structure. This type of house is classified as a non engineered structure and will experience damage during an earthquake, especially at the corner of wall opening.



*Figure 2.12 Masonry house without tie beam, during construction (Depok – 2005)*





*Figure 2.13 Masonry house without tie beam and column, viewed from front (Porong – 2006)*



*Figure 2.14 Masonry house without tie beam and column, viewed from corner direction (Porong - 2006)*

## 2.4 Production of local bricks in Cikarang – Indonesia

Local bricks used for building construction in JABODETABEK region are mainly produced in Cikarang (Indonesia). Cikarang is a suburb located about 40 km to the east of Jakarta and 140 km northwest of Bandung as shown in Figures 2.15. This place has been well known for many generations as a village of solid clay brick home factories. Generally, in the most part, the rural houses and low-rise buildings in the JABODETABEK region, are constructed from Cikarang solid clay bricks.

The solid clay brick factories are surrounded by rice farm fields, as shown in Figure 2.16. They are made up of many short houses for brick storage, called “*lio*”, as shown in Figure 2.17.



*Figure 2.15 The location of Jakarta, Cikarang and Bandung*



*Figure 2.16 Clay brick factory in Cikarang – Jakarta*



*Figure 2.17 Place of brick storage for drying process called "lio"*

#### 2.4.1 Process of brick production

The process of making clay bricks can be divided into several steps. Starting with clay extraction from the ground, then mixing the clay with rice husks, adding the water, forming, cutting, air drying, firing and sorting the bricks.

##### **2.4.1.1 Clay extraction, addition of water and mixing of the ingredients for making bricks.**

The bricks are mainly made of clay taken from the ground, known as a place of clay extraction, as seen in Figure 2.18, this is. Then the clay paste is mixed with rice husks by following the traditional way of mixing the portions as shown in Figures 2.19 (a) and (b). Generally, worker mixes two portions of husks with one portion of clay by using their own hands. They measure out desired quantities using the approximation and feeling method, which is not technically sound. Then they keep adding water until the mixing dough appears acceptable. The acceptable consistency of the mixture is determined by visual and tactile examination.

##### **2.4.1.2 Brick forming, cutting, drying, firing and sorting.**

After mixing the required ingredients of clay, rice husks and water to form a brick paste, workers portion out this mixture into a simply electrical rotary machinery as



seen in Figure 2.20, for pressing the paste in Figures 2.21 (a) and (b). The mixture is placed over two rotating rolls to homogenise the mix to reduce air pockets.



*Figure 2.18 Place of clay extraction  
(a) Field around factory, (b) Near factory*



*Figure 2.19 Process of mixing brick ingredients  
(a) Mixing clay paste and rice husk, (b) Rice husks*

Subsequently, the paste is compressed into a continuous block with section size of 210 mm x 110 mm as seen in Figure 2.22 (a). Finally, bricks are cut manually using sets of steel wire cutters into three clay blocks each 50 mm thick as seen in Figure 2.22 (b). Later, while still wet, bricks are manually collected into a carriage as seen in Figure 2.22 (c), and then placed in an open air storage space. This storage place is called *lio* and is protected from direct sunlight, as shown in Figure 2.23. In the final step, the bricks are fired in a traditional wood-fired kiln, as shown in Figure 2.24 and

2.25 until firing is completed and bricks are ready to be customised, as seen in Figures 2.26 and 2.27.



*Figure 2.20 Machinery apparatus for pressing the brick paste*



*Figure 2.21 Moulding process  
(a) Labourers working with moulding machine, (b) Blending raw dough*





*Figure 2.22 Wet brick cutting process  
(a) Brick forming, (b) Manual cutting, (c) Manual collection for transporting*



*Figure 2.23 Treatment for natural air drying process  
(a) Transporting wet bricks, (b) Air drying process in lio*

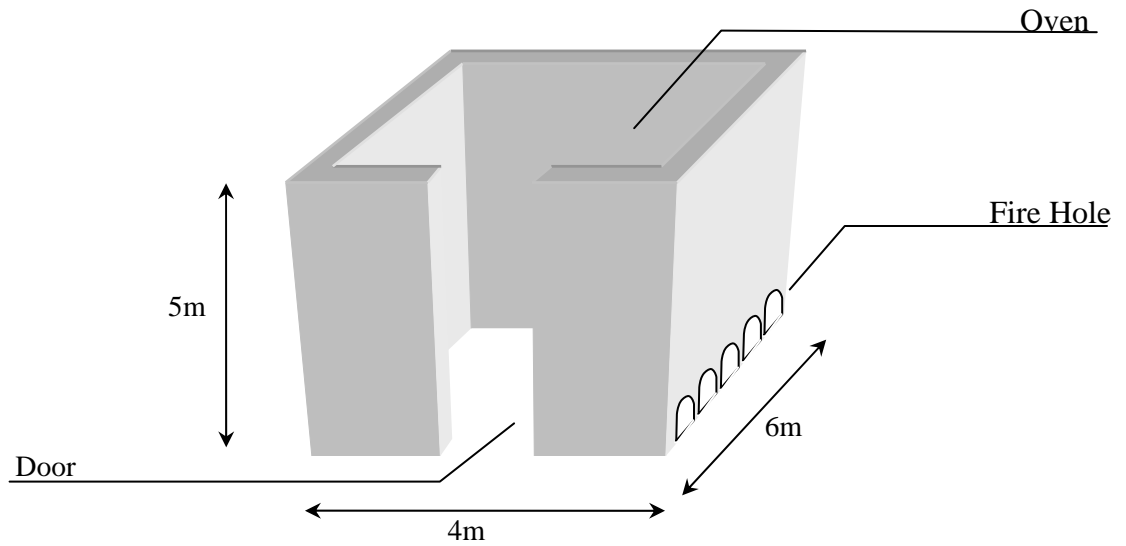


*Figure 2.24 General scheme of the oven*



*Figure 2.25 The traditional wood-fired oven*



*Figure 2.26 Well done ready to use solid clay bricks  
(a) Brick deposit before selling, (b) Clay brick products in different colour*

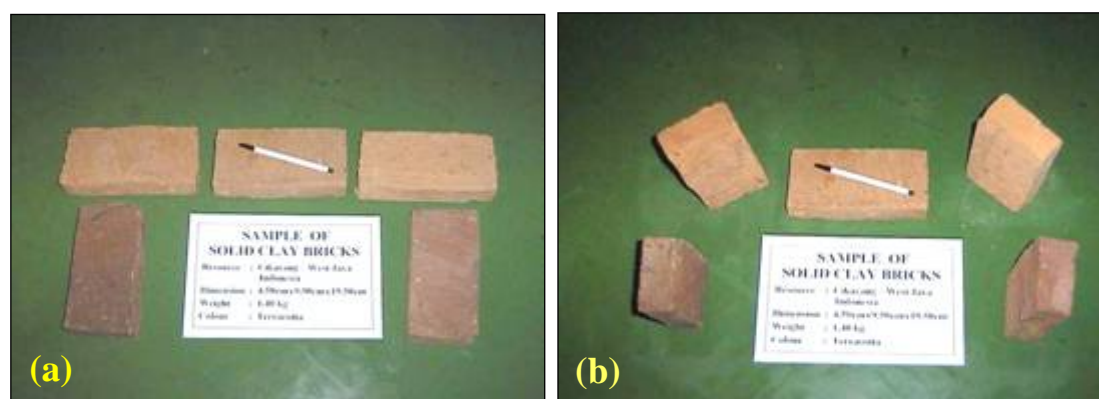


*Figure 2.27 Brick samples used for experimental laboratory work  
(a) Lying position as in construction site, (b) Standing position*

## 2.5 The review of previous research on masonry

The study on mechanical behaviour of masonry walls in the United States and Canada started before 1980's, The majority if the research on masonry and in the United States was focused on high quality bricks' compressive strength, range from 69.8 MPa to 101.7 MPa, (Mc Nary and Abrams, 1985). Compared to Indonesian clay bricks, especially those found in Jakarta rural areas, such bricks are considered to be of a very low quality in compressive strength. Although the bricks are strong enough and safe to retain gravity loads, their behaviour under external load, especially under the lateral in-plane loads representative of static earthquake loads, in veru unpredictable.

### 2.5.1 Research Prior to 2000

The basic research in evaluating the material behaviour of masonry walls subjected to uniaxial monotonic compressive loads started in the early 60's and continued into the 70's and it was carried out in Europe, Canada and the United States of America (McNary and Abrams, 1985). From the late 70's and in the 80's researchers started to evaluate the material behaviour of masonry structures under cyclic loading. The results of these research projects concluded that the masonry wall is generally safe and can adequately resist gravity loads, but it is considered to be weak and vulnerable under lateral loads caused by the earthquake motion (Naraine and Sinha, 1989).



The question therefore arises as to the ability of masonry walls to resist seismic loads. To answer this question, the masonry walls need to be categorised into two different types of structures; firstly, the un-reinforced masonry walls (URM) or un-reinforced brick masonry walls (UBM), secondly, the reinforced masonry walls (RM). These URM, UBM and RM structures can be either unconfined or confined by frames such as wood, concrete or steel frames, and/or by a mortar plastered over the wall surface. The mortar plastered is not considered to be a confinement system to the wall because surface mortar plastered walls is rarely found in Europe, America, Canada and Australia.

Though masonry bricks are cheap in Indonesia and hence used extensively, they are low in quality and strength. As observed in real case studies found in Indonesia, most clay brick masonry walls or houses are strengthened by mortared surface confinement. This type of structures can be found in many villages all over the country in rural low cost houses built for low income people. These structures are usually built without following any technical guidelines or supervision. They are categorised as non engineered structures and many of them are located in regions of moderate to high seismic risk.

Hamid and Drysdale (1981) investigated failure theories and proposed failure hypotheses for masonry under combined stresses. The applicability of the failure theories for composite materials to masonry was examined by utilizing experimental results of concrete block masonry tests. It was concluded that failure theories for isotropic materials are not applicable to masonry. Also, failure theories for composite materials couldn't be directly applied to predict the masonry strength under biaxial stresses. Failure criteria for masonry under biaxial stresses were proposed, taking into consideration its anisotropic nature as a composite material. Two failure criteria were determined each describing a single mode of failure and shear failure along one of the critical bed or head joint direction, and a tension failure incorporating the interaction of the block, mortar and grout. The proposed criteria are capable of predicting both, the mode of failure and the strength of concrete block masonry under biaxial stresses.

Anand and Young (1982) developed a two-dimensional composite element that is capable of predicting the out-of-plane inter-laminar shearing stresses between the brick without using a three-dimensional finite element model. This composite element was utilized in two-dimensional analyses in a plane-strain condition. The results of these analyses were compared with those using the plane-strain finite element models. These comparisons indicated that the two-dimensional composite element models predicting inter-laminar shearing stresses in the collar joint were in good agreement with those obtained from the plane-strain models. Although the composite element was initially developed only for elastic conditions in an unreinforced collar joint without any consideration to fracture and failure, these criteria can be easily incorporated in the proposed model.

Dhanasekar et al. (1985) evaluated simple nonlinear stress-strain relation for brick masonry constructed with solid pressed bricks, based on the results of a large number of biaxial tests on square panels with various angle of the bed joint to the principal stress axes. The results from this research were as follows. In the initial elastic behaviour the brick masonry was isotropic. Panels that failed by tensile splitting can be assumed to be elastic up to failure. Strains derived using the assumption of an associated flow rule and an isotropic strain-hardening yield surface were not consistent with the measured strains. Further tests, are required to define the boundary between the region, in which a power law is appropriate and the important region, where bed joint sliding develops.

Grimm and Tucker (1985) investigated the combination of masonry units and mortar. They concluded that the flexural strength of masonry is dependent on the quality of workmanship, the method of loading, and the number of mortar joints in the span. The weakest link theory was applied to establish the relationship between flexural strength test data obtained for the same materials and workmanship by different loading conditions and sizes of masonry units.

McNary and Abrams (1985) investigated the strength and deformation of clay-unit masonry under uniaxial concentric compressive force. Biaxial tension-compression tests of bricks and triaxial compression tests of mortar were done to establish constitutive relations for each material. Mortar strengths and brick types were varied.

Using four different types of mortar with proportion of cement: lime: sand were 1 : ¼ : 3 for mortar type M, 1 : ½ : 4 ½ for mortar type S, 1 : 1 : 6 for mortar type N, 1 : 2 : 9 for mortar type O. Water/cement ratios for mortar types M, S, N, O were 0.55, 0.85, 1.19, 1.96 and the strength of these mortar types were 52.6 MPa, 26.4 MPa, 13.7 MPa, and 3.4 MPa respectively. Two brick types were used for compressive tests. Brick type 1 was standard modular paving with a flat compressive strength of 101.7 MPa and brick type 2 was a modular cored unit with a flat compressive strength of 69.8 MPa. The authors found that brick masonry prisms built using strong mortars type M and S cracked suddenly and failed explosively at the ultimate load. For prisms built using weaker mortars type N or O, the progression of cracking was slower and the failure was more ductile than that observed for prisms with strong mortars.

Interaction effects of these two materials were examined using a theory proposed by others. A numerical model based on this theory was used to compute the force-deformation relationship for a stack-bond prism, and was compared with measured strengths and deformations of test prisms taken from experimental work as shown in Figure 2.28.

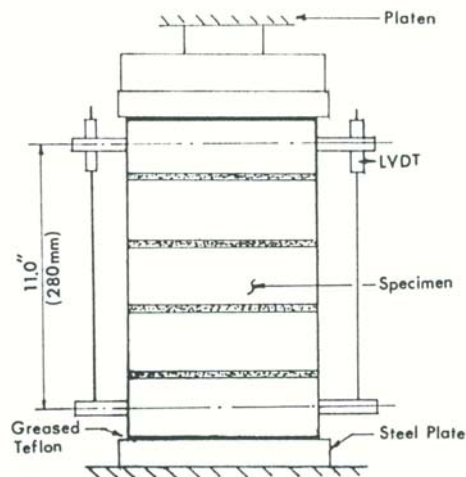


*Figure 2.28 Test configuration by McNary and Abrams (1985)*

The relation between stress and strain as shown in Figure 2.29, became increasingly nonlinear as mortar strength decreased, which indicated that the properties of mortar had a strong influence on prism deformation.

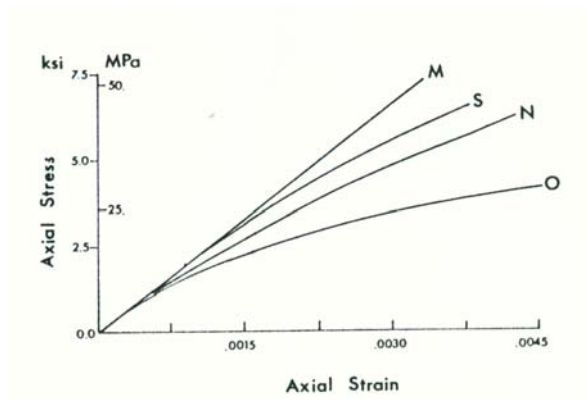


*Figure 2.29 Stress-strain relation measured from experimental test by McNary and Abrams (1985)*

Results of the study indicated that mechanics of clay-unit masonry in compression could be well represented by a relatively simple model, and the most significant parameter to consider was the connection behaviour of the mortar with bricks.

Hamid and Chukwunenye (1986) developed an analytical procedure using three-dimensional finite element model to study the complex behaviour of hollow block prismatic masonry under axial compression. In this analysis, the effect of mortar bedding, mortar deformation characteristics, block size, height to thickness ratio, a number of mortar joints and stiffness of bearing plates were considered. The results showed that the most significant parameters were the type of mortar bedding, prism geometry, and the stiffness of bearing plates.

Biolzi (1988) determined the bearing capacity of masonry elements subjected to compression with respect to the difference of mechanical properties of the constituents. The results showed that the collapse mechanism occurred due to tensile rupture of mortar/brick complex but not due to the compression of the mortar joints. The improvement of mortar quality resulted in only limited variations of the collapse load and the excessive thickness of mortar joints considerably reduced the masonry strength.

Atkintson et al. (1989) examined the horizontal bed joint shear failure mode and the shear load-displacement behaviour of un-reinforced brick masonry during static and cyclic loading, based on laboratory and field tests. The results of this research indicate that the residual strength does not seem to be affected by the number of

shear cycles. Masonry bed joints show peak strength for the first cycle, followed by residual shear strength afterwards.

Naraine and Sinha (1989 a, b) investigated the behaviour of brick masonry under cyclic compressive loading and evaluated the loading and un-loading stress-strain curves. The results showed that experimentally and analytically, the envelope curve under cyclic loading coincide with the stress-strain curve under monotonic loading.

According to Shing et al. (1990), simple flexure theory based on the plane-section assumption can be applied to square wall panel with good accuracy. The actual flexural strength of a masonry shear wall subjected to seismic loads can be slightly higher than that is predicted by the flexure theory, due to the more severe strain hardening under cyclic loads. The ductility of a flexure-dominated wall can be reduced substantially by increasing the axial stresses, which leads to more severe crushing at the bed joint. Further experimental works are still needed with different aspect ratios of specimen size subjected to different load conditions.

Naraine and Sinha (1991, 1992) investigated stress-strain behaviour based on an experimental investigation on brick masonry under cyclic biaxial compressive loading. The experimental investigation involved biaxial tests on 45 half-scale brick masonry specimens. Three types of tests were conducted to establish the envelope stress-strain curve, the common point curve, and the stability point curve. A general empirical equation was proposed for these curves that compares well with the experimental data. The research outcomes were: (1) failure criterion expressed in terms of principal stress invariants; (2) the use of the stability point curve as an aid in defining the permissible stress level for brick masonry under cyclic biaxial compressive loading; and (3) the importance of relating the stability point to the level of residual strain in the material.

Fahmi and Ghoneim (1995) developed a nonlinear three-dimensional finite element model to study the complex behaviour of un-grouted and grouted concrete block masonry prisms under axial compression. The model detects crack initiation and traces crack propagation in the masonry assemblage. Variable strengths for block, mortar, and grout were used to study the effect of mechanical properties of prism

constituents, and their combination of prism strength and modulus of elasticity. The results of this analysis showed that crack pattern, failure mode, compressive strength and initial modulus of elasticity, all depend on the relative rather than the individual material properties.

Lafuente et al. (1995) evaluated analytical procedures for the scope and limitation of standard masonry testing according to the codes. By assuming that masonry is modelled as a homogeneous material, the findings of this research were: the interaction between brick and mortar component highly influenced the structural behaviour of masonry wall; final behaviour of a framed confined masonry panels depended on the infill cracking pattern; higher resistances and ductility factor were associated with friction failure mechanisms; correction factors must be used with design purposes.

Magenes and Calvi (1995) showed the laboratory experimental work of masonry wall on shaking table test. The result of this experiment stated that the structural behaviour of masonry walls was influenced by the effect of stiffness difference between mortar and masonry units; thickness of mortar joints; and presence of vertical joints.

Romano et al. (1995) analysed the calcareous tufa masonry walls subjected to vertical load and cyclic shear load, using two types of mortar joints with different mechanical properties. The material behaviour of masonry was represented by an equivalent homogeneous orthotropic. The results of this analysis showed that the level of vertical load had much more influence on the shear strength and their behaviour of the wall than the mortar strength.

Subramaniam and Sinha (1995) developed mathematical model using polynomial function for analysing uniaxial cyclic behaviour of clay brick masonry under compressive loading. The model facilitates the reproduction of the reloading and unloading stress-strain curves for both cases of loading, for loading perpendicular to the bed joint and loading parallel to the bed joint. The algorithm of the model is simple and can be computed easily, it also gives good result compared to model predictions and the experimental stress-strain curves.

Tomazevic (1995) stated that different method of testing the masonry walls under seismic loads will give different results. Therefore, it needs the relevant correction procedure and it is developed by using a special computer program in order to optimise values of ground displacements. Practical limitations of modelling techniques and simulation of earthquake ground motion require additional experiments to determine the characteristics of model materials and model structural elements, as well as simulated earthquake ground motion in order to evaluate the effect of this limitation.

Zarnic (1995) evaluated two mathematical models, one for the simulation of inelastic response to monotonous load and the other for simulation of inelastic response to dynamic load. The first analytical model is created for the calculation of tri-linear relationship between the deformation and the base shear. The second model enables dynamic analysis of in-filled frame structures incorporated in a computer program for dynamic analysis of structures. By using finite element DRAIN-2D program, the proposed models are suitable for further experimental and analytical research into the behaviour of in-filled frames. Further investigations are still needed regarding the additional testing of the proposed model by means of experiments of multi-storey and multi-bay specimens

Anand and Yalamancili (1996) presented results of three-dimensional finite-element failure analysis of composite masonry walls subjected to both vertical and horizontal loads. The wall was modelled by using eight-node solid elements and cracking at the interfaces was defined by a simple Mohr-Coloumb failure criterion. The smeared crack technique was used to model the cracks. It was shown that cracking in the collar joint was initiated at a much smaller magnitude of the horizontal in-plane load, compared to the vertical load. This phenomenon may be attributed to the relatively high rigidity of the wall in the vertical direction. The failure loads for composite walls are computed using the three-dimensional analysis and were compared with those obtained from an approximate method and experimental values. It was shown that the computed failure loads follow the same trend as the experimental results.

Andreas (1996) investigated the failure criteria of masonry panels under in-plane loading, which can be attributed to three simple modes: slipping of mortar joints, cracking of clay bricks and splitting of mortar joint and middle plane spalling. In this paper, a suitable strength criterion is connected to each collapse mode. In more detail, as referred to the modified Mohr-Coulomb criterion of intrinsic curve, a frictional law is associated with the slipping, which accounts for the shear strength depending nonlinearly on normal stress. Splitting can be expected by the maximum Saint Venant tensile strain criterion, orthotropic non-symmetric elasticity being assumed for the material. Eventually panels exhibit spalling when the maximum Navier criterion compressive stress was attained under biaxial loading. Strength parameters are then identified on the basis of experimental results and a comparison with the reliable criteria found in the literature was carried out. The validity of the failure criteria to predict the experimental failure modes with respect to the normal stress has been tested in a qualitative manner for the three fundamental failure modes. A quantitative comparison between experimental and analytical results has been carried out for the cases, where significant scatters are concerned. The proposed failure criteria seem to be in a good agreement with experimental results, within the limits of: small-size panels, single courses, solid units, regular mortar joints, and in-plane loads. Further, these criteria can be used together with a suitable 2D finite-element model, and then directly used to carry out the limit analysis of masonry walls, modelled by a discrete number of panels of finite size. The potential application of the proposed criteria to actual cases is also illustrated. In fact, a specific example is worked out to show, how to apply these criteria to predict the failure load and failure mode of a particular masonry panel.

Tomazevic and Lutman (1996a, b) mostly investigated nonlinear behaviour of masonry wall / structures by doing laboratory experimental work for masonry building structural model due to seismic loading. The result of this research gives a conclusion that masonry walls take a considerable participation in absorbing the energy caused by cyclic loading.

Anthoine (1997) evaluated the relevance of the plane stress and generalised plane strain assumptions in applying the homogenisation theory for periodic media to masonry in the linear range elasticity. Both brick and mortar were assumed to be



homogenous elastic materials subjected to isotropic damages. The result from numerical computation showed that this assumption had little influence on the macroscopic elastic behaviour of masonry, but may significantly affect its non-linear response.

Khalaf (1997) investigated the response of block-work masonry compressed in two orthogonal directions. An experimental investigation was conducted to study the difference in strength and behaviour of unfilled and filled blocks and prisms compressed in two orthogonal directions, normal and parallel, to unit bed face. In some codes and standards no consideration was given to the way the prisms constructed, nor to the way of the blocks or prisms should be loaded to meet situations, where the acting external forces are applied in a direction parallel to the unit bed face. The effects of using different grout mixes and mortar joint types on the samples' strength were also investigated. The results showed that changing the mortar strengths have little influence on unfilled prisms strength compressed parallel to bed face, compared to those compressed normal to bed face. The presence of grout significantly increased the filled prisms section capacity compared to unfilled prisms, but for the range of grout strengths used, the contribution of grout to the prisms section capacity was small.

La Mendola (1997) evaluated the influence of nonlinear constitutive law on masonry pier stability. The stability condition of cantilevered masonry piers subjected to their own weight and to a concentrated compressive top load was investigated, considering material with small tensile strength and nonlinear stress-strain law in compression, of an experimental-nature, and including softening behaviour. The analysis was carried out by improving a numerical approach adopted in previous works, where stability problems were solved assuming an infinitely elastic linear constitutive law in compression. Before the geometrical nonlinearity is considered, the limit equilibrium of a typical pier rectangular cross section is detected assuming unlimited available compressive strain. This preliminary analysis allows one to determine analytically the limit value that has to be imposed on the eccentricity of the resultant compressive force and to derive the moment-curvature relationships, on which the second-order effects depend. Then the stability domains are derived in dimensionless form and their boundaries are modelled by analytical approximate

expressions of practical use. Some numerical examples show that, depending on the average normal stress level, the assumption of an approximate linear constitutive law in compression, affected by the same elasticity modulus as that at the origin of the actual stress-strain law, can provide an unacceptable overestimate of the critical load.

Madan et al (1997) developed an analytical macro-model based on an equivalent strut approach integrated with a smooth hysteretic model and proposed this model for representing masonry infill panels in nonlinear analysis of frame structures. The hysteretic model uses degrading control parameters for stiffness and strength degradation and slip "pinching" that can be implemented to replicate a wide range of hysteretic force-displacement behaviour, resulting from different design and geometry. The development of the hysteretic model and the definitions of the control parameters, which can be determined using any suitable theoretical model for masonry in-fills, are also presented. An available theoretical model for simplified engineering evaluation of masonry in-filled frames was explored, for estimating the control parameters of the proposed macro-model. The macro-model was incorporated in a nonlinear structural analysis program, IDARC2D Version 4.0, for quasi-static cyclic and dynamic analysis of masonry in-filled frames. Simulations of experimental force-deformation behaviour of prototype infill frame subassemblies were performed to validate the proposed model. A lightly reinforced concrete framed structure was analysed for strong ground motions to evaluate the influence of masonry infill panels on the dynamic response.

Magenes and Calvi (1997) observed the diagonal shear cracking failure and flexural failure of masonry wall panels subjected to seismic in-plane loading. The result of this research stated that the ultimate deformation capacity in shear was very stable, when expressed in terms of drift and corresponds approximately to 0.5 percent. The large deformation capacity was also available with an ultimate drift level equal to 1 percent and it was recommended for the purpose of non-structural damage limitation.

Mehrabi and Shing (1997) developed a finite element modelling of masonry in-filled reinforced concrete frames. A set of experimental and analytical studies has been carried out to investigate the performance of masonry-in-filled RC frames under in-plane lateral loadings. The experimental results were concisely summarized, and a

constitutive model was presented for the model of masonry mortar joints and cementitious interfaces in general. A smeared-crack finite element model was used to model the behaviour of concrete in the RC frames and masonry units. It was shown that the finite element models are able to simulate the failure mechanisms exhibited by in-filled frames, including the crushing and cracking of the concrete frames and masonry panels, and the sliding and separation of the mortar joints. The lateral strengths obtained with these models were in good agreement with those obtained from the tests.

Mojsilovic and Marti (1997) developed a mathematical model to analyse strength of masonry subjected to combined in-plane forces and moments, using sandwich model based on the theory of reinforced concrete plate elements. The conclusions stated that using sandwich model could reduce the interaction problem of six stress resultants to two interaction problems of three membrane force components.

Tomazevic and Klemenc (1997) observed the seismic behaviour of confined masonry walls. In this research, a tri-linear model of lateral resistance-displacement envelope curved has been proposed, where the resistance was calculated as a combination of the shear resistance of the plane masonry wall panel and dowel effect of the tie-columns reinforcement.

Al-Shebani and Sinha (1999) developed a nonlinear behaviour of stress-strain characteristics of brick masonry under uniaxial cyclic loading. This research was mainly based on the previous work done by Dhanasekar et al. (1985), Naraine and Sinha (1989a, b, 1991, 1992), Subramaniam and Sinha (1995). In this research, 42 panels of brick masonry walls were loaded in two cases: normal to the bed joint and parallel to the bed joint. Some conclusions from this research are: (1) failure in tension occurred in mortar joint and it was brittle with a limited number of cycles; (2) failure in compression occurred by splitting in bed joints for loads parallel to the bed joint; (3) for loads normal to the bed joint, the failure was characterised by combined failure in the brick units and head joint; (4) and the stress ratios of 0.69 for loading normal to the bed joint and 0.67 for loading parallel to the bed joint were taken to initiate the process of strength deterioration. These ratios were shown by the relation between residual strain and energy dissipation.

Bati (1999) proposed a micromechanical model for determining the overall linear elastic mechanical properties of simple-texture brick masonry. The model, originally developed for long-fibre composites, relies upon the exact solution and describes brickwork as a mortar matrix with insertions of elliptical cylinder-shaped bricks. Macroscopic elastic constants were derived from the mechanical properties of the constituent materials and phase volume ratios. Conformity of the suggested model to real brickwork behaviour was verified by performing uniaxial compression tests on masonry panels composed of fired bricks and mud mortar. Composite masonry panels of varying phase percentages were then constructed and tested by replacing several of the fired bricks with mud bricks. Comparison of experimental results with theoretical predictions demonstrates that the model is suitable even in the presence of strongly differentiated phases, and is moreover able to predict different behaviour as a function of phase concentration. The model fits experimental results more closely than the micromechanical models previously reported in the literature.

From the extensive review of the existent literature it is evident that no research has been carried out on the mechanical and structural behaviour of un-reinforced masonry clay brick walls with surface mortared confinement subjected to lateral earthquake / cyclic / dynamic loading.

### 2.5.2 Research Beyond 2000

Al-Shebani and Sinha (2000) developed Stress-Strain characteristics of brick masonry under cyclic biaxial compression. Tests on half-scale sand calcium-silicate brick masonry specimens subjected to cyclic biaxial compression were conducted for five principal stress ratios. An interaction curve for the principal stresses at failure was obtained experimentally and expressed mathematically in terms of stress invariants. The failure under biaxial compression was characterized by mid-thickness splitting of the bearing area. The failure was quantified by the critical orthogonal strain that governed the failure, which in turn defines the critical stress-strain envelope curves. The critical envelope curve and the corresponding common point and stability point curves were expressed in mathematical form by general exponential formulas. The stability point curves can be used to establish the

permissible stress level under in-plane cyclic loading and approximately close to 0.60 – 0.70 to the maximum stress level.

Lourenco (2000) developed a model for the numerical analysis of masonry subjected to out-of-plane loading. The proposed composite plasticity model is able to reproduce elastic and inelastic behaviour in two orthogonal directions, coinciding with the orientation of the bed and head joints of masonry. The implementation of the model is described, and a comparison with experimental data on masonry strength is provided. Good agreement is found for different masonry types. Further validation of the model with experimental results on masonry panels subjected to out-of-plane loading demonstrated the accuracy of the proposed approach and the possibilities offered by numerical analysis for the understanding of the complex nonlinear phenomena involved in the failure of masonry plates and shells. The research outcomes issues were: adequacy of yield-line analysis for the design of masonry structures subjected to out-of-plane loading, the influence of the aspect ratio of the panels, and the influence of in-plane normal pressure.

Ma et al. (2001) developed a method of homogenization of masonry using numerical simulations. Homogenization was one of the most important steps in the numerical analysis of masonry structures where the continuum method was used. In this study, equivalent elastic properties, strength envelope, and different failure patterns of masonry material were homogenized by numerically simulating responses of a representative volume element (RVE) under different stress conditions. The RVE was modelled with distinctive consideration of the material properties of mortar and brick. In the numerical simulation, various displacement boundaries were applied on the RVE surfaces to derive the stress-strain relation under different conditions. The equivalent overall material properties of the RVE were averaged by integrating the stresses and strains over the entire area. Failure of masonry is defined by three different modes, namely, tensile failure of mortar (Mode I), shear failure of mortar or combined shear failure of brick and mortar (Mode II), and compressive failure of brick (Mode III). The homogenized elastic properties and failure model can be used to analyse large-scale masonry structures.

Sakr and Neis (2001) developed a new analysis method for un-reinforced masonry double walls. The technique uses empirical formulas for the effective flexural rigidity of a masonry wall, as obtained from a finite-element analysis of a masonry couplet. These formulas, together with equations that relate the moments in the blocks, bricks and the ties, are used in a one dimensional analysis of the masonry wall. The method rationally accounts for material nonlinearities, flexural tensile bond failure mechanism, types of ties, cavity width, load eccentricity, slenderness ratio, load-displacement, and moisture and temperature deformation effects. The simplicity of the analysis technique is illustrated by instituting the procedure into a spreadsheet application. Complete load-deflection curves generated for some test walls compared well with the experimental data. The analysis method is accurate and extendable in predicting the ultimate load and the load-deflection relationships of masonry walls.

Syrmakezis and Asteris (2001) investigated the masonry failure criterion under biaxial stress state. Masonry is a material that exhibits distinct directional properties because the mortar joints act as planes of weakness. To define failure under biaxial stress, a three dimensional surface in terms of the two normal stresses and shear stress (or the two principal stresses and their orientation to the bed joints) is required. A method to define a general anisotropic (orthotropic) failure surface of masonry under biaxial stress, using a cubic tensor polynomial was developed. The evaluation of strength parameters was performed using existing experimental data through a least-squares approach. The validity of the method is demonstrated by comparing the derived failure surface with classical experimental results. The ability to ensure the closed shape of the failure surface, the unique mathematical form for all possible combinations of plane stress, and the satisfactory approximation with the results of the real masonry behaviour under failure conditions, were some of the advantages of the proposed method.

Al-Shebani (2001) provided research outcomes based on the former test done to the calcium silicate brick masonry panels, measuring 360 mm x 360 mm x 115 mm under cyclic loading. The findings were: the cyclic test can produce three distinct stress-strain curve; envelope, common point, and stability point curves; residual strains accumulate as the number and peaks of the cycles increase; the variation of residual strain with axial strains follows a polynomial function of single term; the

level of residual strain can be used to predict the degree of the material deterioration; the cyclic permissible stress is based on the plastic deformation of brick masonry, and maximum permissible stress is corresponding to the residual strain associated with unloading from the peak of stability point curve.

Danasekar (2001) developed three dimensional modelling of complex state of stress of hollow masonry, when it is subjected to simple state of loading, such as uniaxial compression using ABAQUS finite element package program. The case study was applied to hollow masonry walls and categorised as face shell bedded and full-bedded masonry, where the hollow cores are grouted. The outcomes of this research were: (1) the vertical stress distribution along a mortar bed joint is more uniform in full bedded masonry than the face shell bedded masonry; (2) the horizontal and lateral stresses in face shell bedded masonry was in the order of 28% of the dominant vertical compressive stress ( $\sigma_y$ ); (3) the lateral stress ( $\sigma_z$ ) in the full bedded masonry is as high as 48% of the  $\sigma_y$ ; and (4) face shell bedded masonry developed tensile stresses in the web shells adjacent to the mortar bed joints in the order of 42% of  $\sigma_y$ .

Sutcliffe et al. (2001) carried out analysis of masonry shear walls, using two modelling techniques based on finite elements and the lower bound limit theorem of classical plasticity. Both techniques were based on simplified micro-modelling approach where the units and the joints are modelled separately, with failure mainly confined to the relatively weak joints. Common to both approaches is the use of a linear of constituent materials. However, the models differ in their assumptions relating to the modes of failure, particularly parallel to the bed joint direction. The effects of variation of tensile, compressive and frictional strength were all studied in relation to their influence on the overall, in-plane strength of a masonry shear panel.

Zhuge (2001) tested six partially reinforced / reinforced clay brick masonry walls experimentally under in-plane lateral loads and observed results, which were quite different to those obtained from tests with concrete block walls. All six walls failed in a brittle manner, which is not acceptable in seismic design. It has been found that the vertical reinforcing bars failed to participate in providing composite action, due to the low compressive strength of the grouting material.

Zhuge (2001) also carried out a three dimensional finite element analysis of masonry walls subjected to foundation movement, using a non-linear approximation of material behaviour. These results were calibrated with the experimental tests on a wall size of 2.40 m high and 6.0 m long, constructed on a reinforced concrete footing 300 mm wide by 250 mm deep, which was cast as a continuous strip on the footing rig.

El-Sakhawy et al (2002) investigated shearing behaviour of joints in load-bearing masonry wall and stated that stress and strain responses during shearing of masonry joints indicate unrecoverable shear and normal deformation that demand use of a constitutive model specifically developed for joints. The study about an elasto-plastic joint constitutive law is proposed to model the shearing behaviour of joints in load-bearing masonry walls. The brick-mortar bed joints were sheared using a shear box test. The physical parameters of the model were obtained from the experimental data. The load-displacement response observed experimentally was analysed using the proposed constitutive law. The model appears to predict the shearing behaviour of brick-mortar bed joints. By applying an elasto-plastic constitutive law for joints and determining its parameters from the shear testing of brick-mortar bed joints, shearing displacement response of brick-mortar bed joints can be determined.

Andreas et al (2002) evaluated simplified models for lateral load analysis of unreinforced masonry buildings, In this study, several parametric analyses involving finite element models of two dimensional and three dimensional structures have been performed, first in the elastic range, using both refined and coarse planar meshes. They were followed by analyses of the same structures using equivalent frames with alternative arrangements of rigid offsets. Subsequently, two-dimensional nonlinear static (pushover) analyses of both finite element and equivalent frame models were performed, to check the validity of the conclusions drawn from the elastic analysis.

Mohamed et al (2003) investigated the cyclic performance of concrete-backed stone masonry walls experimentally. Six 1/3-scale, single-story, single-bay wall samples were tested. Three of these samples were constructed using an old construction method and the other three were constructed using a new construction method. The influence of the type of construction, applied vertical loads, and existence of dowels



between the infill concrete panel and the base on the lateral resistance, ductility, energy-dissipation, stiffness degradation, and failure mechanisms were investigated. The experimental results indicate that an increase in the applied vertical load resulted in a substantial increase in both, the lateral strength and stiffness of the tested samples. The type of construction had no influence on the ultimate lateral load resistance. The existence of the dowels caused the diagonal cracks to be shifted upward, far from the base. Also, the dowels gave a better distribution and smaller widths for these diagonal cracks. The failure mechanisms of all concrete-backed stone masonry walls were dominated by diagonal shear cracks.

Lourenco and Ramos (2004) developed a characterization of cyclic behaviour of dry masonry joints and stated that the behaviour of dry masonry joints under cyclic loading is a key aspect for seismic actions. The work focuses on the characterization of Coulomb failure criterion and the load-displacement behaviour of dry masonry joints under cyclic loading, including aspects as surface roughness, dilatancy, and inelastic behaviour. For this purpose, a displacement controlled test setup using masonry couplets was used. Besides providing a basis for understanding the behaviour of masonry joints in shear, the experiments contribute also to the definition of advanced nonlinear numeric models.

Lu et al (2004) developed an analysis technique of the influence of tensile strength on the stability of eccentrically compressed slender unreinforced masonry walls under lateral loads. The outcomes was a comprehensive finite element model for the combined material and geometric nonlinear analysis of slender unreinforced masonry walls, with the capability of capturing post-cracking and post-buckling behaviour. Material tensile strength is taken into consideration; an exponential stress-strain relationship is adopted for the compressive region and its smooth linear extension is used for the tensile region. This model is applicable under different load combinations (concentrated and distributed lateral loads, vertical load with eccentricity, as well as self-weight) and different restraint conditions. Numerical results of the model show good agreement with experimental results, as well as with analytical results.

Asteris and Syrmakizis (2005) evaluated the strength of unreinforced masonry walls under concentrated compression loads. The result from this study stated that the strength of masonry walls subjected to concentrated vertical loads is nonlinear. An orthotropic finite-element model was used to simulate the wall behaviour. Nonlinear deformation characteristics of masonry material as well as its anisotropic (orthotropic) behaviour were taken into consideration. A new anisotropic yield/failure surface of a masonry wall under biaxial stress, in a cubic tensor polynomial form, is proposed. A parametric study is carried out using several parameters such as the loaded area length to the total length ratio, the load position in relation to the end of the wall, and the wall geometry. Based on the results of the parametric investigation, a new design rule is proposed.

Roca et al (2005) evaluated the strength capacity of masonry wall structures by the equivalent frame method. The structural assessment of large traditional and historical masonry buildings poses significant challenges due to the need for modelling complex geometries and nonlinear material behaviour. Although sophisticated methods have been developed for the nonlinear analysis of such structural systems mostly based on two- or three-dimensional finite element modelling, they can hardly be used for practical purposes due to very large computational requirements. An alternate method, specifically developed for efficiently simulating the service and ultimate responses of structural systems composed of masonry load-bearing walls, was presented. Its efficiency stems from the technique adopted to model the wall panels, based on treating them as equivalent frame systems composed of one-dimensional elements. In addition, biaxial constitutive equations are included to account for the relevant aspects of the nonlinear response of the material. In spite of the numerical efficiency of the method, it is able to obtain accurate predictions of the overall response of masonry buildings and their failure condition. The method has been successfully used for the analysis of actual large historical constructions and for simulating possible operations of repair and restoration.

Khalaf (2005) developed a new test for determination of masonry tensile bond strength between masonry units and mortar. The flexural bond strength of masonry in particular is needed for the design of masonry walls subjected to horizontal forces applied normal to the face of the wall, such as wind forces. Researchers and

standards have suggested different kinds of specimens and test procedures to determine the flexural bond strength. These include the test on small walls, the bond wrench test, the direct tensile test, and the crossed couplet test. Each of these tests has its own drawbacks and problems. A test method to determine the flexural bond strength,  $f_{fb}$ , by bending was presented. In this work the test can be used for laboratory research to investigate the many factors affecting bond strength and also for deriving design values for masonry standards. The specimen is constructed from two brick units in a Z-shaped configuration, and three-point loading induces a flexural bond failure parallel to the bed joint. Three different types of clay brick, one calcium silicate brick, and three different types of mortar were used in the experimental program. The results derived show that the proposed new specimen and test procedure are easily and accurately capable of determining the flexural bond strength.

Köksal et al (2005) evaluated the compression behaviour and failure mechanisms of concrete masonry prisms. To date, only linear elastic analyses have been used to explain the compression behaviour of the concrete masonry prisms. In this study, nonlinear three-dimensional finite element analyses, based on both an elasto-plastic approach and an isotropic damage model, have been applied to the compression behaviour of hollow block and grouted concrete block prisms. Attention is particularly focused on the derivation of material parameters for concrete, grout, and mortar, and also on the improvement of existing code expressions for prism strength. In this research, the adequate values for the cohesion and friction angle of the Drucker-Prager yield criterion and material damage parameters for the damage model for the constituent materials were introduced. The results of the nonlinear finite element analyses were observed to be in good agreement with the experimental data were in terms of failure mechanisms and ultimate load. Failure modes of grouted prisms, also investigated by evaluating the stress distributions at the outer face shell, along the prism height. Finally, an analytical relation,  $f'_m$  was proposed to predict the compressive strength of concrete masonry prisms.

Sarangapani et al (2005) investigated the brick-mortar bond and masonry compressive strength. This research focuses on some issues pertaining to brick-mortar bond and masonry compressive strength. Failure theories for masonry under

compression make the assumption that the bond between brick and mortar remains intact at the time of failure of the brick or mortar. The influence of bond strength on masonry compressive strength is not fully accounted for in these failure theories. In this investigation, the influence of bond strength on masonry compressive strength was examined through an experimental program using local bricks and mortars. Masonry prism compressive strength was determined when the brick-mortar bond strength is varied over a wide range without altering the strength and deformation characteristics of the brick and mortar. Brick-mortar bond strength was determined through flexure bond strength and shear bond strength tests. A relationship between the masonry prism compressive strength and bond strength was obtained. The results clearly indicate that an increase in bond strength, while keeping the mortar strength constant, leads to an increase in the compressive strength of masonry.

Venkatarama and Gupta (2006-a) investigated tensile bond strength of soil-cement block masonry couplets using cement-soil mortars. Soil-cement blocks and cement-soil mortars are used for the load bearing masonry, with the scantily explored area of tensile bond strength of soil-cement block masonry using cement-soil mortars. Influence of initial moisture content of the block and block characteristics (strength, cement content, and surface characteristics) as well as composition and workability of cement-soil mortar on direct tensile strength of masonry couplets was explored. Major findings of this study were: (1) initial moisture content of the block at the time of construction affects bond strength and use of partially saturated blocks is better than dry or fully saturated blocks; (2) as the cement content of the block increases, its strength increases, and surface pore size decreases leading to higher bond strength irrespective of the type of mortar; (3) cement-soil mortar gives 15.50% more bond strength when compared to cement mortar and cement-lime mortar; and (4) bond strength of cement-soil mortar decreases with increase in clay content of the mortar. The study clearly demonstrates the superiority of cement-soil mortar, over other conventional mortar such as cement mortar. The results can be conveniently used to select a proportion for cement-soil mortar for soil-cement block masonry structures.

Venkatarama and Gupta (2006-b) investigated the strength and elastic properties of stabilized mud block masonry using cement-soil mortars. Stabilized mud blocks (SMBs) are manufactured by compacting a wetted mixture of soil, sand, and

stabilizer in a machine into a high-density block. Such blocks are used for the construction of load-bearing masonry. Cement soil mortar is commonly used for SMB masonry. The compressive strength, stress-strain relationships, and elastic properties of SMB masonry using three types of SMBs and cement-soil mortars were discussed. The influence of a cement-soil mortar's composition and strength on masonry characteristics was examined. The results of masonry using cement-soil mortars were compared with those using conventional mortars (cement mortar and cement-lime mortar). Some of the major findings are: (1) SMB masonry strength is sensitive to block strength and increases with increase in block strength; (2) the strength of SMB masonry using cement-soil mortars is more sensitive to the cement content of the mortar than to the clay fraction of the mortar mix; (3) the masonry modulus increases as the block strength increases; and (4) SMB masonry with cement-soil mortars shows higher modulus than the masonry using cement mortar and cement-lime mortar.

Referencing Yi et al, (2006-a), evaluated the nonlinear response of lateral load on a two-story unreinforced masonry building by testing a full-scale building in a quasistatic fashion to investigate the nonlinear properties of existing URM structures and to assess the efficiency of several common retrofit techniques. The main experimental findings are associated with the nonlinear properties of the original URM structure. The test structure exhibited large initial stiffness and its damage was characterized by large, discrete cracks that developed in masonry walls. Significant global behaviour such as global rocking of an entire wall, and local responses such as rocking and sliding of each individual pier, were observed in the masonry walls with different configurations. In addition, formation of flanges in perpendicular walls and overturning moments had significant effects on the behaviour of the test structure. A comparison between the experimental observations and the predictions of finite element analysis using FEMA 356 provisions shows that major improvements are needed for this latter methodology.

Referencing Yi et al, (2006-b) developed an analyses method of a two-story unreinforced masonry building. A variety of elastic and inelastic analytical approaches were used to investigate the response of a full-scale unreinforced masonry (URM) structure tested in the laboratory. Elastic analyses, employing a

three-dimensional finite element model, revealed little coupling between parallel walls, and pointed to the appropriateness of two-dimensional analytical tools for further simulation of the test structure. The nonlinear analytical methods employed included, in order of increasing complexity, a rigid body analysis, a two-dimensional nonlinear pushover analysis, and a three-dimensional nonlinear finite element analysis. All methods considered important structural characteristics such as failure modes of perforated walls, flange effects, and global overturning moment effect.

Venkatarama et al (2007) evaluated the bond strength and characteristics of soil-cement block masonry, used for the load bearing masonry of two story buildings. The outcomes from this research were the methods of improving the shear-bond strength of soil-cement block masonry, without altering the mortar characteristics, and the influence of shear-bond strength on masonry compressive strength. Altering the texture of bed faces, size and area of the block, and certain surface coatings were attempted to enhance the shear-bond strength. The results indicate that: (1) rough textured bed face of the blocks yields higher shear-bond strength than the plain surface; (2) use of fresh cement-slurry coating on the bed faces improves the shear-bond strength considerably; (3) no significant changes are noticed in the compressive strength and stress-strain characteristics of soil-cement block masonry due to changes in shear-bond strength; and (4) masonry has a higher straining capacity than that of the block and the mortar.

### 2.5.3 Research Done at QUT

The research project presented in this thesis will draw information and guidance from the research carried out at the Physical Infrastructures Centre - Queensland University of Technology (PIC-QUT) in the area of lateral load response of masonry structures by Thambiratnam (1993) and his researchers. This work is reviewed in the following section.

#### **2.5.3.1 Masonry Research by Zhuge (1993 - 1998)**

Zhugue et al. from 1993 to 1998 carried out research on the behaviour of unreinforced masonry walls under in-plane cyclic loading at PIC-QUT. Their research had two distinct phases: the first was an experimental study, (Zhuge and

Thambiratnam, 1993, 1994, 1995a) and the second was an analytical investigation, (Zhuge and Thambiratnam, 1995b, 1996, 1997, 1998).

The results of this research indicate that masonry walls have a substantial deformation capacity after cracking. It was shown that nonlinear behaviour of brick masonry is caused by two major effects: progressive local failure by cracking of the mortar and its non-linear deformation characteristic caused by the combination of uniaxial or biaxial stresses. Based on these results, there is a recommendation to develop further research work to validate the proposed model, especially for non-linear time history analysis and for studying collapse mechanisms, (Zhuge,1995)

The material model of in-plane behaviour of brick masonry under lateral loads has been very limited. One-phase linear homogeneous material model is still commonly used for analysing masonry as it is easy to use and saves computing time. However, it is difficult to simulate the influence of mortar joints acting as a plane of weakness.

To investigate the cyclic behaviour of masonry, the two-dimensional finite element model was adopted. Since the influence of mortar joints acting as a plane of weakness is not fully considered in the models, the authors were unable to predict shear sliding type of failure, which was controlled by mortar joints.

During these investigations, twelve unreinforced brick masonry walls were tested under in-plane cyclic loads. It was found that unreinforced walls had long life after cracking, when a suitable vertical compressive load was applied. The vertical compressive stress had also played an important role in determining the failure pattern of URM. The cracks closed when the load was reversed and the walls regained their lateral load carrying capacity. The effect of vertical loads, which had been disregarded by most design codes, was very significant for both cracking and ultimate strength of URM walls. However, the failure pattern of the wall could only be determined by the local strength of the mortar, when the same vertical compressive load was applied to the walls. Three different failure patterns were observed in the experiments, named as: shear sliding, rocking and diagonal shear. The walls that exhibited a flexural behaviour and failed by rocking were more ductile than those that failed by shear and had higher ultimate load capacity.

A simple procedure for modelling and analysing brick masonry, especially unreinforced masonry subjected to dynamic or seismic loading was also developed. The general research outcomes stated that URM walls could have considerable energy absorption capacity, when used in a building system, where they are subjected to moderate vertical stress. The wall geometry in terms of the aspect ratio L/H effected significantly both the load capacity and the failure pattern for the wall. Both, the cracking and the ultimate strength increased with increase of the aspect ratio up to L/H=2.0.

The vertical compressive stress in a wall plays an important role in determining the ultimate strength, failure pattern and post-failure behaviour of the wall under both static and dynamic loads. The cracking strength increased with the vertical compressive stress. However, when the vertical compressive stress was high, the ultimate strength decreased and the wall fails in a brittle manner.

The conclusions of these studies are in relation to the cracking and ultimate loads, lateral force versus displacement, maximum displacement versus time and failure patterns. It was found that the tensile strength has a significant influence on the cracking and the ultimate load capacity of URM walls only when the vertical compressive load is relatively low. This influence becomes insignificant when the vertical compressive stress is high. The compressive strength of URM does not have significant effect on the load capacity of URM walls, but it does have an effect on the failure patterns of the wall.

#### **2.5.3.2 Giles and Basoenondo (2000)**

A set of laboratory experimental work has been done at QUT by Giles (2000) and Basoenondo et al (2001) to evaluate the response of wall panels to lateral loading. The size of each panel was approximately 1175 mm x 916 mm (9 courses high, 5 bricks in length). A total of 12 walls were built and tested under varying vertical pre-compression and under either monotonic or cyclic in-plane loading. Several walls also had bedding reinforcement on the third, sixth and ninth courses. According to the Standard Australian and New Zealand AS/NZS 4456, material properties of the wall specimens were obtained as given in the Table 2.2.



*Table 2.1 Brick Property in Australia (Brisbane)*

Brick Unit Properties	
Length	229 mm
Width	110 mm
Height	76 mm
Tensile strength	1.67 N/mm <sup>2</sup>
Compressive strength	20 MPa
Dry density	1413 kg/m <sup>3</sup>
Initial rate of absorption	0.957 kg/m <sup>2</sup> /min
Mortar 28 day strength	4.12 MPa
Masonry Properties	
Pier compression test	11.76 MPa
Pier flexural test	1.447 MPa

The result of this research project indicated that diagonal shear cracking was the predominant failure mode of the masonry walls subjected to lateral in-plane loading. The vertical pre-compression had an effect on the strength of the masonry walls when subjected to lateral in-plane loading. Bedding reinforcement system had no significant influence on the strength of the wall under lateral in-plane loading. Cyclic testing caused a reduction in strength and ductility. Further research was needed, including finite element modelling and analysis to obtain conclusive results, which will be applicable only to masonry structures made from local Brisbane bricks.

## 2.6 Code provisions for masonry wall structures in resisting lateral loads

### 2.6.1 Australian Standard

Masonry is designed according to limit states principles. The designer must anticipate all the likely conditions to which the structure will be subjected during its lifetime and design it to ensure satisfactory performance under those conditions. Australian Standard 3700 - 2001 Sections 7.5 and 7.6 provide the guidelines to design for shear under lateral loads on unreinforced masonry walls. Where a wall does not have lateral support on its vertical edges, the wall will span purely

vertically. The strength of cross-section in vertical bending is determined by assuming that the stress-strain relationship is linear until failure, and that the cross-section remains un-cracked until the extreme fibre tension stress equals the ultimate tensile stress capacity of the bed joint.

According to AS 3700 - 2001, design for resistance to sliding and shear failure is carried out using the separate code rules for shear capacity under wind and earthquake loading. The possibility of local failures at the heel and toe should be checked using the tensile and compressive strengths of the masonry and considering the combined effects of bending in the member, caused by the shear force and compression caused by the vertical load.

Adequate shear strength on vertical planes is ensured by the overall code requirements for bonding and tying. The capacity of shear connector across mortar joints within a masonry member and to other masonry members must be checked. Design for shear under earthquake loading is carried out in accordance with AS 3700.

The design shear force is defined as

$$V_d \leq V_0 + V_{1e}$$

where,

$V_0 = \phi f'_{ms} A_{dw}$  represents the shear bond strength,

$V_{1e} = 0.9k_v f_{de} A_{dw}$  represents the shear friction strength,

$f_{de}$  = design compressive stress on the bed joint under gravity load,

$\phi$  = Capacity reduction factor (0.6 for shear in un-reinforced masonry),

$f'_{ms}$  = Characteristic shear strength of the masonry,

$A_{dw}$  = Bedded area,

$k_v$  = Shear factor (0.3 for bed joints in clay masonry).

## 2.6.2 American Standard

Based on Building Code Requirement for Masonry Structures (ACI 530-92/ASCE 5-92/TMS 402-92), Specifications for Masonry Structures (ACI 530.1-92/ASCE 6-

92/TMS 602-92) and Masonry Designer Guide part 8.4.3.9, the shear design of walls depends upon the magnitude of axial load in the wall. If the axial load is sufficient to overcome the flexural tension resulting from lateral loads, the section may be designed as un-reinforced. Shear reinforcement is only required if shear stress  $f_v$  exceed allowable shear strength  $F_v$ . If  $f_v > F_v$  the wall must be increased in size. The shear stress  $f_v$  is evaluated by the formula stated in Masonry Designer Guide part 8.4.3.9.1 and 8.4.3.9.2. for shear wall without and with net flexural tension.

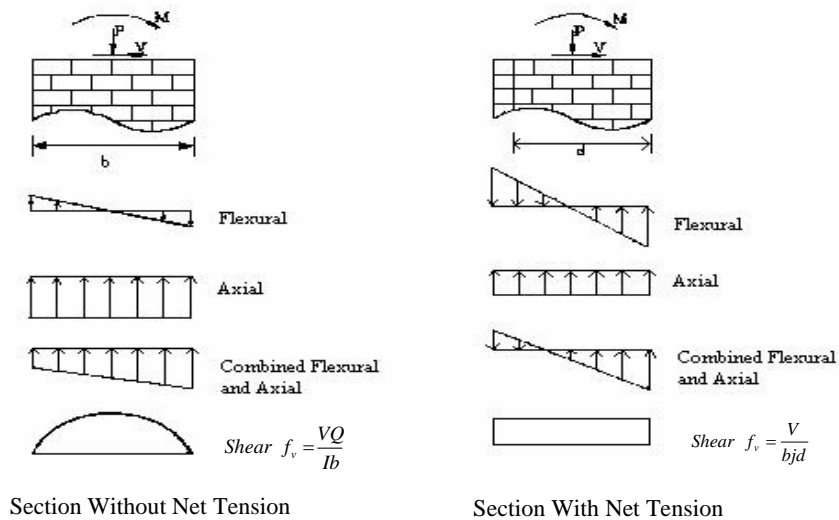


*Figure 2.30 Masonry wall section without tension and with tension*

For shear walls without net flexural tension, if the stress  $M/S$  is less than  $P/A_n$ , then the axial compression exceeds the flexural tension. The actual stress  $f_v$  and allowable shear stress  $F_v$  (psi) are calculated from least value of:

- a)  $1.5\sqrt{f'_m}$  ,
- b) 120 psi ,
- c)  $\nu + 0.45 \frac{N_v}{A_n}$  ,
- d) 15 psi other than running bond with open end units grouted solid,

and

$$f_v = \frac{VQ}{Ib} ,$$

where

V = design shear force, lb ,

Q = first moment about the neutral axis of a section of that portion of cross section lying between the plane under consideration and extreme fibre, in<sup>3</sup> ,

I = moment of inertia of masonry, in<sup>4</sup> ,

B = width of section, in,

f<sub>m</sub> = masonry compressive strength, psi,

N<sub>v</sub> = force acting normal to shear surface, lb,

A<sub>n</sub> = cross-sectional area of masonry, in<sup>2</sup>.

For shear walls with net flexural tension; if M/S exceeds P/A<sub>n</sub> then the wall has net flexural tension. The actual and allowable shear stress should follow these formulations.

$$f_v = \frac{V}{bjd}$$

If  $\frac{M}{Vd} < 1$  , then

$$F_v = \frac{1}{3} \left[ 4 - \left( \frac{M}{Vd} \right) \right] \sqrt{f'_m} ,$$

and

$$F_v \leq 80 - 45 \left( \frac{M}{Vd} \right) \text{ psi} .$$

If  $\frac{M}{Vd} \geq 1$  , then

$$F_v = \sqrt{f'_m} ,$$

and

$$F_v \leq 35 \text{ psi} ,$$

where

M = maximum moment occurring simultaneously with design shear force V at the section under consideration, lb-in,

d = distance from extreme compression fibre to centroid of tension reinforcement,

j = ratio of distance between centroid of flexural compressive forces and centroid of tensile forces to depth d.

If  $f_v$  less than or equal to  $F_v$ , the section is satisfactory. If  $f_v$  exceeds  $F_v$  therefore shear reinforcement is required.  $F_v$  is calculated from:

If  $\frac{M}{Vd} < 1$ ,

$$F_v = \frac{1}{2} \left[ 4 - \left( \frac{M}{Vd} \right) \right] \sqrt{f'_m},$$

and

$$F_v \leq 120 - 45 \left( \frac{M}{Vd} \right) \text{ psi},$$

If  $\frac{M}{Vd} \geq 1$ ,

$$F_v = 1.5 \sqrt{f'_m},$$

and

$$F_v \leq 75 \text{ psi}$$

If  $F_v$  still exceeds  $f_v$ , the wall must be increased in size.

### 2.6.3 British Standard

According to British Standard Code of Practice use of masonry BS5628, Part 2: The structural use of reinforced and prestressed masonry, provides guidelines to design reinforced masonry subjected to horizontal forces in the plane of the element. In walls subjected to in-plane horizontal forces and loaded to failure, cracks typically occur in diagonal shear failure and are caused by diagonal tension. It is usual to treat the design of walls on the basis of the average stress over the plan area. If total

horizontal design force is  $V$ , the shear stress due to design loads is considered to be  $v$ , where:

$$v = \frac{V}{tL}$$

and

$t$  = the thickness,

$L$  = the length of wall.

The code states that adequate provision against the ultimate limit state being reached must be assumed if the average shear stress is less than design shear strength, i.e.:

$$v \leq \frac{f_v}{\gamma_{mv}}$$

and

$f_v$  = the characteristic racking shear strength taken from BS 5628 – 19.1.3.2, and it is equal to  $0.35 + g_B$  MPa, where  $g_B$  is the design vertical load per unit area of wall cross section due to vertical dead and imposed loads calculated from the appropriate loading condition. The shear factor for masonry is  $\gamma_{mv}$ , and the maximum value to be taken for  $f_v$  is 1.75 MPa.

According to the design method, a standard for general application of structural masonry was developed. Some of design procedures for masonry structures have been developed since 1970's. These procedures were concerning the local condition of masonry structures using high quality bricks. The general mechanical characteristics of clay bricks used for constructing masonry in many countries are listed in Table 2.2.

These design concepts developed by Sahlin (1971) and Hendry (1990, 1997), show that the factor of workmanship errors has a strong influence on the compressive strength of masonry, especially on low strength bricks and mortars. This factor was not considered in this research.

*Table 2.2 The characteristics of clay brick masonry*

Design developer:	Characteristics of clay bricks	
Sven Sahlin (1971)	Compressive strength Modulus of rupture Modulus of elasticity	28 – 70 MPa 2.5 – 15 MPa $300 f_b'$
Hendry A.W (1990)	Compressive strength Modulus of rupture Modulus of elasticity	42 – 60 MPa 3.36 – 6.30 MPa $700 f_b'$
Hendry A.W., Sinha B.P., Davies S.R. (1997)	Compressive strength Modulus of rupture Modulus of elasticity	60 - 80 MPa 4.60 – 7.20 MPa $700 f_b'$
Australian Standard AS3700-2001	Compressive strength Modulus of rupture Bond shear strength Modulus of elasticity: - short term loading - long term loading	30 MPa 0 0.15 – 0.35 MPa  $700 f_b'$ $450 f_b'$

#### 2.6.4 Indonesian Standard

According to Ditjen CIPTA KARYA (1993), the method and procedure of constructing masonry buildings are not clearly defined and need to be revised.

Some recommendations from guidelines are:

- unreinforced brick masonry structures are purposed for one story building,
- main structural wall is recommended to be constructed in double wall thickness,
- tie beam or ring balk should be placed over the wall opening such as window or door opening and is to be connected in a closed form as a ring confinement,
- in every corner of wall connection, practical column should be connected to wall structure using anchorage connection, and
- the composition of mortar mix for structural wall is 1 : 3 of cement : sand in weight proportion.

#### 2.6.5 Indonesian seismic zones

Based on SNI-1726-2002 and as shown in Figure 2.31, the map of seismic zones of Indonesia consists of 6 earthquake zones. To determine the base shear force caused

by the earthquake, it is necessary to determine the weight of houses or low-rise buildings. The magnitude of base shear force can therefore be determined by using the following formula:

$$V = \frac{C_i I W_t}{R},$$

where, V is base shear force acting on a house or low-rise building structure,  $C_i$  is coefficient of earthquake response based on the Indonesian Earthquake Response Spectrum, as tabulated in Table 5.6. Coefficient I is the building importance factor. For houses and low-rise buildings, the importance factor I is taken as 1.0.  $W_t$  is the total weight of building. For simple ordinary houses, total weight of structure is 100 kN and R is the coefficient of earthquake reduction factor taken as 1.6.

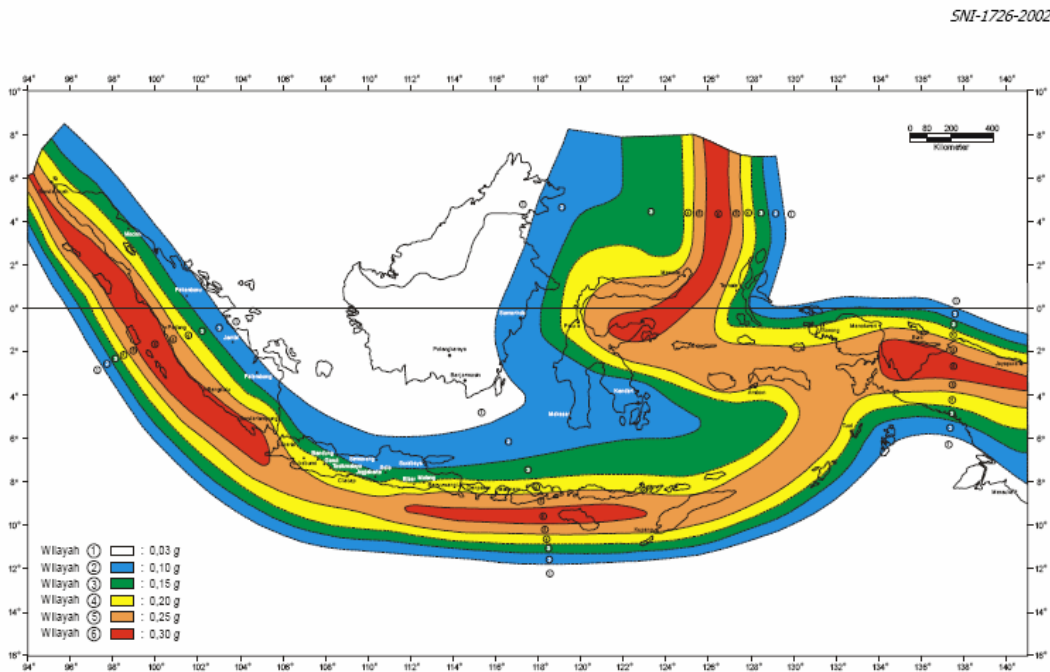


Figure 2.31 Seismic zone in Indonesia with bed stone acceleration within 500 years return period (SNI-1726-2002 Indonesian Seismic Design Code)

Table 2.3 Coefficient of earthquake response  $C_i$

Seismic Zone	Type of Soil		
	Soft	Moderate	Hard
1	0.20	0.13	0.10
2	0.50	0.38	0.30
3	0.75	0.55	0.45
4	0.85	0.70	0.60
5	0.90	0.80	0.70
6	0.95	0.90	0.83



## 2.7 Conclusion

Based on the literature review presented in this chapter, lot of research was conducted on the analytical purpose using either mathematical or numerical approach. However, the laboratory experimental investigation in low quality bricks was very limited. The qualities of bricks used in many countries were mostly in the range of high to very high quality, the masonry buildings were constructed based on their regional or national technical standard. The examples of using low quality bricks to build non engineered houses or low-rise buildings were very rare.

From the records of research carried out in Indonesia, it is evident that there has been very limited number of research work carried out with respect to masonry wall structures. This is especially true in relation to their lateral load response and the characteristic, and mechanical behaviour of specific local brick traditionally produced in rural area. The currently issued guidelines are neither clearly understandable, nor widely accepted in regional construction work.

According to review of existing literature on research carried out in many institutions in many different countries, it is evident that none of these research works investigated the structural behaviour of low quality clay brick masonry walls. Furthermore, they did not considered the effects of mortared surface confinement or mortar plastered confinement of wall and its surface on the structural response.

The findings of the research project presented in this thesis address such gap in knowledge and contribute towards determining the enhanced performance of masonry brick wall structures, built from Cikarang Clay Bricks found in Jakarta – Indonesia. Consequently, the comparative responses of un-reinforced masonry brick walls with and without mortared surface confinement, were extensively investigated.



## Chapter 3. Experimental Investigation on Physical Characteristics of Brick Assemblages

---

### 3.1 Introduction

This chapter presents the experimental works on testing of brick assemblages carried out at the Material Laboratory, Civil Engineering Department, FTUI - Depok, and at the Structural Laboratory, The Ministry of Public Work Research Center, PUSKIM – Bandung.

In this research, some preliminary investigations were carried out for evaluating physical and mechanical characteristics of Cikarang bricks. The parameters were:

- size, unit weight and water absorption,
- mortar compressive strength,
- brick compressive strength, and
- bond shear strength between brick surface and mortar.

The physical characteristics of these bricks are very important and need to be evaluated. Size, unit weight and water absorption will affect the structural size, weight and water cement ratio for mortar mixing. The compressive strength of mortar and brick will affect the capacity of masonry columns and wall in retaining applied loads.

To determine the stress-strain response of masonry assemblage, tests were also done on masonry columns and wall specimens. Four different types of columns and five different types of wall specimens were tested under increasing axial compressive loads until failure. The experiments were classified into two groups:

- masonry columns under compression load, and
- masonry walls under compression load.

Both tests on masonry columns and walls provided curve models presenting general material behaviour in response to the increasing applied compressive loads. Details of the specimens tested can be seen in Table 3.1

*Table 3.1 Number and types of specimens*

Test	Type	Number of specimens
Brick size, unit weight, water absorption	Random bricks	180
Mortar	Type A, B, C, D, E, F	120
Brick	Using Mortar Type A, B, C, D, E, F	180
Triplet Brick	Using Mortar Type A, B, C	144
Short Brick Column	3 layer bricks	20
Brick Column	5 layer bricks	10
Mortared Column	5 layer bricks	10
Comforted Column	5 layer bricks	10
Wall panel under compression load	Brick Wall, Mortared Wall, Comforted Wall	25

*Table 3.2 Research limitation*

Brick type / resource	: Solid clay bricks Cikarang – Jakarta – INDONESIA
Mortar composition	: 1 cement : 4 sand (bonding mortar and surface mortar Type B) : 1 cement : 3 sand (surface mortar type A)
Water/cement ratio	: 0.9 – 1.0 in weight scale of cement
Mortar bonding thickness	: 10 mm
Surface mortar thickness	: 10 mm
Loading type	: Static-monotonic, repeated, semi cyclic
Loading direction	: In-plane
Specimen type	: Brick assemblages, Columns, Wall panels
Surface mortar strength variation	: Type B, 1 cement : 4 sand Type A, 1 cement : 3 sand (in comparison for surface mortar only)
Workmanship error	: not considered
Change of ambient temperature	: not considered
Loading rate	: not considered
Creep and shrinkage of mortar	: not considered
Initial defects of bricks	: not considered
Brick size variation	: not considered

### 3.2 Research scope and limitations

The scopes considered in this experimental work are type of bricks, mortar, type of specimens and loadings. All the aspects treated in this research project together with the limitations in the investigation are as stated in Table 3.2.

### 3.3 Physical characteristic of bricks based on Indonesian National Standard, SNI 15. 1328 – 1989

To observe general physical characteristics of Cikarang bricks, sets of laboratory experimental works were done on brick specimens randomly taken from the factory, to evaluate brick size, unit weight, and water absorption across brick surface.

To evaluate the size of individual bricks, 180 bricks were considered as a group of brick samples. Refer to SNI 15. 1328 – 1989, brick physical data were collected by measuring all samples, as shown in Figure 3.1 such as individual brick's length, width, thickness using Vernier Caliper instruments, as shown in Figure 3.2 and measuring unit weight, using weighing balance instrument, as shown in Figure 3.3.

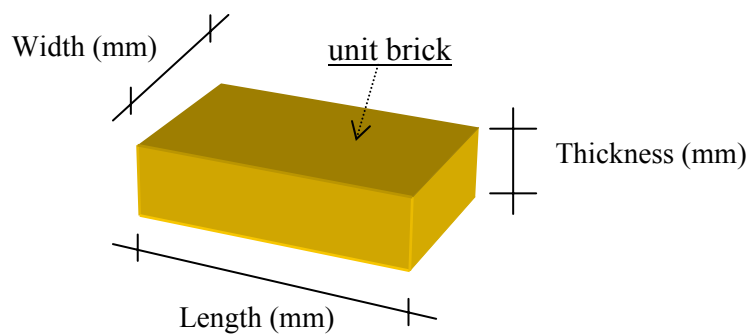


*Figure 3.1 Size measurement in mm*



*Figure 3.2 Vernier Caliper*



*Figure 3.3 Weighing balance instruments*

To prepare a proper mortar mix, water absorption is very important to be considered in the calculation of water cement ratio. To evaluate water absorption characteristics; firstly, the weight of each single brick is measured as  $W_1$ . Then the brick is placed into 1 cm depth of water for 60 seconds, as shown in Figure 3.4. Finally, the brick is removed from water and its weight is measured as  $W_2$ .

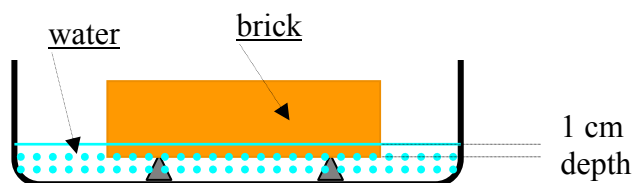


*Figure 3.4 Test scheme for water absorption*

Collecting the data of  $W_1$  and  $W_2$ , therefore, the water absorption can be determined as Initial Rate of Absorption (IRA) =  $(W_2 - W_1)/\text{Contact Area}$  measured in  $(\text{gram}/\text{mm}^2)/\text{minute}$ , and the unit weight or mass density =  $W_1/\text{volume}$  of single brick in  $\text{gram}/\text{mm}^3$ .

All site collected data were statistically evaluated based on normal distribution and the results are tabulated in Table 3.3. In this table, the bias of water absorption is widely scattered in a range of 33%. This was caused by surface porosity condition of each single brick.

*Table 3.3 Physical characteristic of Cikarang bricks*

Number of sample = 180 bricks						
	Thickness (mm)	Width (mm)	Length (mm)	Density ( $\text{gram}/\text{cm}^3$ )	IRA ( $\text{gram}/\text{mm}^2/\text{minute}$ )	Water Penetration
Average	46.11	90.43	189.68	1.690	0.00214	0.036 (mm/sec) or 2.14 (mm/minute)
S-Dev	1.230	1.320	2.350	0.043	0.0007	
COV	0.0267	0.0146	0.0124	0.0255	0.3277	
Bias Index	2.67 %	1.46 %	1.24 %	2.55 %	32.77 %	

In general and as determined by evaluation in this thesis, the physical characteristic of Cikarang bricks are:

- Length =  $190 \pm 2.5$  mm,
- Width =  $90 \pm 1.5$  mm,
- Thickness =  $46 \pm 1.5$  mm,
- Density =  $1.69 \pm 0.04$   $\text{gram}/\text{mm}^3$ ,
- Water Absorption =  $0.00214 \pm 0.0007$   $(\text{gram}/\text{mm}^2)/\text{minute}$ .

### 3.3.1 Mortar compressive strength

Six different types of mortar were tested to evaluate their compressive strength at 28 days of mortar age. Mortar type A, B, C, D, E, F, using cement : sand composition of 1:3, 1:4, 1:5, 1:6, 1:7, 1:8 respectively, as described in Table 3.4, were tested based on Indonesian National Standard, SNI 03-6825-2002.

20 specimens of each type of mortar were tested under monotonic compression loads, using a compressive crushing machine of 150 kN capacity, as shown in Figure 3.5, until failure. Then the loads were recorded at the maximum values, assumed to be uniformly distributed. Mortar compressive strength was obtained by dividing these maximum compression loads by contact area of cube specimens measured in N/mm<sup>2</sup> or MPa. The compressive strengths of each type of mortar are given in Table 3.4.



*Figure 3.5 Compressive crushing machine*

*Table 3.4 Types and categories of mortars*

Mortar Type	Composition of Cement : Sand	Water/Cement Ratio	Category
A	1 : 3	0.67	Structural
B	1 : 4	0.85	Structural
C	1 : 5	1.05	Non Structural
D	1 : 6	1.24	Non Structural
E	1 : 7	1.43	Non Structural
F	1 : 8	1.62	Non Structural

The size of mortar specimens shown in Figure 3.6 were 50 mm × 50 mm × 50 mm. The specimens were prepared by using casting or moulding apparatus, as shown in Figure 3.7. After 24 hours of mortar casting, cube specimens were taken from moulding apparatus and were placed in a watered curing basin for 26 days. They were tested at 28 days of mortar's age.





*Figure 3.6 50mm × 50mm × 50 mm mortar specimens*



*Figure 3.7 Moulding apparatus for 50 mm × 50 mm × 50 mm mortar cubes*

*Table 3.5 Mortar compressive strength*

Compressive strength						
Mortar Type	A	B	C	D	E	F
Compressive Strength (MPa)	28.87	17.64	11.88	10.54	5.71	4.85
S-Dev	5.12	3.80	3.62	3.06	1.54	0.86
COV	0.177	0.215	0.304	0.290	0.270	0.166
Number of specimens of each type of mortar = 20 cubes						

According to test results and as anticipated, higher portion of cement : sand ratio produces higher mortar compressive strengths than using low cement : sand ratio, as seen in Figure 3.8. Taking the trend-lines as shown in Figure 3.9, the variation of mortar compressive strength according to 6 different mortar types is to be expressed as logarithmic curves.

As observed in recent civil engineering construction sites, mortar type A is never used due to cost reasons. Therefore, mortar type B was chosen and used to construct

all specimens of brick columns and masonry wall panels in this experimental work. It is also stated by SNI 15-3758-1995, that mortar type B is to be used for constructing structural masonry. In this experimental investigation, mortar type A is also used for surface mortar plaster for mortared wall and comformed wall type A.

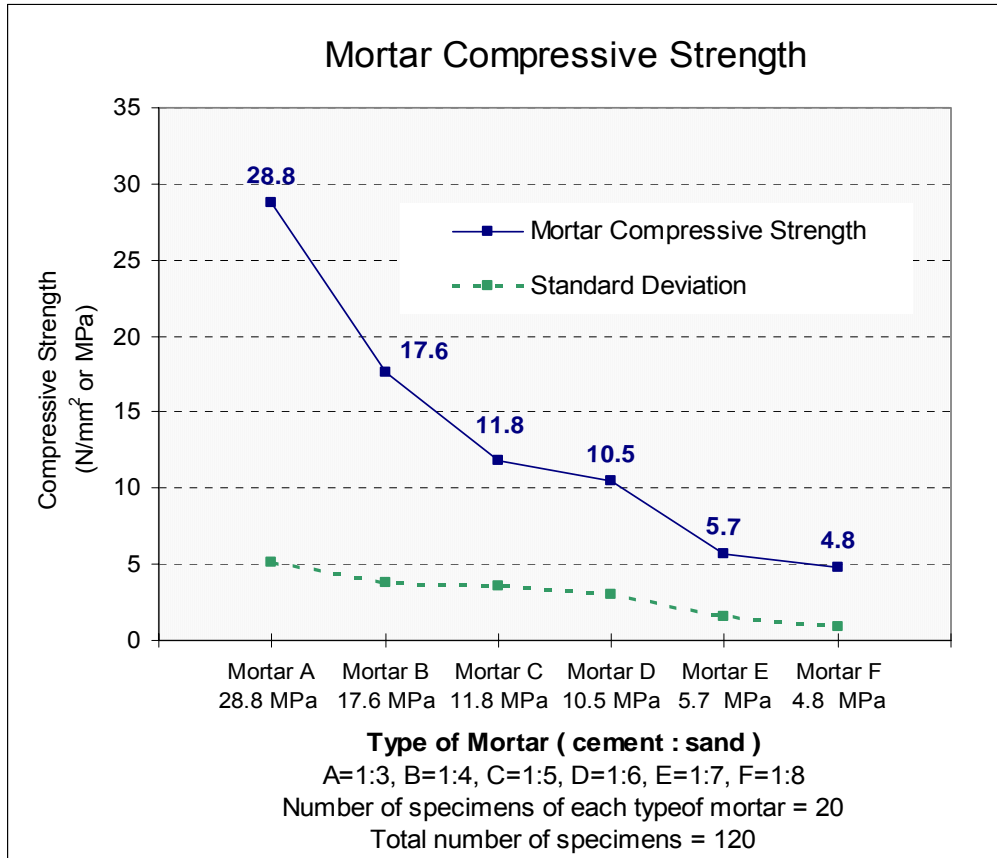


Figure 3.8 Mortar compressive strength

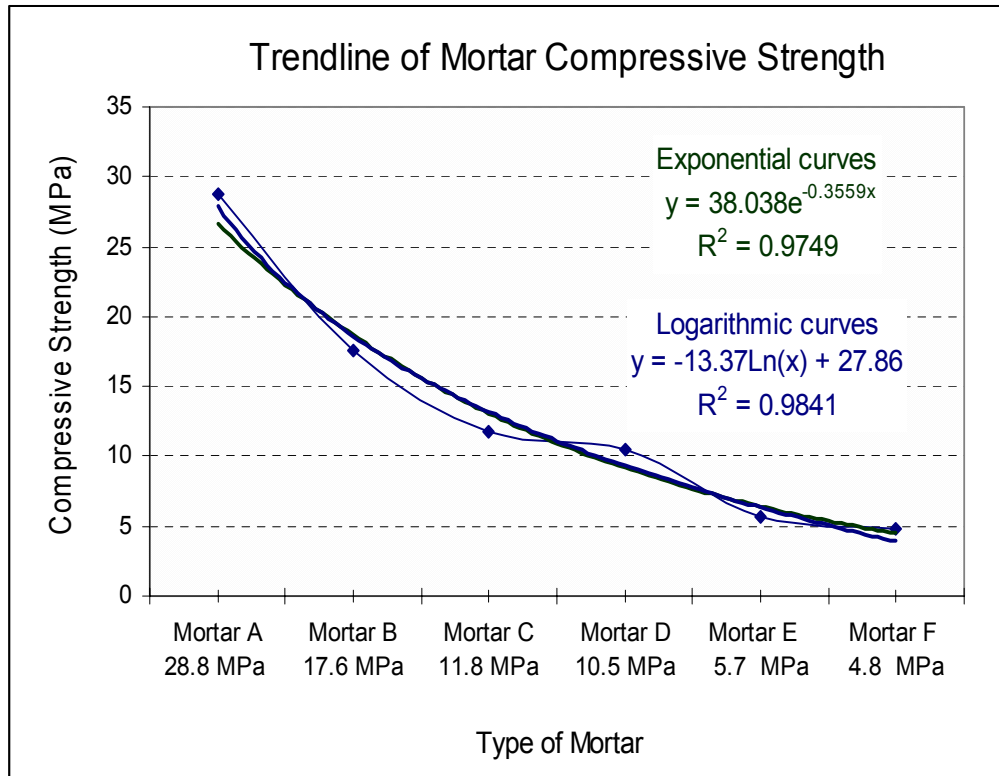


Figure 3.9 Exponential and logarithmic model of mortar compressive strength

### 3.3.2 Brick compressive strength

Indonesian National Standard SNI 15-2094-2000 states that testing brick compressive strength should be done on two pieces of half portion of brick specimens, which are connected together using mortar bonding.

To construct a compressive brick specimen, one unit brick is cut into two equal sized pieces and bonded together with 10 mm mortar, as shown in Figure 3.10. To enable the applied axial compressive load to be uniformly distributed, the specimens are also covered over the top and bottom surface with thin layer of sulphur capping.

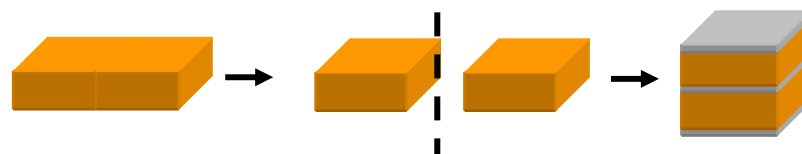


Figure 3.10 One unit brick cut into two pieces and connected together with mortar

Figure 3.11 shows the cutting machine instrument and a half portion of brick including the cross section area of individual brick. From Figure 3.11 b, c and d it is

seen that cross section area of each brick is different in colour and shape. This variance is caused by inside kiln temperature during burning process. Brick with red colour is traditionally considered to be a normal brick and the brick with black colour is to be an over burnt brick. Some of compressive brick specimens before and after capping are shown in Figures 3.12 and 3.13. The average size of these specimens is  $90 \times 90 \times 100 \text{ mm}^3$  and the numbers of brick specimens to be tested in this experimental work are given in Table 3.6.

*Table 3.6 Number of compressive brick specimens*

Type of Brick Specimens	Number of Specimens
Brick with mortar type A	30
Brick with mortar type B	30
Brick with mortar type C	30
Brick with mortar type D	30
Brick with mortar type E	30
Brick with mortar type F	30



*Figure 3.11 (a) Cutting Machine, (b) Half part of unit brick, (c) Cross section area of brick, (d) Cross section area of over burnt brick*



*Figure 3.12 Compressive brick specimens before capping*



*Figure 3.13 Compressive brick specimens after capping*



*Figure 3.14 Compression test on brick specimen without and with LVDT configuration*

As it is seen in Figure 3.14, each specimen was then axially compressed using vertical hydraulic jack of 60 ton-f capacity until failure. The load at failure is

recorded as the maximum compressive load and divided by the surface area of brick to obtain the maximum compressive brick strength in  $\text{N/mm}^2$  or MPa.

To measure vertical and horizontal displacements, 4 vertical LVDTs were located at each corner at the top of specimens and 4 horizontal LVDTs were located at each side of specimens. The axial and lateral strains therefore can be analysed based on the ratio of vertical or horizontal displacement to the original length of specimens. The effect of capping layers is neglected as the thickness is 3 mm and the compressive strength of capping material is 20 MPa. The compression load was applied monotonically at a rate of 2 kN/sec (or  $0.05 \text{ N/mm}^2/\text{sec}$ ), which it is about 1/3 scale of ASTM C-39-96.

Observing the failure mechanism during the tests, most specimens collapsed in brittle failure mechanism, without appearance of ductility. As a result, these Cikarang clay bricks are considered to be a brittle material.

The results from this investigation show that the pattern of brick compressive strength is not similar to the pattern of mortar compressive strength. This pattern is different to that reported by McNary and Abrams (1985) and is due to the fissure closing of the low compressive strength Cikarang bricks treated in this thesis. This feature was also observed in the testing of brick columns and walls. In the present investigation, higher mortar compressive strength does not significantly affect brick compressive strength, as shown in Figure 3.15. The ratio of brick compressive strength to mortar compressive strength is given in Table 3.7.

*Table 3.7 Ratios of brick to mortar strength*

	Mortar Type					
	A	B	C	D	E	F
Mortar compressive strength (MPa)	28.87	17.64	11.88	10.54	5.71	4.85
Brick compressive strength (MPa)	15.22	13.45	11.78	11.51	10.49	10.28
Ratio of brick to mortar strength	0.53	0.76	0.99	1.09	1.83	2.12



During the test, vertical and horizontal displacements of specimens caused by increasing compressive load were also recorded, using Linear Variable Displacement Transducer (LVDT). Dividing the vertical and horizontal displacements by the corresponding original length, the axial and lateral strains were determined. The ratio between lateral and axial strain was determined as brick Poisson's ratio  $\nu$  and the stress-strain response of each type of brick is presented in sub section 3.3.3.

Ignoring the influence of mortar compressive strength, the average compressive strength of brick is 12.12 MPa, standard deviation is 1.89 MPa, and coefficient of variance is 15.6 %. In Figure 3.15, the compressive strength of brick and mortar type C coincide.

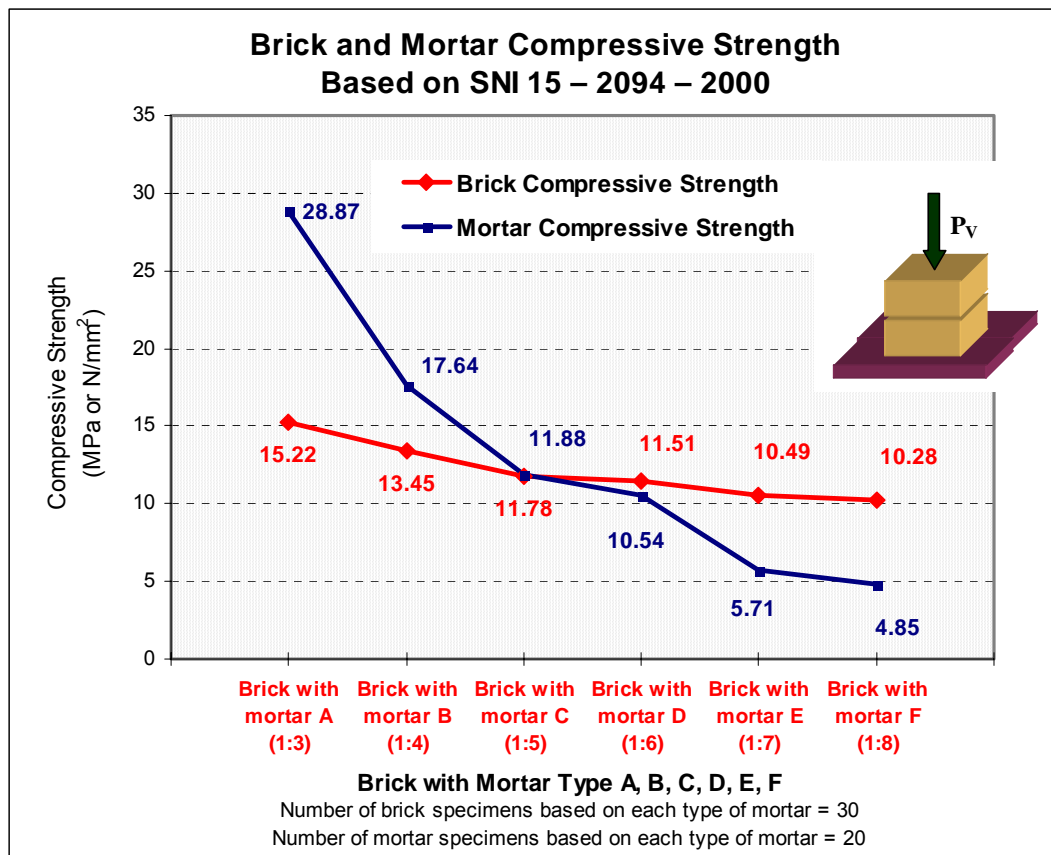


*Figure 3.15 Brick and mortar compressive strength*

### 3.3.3 Modulus of elasticity and Poisson's ratio of bricks

Material characteristics of bricks are represented by their modulus of elasticity and Poisson's ratio, which are measured from the tests. Stress-strain curve of each type of

brick, using six different types of mortar are graphically shown in Figure 3.16 and briefly tabulated in Table 3.8

*Table 3.8 Modulus of elasticity of bricks at each range of compressive stress*

Modulus of elasticity of brick with 6 types of mortar (MPa)							
Compressive stress (MPa)	Mortar type						Average
	A	B	C	D	E	F	
0 – 2	245.04	186.17	199.72	219.49	244.30	245.39	223.35
2 – 6	786.48	476.44	579.68	602.58	506.94	527.47	579.93
6 – 10	936.02	594.24	633.27	666.03	430.40	351.93	601.98
10 – 12	733.07	637.69	527.42	490.15	471.78	354.25	535.73
Max. compressive strength	15.22	13.45	11.78	11.51	10.49	10.28	12.12

From the information recorded in Table 3.8, it can be seen that the brick using mortar type A is stronger than others. The stress-strain curves presented similar trends in their shapes and generally, they can be expressed as bilinear inelastic models. The stress-strain response is generally weak at the beginning at stress less than 2 MPa, and then becomes stronger as stress increases above 2 MPa, until the specimens reach the stage of sudden brittle collapse. The stress-strain curve for the average response nearly coincides with stress-strain response of brick using mortar type C, and it confirms the statement made in the previous section with reference to Figure 3.16.

In general, stress-strain behaviour of brick is expressed by bilinear inelastic model as shown in Figure 3.17. The value of modulus of elasticity  $E_{br \leq 2} = 220$  MPa for compressive stress  $p_v \leq 2$  MPa, and  $E_{br > 2} = 546$  MPa for compressive pressure  $p_v > 2$  MPa. The maximum compressive strength of bricks in this experimental work was determined as nearly equal to 12.12 MPa. It is also recorded in Table 3.9. This phenomenon is also found in the behaviour of soft rock or very hard clay under volumetric compression, known as fissure closing (Goodman, 1989)



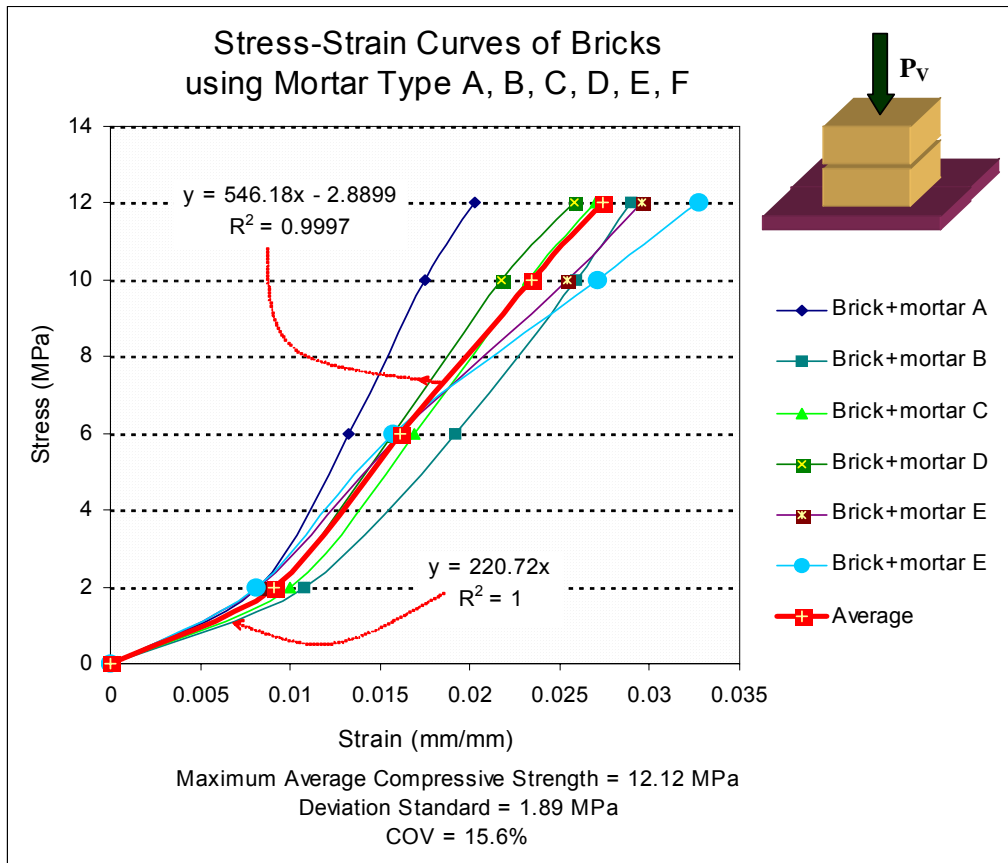


Figure 3.16 Stress-strain curves of bricks using different type of mortars

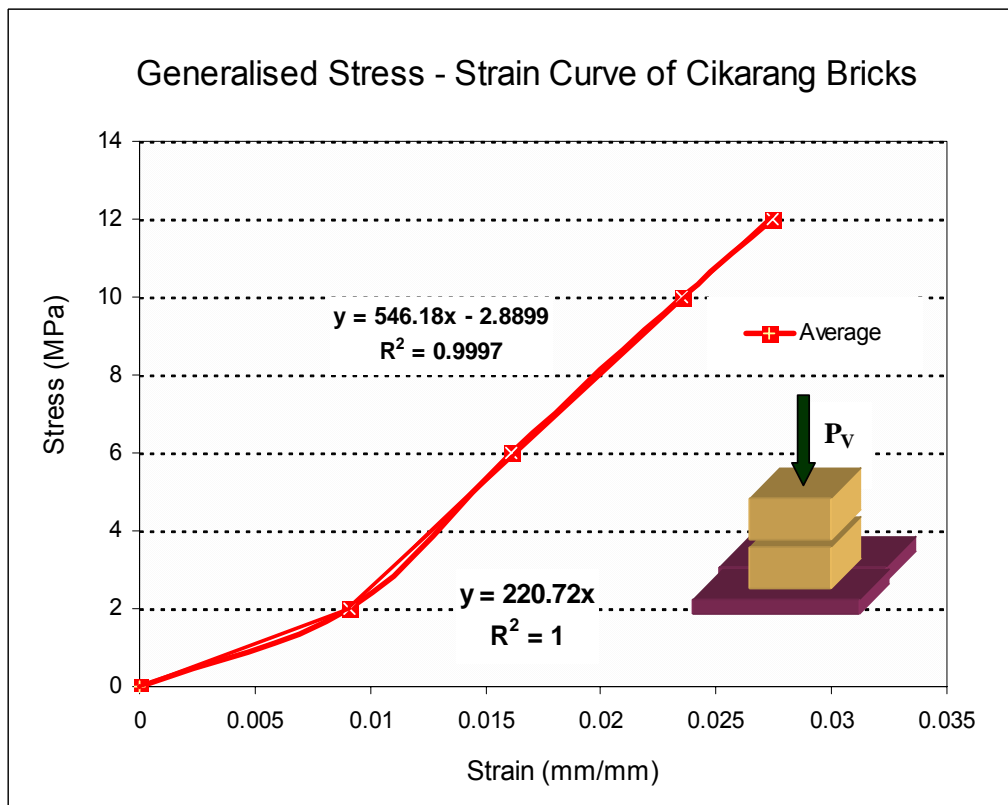


Figure 3.17 General stress-strain curve for bricks

Table 3.9 Modulus of elasticity of brick

Compressive pressure	Modulus of elasticity
$p_v \leq 2$ MPa	220 MPa
$p_v > 2$ MPa	546 MPa
Brick compressive strength = 12.12 MPa	

Evaluating the ratio of lateral strain to the axial strain as shown in Figure 3.18, the average value of Poisson’s ratio  $\nu$  can be determined as 0.254, which is rounded to be equal to 0.25 (Hendry, 1990).

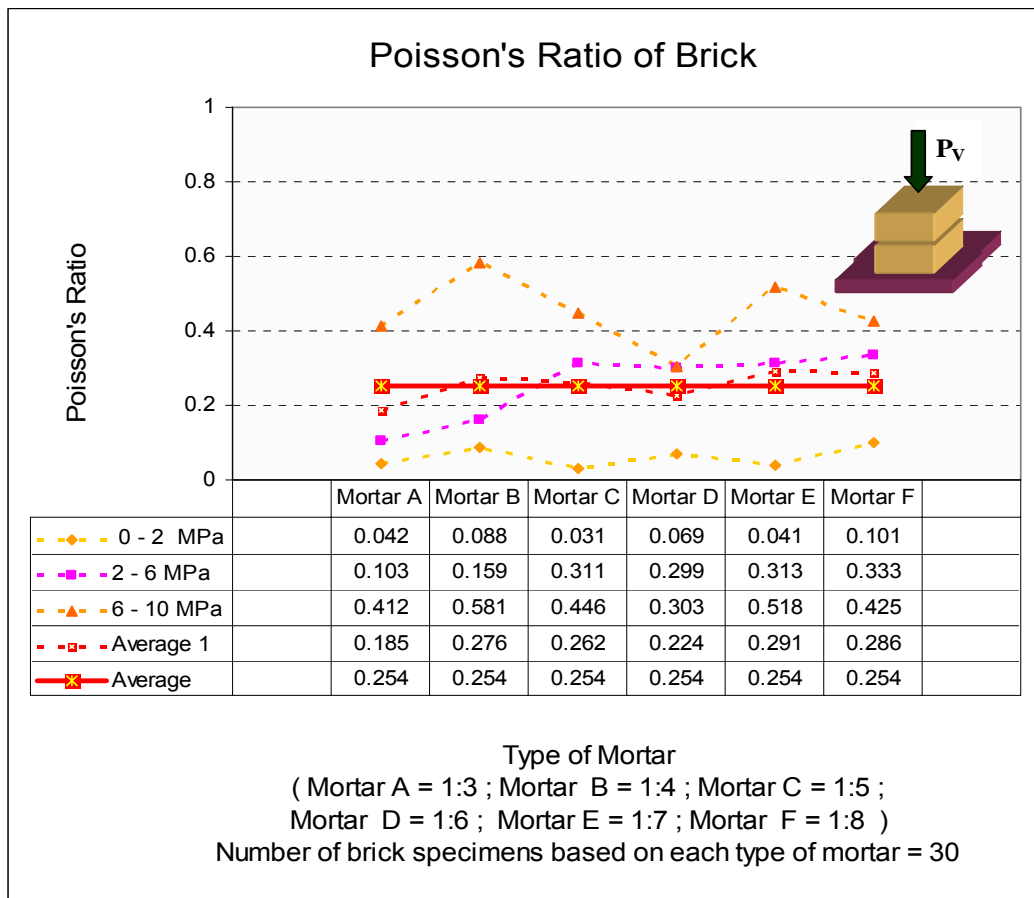
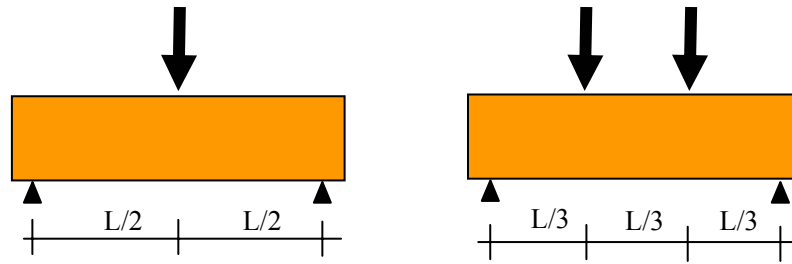


Figure 3.18 Poisson’s ratio of brick

### 3.3.4 Modulus of rupture

To evaluate the bending tensile capacity of these clay bricks, one point and two point bending tests were performed using of 20 bricks in each test type. The bending test configuration and the photographs from the test activity are shown in Figures 3.19 and 3.20 respectively.



*Figure 3.19 The scheme of one point and two point load test for bending*



*Figure 3.20 Tests set up for determining the modulus of rupture*

From these tests it was determined that the average modulus of rupture or bending tensile capacity of Cikarang bricks is 3.0 MPa, with the coefficient of variance 46%, as given in Table 3.10.

Table 3.10 Modulus of rupture of Cikarang bricks

Bending Test	1 point	2 point	Average
Modulus of rupture	3.366	2.639	3.003
Dev. standard	1.560	1.188	1.384
COV	0.463	0.45	0.461

### 3.4 Brick-mortar bond shear strength

The purpose for testing an assemblage of triplet brick, as pictured below, is to determine the maximum bond-shear strength retained by the joint between mortar and brick under compressive pressure, caused by constant vertical load  $P_V$  and monotonically increasing horizontal load  $P_H$ . The test scheme is shown in Figure 3.21.

Bond shear stress occurring between brick and mortar joint of each specimen is assumed to be uniformly distributed over the contact area and it is equal to  $P_H/A_b$ , where  $A_b$  is contact area in  $N/mm^2$ . To evaluate bond shear strength between mortar and brick surface, mortar type A, B and C were chosen to construct triplet brick specimens.

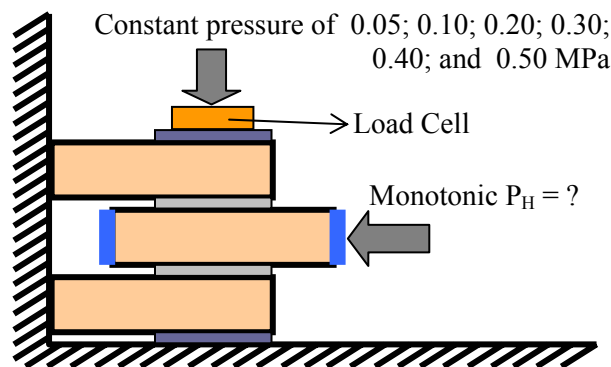


Figure 3.21 Triplet bricks under constant  $P_V$  and increasing  $P_H$  monotonically

For each type of mortar, eight specimens were tested under constant pressure to simulate static gravity load acting on wall structures. Six different pressure parameters chosen were 0.05 MPa, 0.10 MPa, 0.20 MPa, 0.30 MPa, 0.40 MPa and 0.50 MPa. Total number of 144 triplet brick specimens were tested, with details noted in Table 3.11. The ready to test specimens are shown in Figure 3.22.

Using a hydraulic jack of 20 ton-f capacity, triplet brick specimens were placed in a testing machine in horizontal position. Constant vertical compressive pressure was applied through the vertical jack, and increasing horizontal load through horizontal jack was then applied monotonically. Horizontal load at failure is recorded as the maximum capacity of shear force retained by brick-mortar connection. The maximum bonding shear strength is calculated by taking maximum horizontal load distributed uniformly into total two sides of bonding area and measured in  $\text{N/mm}^2$  or MPa. The laboratory test configuration is shown in Figure 3.23

*Table 3.11 Number and type of test of triplet brick specimens.*

Mortar Type	Compressive stress caused by constant $P_V$ (MPa)					
	0.05	0.10	0.20	0.30	0.40	0.50
A	8	8	8	8	8	8
B	8	8	8	8	8	8
C	8	8	8	8	8	8
Total number of specimens = 144						

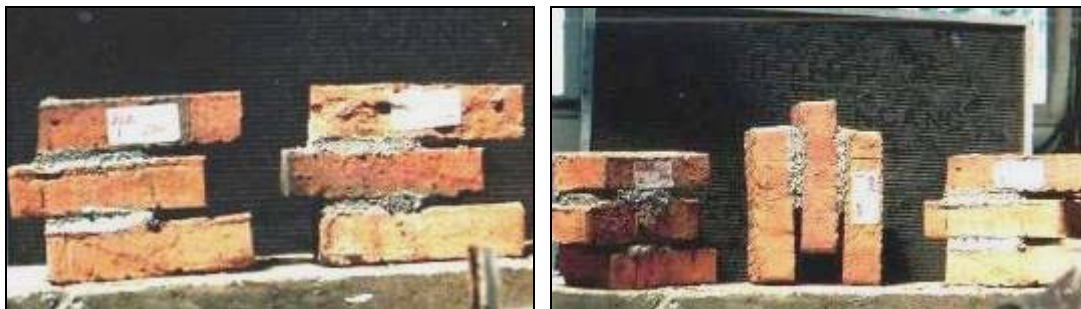


*Figure 3.22 Triplet brick specimens*

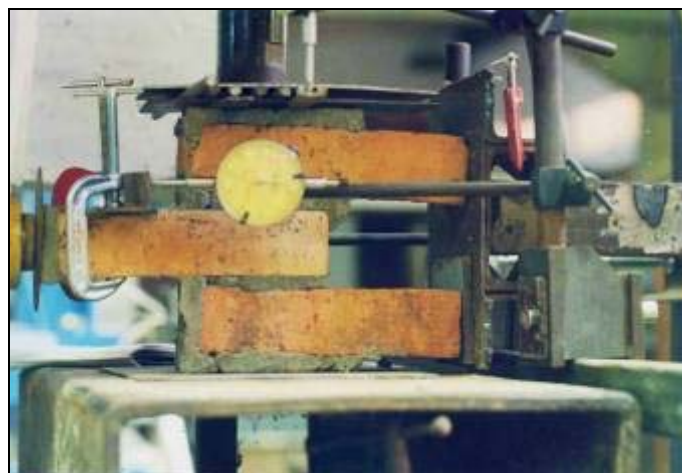


*Figure 3.23 Shear test acted on triplet bricks*

Bond shear strengths without vertical pressure were also evaluated by compressing triplet bricks in vertical direction as shown in Figure 3.24. The tests were performed on sets of 6 triplet bricks for each type of mortar. The results are given in Table 3.12 and are graphically presented in Figure 3.25 as logarithmic curves. The equations of either logarithmic or power trend-lines expressing the capacity of bond shear strengths in term of compressive pressures are given in Table 3.13.

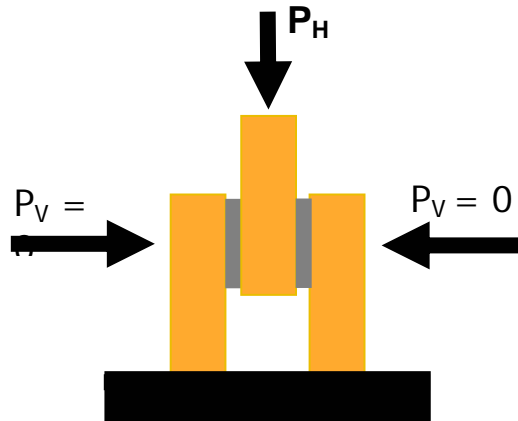


*Figure 3.24 Bond-shear test without pressure*

*Table 3.12 Bond-shear strength between mortar and brick surface*

Mortar Type	Compressive pressure caused by constant $P_V$ (MPa)							Bond-Shear Strength (MPa)
	0	0.05	0.10	0.20	0.30	0.40	0.50	
A	0.35	1.12	1.25	1.61	1.28	1.38	1.53	
B	0.33	0.85	1.05	1.04	1.18	1.30	1.55	
C	0.29	0.62	0.80	0.97	0.82	1.09	1.03	

As seen from Table 3.12 and Figure 3.25, brick-mortar bond shear strength increased as the lateral compressive pressure increased. For triplet bricks without compression, there is no significant difference in bond shear strength between mortar and brick surface. As compressive pressure was applied to specimens, mortar A produced higher shear strength than mortar B and mortar B also produced higher shear strength than mortar C. The bond shear strengths of mortar A and B are 50% and 30% higher than that of mortar C respectively. Based on these results, the best-fit equations relating the bond shear strength to the compressive pressure were developed. Two

different forms of these equations based on either logarithmic or power trends are presented in Table 3.13. Near the origin, the theoretical curves somewhat differ from the experimental curves. However, these are regions of low compressive pressure and low bond shear strength and are not very significant.

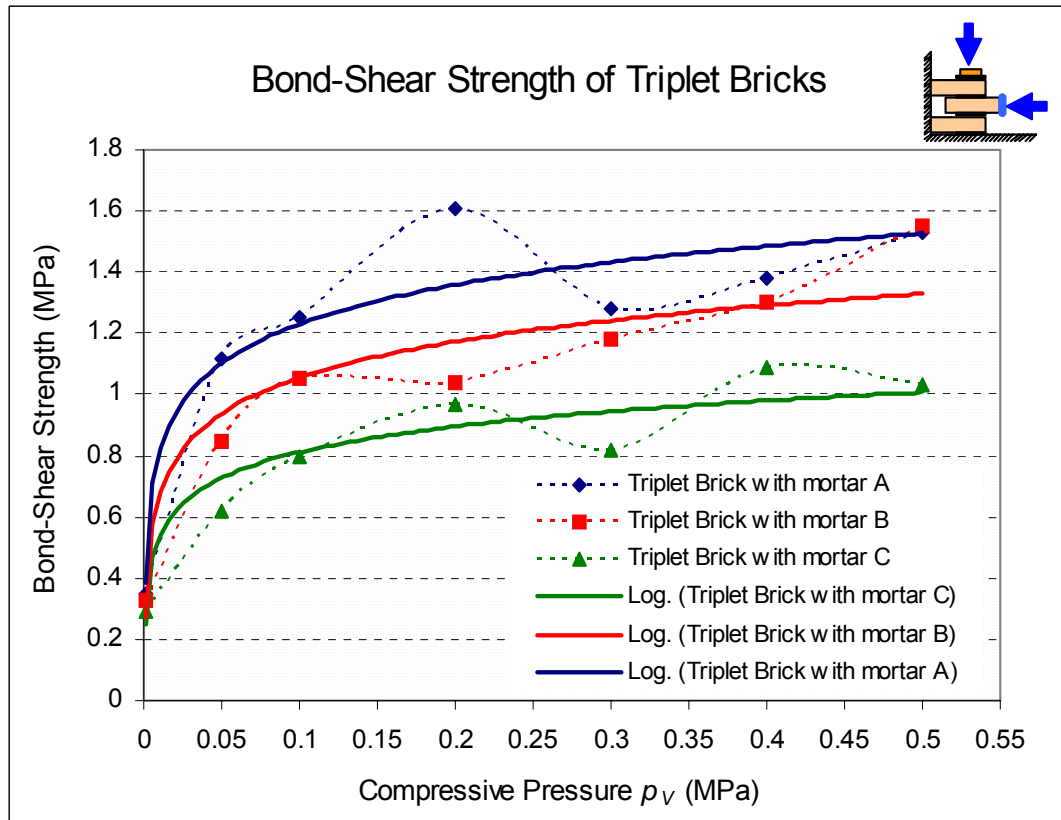


Figure 3.25 Bond shear strength of triplet bricks

Table 3.13 Trend-lines of bond shear strength between brick and mortar

Specimens	Log trend-line	Power trend-line
Triplet Brick with mortar A	$y = 0.1842 \ln(x) + 1.6548$ $R^2 = 0.9046$	$y = 1.947 x^{0.235}$ $R^2 = 0.9288$
Triplet Brick with mortar B	$y = 0.1701 \ln(x) + 1.447$ $R^2 = 0.9081$	$y = 1.6601 x^{0.2324}$ $R^2 = 0.9812$
Triplet Brick with mortar C	$y = 0.1216 \ln(x) + 1.0917$ $R^2 = 0.8978$	$y = 1.2244 x^{0.2086}$ $R^2 = 0.9638$

The failure types of specimens mostly occurred in the form of slip failure between mortar and brick surfaces, which means that the surfaces of bricks were not strong enough to resist bond shear strength caused by lateral loads. The failure patterns are shown in Figure 3.26.





*Figure 3.26 Triplet specimens after testing with slip failure pattern*

### 3.5 Brick column under compression load

Mechanical response of stress-strain behaviour of masonry was also evaluated by observing brick column assemblage under axial compression load. The specimens were constructed in prismatic column shape. Four different types of column specimens named as Short Brick Column SBC, Brick Column BC, Mortared Column MC and Comforted Column CC, were treated.

Short Brick Column is a column with three brick layers bonded together by using mortar type B without any plastering on its surface, as shown in Figure 3.27 and it was named as Column SBC.

Brick Column is a column of five brick layers bonded together by using mortar type B without any plastering on its surface, as shown in Figure 3.28 (a) and it was named as Column BC.

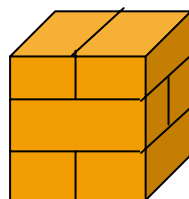


*Figure 3.27 Short Brick Column*



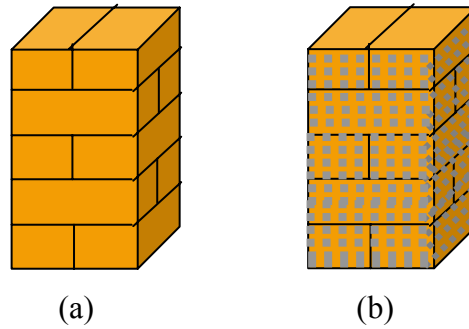


Figure 3.28 (a) Brick Column, (b) Mortared and Comforted Column

Mortared Column MC is a column of five brick layers bonded together by using mortar type B with direct plastering on its surface during construction. This type of column is shown in Figure 3.28 (b) and it was named as Column MC. Comforted Column CC is a column in five brick layers bonded together by using mortar type B with two steps of plastering on its surface and it is named as Column CC. Two steps of plastering in Column CC means: first, a 5 mm thick rough mortar layer (*kamprot*) is applied, which is then allowed to dry for more than 24 hours. Later, a second mortar plaster is applied on the first surface to make the surface look nice.

For the method of constructing column SBC, BC, MC, CC specimens, it was referred to the Indonesian Guidelines for Masonry Construction. All specimens were cured for 27 days by using damp cover to prevent the loss of moisture in mortar. Details of column specimens are given in Table 3.14.

Table 3.14 The number of column specimens

Type of Compressive Column Specimens	Size (mm <sup>3</sup> )	Number of Specimens
Short Brick Column SBC (3 layer bricks)	190×190×185	20
Brick Column BC (5 layer bricks)	190×190×295	10
Mortared Column MC (5 layer bricks)	210×210×295	10
Comforted Column CC (5 layer bricks)	210×210×295	10

The procedure for testing columns SBC, BC, MC, and CC were the same as those performed on individual bricks as described in Section 3.4. Results from these tests are discussed in the following section.

### 3.5.1 Columns SBC

The average capacity of compressive strength evaluated from 20 specimens of SBC is 13.30 MPa. This is about 10% higher than the maximum average compressive strength of single brick, which is approximately equal to 12.12 MPa.

Each specimen had its stress-strain response recorded, and all stress-strain curves have the same pattern as those given by brick specimens. They are mostly weak at the beginning and become stronger when compressive pressure increases above 2 MPa. In general, the value of the modulus of elasticity of column SBC is lower than that of bricks.



*Figure 3.29 Failure type of short brick column specimens*

Most SBC column specimens collapsed in brittle failure, as shown in Figure 3.29. Bricks and mortar were mostly crushed without slip failure and appeared weak without any ductility. The stress-strain behaviour of these columns is shown in Figure 3.30. Statistically, it can be expressed as bilinear inelastic model, weak at the beginning and becoming stronger as pressure  $p_v$  increases above 2 MPa.

In Figure 3.30, it can be noticed that the average compressive strength of column SBC is 13.30 MPa, with coefficient of variation of 17.56 %. In general, the stress-strain curve of short brick column SBC can be simply expressed in a bilinear curve, as shown in Figure 3.31. It presents a similar type of stress-strain curves of brick explained in the previous section.

At compressive pressure  $p_v \leq 2$  MPa,  $E_{SBC \leq 2} = 194$  MPa or 88% of  $E_{br \leq 2}$ ; and as compressive pressure  $p_v > 2$  MPa,  $E_{SBC > 2} = 410$  MPa or 75% of  $E_{br > 2}$ . The weakness in performance of column SBC is caused by discontinuity condition of material homogeneity between brick and mortar, in transferring compressive stress due to compression load.

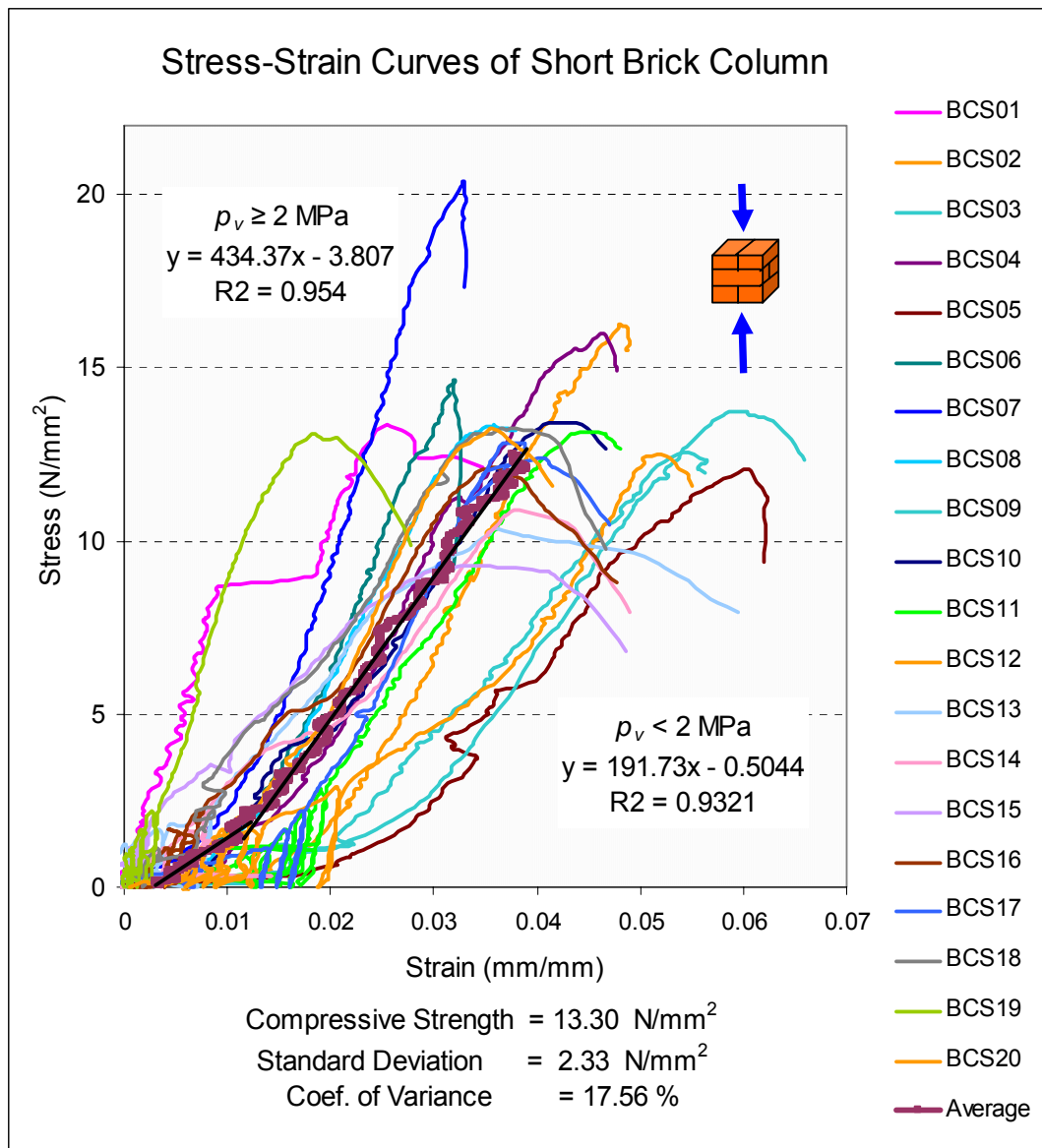


Figure 3.30 Stress-strain curves of column SBC

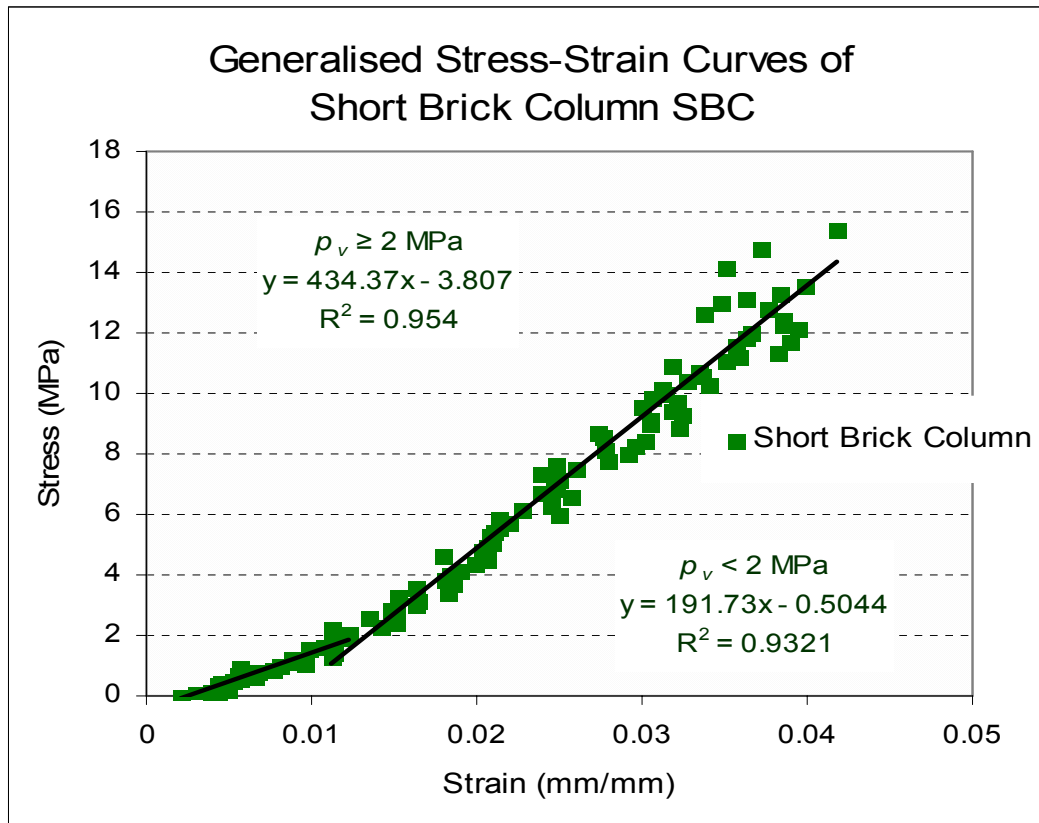


Figure 3.31 General stress-strain curves of column SBC

### 3.5.2 Columns BC, MC and CC

The effects of compressive pressures on five layer brick columns were also evaluated. Three types of columns as shown in Figure 3.28, were loaded increasingly until failure. The average compressive strength capacity of column BC is 8.91 MPa, column MC is 9.96 MPa, and column CC is 12.61 MPa. The curves of stress-strain behaviour of Column BC, MC and CC mostly have the similar trends. The stress-strain curves and generalised stress-strain behaviour of column BC are given in Figure 3.32, those of column MC are given in Figure 3.33, as those column CC in Figure 3.34.

From the six diagrams in Figures 3.32, 3.33 and 3.34, stress-strain behaviour of columns BC, MC and CC is first modelled as bilinear inelastic having no ductility. The curves for stress-strain responses of bricks and columns are represented in one diagram, as shown in Figures 3.35 and 3.36. From these figures, it can be noticed that column CC is stronger than MC, and columns CC and MC are stronger than BC.

As both, columns SBC and Brick are weaker than columns BC, MC and CC, it can be concluded that plastering column surface using mortar plaster or comforted plaster significantly improved the axial stiffness of this type of brick masonry. The modulus of elasticity of SBC, Bricks, BC, MC and CC is given in Table 3.15.

*Table 3.15 Modulus of elasticity of SBC, Brick, BC, MC, CC*

Modulus of Elasticity (MPa)					
Pressure	Type of specimens				
	SBC	Brick	BC	MC	CC
$\leq 2$ MPa	192	220	640	828	981
$> 2$ MPa	434	546	932	1110	1647
Max. compressive strength (MPa)	13.30	12.12	8.44	10.03	12.37

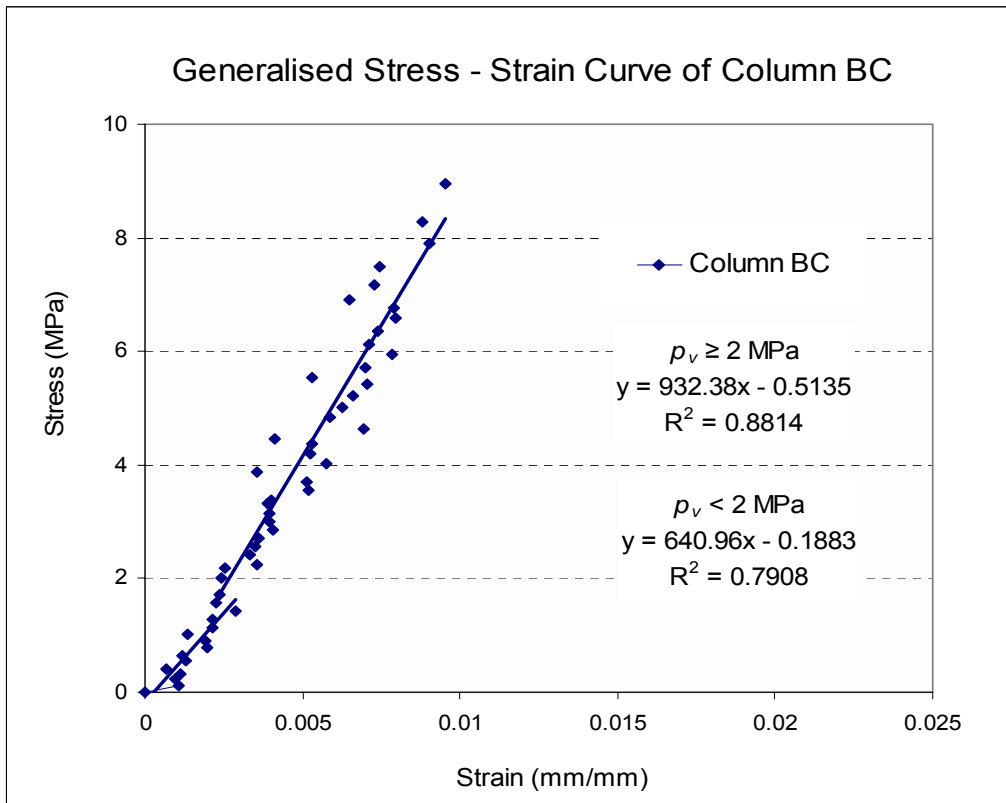
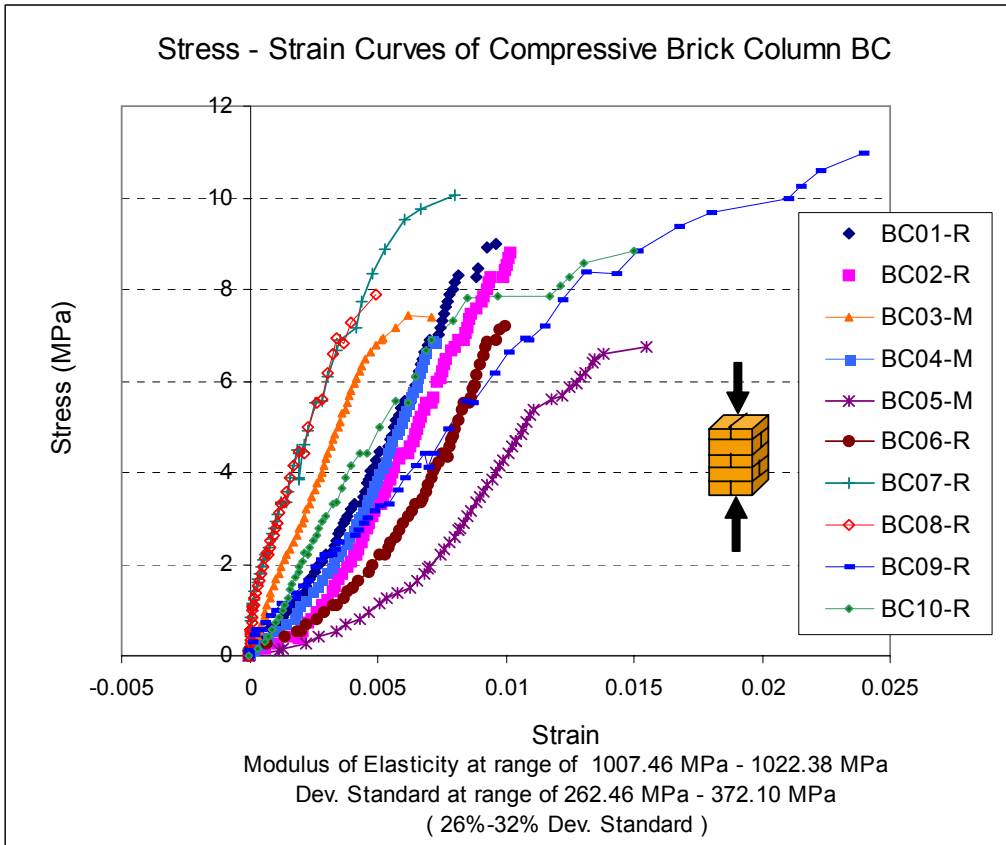


Figure 3.32 (a) Stress-strain curves of brick column BC, (b) Generalised stress-strain curves of brick column BC

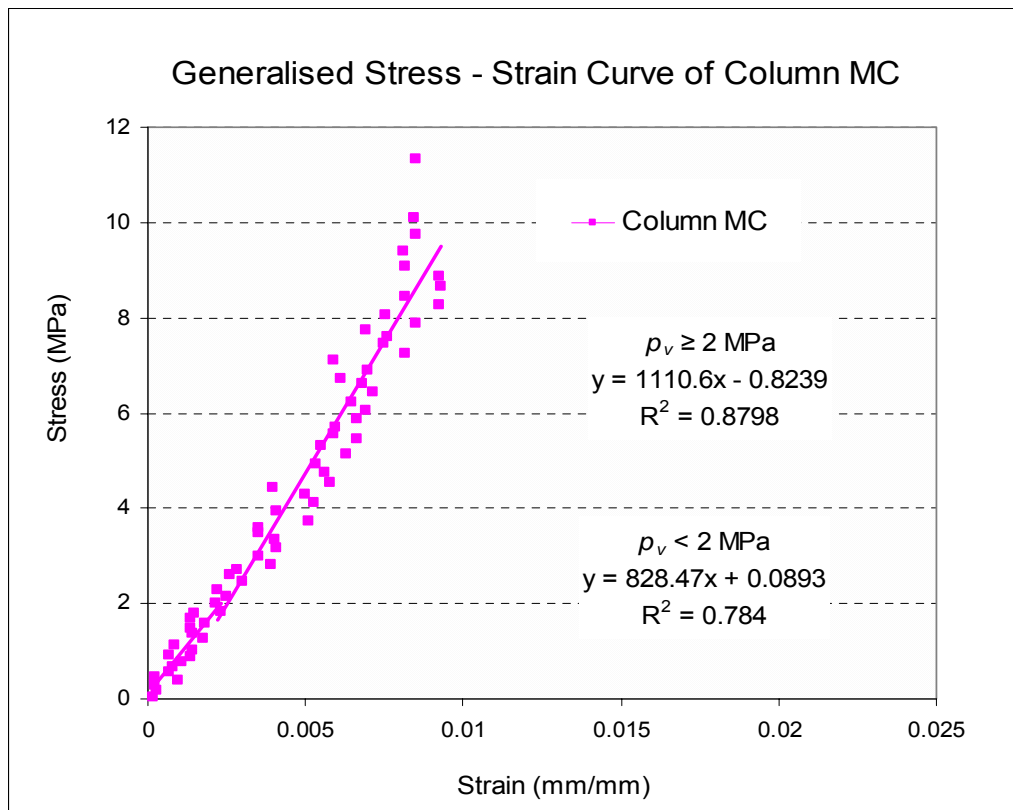
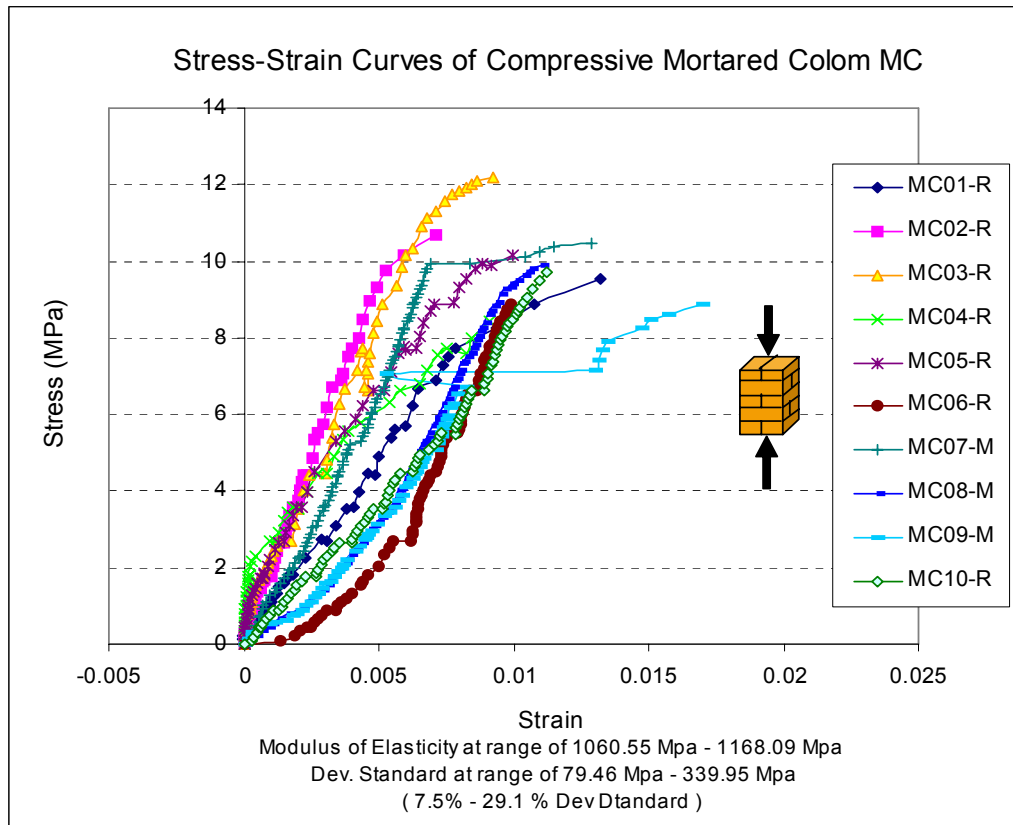


Figure 3.33 (a) Stress-strain curves of mortared column MC, (b) Generalised stress-strain curves of mortared column MC

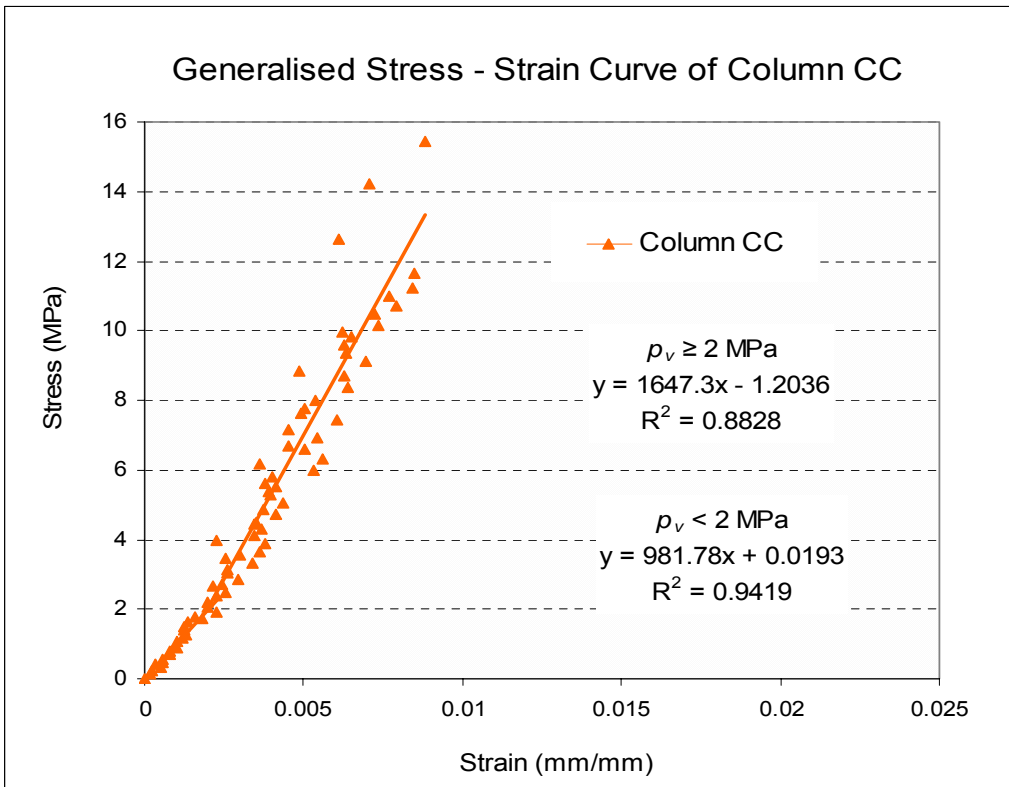
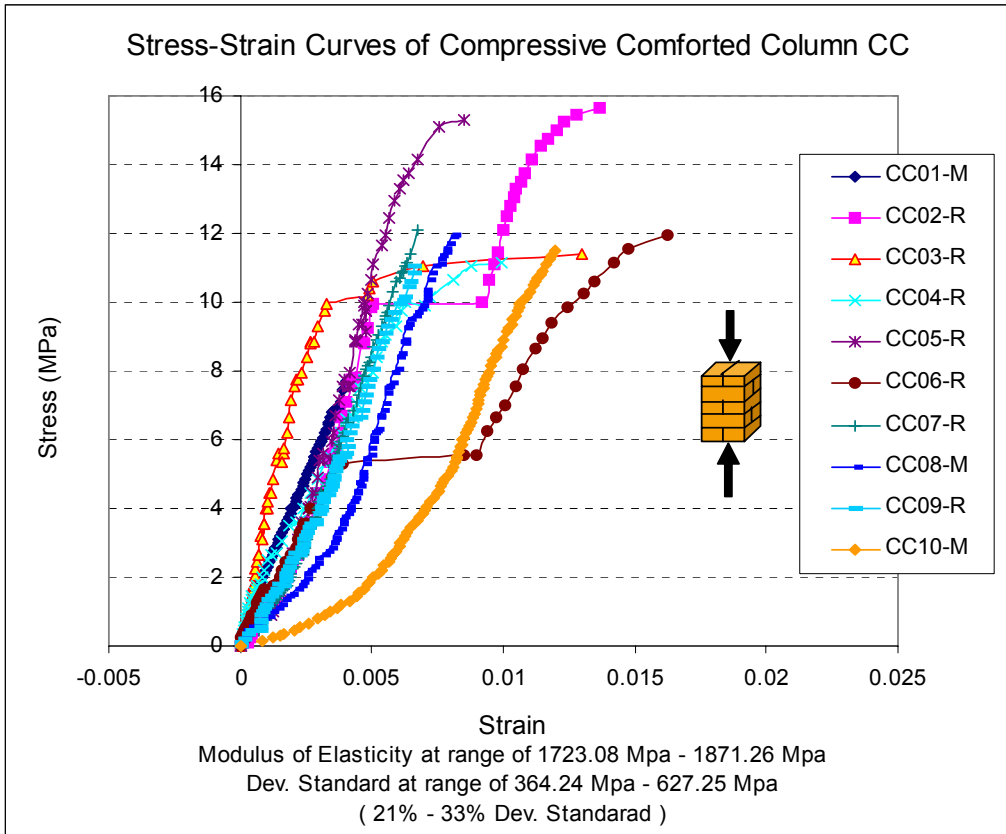


Figure 3.34 (a) Stress-strain curves of comforted column CC, (b) Generalised stress-strain curves of comforted column CC



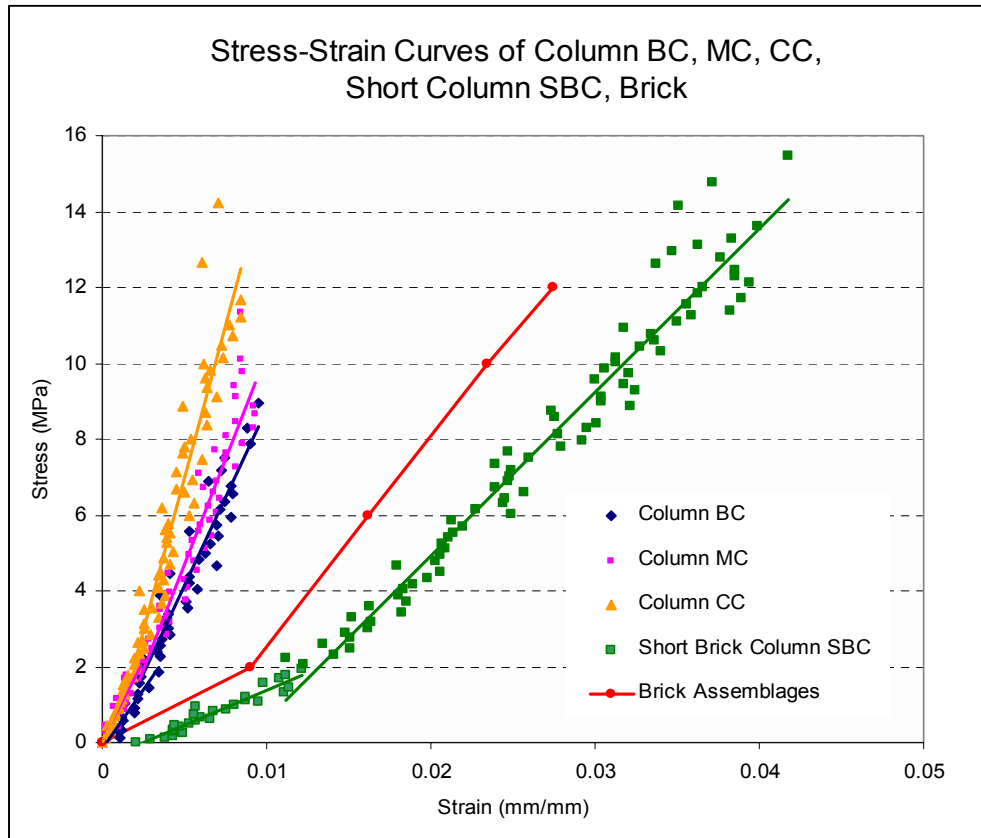


Figure 3.35 Stress-strain curves of columns SBC, Brick, BC, MC and CC

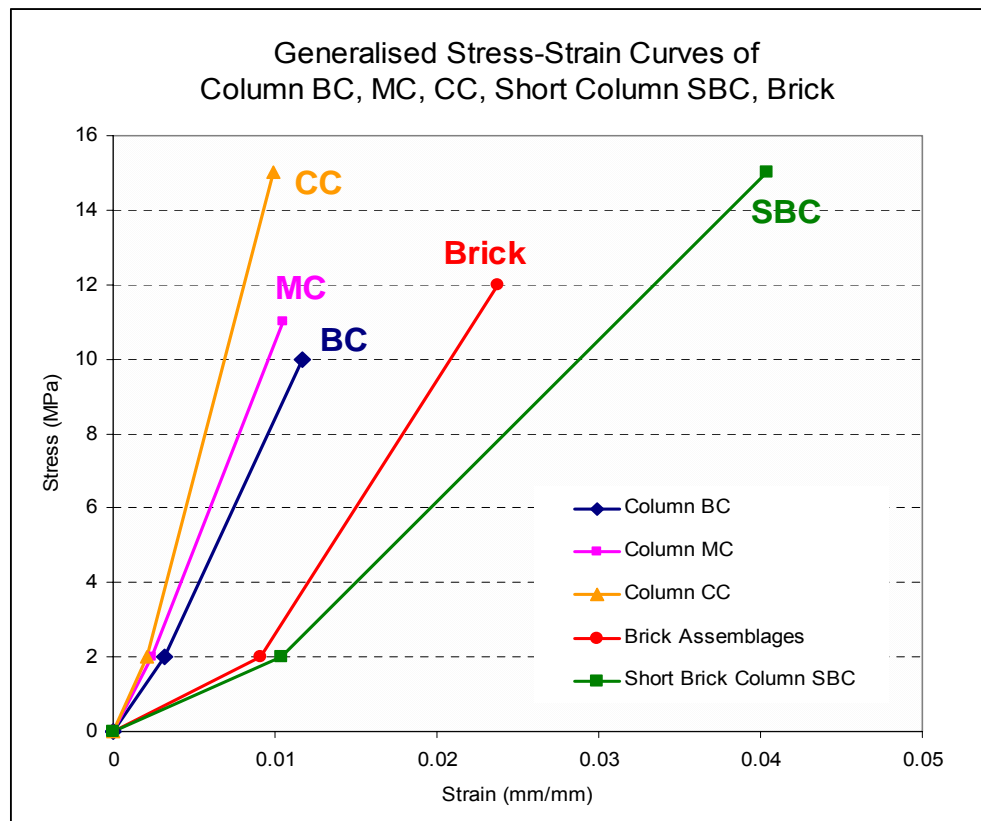


Figure 3.36 Generalised stress-strain behaviour of bricks and columns

From the above results, it can be concluded that brick columns MC, CC and BC are stiffer than individual brick and short column SBC. Assuming all compressive pressure were done to a uniform compressive cross section area  $A$ , taking the length of compressive element as  $L$ , and assuming the stiffness of brick equal to 1 unity, an improvement of axial stiffness ratios of columns to brick can be determined and it is given in Table 3.16.

*Table 3.16 Axial stiffness ratio of columns to bricks*

Ratio of axial stiffness of brick assemblages					
Specimens	SBC	Brick	BC	MC	CC
Axial stiffness	0.79	1	1.73	1.88	2.79

During the tests, it was also found that most columns collapsed in brittle failure mechanism, without any ductility and cracks mostly occurred across bricks and mortar, as shown in Figure 3.37. Most specimens of column SBC, BC, MC and CC collapsed by brittle failure mechanisms without apparent ductility.

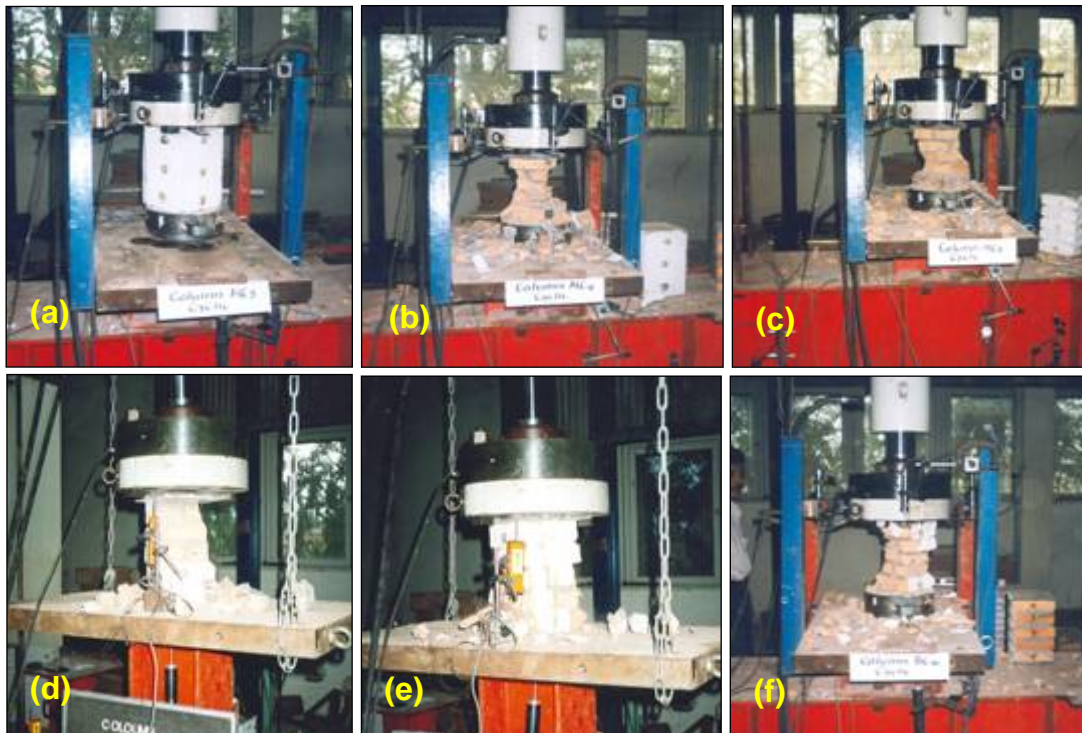


*Figure 3.37 (a) Column specimen before testing, (b) to (f) Brittle failure of column specimens*

### 3.6 Wall panels subjected to vertical compression load

This section, reports on the test results of wall panels also tested under compression load. Evaluating mechanical properties of column assemblages as determined in section 3.5, were here repeated on the brick wall panels. Five types of wall specimens, named as Brick Wall, Mortared Wall, Comforted Wall, Mortared Wall Type A and Comforted Wall type A, in total numbers of 25 wall panels, were tested under compression loads. Details are given in Tables 3.17 and 3.18 respectively.

*Table 3.17 Description of wall specimens, types and coding*

Type of wall	Coding	Description
Brick Wall	BW	Wall without plaster, using mortar 1:4
Mortared Wall	MW	Wall with mortared plaster, mortar 1:4
Comforted Wall	CW	Wall with comforted plaster, mortar 1:4
Mortared Wall type A	MWA	Wall with mortared plaster, mortar 1:4, surface mortar 1:3
Comforted Wall type A	CWA	Wall with comforted plaster, mortar 1:4, surface mortar 1:3

*Table 3.18 Total number of compressive wall specimens*

Type of compressive wall specimens	Size (mm <sup>3</sup> )	Number of specimens
Wall BW	600 × 600 × 90	6
Wall MW	600 × 600 × 110	7
Wall CW	600 × 600 × 110	6
Wall MWA	600 × 600 × 110	3
Wall CWA	600 × 600 × 110	3
Total number of specimens = 25 walls		

#### 3.6.1 Experimental set-up

Wall specimens were placed on a universal testing machine with capacity of 1000 kN. The compression loads were performed on specimens through a hydraulic jack and detected by an installed load cell. Vertical displacement transducers were also located in the same direction of applied compression loads, to measure and record all displacements data during the test.

Two types of compression tests were conducted on wall panels:

- Compression load parallel to brick layers.
- Compression load perpendicular to brick layers.

The test set-ups for parallel and perpendicular loads to brick layers are shown in Figure 3.38 and Figure 3.39 respectively.

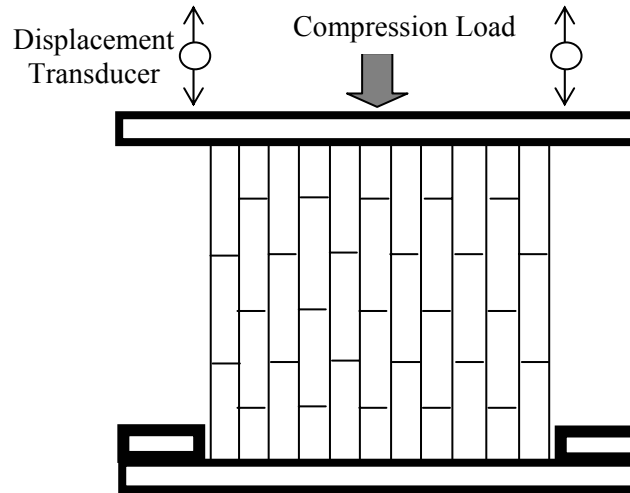


*Figure 3.38 Compressive pressure parallel to brick layers*

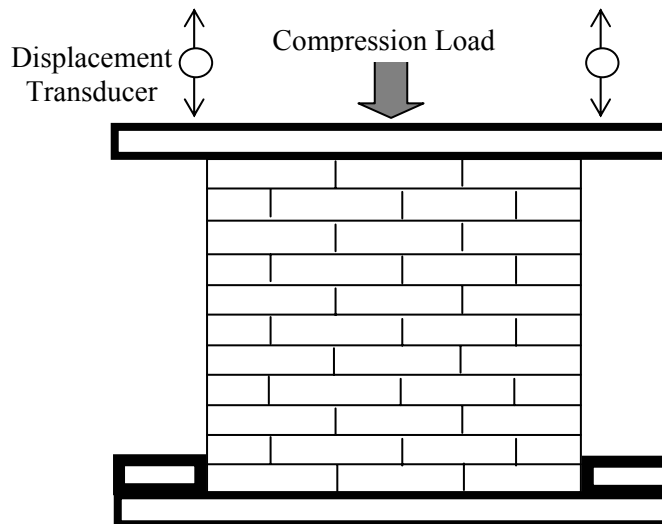


*Figure 3.39 Compressive pressure perpendicular to brick layers*

### 3.6.2 Test procedure

Axial displacements were measured and recorded during the tests while wall specimens were being loaded under increasing axial loads. Axial compressive

pressures were determined by dividing the compressive force by cross section area and measured in  $\text{N/mm}^2$ . The axial strains were analysed as axial displacement divided by the original axial length in  $\text{mm/mm}$ .

### 3.6.3 Test specimens

Type and coding of wall panel specimens tested under compression loads in the parallel or perpendicular direction to bricks layers are detailed in Table 3.19. Most specimens were loaded monotonically, and only 6 walls were under repeated loads.

*Table 3.19 Compressive wall specimens under monotonic and repeated compression loads*

$P_V \perp$ and $P_V //$ brick layer			
Type of Wall	Compression load $P_V$ to be recorded		
	$P_V = ?$	$P_V = ?$	$P_V = ?$
Brick Wall	BW11 $\perp$ - M	BW12 $\perp$ - R	BW13 $\perp$ - R
Mortared Wall	MW09 $\perp$ - M MW12 $\perp$ - M	MW10 $\perp$ - R	MW11 $\perp$ - R
Comforted Wall	CW09 $\perp$ - M	CW10 $\perp$ - R	CW11 $\perp$ - R
Brick Wall	BW14 $//$ - M	BW15 $//$ - M	BW16 $//$ - M
Mortared Wall	MW13 $//$ - M	MW14 $//$ - M	MW15 $//$ - M
Comforted Wall	CW12 $//$ - M	CW13 $//$ - M	CW14 $//$ - M
Mortared Wall type A	MWA13 $//$ - M	MWA14 $\perp$ - M	MWA15 $\perp$ - M
Comforted Wall type A	CWA13 $//$ - M	CWA14 $\perp$ - M	CWA15 $\perp$ - M
Total number of specimens = 25 compressive walls			

### 3.6.4 Test results

All stress strain responses of walls under compression loads are drawn in Figure 3.40. It can be observed that wall BW panels, which were loaded parallel to brick layers, were the weakest walls in retaining compression loads. These walls have the lowest axial stiffness. For compression load perpendicular to brick layer, the axial stiffness is higher, as can be seen through the curves of stress-strain response of wall BW, MW, CW, MWA and CWA which are loaded perpendicular to brick layers. There is also no significant difference in stress-strain response of wall MW, CW, MWA, CWA loaded parallel to brick layers.

The value of modulus of elasticity of wall panels BW, MW, CW, MWA, CWA are given in Table 3.20. During the tests, most specimens collapsed in brittle failure mechanism without ductility, with the failure pattern mostly occurring in the

connection between mortar plaster and brick surface. The specimens are shown in Figure 3.41 and 3.42.

Table 3.20 Modulus of elasticity of walls under compression load (MPa)

Type of wall and loading \ Compressive stress (MPa)	0-1	1-2	2-6	6-10
BW $\perp$	1488.3	2466	1977.15	1133.5
MW $\perp$	1230.9	2260.5	1745.7	2232.3
CW $\perp$	530.19	1841.6	1185.9	1969.2
BW//	33.69	52.43	74.91	74.69
MW//	900.11	1367.79	2200.56	1460.43
CW//	830.42	1457.92	1598.23	1300.18
MWA//, $\perp$	406.85	734.23	903.06	
CWA//, $\perp$	419.22	735.08	730.72	

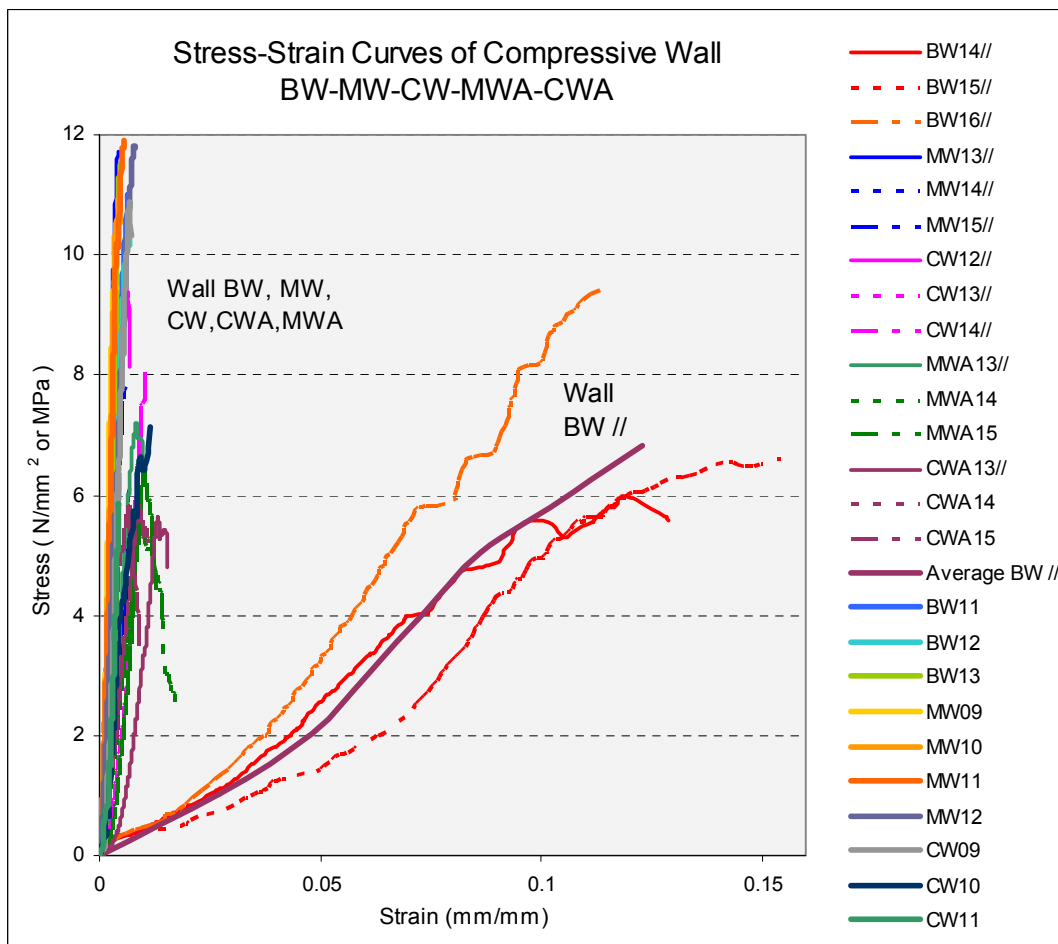
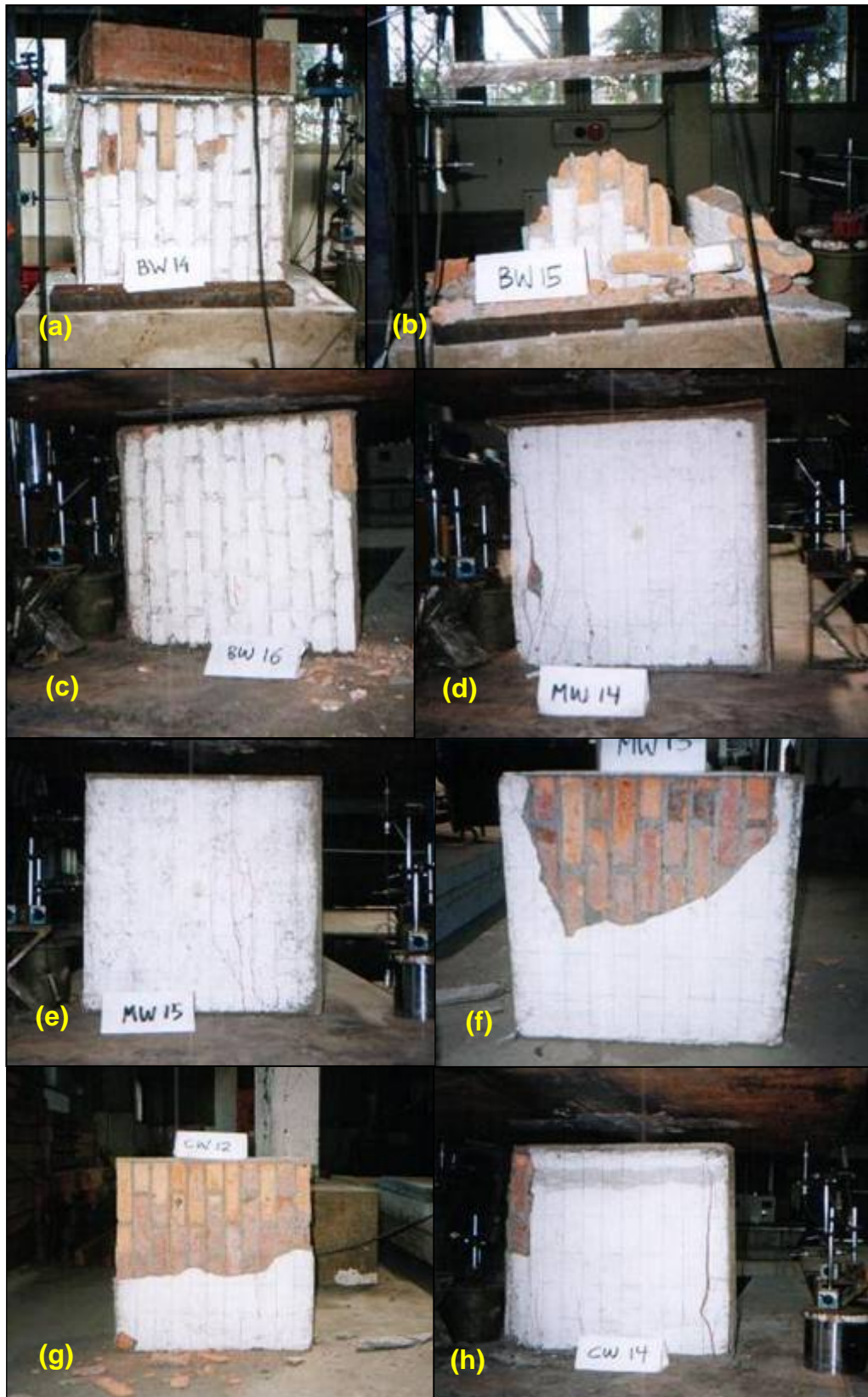


Figure 3.40 Stress-strain behaviour of compressive wall panel



*Figure 3.41 Failure patterns of compressive walls, loaded parallel to brick layers (a), (b), (c) Mortar bonding failure, (d), (e) Compressive failure, (f), (g), (h) Spalling failure*





*Figure 3.42 (a) to (c) Failure pattern of compressive wall MWA and CWA  
(d) Wall MWA before testing, (e) to (g) Mortar plaster failure of wall CWA*

### **3.6.4.1 Wall BW**

All results representing the performance characteristic of wall BW under compression load are shown in Figures 3.43 and 3.44. It can be noticed in Figure 3.43, that wall BW loaded parallel to brick layer is physically weak. The failure is mainly caused by the weakness of brick-mortar bonding strength in brick surfaces. The Figure 3.44 demonstrates that the stress-strain behaviour of wall BW loaded perpendicular to brick layer is stronger. All BW11, BW12 and BW13 responded in similar stress-strain trends. As the compressive pressure lowered below 2 MPa, BW were still weak, however they started to show more strength as the pressure raised



above 2 MPa. This phenomenon was found in columns specimens tested under compression loads.

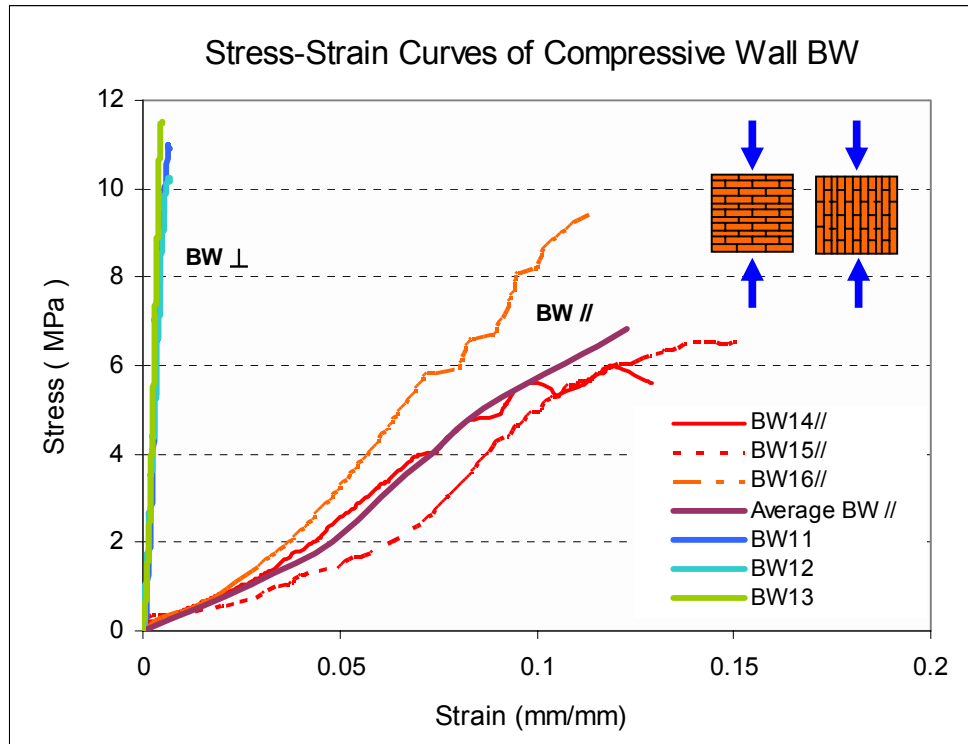


Figure 3.43 Stress-strain curves of wall BW

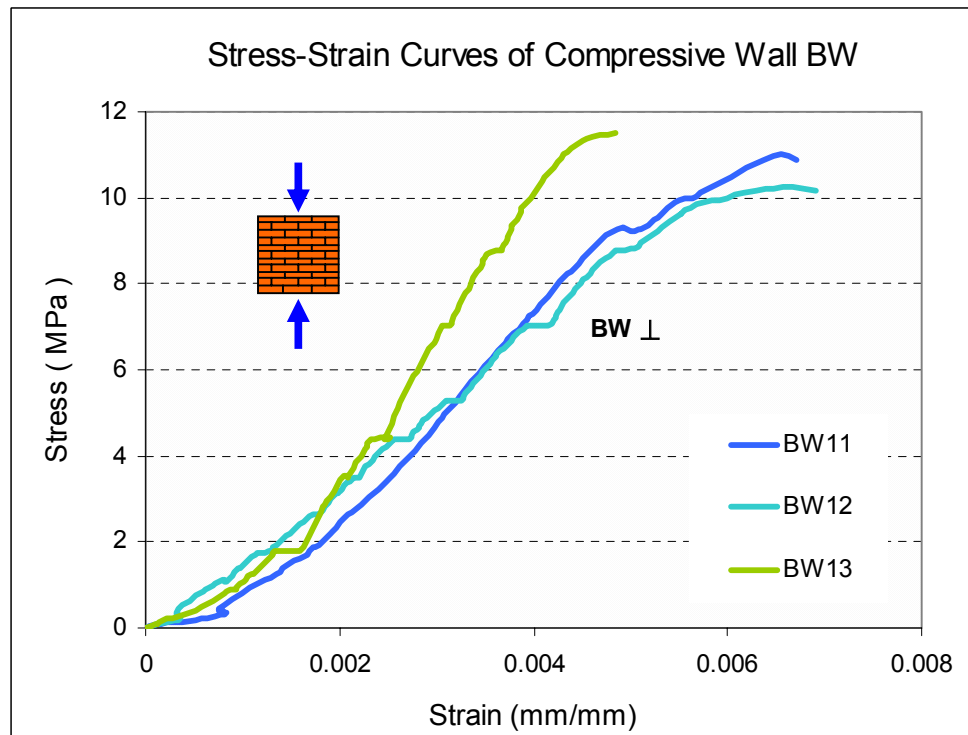


Figure 3.44 Stress-strain curves of wall BW $\perp$

### 3.6.4.2 Wall MW

The results representing the performance characteristic of wall MW under compression load are shown in Figures 3.45, 3.46 and 3.47. In Figure 3.45, it can be seen that wall MW14 loaded parallel to brick layer is physically weak. Walls MW15 and MW09 exhibited similar stress-strain response. Walls MW10, MW11, MW12 and WW13 are stronger. As the graphs of stress-strain curves were drawn separately for wall MW loaded parallel and perpendicular to brick layers, three walls MW10, MW11 and MW12 produced similar stress-strain curves as shown in Figure 3.46. In Figure 3.47, stress-strain response of walls MW13, MW14 and MW15 are widely scattered. The bond shear strength between brick surface and mortar has dominant affect on the wall strength. In general, as the compressive pressure reduced bellow 2 MPa, MW walls were weak, however they increased in stiffness as the pressure raised above 2 MPa.

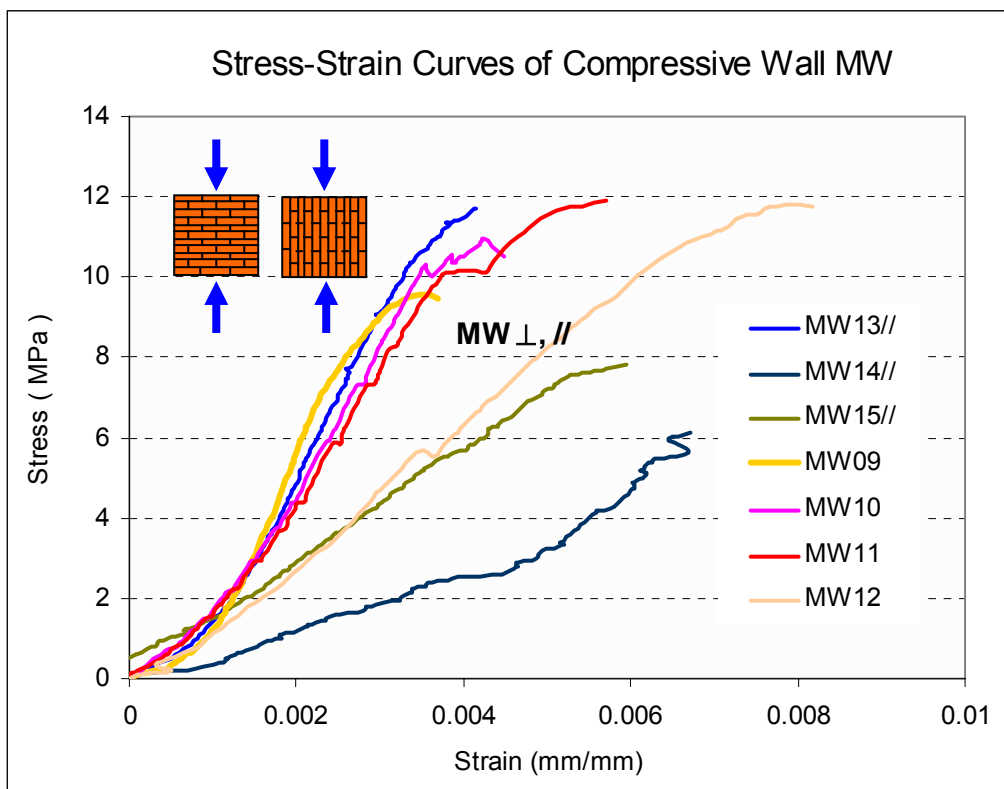


Figure 3.45 Stress-strain curves of wall MW

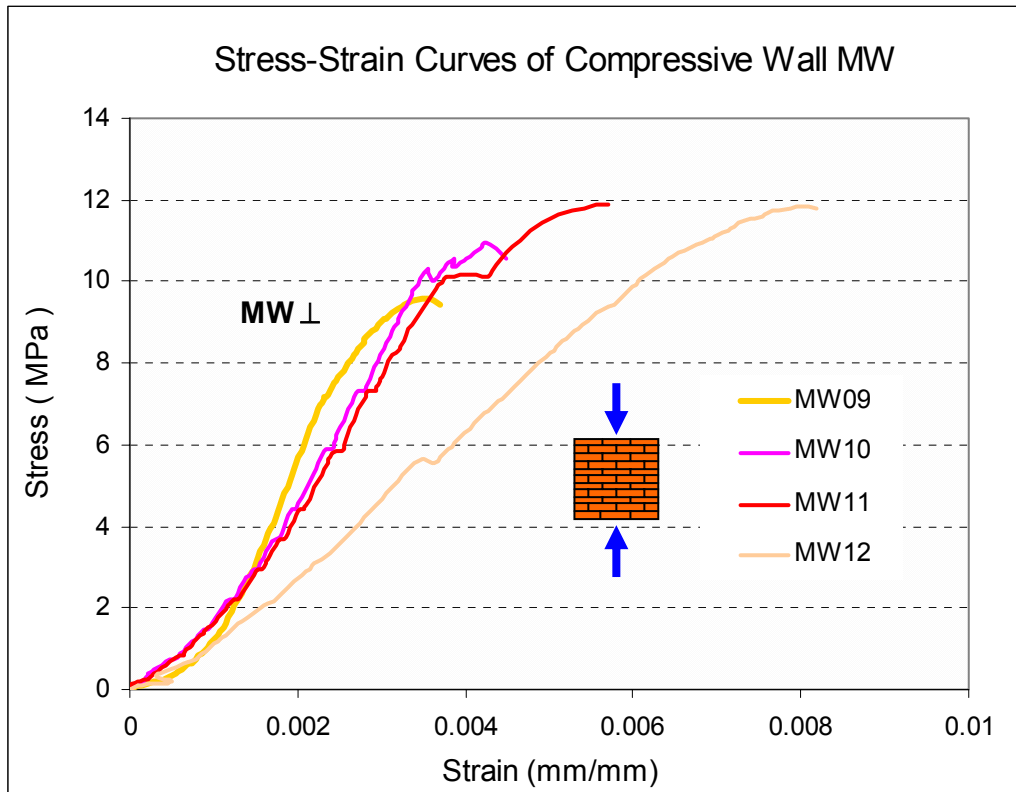


Figure 3.46 Stress-strain curves of wall MW $\perp$

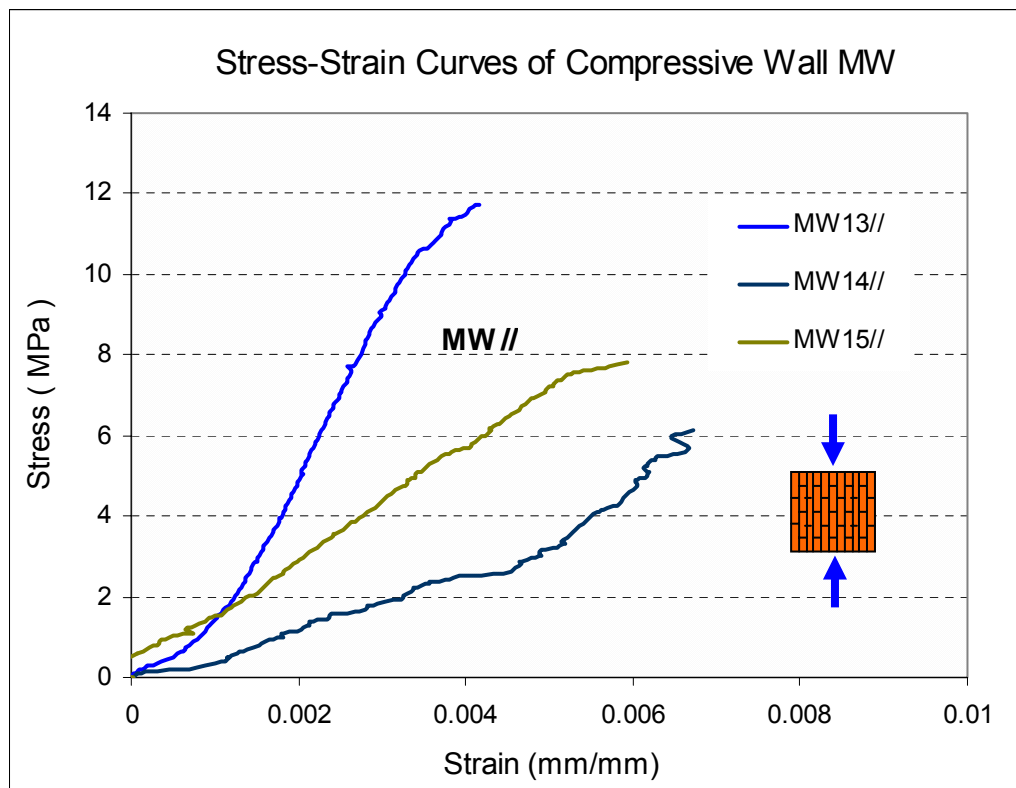


Figure 3.47 Stress-strain curves of wall MW//

### 3.6.4.3 Wall CW

Observing wall CW under compression load, the results representing the performance characteristic can be seen in Figures 3.48, 3.49 and 3.50. In Figure 3.48, it can be seen that wall CW14 loaded parallel to brick layer is physically weak. Walls CW09 and CW11, CW12 and CW13 exhibited similar stress-strain response, while walls CW10 and CW1 are weaker. In Figure 3.50, the stress-strain response of walls CW09 and CW11 are similar. Wall CW11 has very low compressive strength caused by a technical fault during test. The bond shear strength between brick surface and mortar is dominant affect on the wall strength. In general, as the compressive pressure reduced below 2 MPa, CW walls were weak, however they increased in stiffness as the pressure raised above 2 MPa.

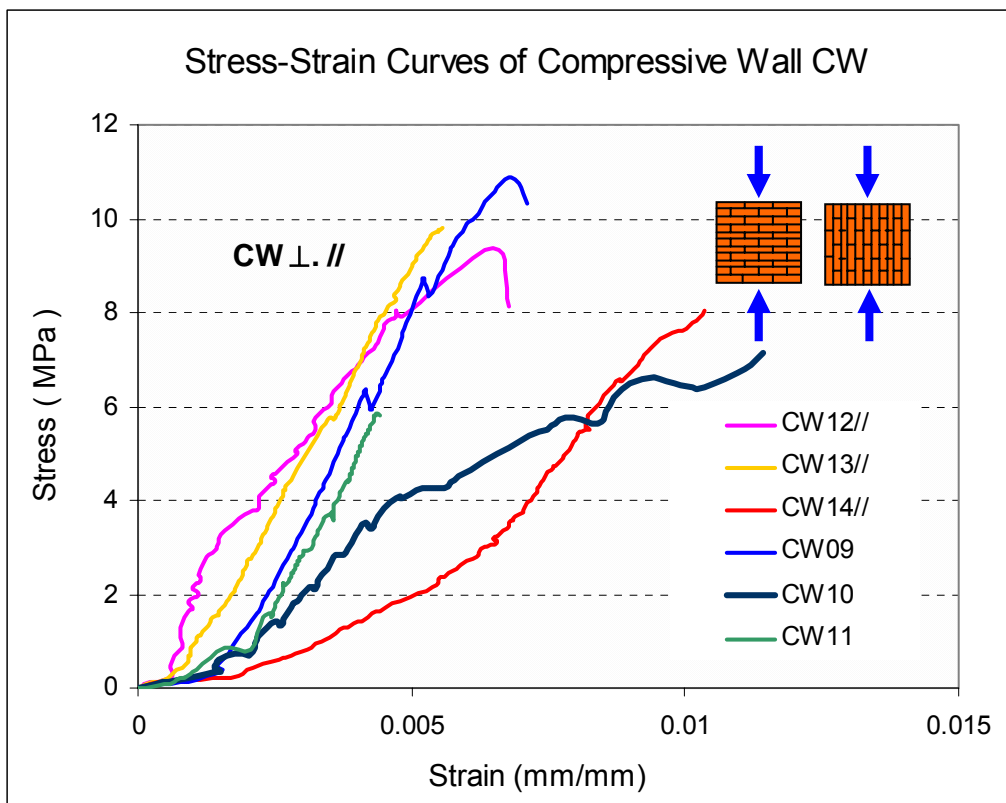


Figure 3.48 Stress-strain curves of wall CW

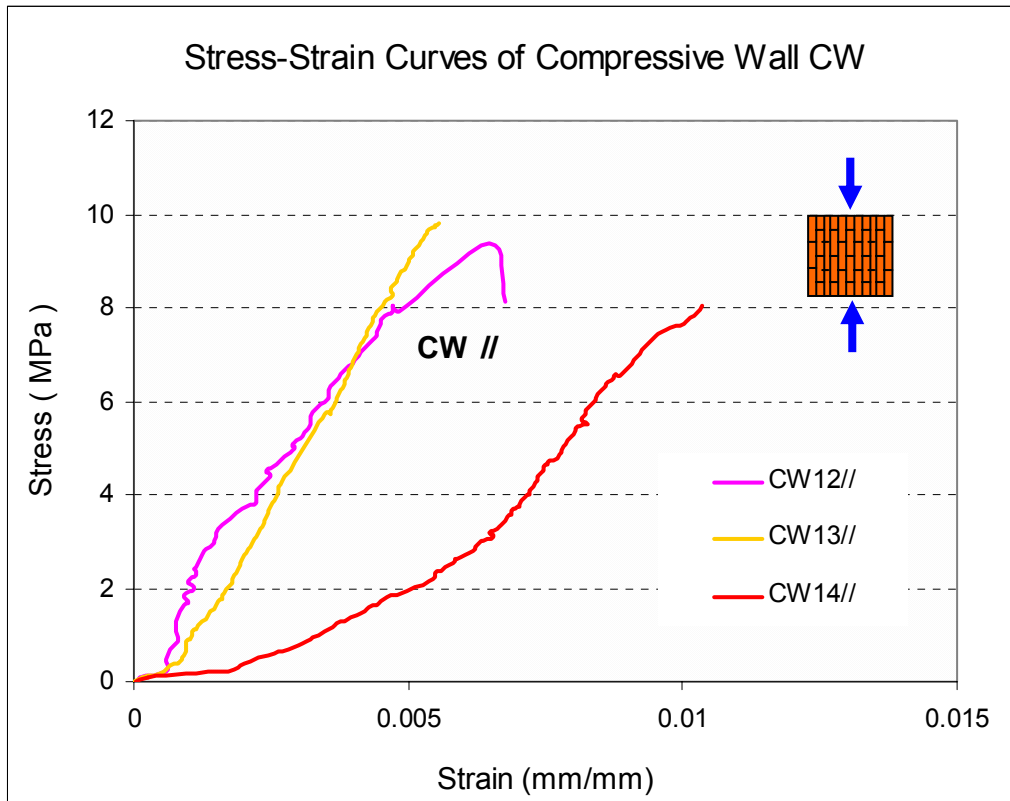


Figure 3.49 Stress-strain curves of wall CW//

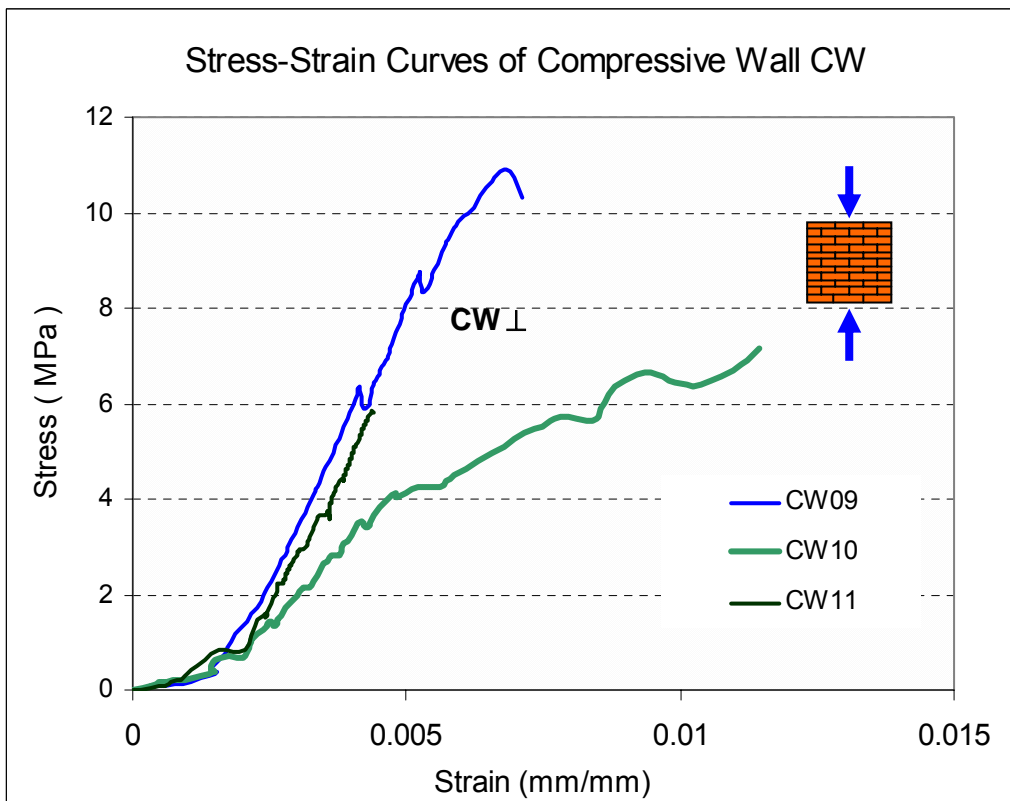


Figure 3.50 Stress-strain curves of wall CW⊥

### 3.6.4.4 Wall MWA and CWA

In Figures 3.51 and 3.52, the stress strain response of MWA and CWA walls loaded parallel and perpendicular to brick layers is similar. In compressive stress below region 2 MPa, the characteristics of stress strain are always presenting low slope of stress-strain relation. As the compressive stress increased above 2 MPa, most walls became stronger and exhibited similar trends in their stress-strain relation. The general response of walls to the applied compressive load is drawn in stress-strain curves diagram as shown in Figure 3.53.

According to the real in site conditions, masonry wall for houses and low rise buildings never retain compressive load above 2 MPa. The testing performed showed that the stress-strain behaviour of walls BW, MW, CW, MWA and MWA under compressive pressure below 2 MPa is generally weak. The modulus of elasticity of any type of wall is widely spread, according to the stage of fissure closing that happened to this brick masonry. This fissure closing stage has not been found in any former research work.

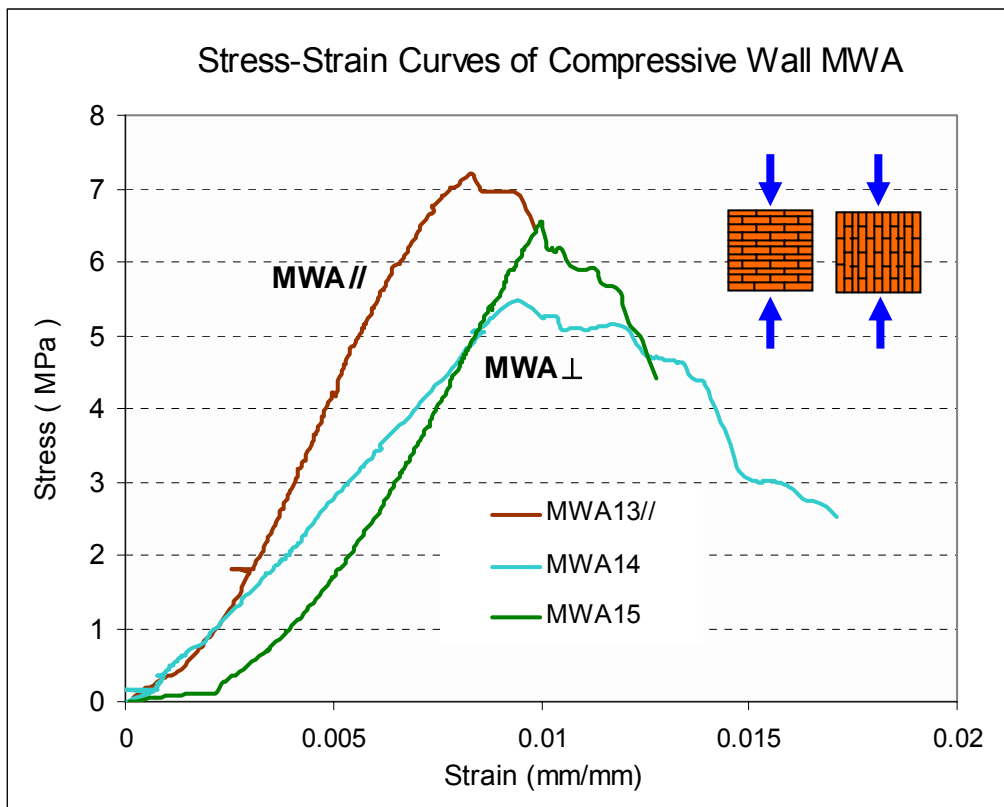


Figure 3.51 Stress-strain curves of wall MWA

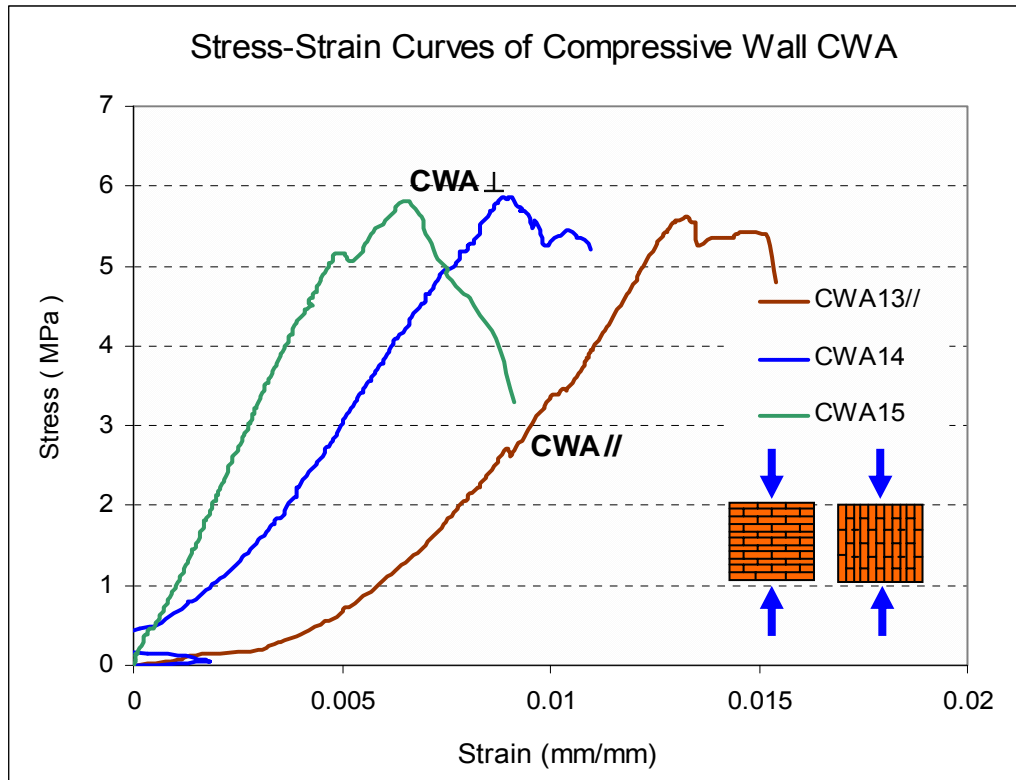


Figure 3.52 Stress-strain curves of wall CWA

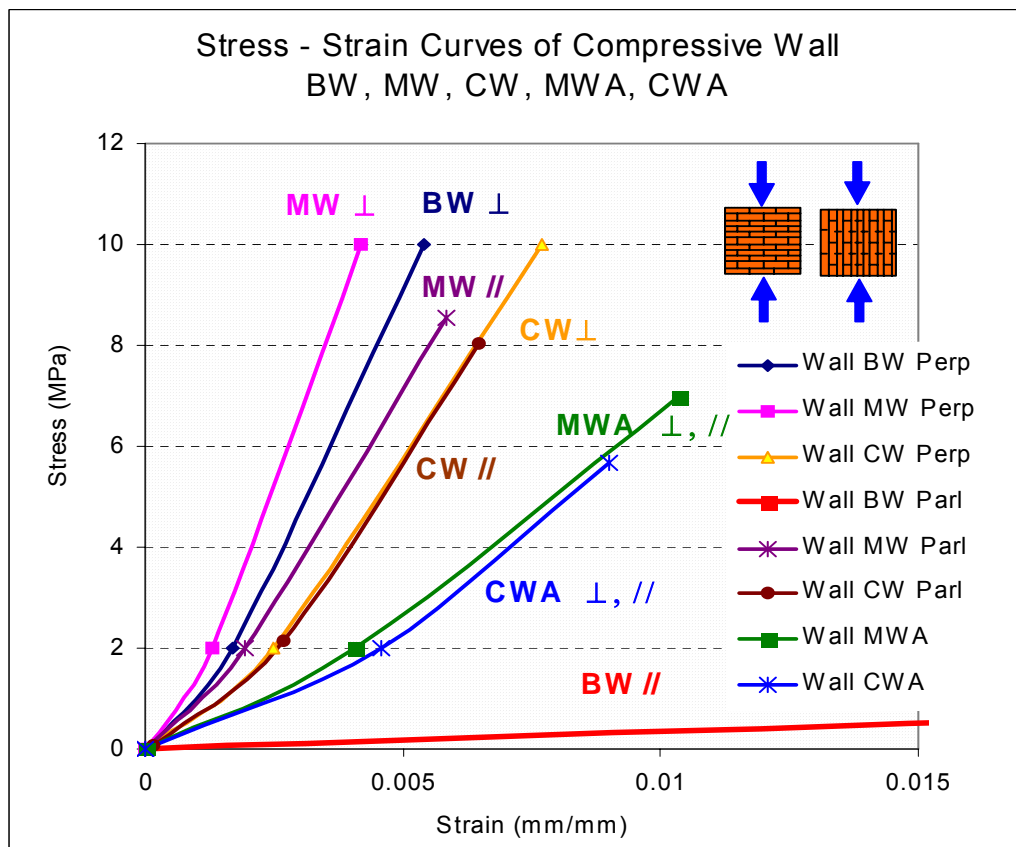


Figure 3.53 Stress-strain behaviour of compressive walls

Observing Figure 3.53, wall BW loaded parallel to brick layer is not recommended to be used in structural brick wall. Bond strength between mortar and brick surface is low and does not resist the applied load parallel to brick layers. Wall MW loaded perpendicular to brick layer exhibited the strongest performance. Its strength was due to homogeneity condition of the wall. The response of wall CW is the lowest among two other walls BW and MW. Its low response was caused by the discontinuity condition between comforted mortar and wall surface. Walls MWA and CWA performed unsatisfactorily. Their bad performance was caused by the discontinuity condition between mortar type A and wall surface. Spalling failure mechanism happened to surface mortar plaster in these walls, as seen in Figure 3.42.

Based on the values of Modulus of Elasticity as listed in Table 3.20, the axial stiffness of wall panels can be determined and is given in Table 3.21. These axial stiffness values are then used for developing a simple model for diagonal stiffness of wall elements, as derived in Chapter 5.

*Table 3.21 Axial stiffness of wall panels*

Axial stiffness of wall panes under compression load (kN/mm)					
Compressive pressure (MPa) \ Type of wall	0 to 1	1 to 2	2 to 6	6 to 10	Number of specimens
BW $\perp$	148.83	246.60	197.72	113.35	3
MW $\perp$	135.40	248.66	192.03	245.55	4
CW $\perp$	58.32	202.58	130.45	216.61	3
BW//	3.71	5.77	8.24	8.22	3
MW//	99.01	150.46	242.06	160.65	3
CW//	91.35	160.37	175.81	143.02	3
MWA//, $\perp$	44.75	80.77	99.34		3
CWA//, $\perp$	46.11	80.86	80.38		3
Total Number of Specimens					<b>25</b>

### 3.7 Conclusion

The results from this experimental work can be summarised in four categories: brick compressive strength, stress strain behaviour of bricks, stress strain behaviour of columns and stress strain behaviour of walls.



Brick compressive strengths were evaluated using six different types of mortar. It was observed that mortar compressive strength does not affect significantly the brick compressive strength. Compressive strength of mortar type C is nearly the same as that of brick using mortar type C. The average compressive strength of Cikarang bricks is 12.12 MPa.

Modulus of elasticity of bricks was evaluated from stress strain response during compression test. As the stress-strain response of bricks using mortar type A, B, C, D, E and F resulted in a similar trends and forms, the modulus of elasticity of these bricks was simplified as the average of tangent modulus taken from six stress strain curves. As the compressive stress is equal or lower than 2 MPa, the modulus of elasticity of bricks is 220 MPa. When the compressive stress rises above 2 MPa, the modulus of elasticity increases to 546 MPa.

Modulus of elasticity of columns SBC, BC, MC and CC were also evaluated based on the stress strain response from compression test. Column SBC was the weakest among the three other columns BC, MC and CC. Column CC produced the highest modulus of elasticity, 2.79 times that of the brick.

Evaluating the stress-strain response of walls BW, MW, CW, MWA and CWA, it was observed that the wall BW was very weak to resist compression load parallel to brick layers. Walls MC and CC gave better performance in axial stiffness than walls MWA and CWA. The compressive strength of wall MWA and CWA were lower than that of walls BW $\perp$ , MW, and CW. Consequently, it was concluded that there is no significant benefit of using mortar type A for surface plaster.

The stress-strain response of wall CW loaded parallel to brick layers was equal to that of wall CW loaded perpendicular to brick layers. Both CW wall responses were lower than that of wall MW, therefore, wall MW is recommended to be used in structural application.



## Chapter 4. Experimental Investigation of Walls under Lateral In-plane Loads

---

### 4.1 Introduction

The main purpose of the research presented in this thesis is to evaluate the response of gravity and horizontal earthquake loads on brick masonry structures in Indonesia. To simulate these types of loads, wall panels were loaded under constant vertical compression, ranging from 1.0 ton-f to 2.5 ton-f or from 0.15 MPa to 0.5 MPa and subjected to increasing lateral in-plane load in horizontal direction. These tests are considered to be masonry wall panels under compression and lateral in-plane loads.

In these experiments, 6 types of wall panels were tested and coded as:

- BW = brick wall without surface mortar plaster,
- MW = brick wall with surface mortar plaster,
- CW = brick wall with comforted surface mortar plaster,
- MWA = brick wall with surface mortar plaster type A,
- CWA = brick wall with comforted surface mortar plaster type A,
- MWE = extra brick wall with surface mortar plaster.

Four different types of vertical compression load parameter  $P_v = 1$  ton-f; 1.5 ton-f; 2 ton-f, 2.5 ton-f were applied to these types of wall panels, which respectively produced compressive pressure  $p_v = 0.165$  MPa, 0.245 MPa, 0.325 MPa, and 0.42 MPa. In addition, wall MW, CW and MWE were also evaluated under compression load  $P_v = 0.5$  ton-f or compressive pressure  $p_v = 0.08$  MPa. These compressive loads and pressure parameters are listed in Table 4.1.

As tabulated in Table 4.2, total of 75 wall panels were tested under monotonic, repeated and cyclic lateral loads in horizontal direction until collapse, and the failure mechanisms were observed.

Table 4.1 Compressive pressure acted on wall specimens

Vertical compression load $P_V$ ( ton-f )	Compressive pressure $p_v$ ( MPa )
0.5	0.08
1	0.165
1.5	0.245
2	0.325
2.5	0.42

Table 4.2 Type and number of wall panels tested under  $P_V$  and  $P_H$

Wall type	Type of horizontal load $P_H$	Vertical compression load $P_V$				
		0.5 ton-f	1.0 ton-f	1.5 ton-f	2.0 ton-f	2.5 ton-f
		Compressive pressure $p_v$				
		0.08 MPa	0.165 MPa	0.245 MPa	0.325 MPa	0.42 MPa
BW	Monotonic		1	1	1	1
	Repeated		1	1	2	1
	Cyclic		1	1	1	1
MW	Monotonic		1	1	1	1
	Repeated		1	1	1	1
	Cyclic	2	2	1	1	1
CW	Monotonic		1	1	1	1
	Repeated		1	1	1	1
	Cyclic	2	2	2	2	2
MWA	Monotonic		1	1	1	1
	Repeated		1	1	1	1
	Cyclic		1	1	1	1
CWA	Monotonic		1	1	1	1
	Repeated		1	1	1	1
	Cyclic		1	1	1	1
MWE	Monotonic	1	1	1	1	1
Total number of wall specimens = 75 walls						

## 4.2 Experimental scheme

### 4.2.1 Wall under compression and lateral in-plane load

To resist lateral displacement at support, wall specimens were placed on a rigid bed joint made of concrete block. Uniformly distributed compression loads were applied through transfer beams and roller plates to avoid horizontal displacement of jack head. Lateral in-plane loads were then applied through horizontal jack located firmly at a loading frame of 100 ton-f capacity. The diagram of the test set-ups is shown in Figure 4.1 and the photograph of the set-up is shown in Figure 4.2.

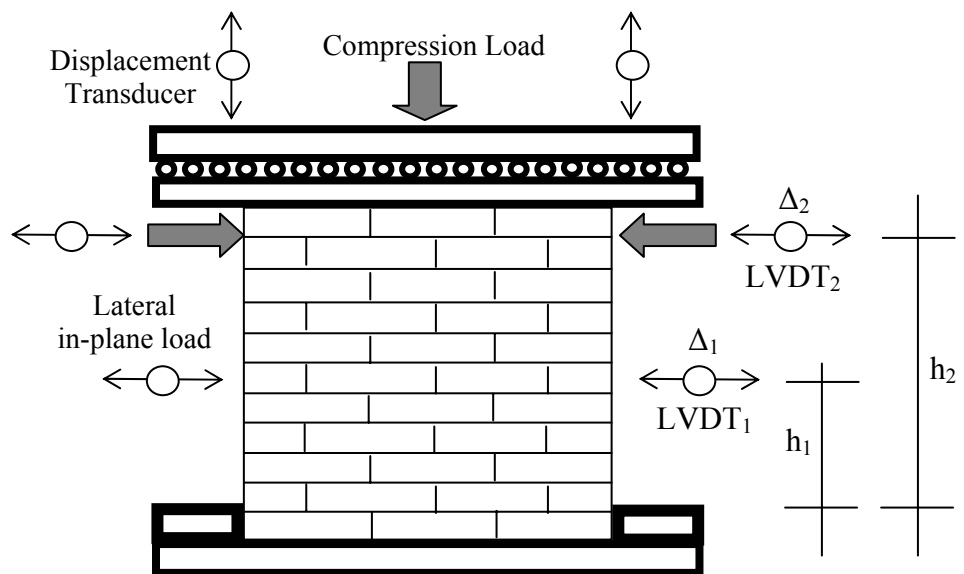


Figure 4.1 Wall under compression load  $P_V$  and increasing lateral in-plane load  $P_H$

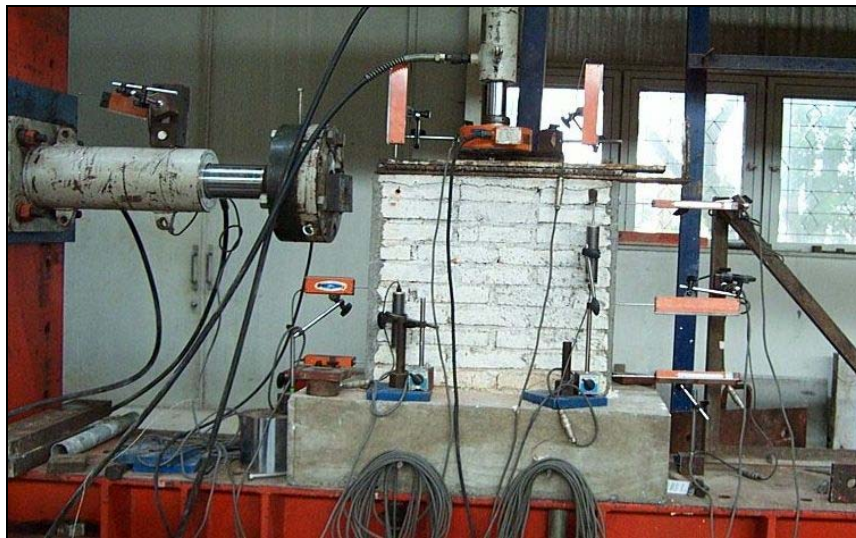
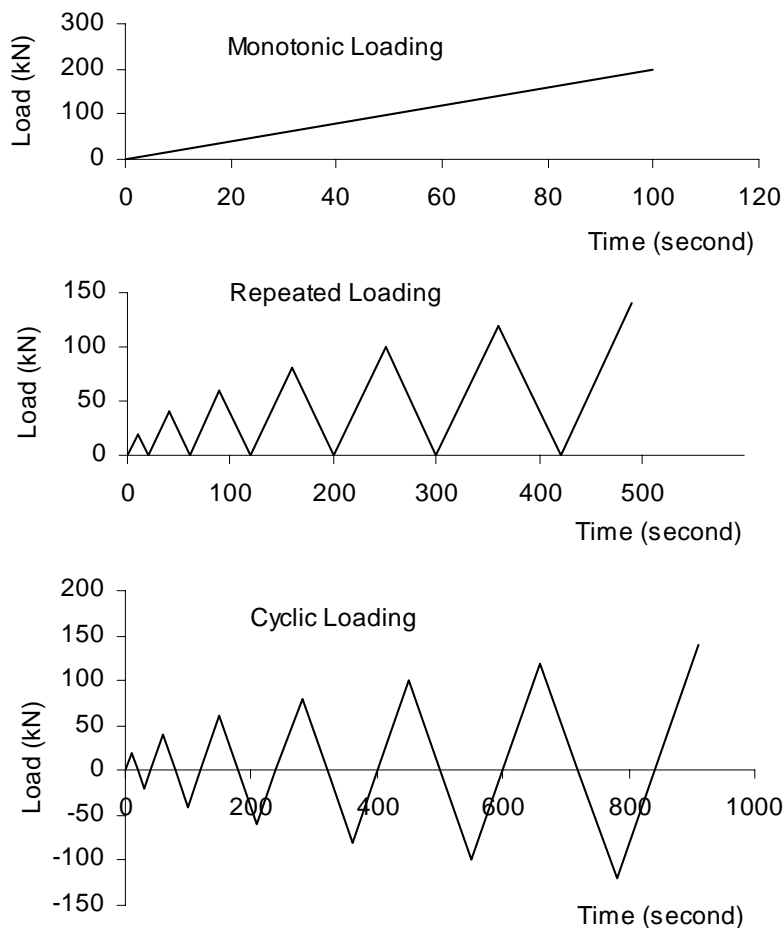


Figure 4.2 Test configuration of wall panel

The vertical compression loads were applied constantly by locking pressure control valve of vertical hydraulic jack. Horizontal loads were increased gradually from zero up to failure load, based on the pattern described in Figure 4.3. Horizontal displacements of walls, maximum lateral load, and failure patterns were recorded from each test performed on every single wall specimen.

#### 4.2.2 Loading pattern

The patterns of increasing applied horizontal loads are shown in Figure 4.3. Loading rate velocity of 2 kN/sec or 0.05 N/mm<sup>2</sup>/sec was used, which it is about 1/3 scale of ASTM C-39-96.



*Figure 4.3 Type of horizontal load applied to specimens*

During the experimental tests, wall specimens were grouped into three types of lateral loadings: monotonic, repeated and cyclic loadings. Types of wall specimens and coding are given in Table 4.3. The storage area of wall specimens before testing

is shown in Figure 4.4. Wall specimens were cured with damp cover for 28 days after construction and placed in a room with ambient temperature ranging from 25-30°C and relative humidity of 70-80%.

*Table 4.3 Wall specimens under compression Load  $P_V$  and horizontal load  $P_H$*

Wall under vertical compression load $P_V$ and horizontal load $P_H$					
Horizontal load $P_H$	Compression load $P_V$				
	0.5 ton-f	1 ton-f	1.5 ton-f	2.0 ton-f	2.5 ton-f
	Compressive pressure $p_v$				
	0.08 MPa	0.165 MPa	0.245 MPa	0.325 MPa	0.42 MPa
Monotonic (25)		BW04	BW03	BW05	BW21
		MW08	MW07	MW01	MW06
		CW07	CW08	CW01	CW06
		MWA01	MWA02	MWA03	MWA04
		CWA01	CWA02	CWA03	CWA04
	MWE01	MWE02	MWE03	MWE04	MWE05
Repeated (23)		BW06	BW09	BW07 BW08	BW10
	MW20	MW02	MW03	MW04	MW05
	CW19	CW02	CW03	CW05	CW04
		MWA05	MWA06	MWA07	MWA08
		CWA05	CWA06	CWA07	CWA08
Cyclic (27)		BW17	BW18	BW19	BW20
	MW21	MW16 MW22	MW17	MW18	MW19
	CW20	CW15 CW21	CW16 CW22	CW17 CW23	CW18 CW24
		MWA09	MWA10	MWA11	MWA12
		CWA09	CWA10	CWA11	CWA12
Total of wall specimens = 75					



*Figure 4.4 Storage of wall specimens*

### 4.2.3 Test set-up and instrumentation

The main instruments used for recording the displacement of specimens during test activities were Linear Variable Displacements Transducers (LVDT) with specification of 50 mm and 100 mm displacement recording capacity.

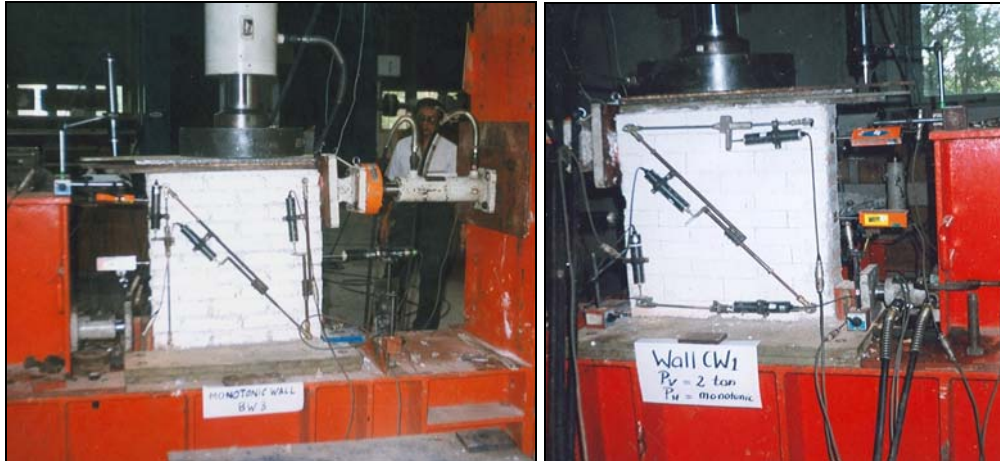


*Figure 4.5 Test configuration of walls with diagonal LVDT*

Formerly, 3 LVDTs were located inside the area of wall surface to measure diagonal, vertical, and horizontal relative displacements, as shown in Figure 4.5. As horizontal load kept increasing on the specimens, these LVDTs did not work properly. Therefore, all recorded inner relative displacements were not considered. The only displacements correctly recorded were horizontal displacements, which were evaluated in the same direction of acted lateral loads. Two hydraulic jacks of capacity of 20 ton-f and 30 ton-f, were installed on a loading frame with capacity of 100 ton-f, to produce vertical and horizontal force respectively. Seven LVDTs were also installed to measure vertical and horizontal displacement occurring during the test. All displacements then recorded by using electronic device recorder and transferred directly into computer formatted data. The failure mechanisms were also recorded visually and the samples of two models of wall failure pattern are shown in Figure 4.6.





*Figure 4.6 Wall failure pattern caused by lateral loads*

### 4.3 General response of walls under monotonic, repeated and cyclic lateral in-plane loads

#### 4.3.1 Walls BW

In this experiment, lateral in-plane loads applied on wall panels were not only of the monotonic type but they also acted in repeated and cyclic manner. The failure patterns and load-horizontal displacements of specimens were also evaluated by grouping each type of wall taken from every single test done to wall specimen, under parameter of compressive pressure and type of lateral load. The results reported in the following sections were recorded according to the classification of each type of wall, with the same magnitude of compressive pressure.

##### **4.3.1.1 Walls BW under vertical pressure $p_v = 0.165$ MPa ( $P_v = 1.0$ ton-f)**

The test results of brick wall without surface mortar plaster, otherwise noted as wall BW under compressive pressure of  $p_v = 0.165$  MPa, are shown in Figures 4.7, 4.8, and 4.9. By observing the failure pattern of walls BW04, BW06 and BW17 under increasing monotonic, repeated and cyclic lateral loads, the major failure types of these three walls are slip failures. The maximum capacities of walls to retain lateral load were also recorded. Under this magnitude of compressive pressure, the wall BW04 retained 74.38 kN of monotonic lateral load, wall BW06 retained 58.85 kN of repeated lateral load and wall BW17 retained 47.38 kN of cyclic lateral load. The capacity of wall BW17 decreased to 64% of that of wall BW04.

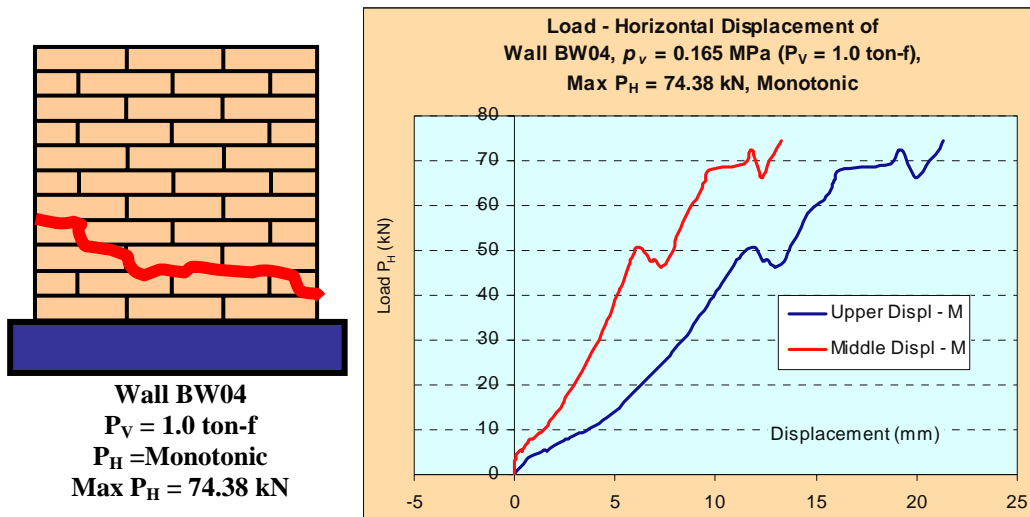


Figure 4.7 Failure pattern and load-displacement of wall BW04

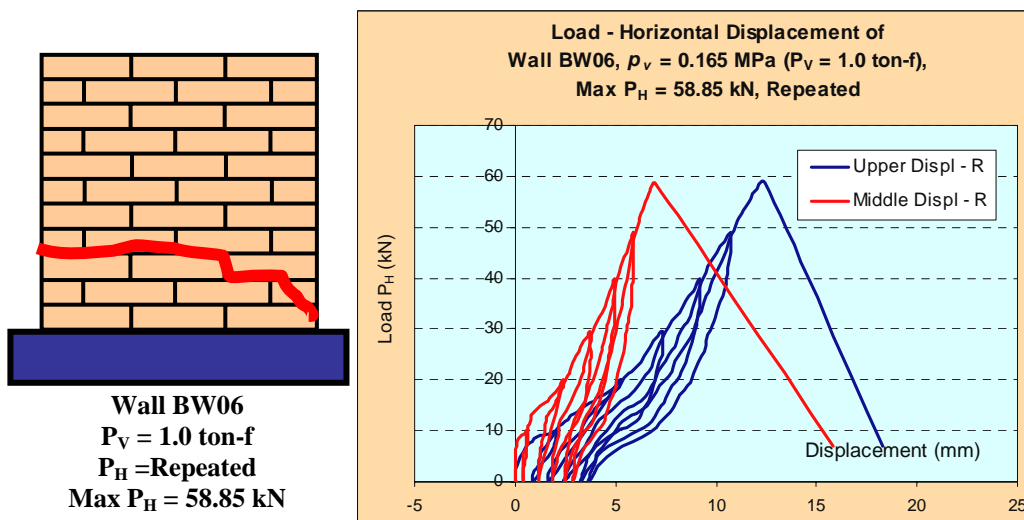


Figure 4.8 Failure pattern and load-displacement of wall BW06

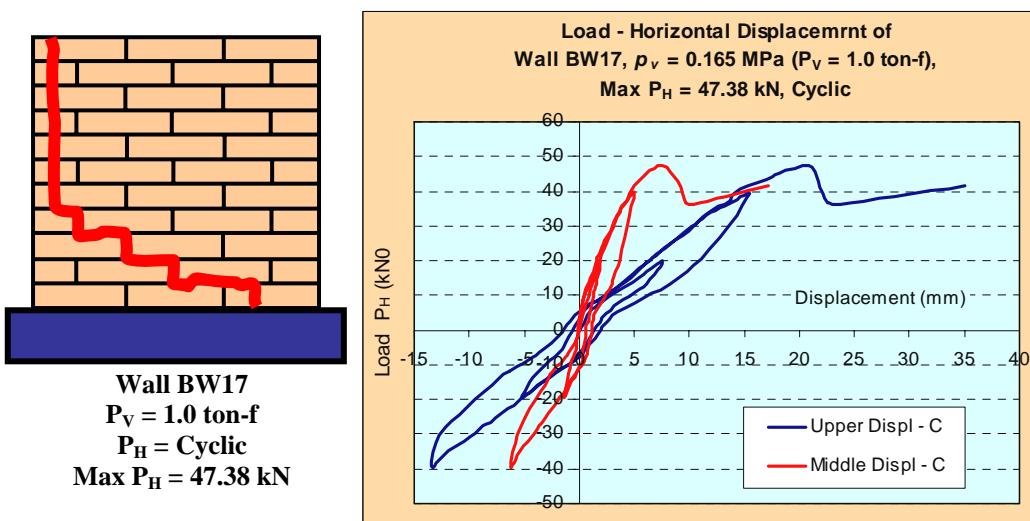


Figure 4.9 Failure pattern and load-displacement of wall BW17

#### 4.3.1.2 Walls BW under vertical pressure $p_v = 0.245$ MPa ( $P_V = 1.5$ ton-f)

Vertical pressures of  $p_v = 0.245$  caused by  $P_V = 1.5$  ton-f were applied to walls BW03, BW09 and BW18 in combination with monotonic, repeated and cyclic lateral loads. Walls BW03 and BW09 collapsed in slip and diagonal shear failure pattern. Both walls BW03 and BW09 were stronger than wall BW18. The capacity of wall BW18 in retaining lateral load was less than 30% of those found in walls BW03 and BW09. The wall BW18 collapsed in brittle failure mechanism with combination of compression, slip and diagonal failure. All failure patterns of walls BW03, BW09 and BW18 are shown in Figures 4.10, 4.11, 4.12 and 4.13. The failure pattern of wall BW18 is similar to that of wall BW17. As the cyclic load was applied, the compressive failure pattern occurred with combination of slip and crushing failure.

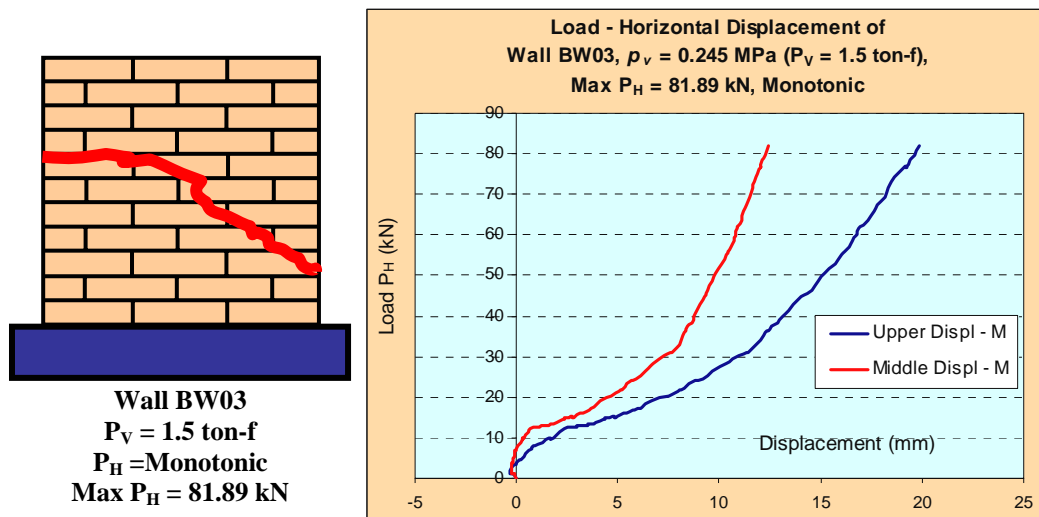


Figure 4.10 Failure pattern and load-displacement of wall BW03

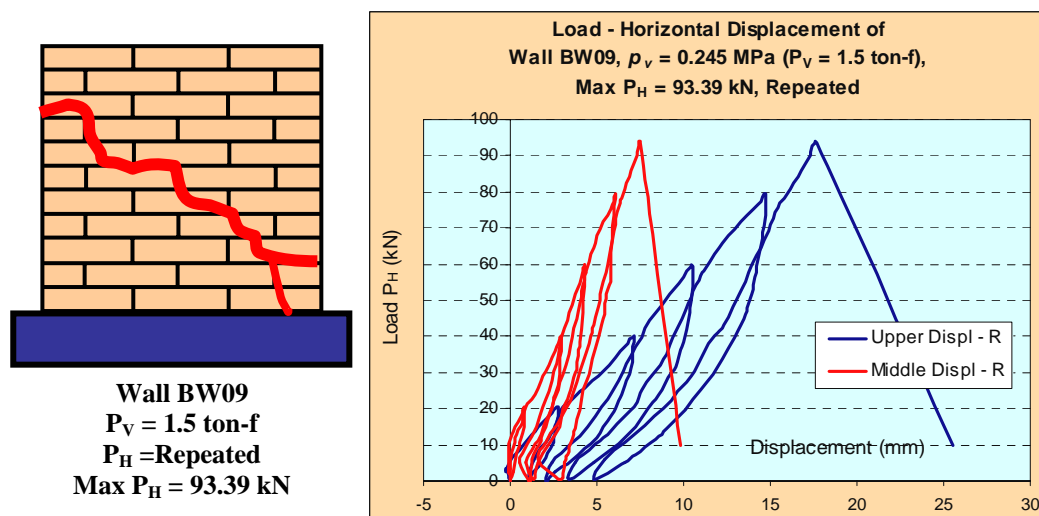


Figure 4.11 Failure pattern and load-displacement of wall BW09



Figure 4.12 Failure pattern of wall BW09

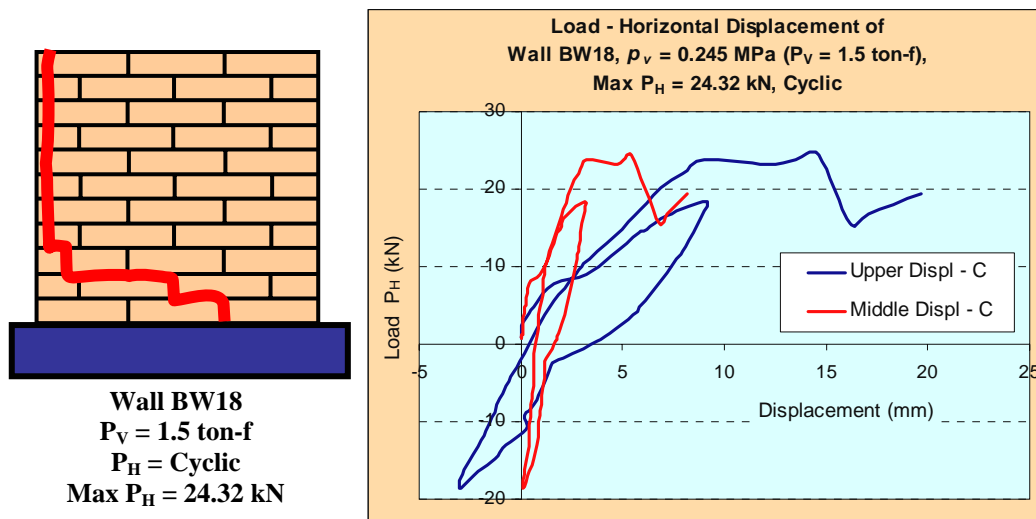


Figure 4.13 Failure pattern and load-displacement of wall BW18

#### 4.3.1.3 Walls BW under vertical pressure $p_v = 0.325 \text{ MPa}$ ( $P_V = 2.0 \text{ ton-f}$ )

Figures 4.14, 4.15, 4.16, 4.17 and 4.18 show the response of wall BW under vertical pressure of 0.325 MPa. Slip failure occurred in walls under monotonic and repeated lateral loads, as seen in Figures 4.14 and 4.15. Walls BW07 and BW08 were compressed by the same pressure, but the failure types were different. Wall BW07 was weaker than wall BW08; the weakness was caused by the capacity of bond shear strength between mortar and brick layers, which was not uniform. Wall BW07 exhibited slip failure pattern. Walls BW08 under repeated load and BW19 under cyclic load collapsed in diagonal shear failure pattern, as shown in Figures 4.16 and 4.18. The capacities of retaining lateral loads were 71.57 kN and 50.91 kN respectively. As the compressive stress increased, diagonal failure pattern occurred

in walls BW08 and BW19. Brittle collapse mechanism of wall BW08 is shown in Figure 4.17, with some crushing failure at the bottom support. The capacity of wall BW19 under cyclic load was 60% of that of the wall BW05 under monotonic load.

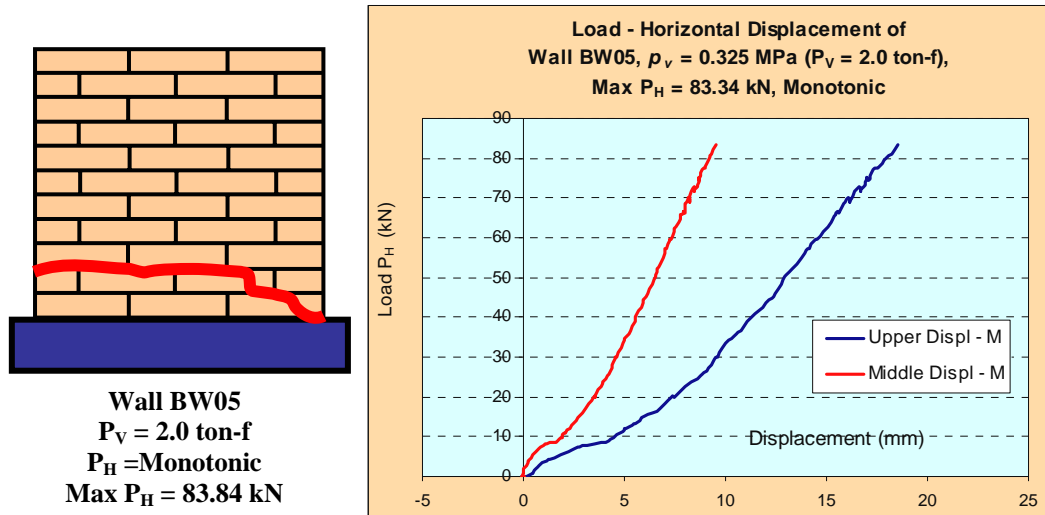


Figure 4.14 Failure pattern and load-displacement of wall BW05

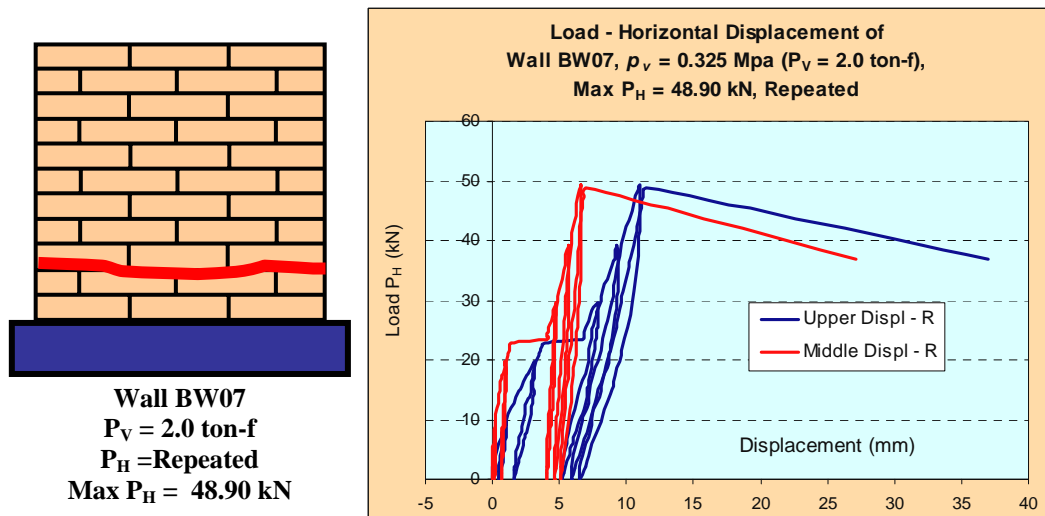


Figure 4.15 Failure pattern and Load-displacement of wall BW07

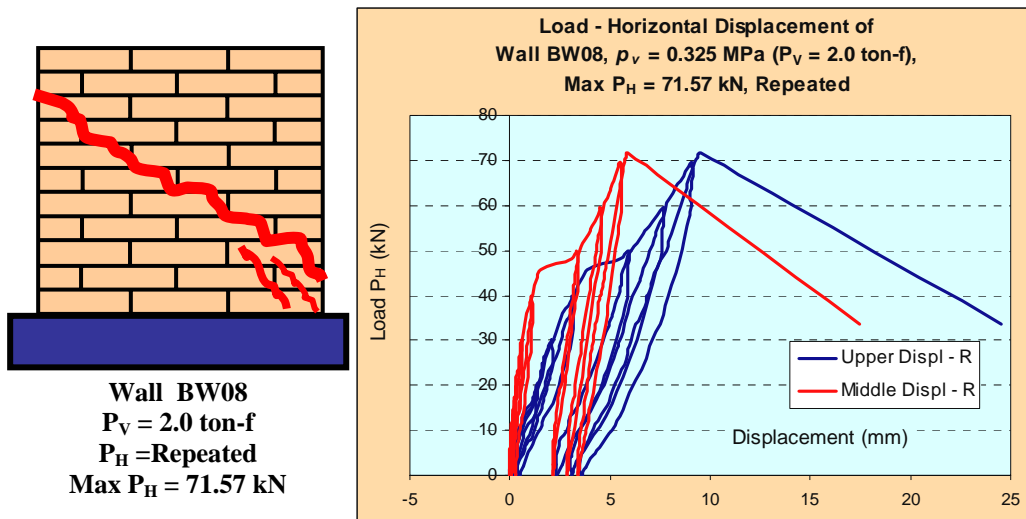


Figure 4.16 Failure pattern and load-displacement of wall BW08

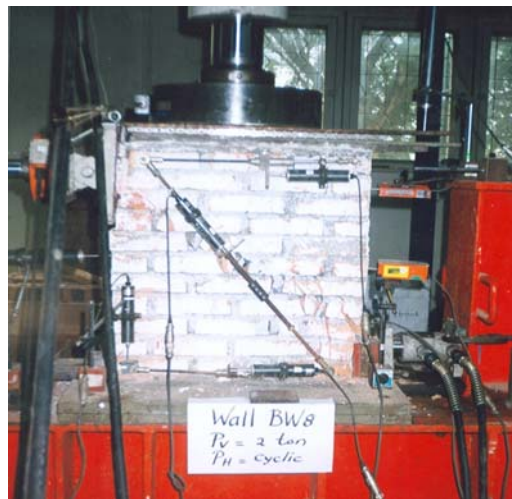


Figure 4.17 Failure pattern of wall BW08

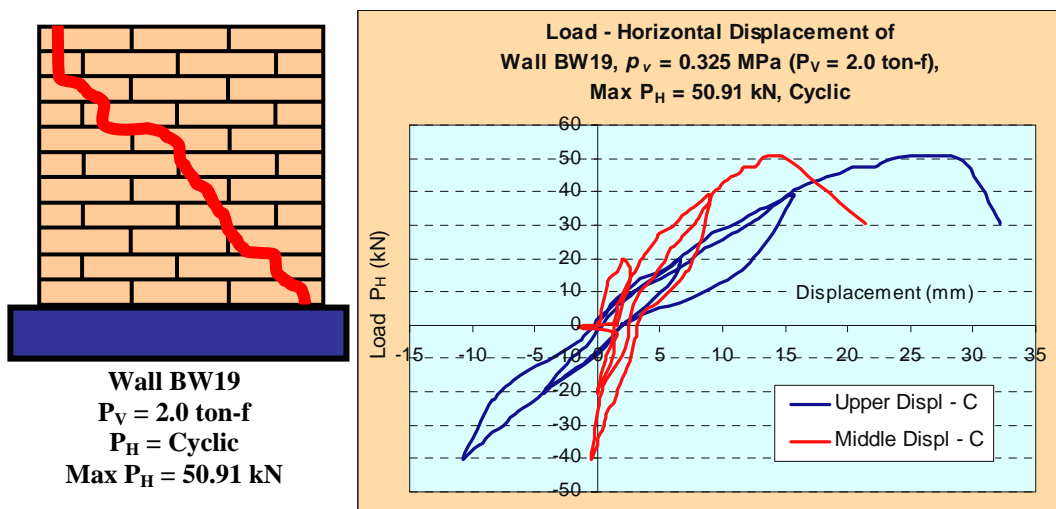


Figure 4.18 Failure pattern and load-displacement of wall BW19



#### 4.3.1.4 Walls BW under vertical pressure $p_v = 0.42$ MPa ( $P_v = 2.5$ ton-f)

The response of walls BW to the lateral loads combined with compressive pressures of 0.42 MPa are shown in Figures 4.19, 4.20, 4.21 and 4.22. Slip failure did not occur as the compressive pressure became higher. Wall panels became more compact under this pressure and diagonal shear failures crossing the bricks were found in walls BW21 and BW10. Figure 4.20 shows a real condition of wall BW21 before and after testing.

Wall BW20 was tested under cyclic load. Compressive crushing failure combined with diagonal shear failure happened during the test. As the four different magnitude of compressive pressures of cyclic lateral loads were applied to walls BW, all these wall were considered to be the weakest compared to those subjected to either monotonic or repeated loads.

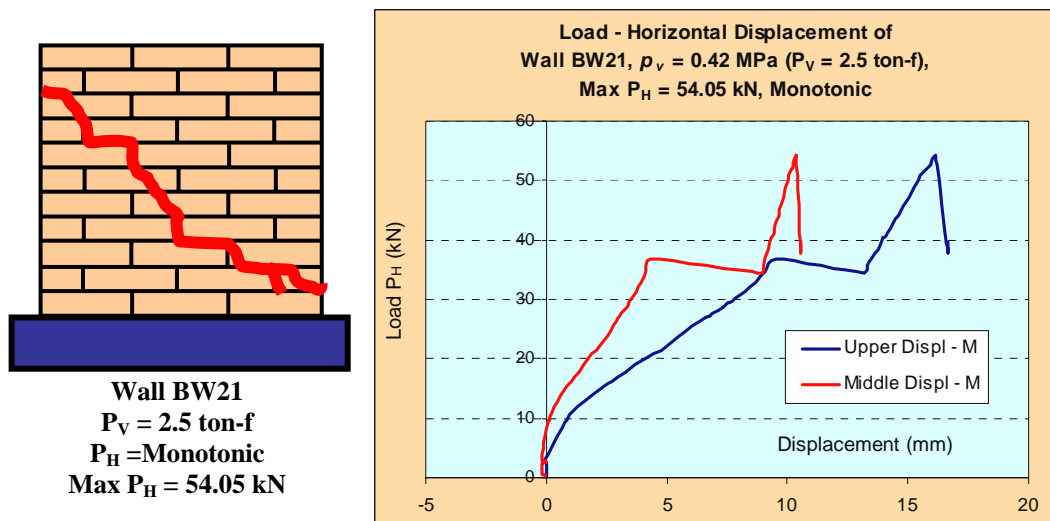


Figure 4.19 Failure pattern and load-displacement of wall BW21



Figure 4.20 Wall BW 21 before and after testing

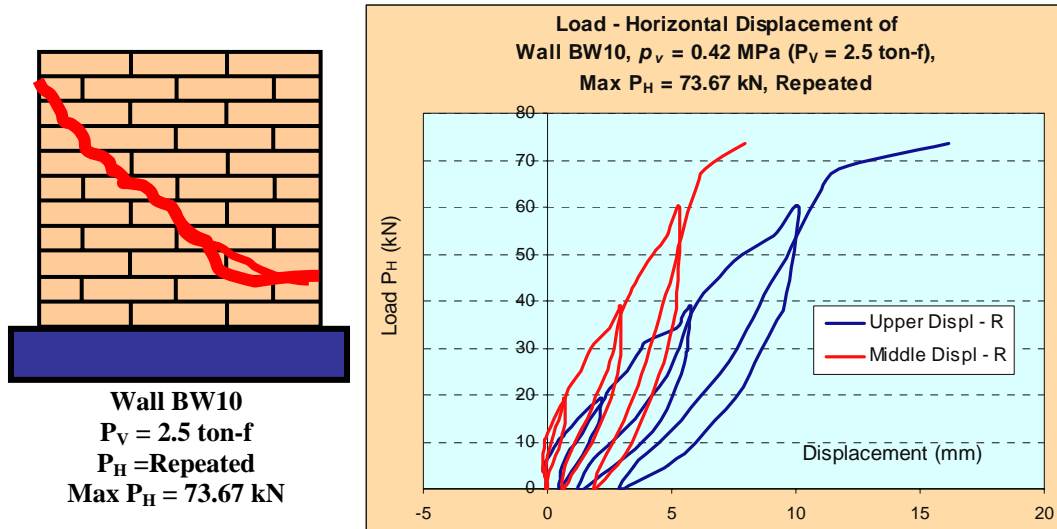


Figure 4.21 Failure pattern and load-displacement of wall BW10

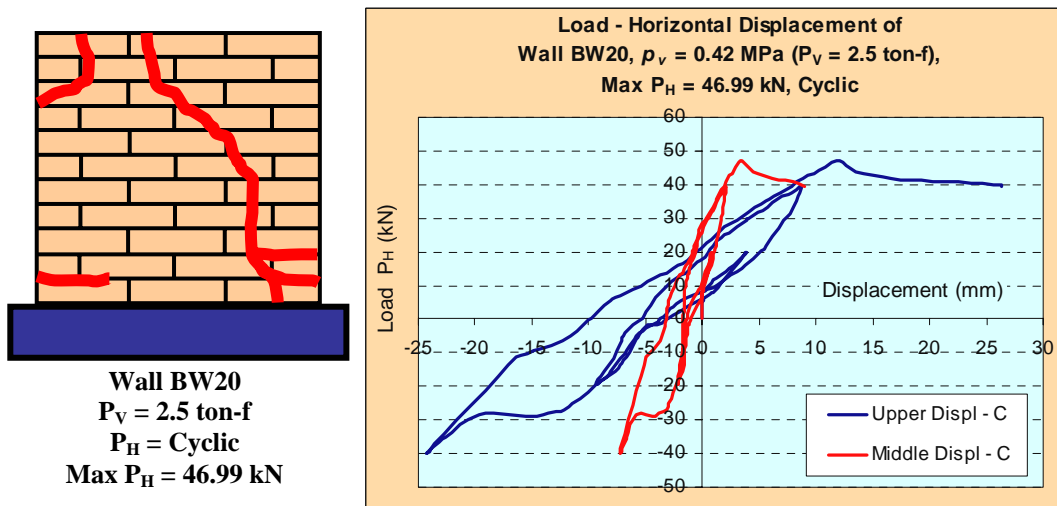


Figure 4.22 Failure pattern and load-displacement of wall BW20

### 4.3.2 Walls MW

In these experimental tests, walls MW were evaluated under combination of vertical pressures of  $p_v = 0.08 \text{ MPa}$ ,  $0.165 \text{ MPa}$ ,  $0.245 \text{ MPa}$ ,  $0.325 \text{ MPa}$ ,  $0.42 \text{ MPa}$  and monotonic, repeated and cyclic horizontal loads. The following section describe responses of each wall MW to applied vertical and horizontal loads.

#### 4.3.2.1 Walls MW under vertical pressure $p_v = 0.08 \text{ MPa}$ ( $P_V = 0.5 \text{ ton-f}$ )

Walls MW20 and MW21 were tested under  $p_v = 0.08 \text{ MPa}$  in combination of repeated and cyclic lateral loads respectively. Wall MW21 under cyclic load was weaker than wall MW20 under repeated load. The capacity of Wall MW21 was 52%



of that of the wall MW20. Both walls collapsed in brittle failure mechanism with very small ductility. Shear diagonal failure patterns were found in both specimens, as shown in Figures 4.23 and 4.24. The photograph of failure pattern of wall MW21 is also shown in Figure 4.25. It can be seen that the crack propagated gradually, as failure mechanism started at mortar plaster portion. There is no slip between mortar and brick during failure. The collapse mechanism of wall MW was significantly affected by the contribution of mortar plaster over wall surface.

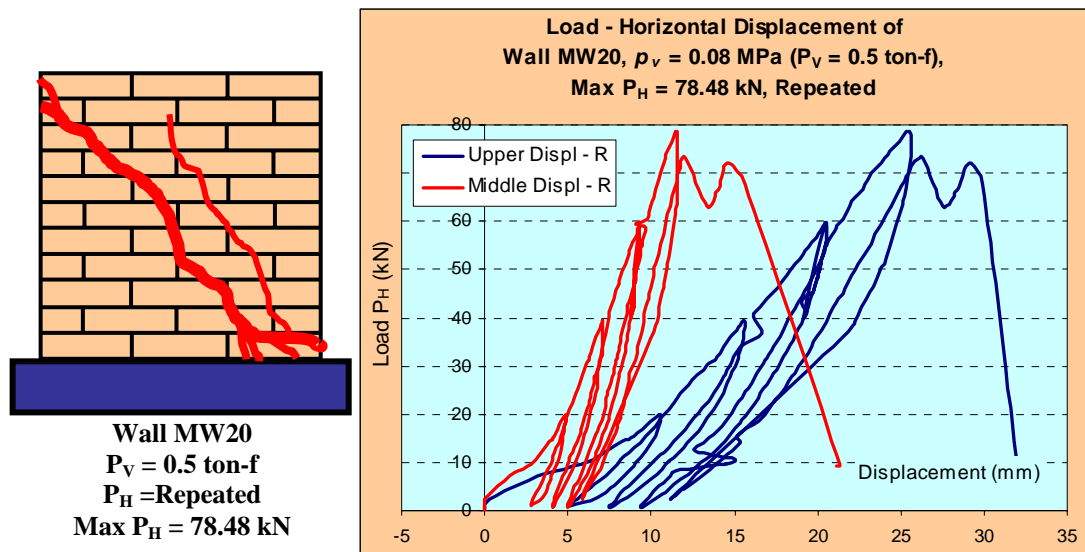


Figure 4.23 Failure pattern and load-displacement of wall MW20

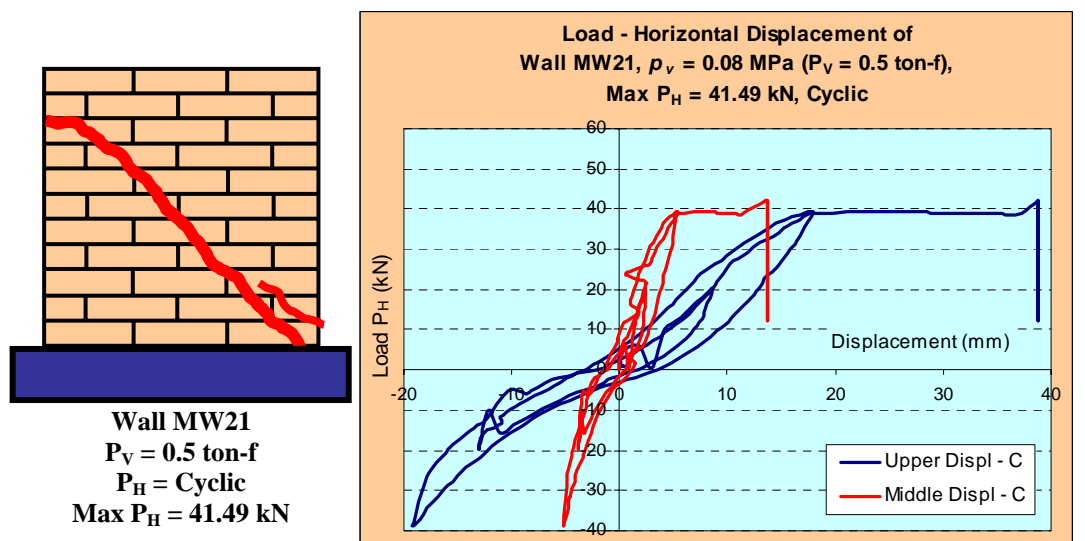


Figure 4.24 Failure pattern and load-displacement of wall MW21



*Figure 4.25 Failure type of wall MW21*

#### **4.3.2.2 Walls MW under vertical pressure $p_v = 0.165$ MPa ( $P_v = 1.0$ ton-f)**

Compressive pressure of 0.165 MPa was applied to walls MW08, MW02, MW22, and MW16. As seen in Figure 4.26, wall MW08 collapsed in brittle failure, and its capacity of retaining lateral force was 176.78 kN. When lateral load reached 168 kN, crack propagated in combination of slip and diagonal shear type, until the specimen collapsed completely. From this experiment, it can be seen that the role of mortar plaster significantly increases the capacity of the wall in retaining lateral load.

In Figure 4.27, wall MW02 collapsed in diagonal shear failure, without ductility. The capacity of wall MW02 is 67% of that of the wall MW08. Brittle failure and gradual collapse happened. Figures 4.28 and 4.29 illustrate the responses of walls MW22 and MW16, both under compression force of 1 ton-f and cyclic lateral load. Shear diagonal failure pattern occurred in both specimens, and compressive failure was more dominant in wall MW22. The capacity of walls MW22 and MW16 is low compare to that of walls MW08 and MW02. In general, the capacity of walls MW22 and MW16 was 27% of that of the wall MW08 under monotonic load.

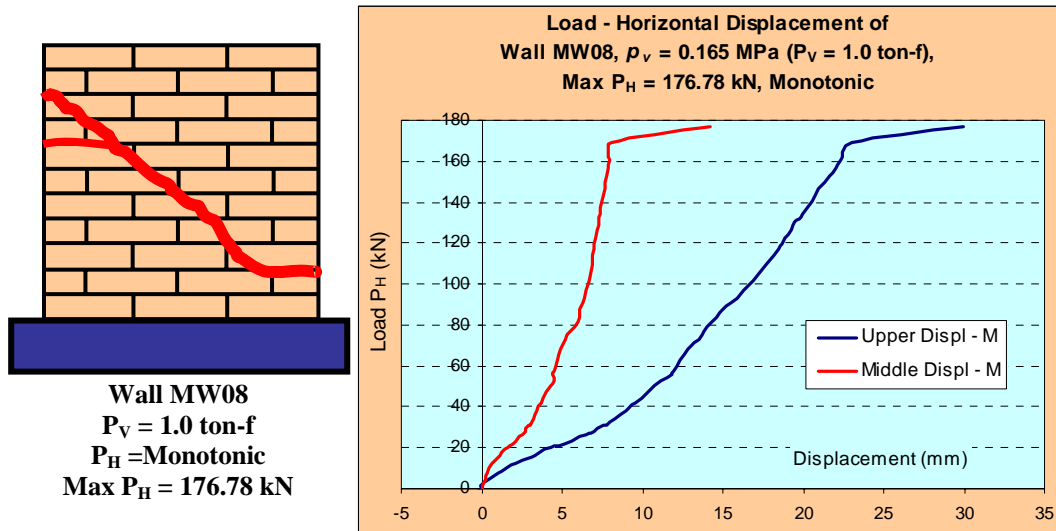


Figure 4.26 Failure pattern and load-displacement of wall MW08

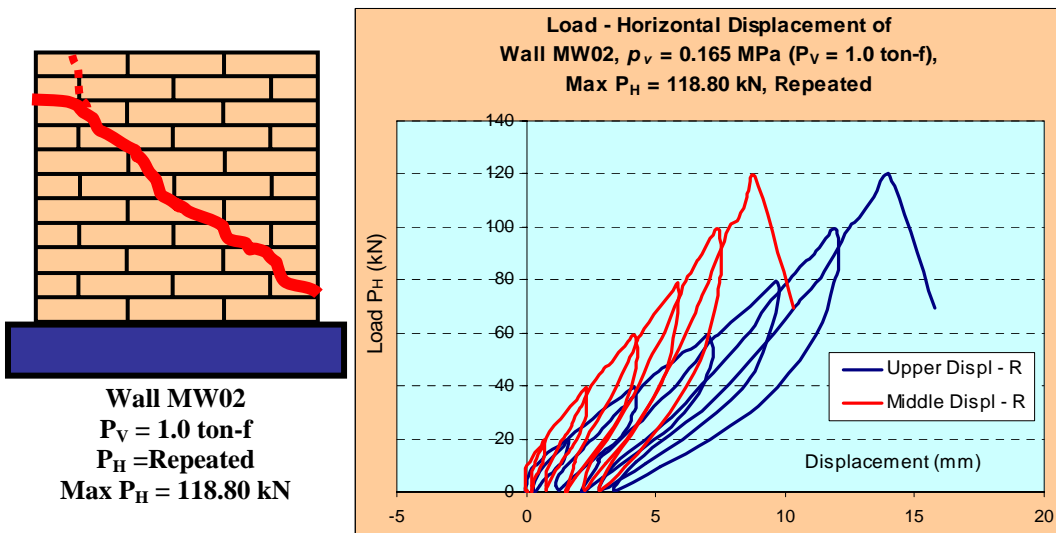


Figure 4.27 Failure pattern and load-displacement of wall MW02

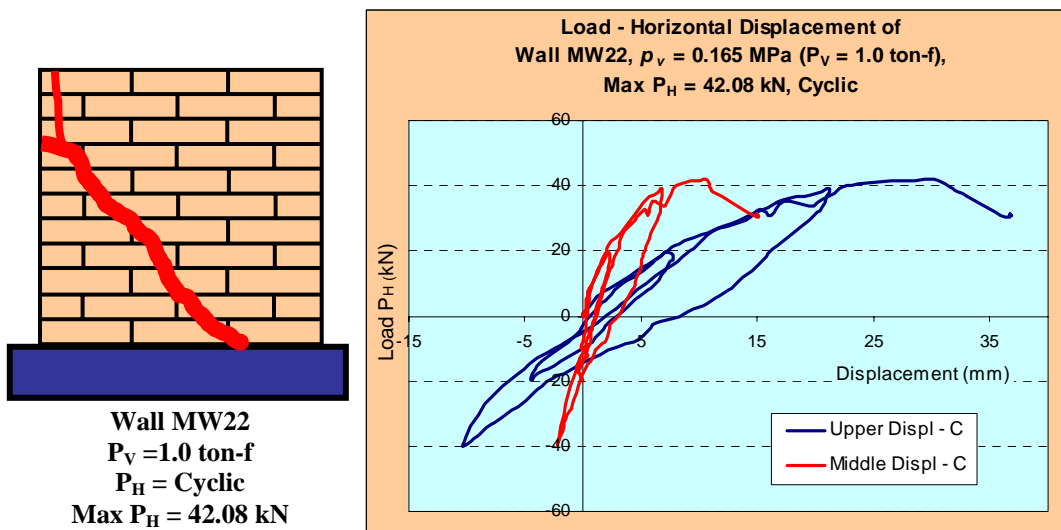


Figure 4.28 Failure pattern and load-displacement of wall MW22

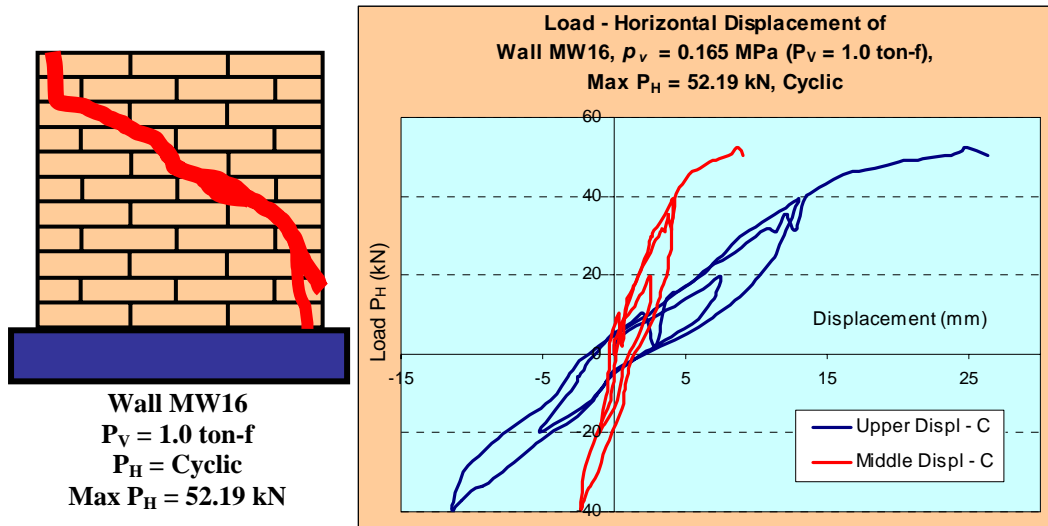


Figure 4.29 Failure pattern and load-displacement of wall MW16

#### 4.3.2.3 Wall MW under vertical pressure $p_v = 0.245 \text{ MPa}$ ( $P_V = 1.5 \text{ ton-f}$ )

Walls MW07, MW03, MW17 were tested under  $p_v = 0.245 \text{ MPa}$ , with  $P_H$  monotonic, repeated and cyclic types respectively. The failure patterns were mostly in diagonal shear failure, combined with slip at the bottom support and near the applied lateral load. Compressive crack did not appear in these three specimens, as shown in Figures 4.30, 4.31 and 4.32. In Figures 4.30 and 4.31, walls MW07 and MW03 performed to a higher capacity in resisting lateral load, compared to wall MW17. In Figure 4.32, wall MW17 collapsed gradually in diagonal shear failure pattern with brittle collapse mechanism. The capacity of wall MW17 under cyclic load was 27% of that of the wall MW07 under monotonic load.

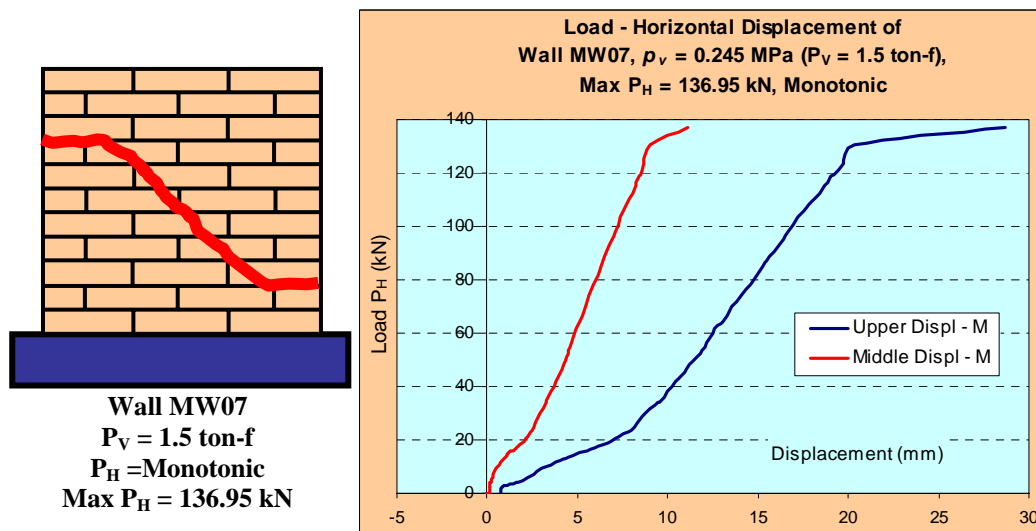


Figure 4.30 Failure pattern and load-displacement of wall MW07

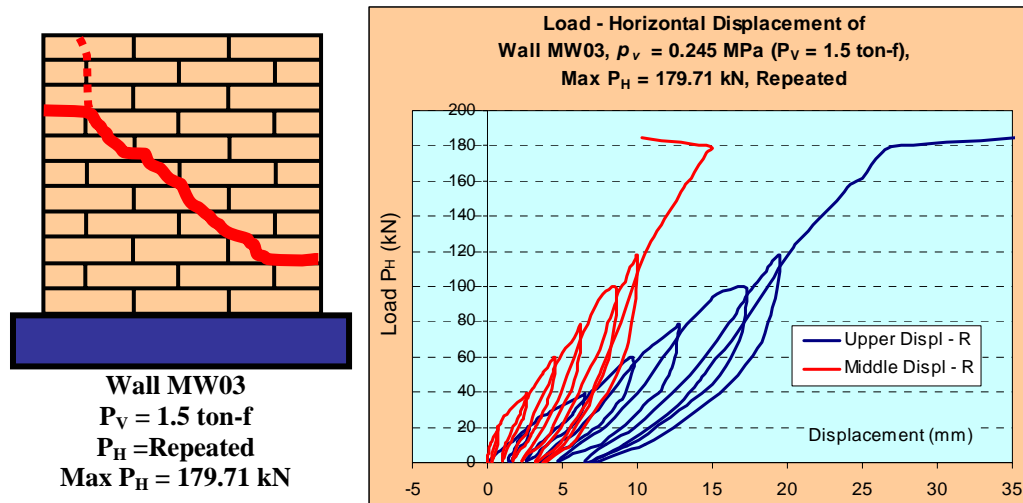


Figure 4.31 Failure pattern and load-displacement of wall MW03

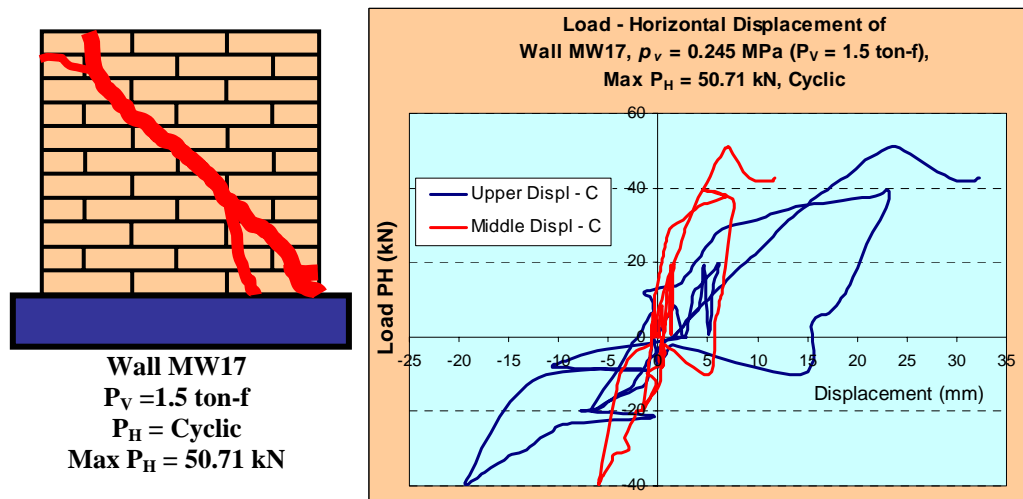


Figure 4.32 Failure pattern and load-displacement of wall MW17

#### 4.3.2.4 Walls MW under vertical pressure $p_v = 0.325 \text{ MPa}$ ( $P_V = 2.0 \text{ ton-f}$ )

In Figures 4.33, 4.34 and 4.35 vertical compressive pressure of  $p_v = 0.325 \text{ MPa}$  caused similar response in walls MW under monotonic and repeated load. Walls MW01 and MW04 were stiffer than wall MW18. Walls MW01 and MW04 collapsed in diagonal shear failure pattern. Capacity of wall MW18 in retaining cyclic load was about 30% of that of the walls MW01 and MW04, and its failure pattern was a combination of shear diagonal and compressive failure. It can also be seen that wall failure pattern was dominated by the presence of surface mortar over wall surface.

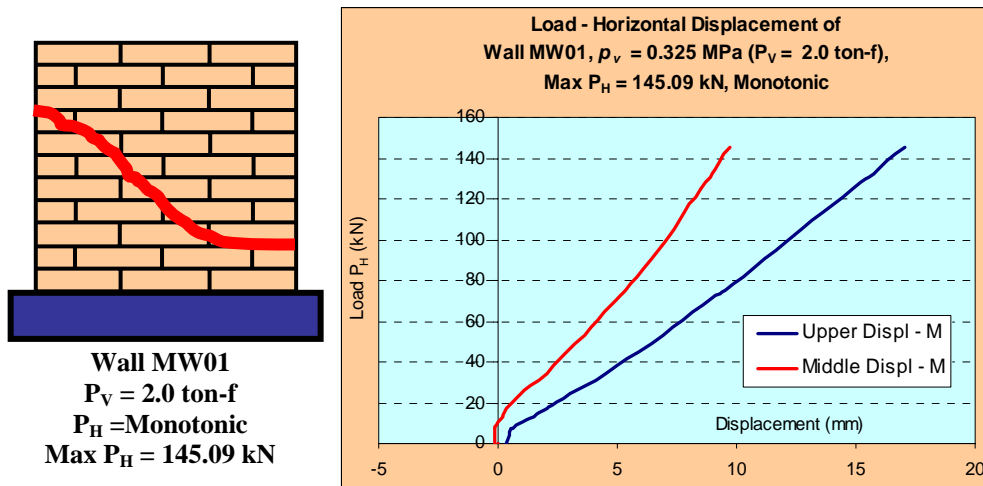


Figure 4.33 Failure pattern and load-displacement of wall MW01

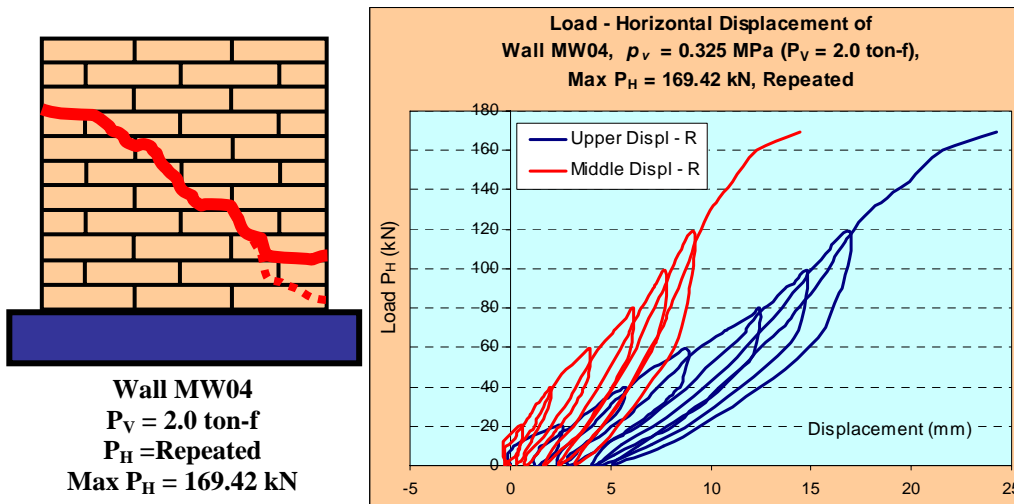


Figure 4.34 Failure pattern and load-displacement of wall MW04

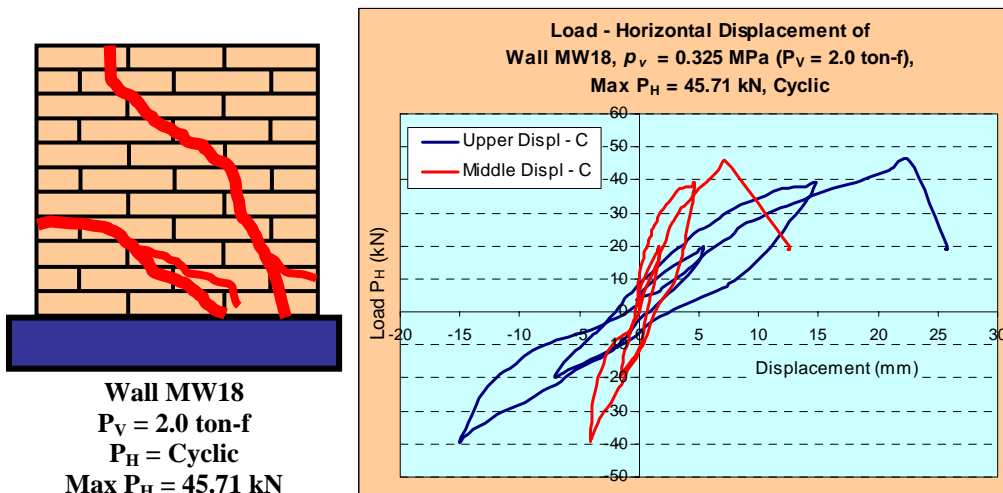


Figure 4.35 Failure pattern and load-displacement of wall MW18

#### 4.3.2.5 Walls MW under vertical pressure $p_v = 0.42$ MPa ( $P_V = 2.5$ ton-f)

As  $p_v$  increased up to 0.42 MPa, the failure of walls MW06, MW05 and MW19 appeared in shear diagonal failure pattern. These patterns are shown in Figures 4.36, 4.37 and 4.38. Wall MW19 under cyclic lateral load was the weakest among them all. The capacity of wall MW19 was 30% of that of wall MW05 and its lateral stiffness was 40% of that of the wall MW06 or MW05. No ductility occurred in this test. Combination of slip and shear diagonal failure was found in wall MW05.

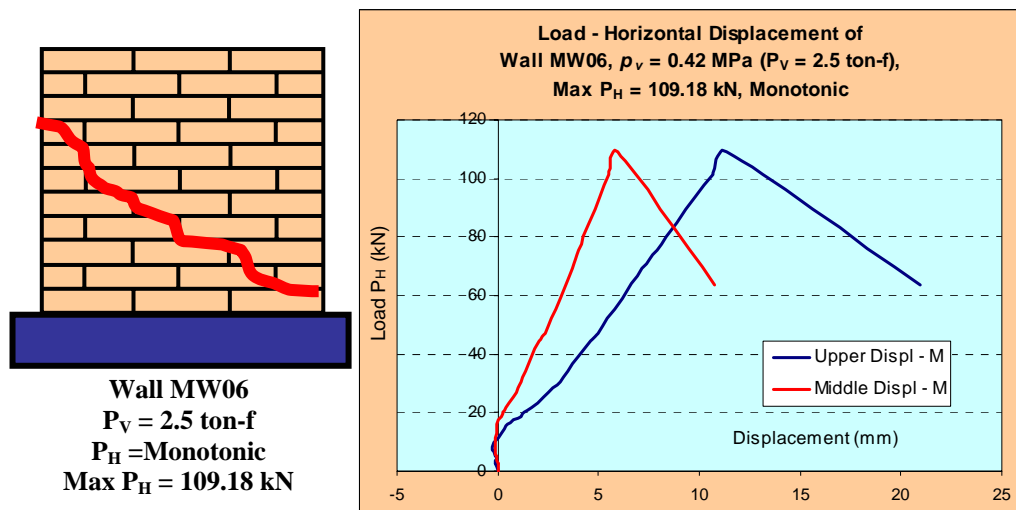


Figure 4.36 Failure pattern and load-displacement of wall MW06

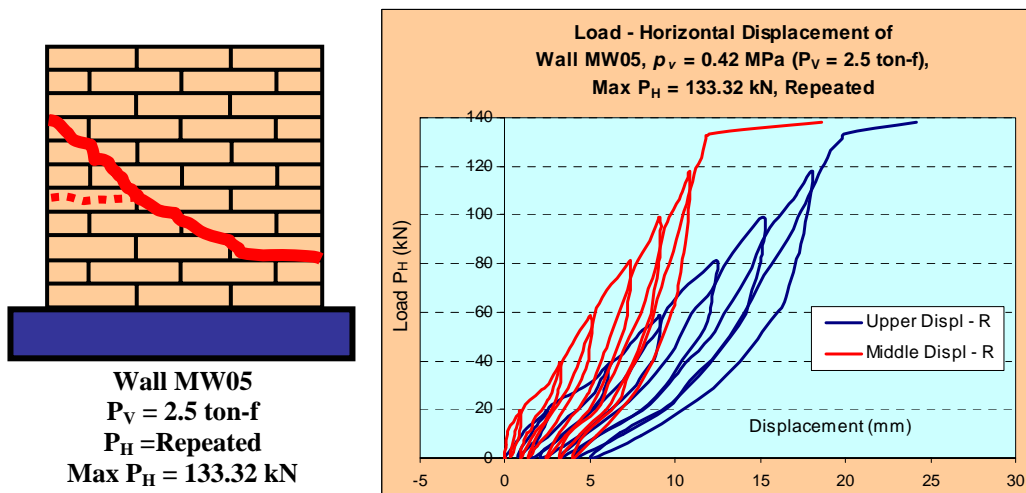


Figure 4.37 Failure pattern and load-displacement of wall MW05

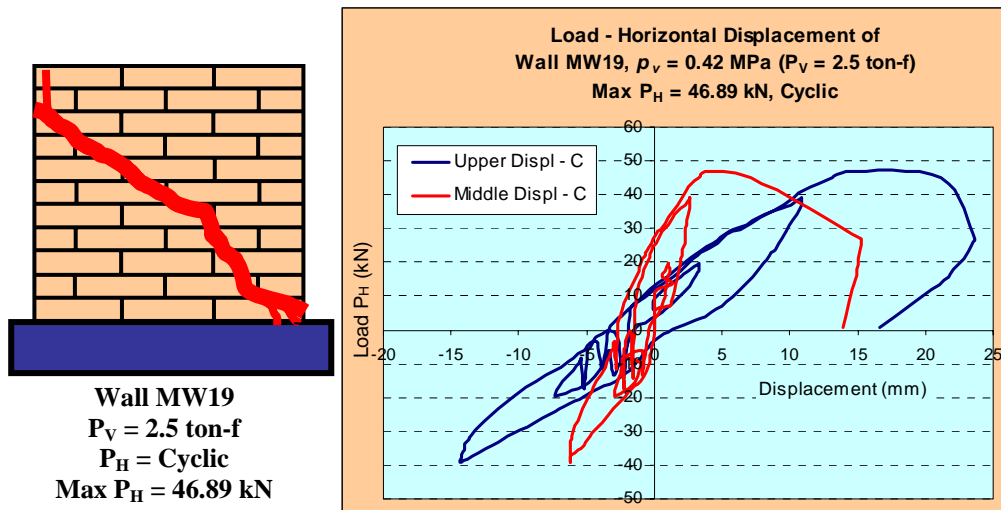


Figure 4.38 Failure pattern and load-displacement of wall MW19

### 4.3.3 Walls CW

Combination of compressive pressure  $p_v = 0.08 \text{ MPa}$ ,  $0.165 \text{ MPa}$ ,  $0.245 \text{ MPa}$ ,  $0.325 \text{ MPa}$ ,  $0.42 \text{ MPa}$  and monotonic, repeated and cyclic horizontal load were applied to walls CW. All responses of wall CW are explained in the following sections.

#### 4.3.3.1 Walls CW under vertical pressure $p_v = 0.08 \text{ MPa}$ ( $P_V = 0.5 \text{ ton-f}$ )

Walls CW19 and CW20 were compressed under  $P_V = 0.5 \text{ ton-f}$  and loaded under repeated and cyclic lateral loads. Wall CW20 was 52% weaker than wall CW19. Wall CW19 collapsed in diagonal shear failure pattern, but wall CW20 collapsed partially at corner local region, which was affected by compressive pressure. The responses are shown in Figures 4.39 and 4.40.

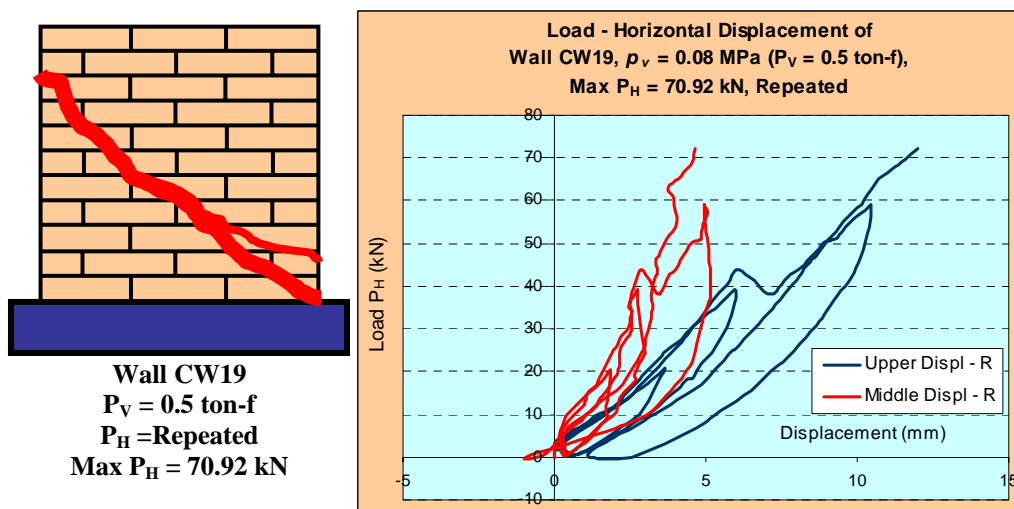


Figure 4.39 Failure pattern and load-displacement of wall CW19



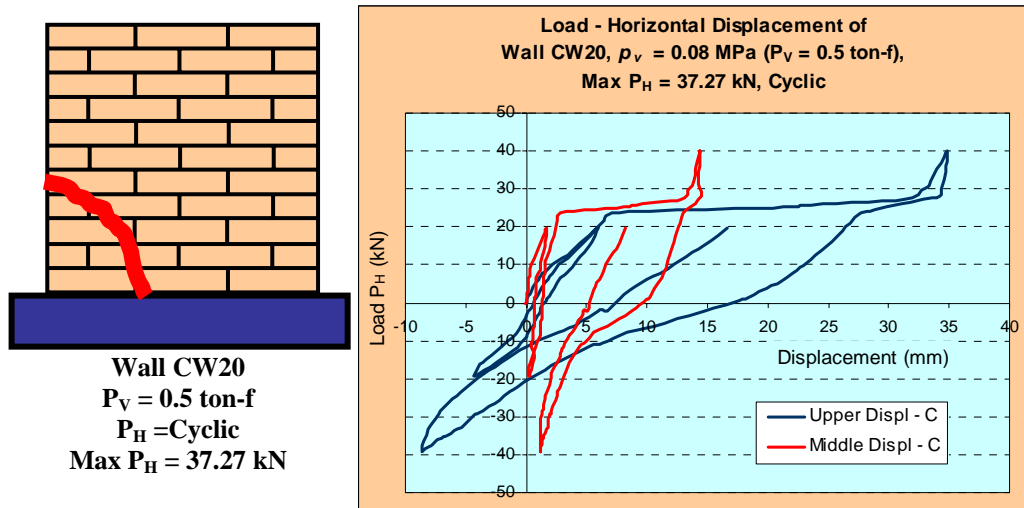


Figure 4.40 Failure pattern and load-displacement of wall CW20

#### 4.3.3.2 Walls CW under vertical pressure $p_v = 0.165 \text{ MPa}$ ( $P_V = 1.0 \text{ ton-f}$ )

In Figures 4.41, 4.42 and 4.43, failure patterns of walls CW07 and CW02 were similar in types. Walls' capacities in retaining lateral loads were almost the same and their stiffness patterns were similar. In Figures 4.44 and 4.45, walls CW15 and CW21 were loaded under cyclic lateral loads and collapsed in very brittle failure mechanisms. For wall CW15, the failure pattern happened locally, at upper part near compression load. Failure type of wall CW21 was predominantly influenced by compressive failure. The capacities of walls CW15 and CW21 in retaining cyclic lateral loads were 50% lower than those of the walls CW07 and CW02.



Figure 4.41 Failure type of Wall CW07

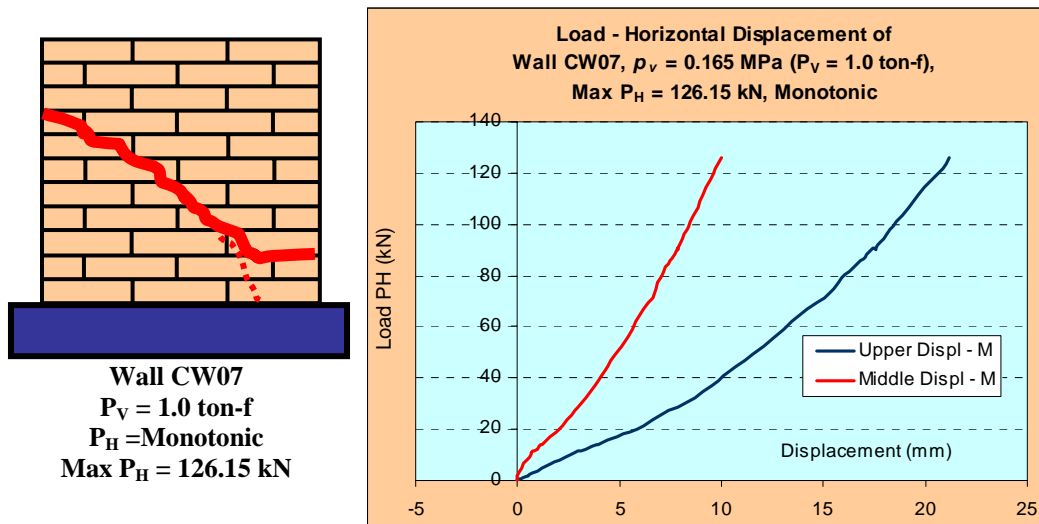


Figure 4.42 Failure pattern and load-displacement of wall CW07

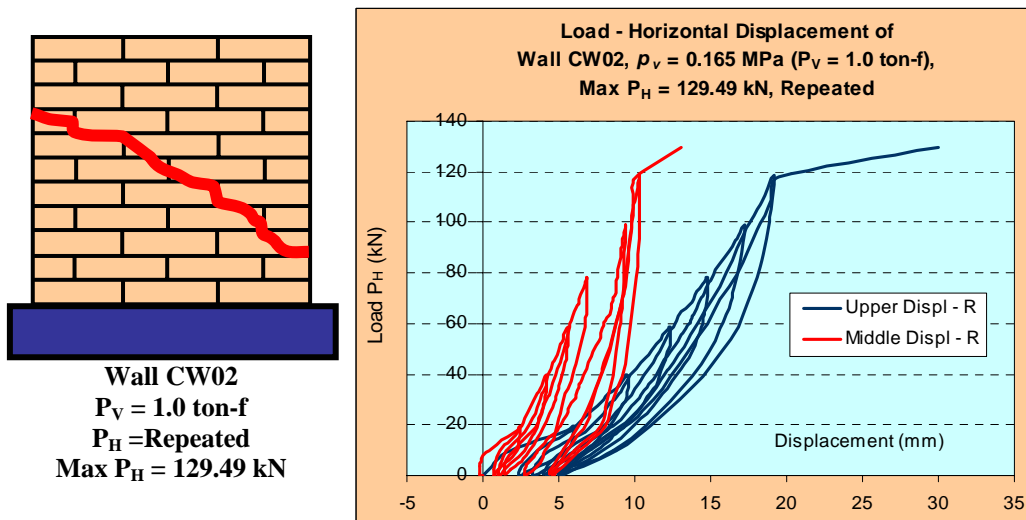


Figure 4.43 Failure pattern and load-displacement of wall CW02

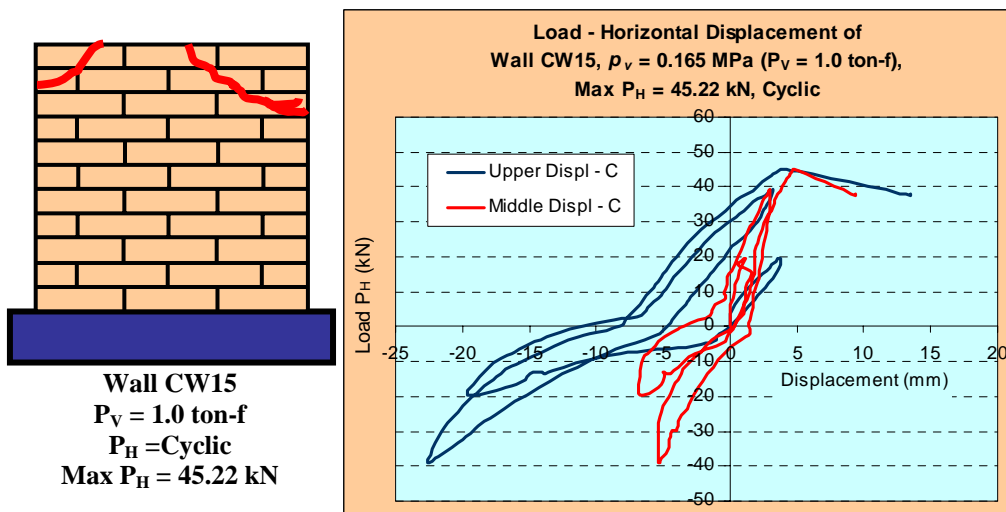


Figure 4.44 Failure pattern and load-displacement of wall CW15

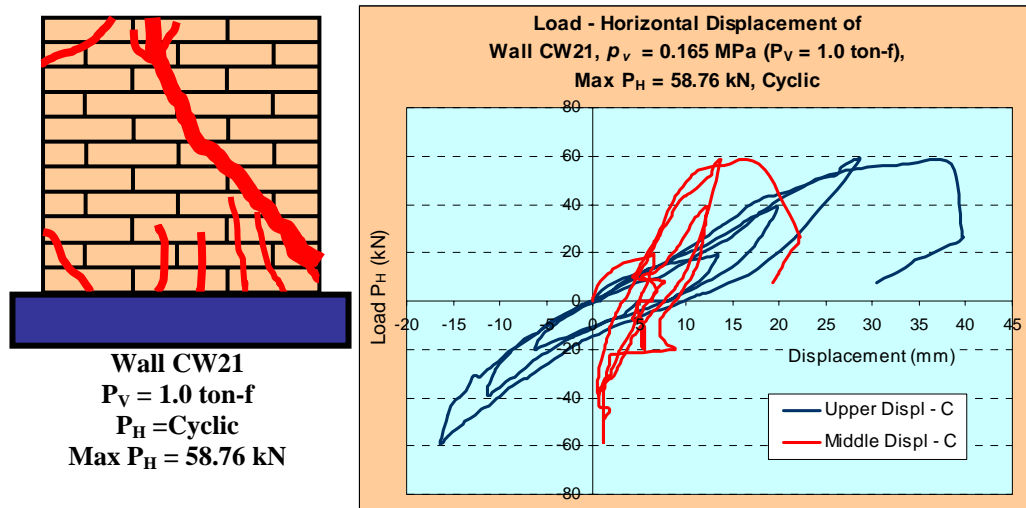


Figure 4.45 Failure pattern and load-displacement of wall CW21

#### 4.3.3.3 Walls CW under vertical pressure $p_v = 0.245 \text{ MPa}$ ( $P_V = 1.5 \text{ ton-f}$ )

Shear diagonal failure pattern of walls CW08 and CW03 are shown in Figures 4.46 and 4.47. Load-displacement responses of both walls are similar and wall capacities in retaining lateral load are 122.52 kN and 103.49 kN respectively. As lateral cyclic load was applied to walls CW22 and CW16, wall capacities in retaining cyclic lateral load were 30 – 40 % lower than those of walls CW08 and CW03. Combination of compressive crushing and diagonal shear failure pattern happened to walls under cyclic lateral loads. These phenomena are shown in Figures 4.48 and 4.49

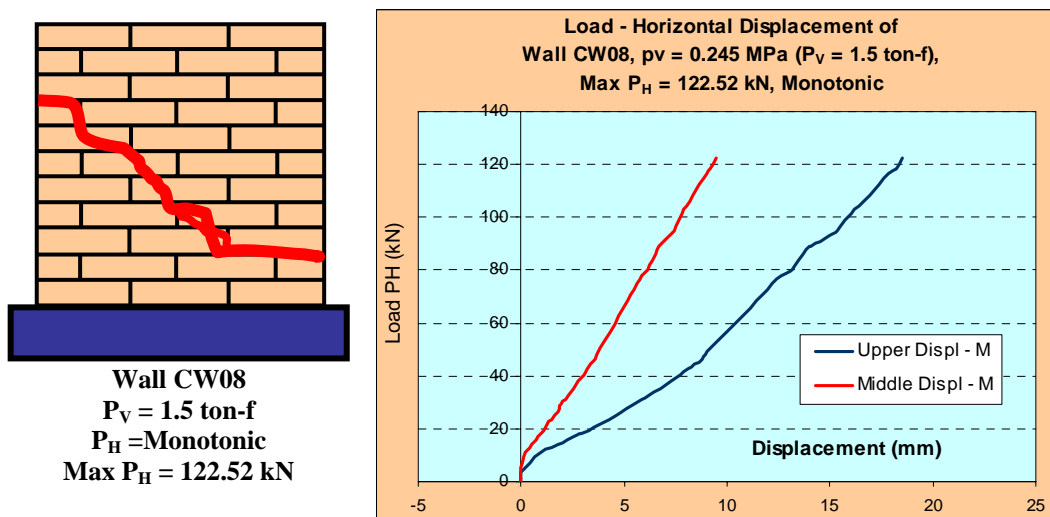
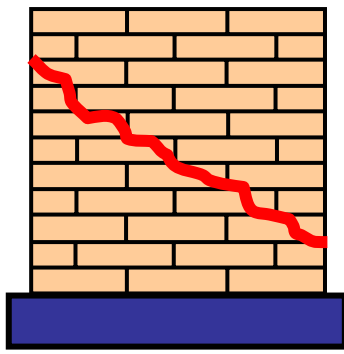


Figure 4.46 Failure pattern and load-displacement of wall CW08



**Wall CW03**  
 $P_V = 1.5 \text{ ton-f}$   
 $P_H = \text{Repeated}$   
 $\text{Max } P_H = 103.49 \text{ kN}$

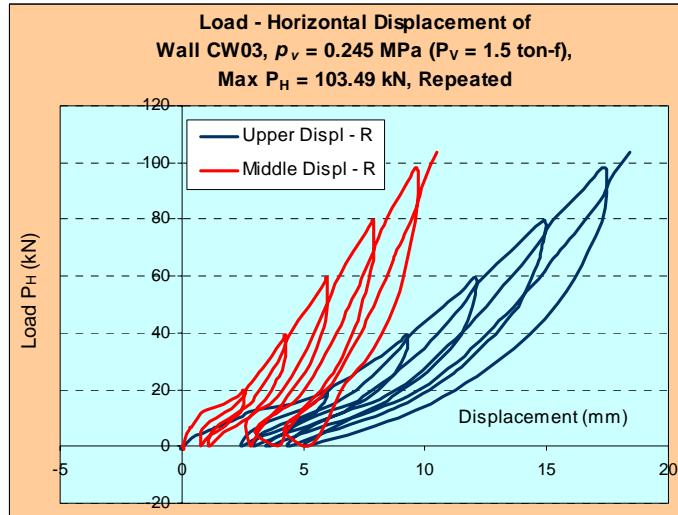
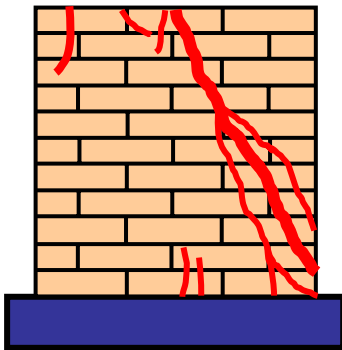


Figure 4.47 Failure pattern and load-displacement of wall CW03



**Wall CW22**  
 $P_V = 1.5 \text{ ton-f}$   
 $P_H = \text{Cyclic}$   
 $\text{Max } P_H = 47.48 \text{ kN}$

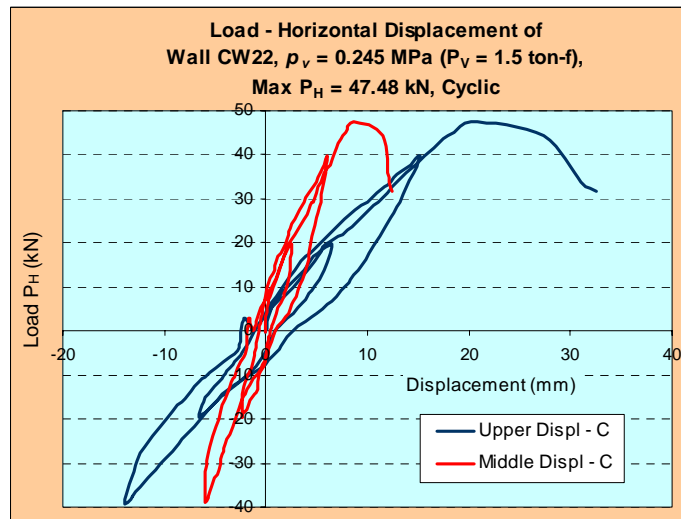
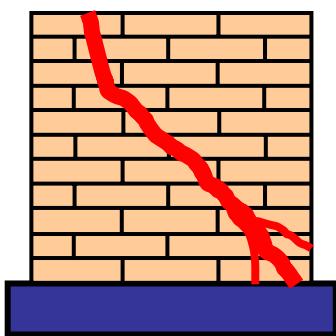


Figure 4.48 Failure pattern and load-displacement of wall CW22



**Wall CW16**  
 $P_V = 1.5 \text{ ton-f}$   
 $P_H = \text{Cyclic}$   
 $\text{Max } P_H = 35.41 \text{ kN}$

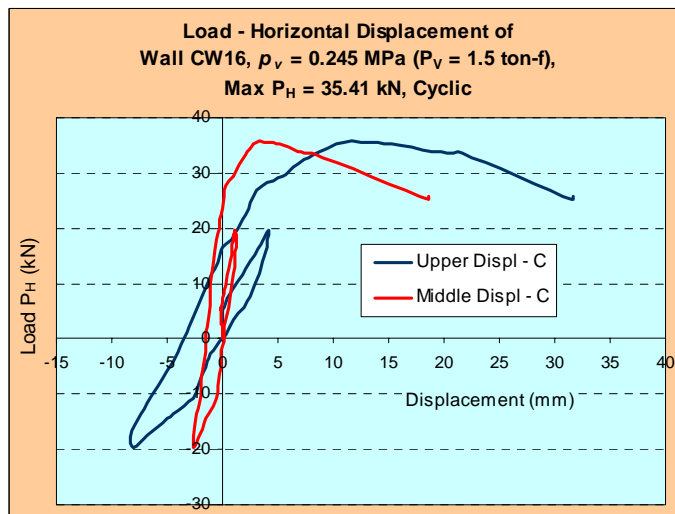


Figure 4.49 Failure pattern and load-displacement of wall CW16

#### 4.3.3.4 Walls CW under vertical pressure $p_v = 0.325 \text{ MPa}$ ( $P_V = 2.0 \text{ ton-f}$ )

In Figure 4.50, as compressive pressure increased, the failure pattern of wall CW01 resulted in shallow diagonal shear failure type. Similar pattern can be seen in Figure 4.51 for wall CW05 under repeated lateral load. Capacity of wall CW05 in retaining lateral load, was lower than that of wall CW01. In Figures 4.52 and 4.53, walls CW17 and CW23 are weaker than walls CW01 and CW05. Wall capacity in retaining cyclic lateral load was 50% of those of the walls CW01 and CW05 under repeated lateral load. Wall CW17 and CW23 collapsed in shear diagonal failure pattern, with very small ductility.

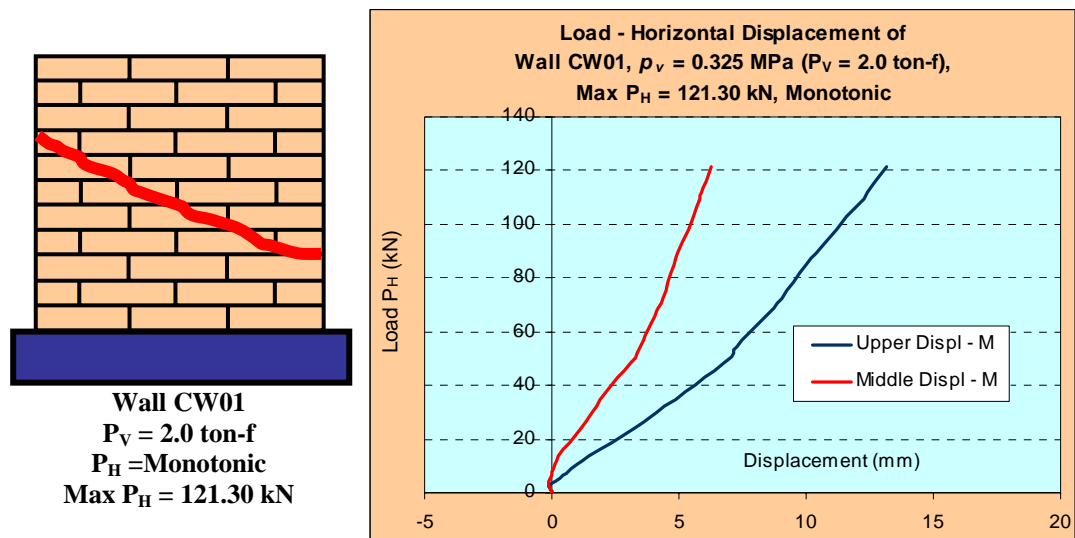


Figure 4.50 Failure pattern and load-displacement of wall CW01

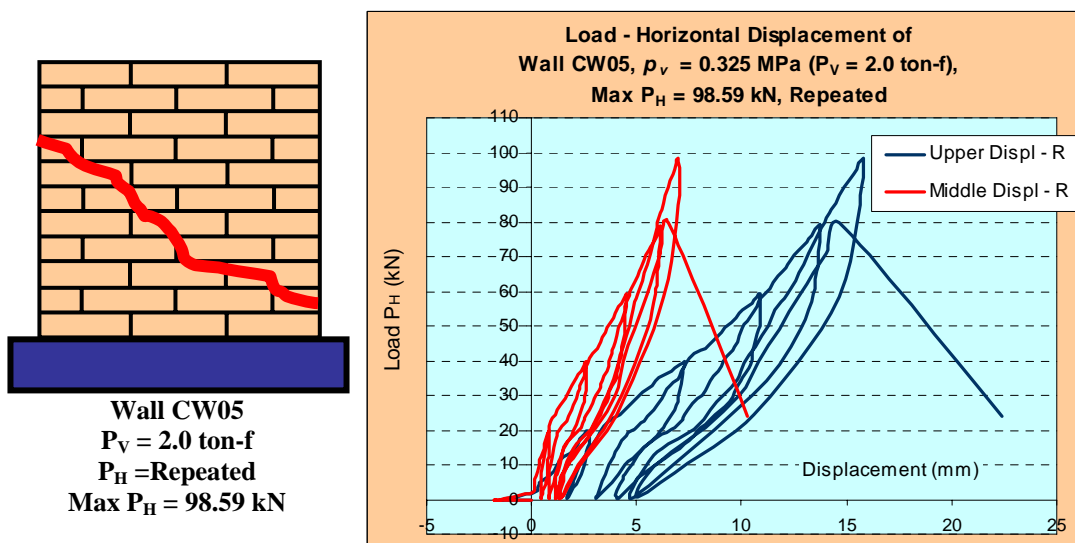


Figure 4.51 Failure pattern and load-displacement of wall CW05

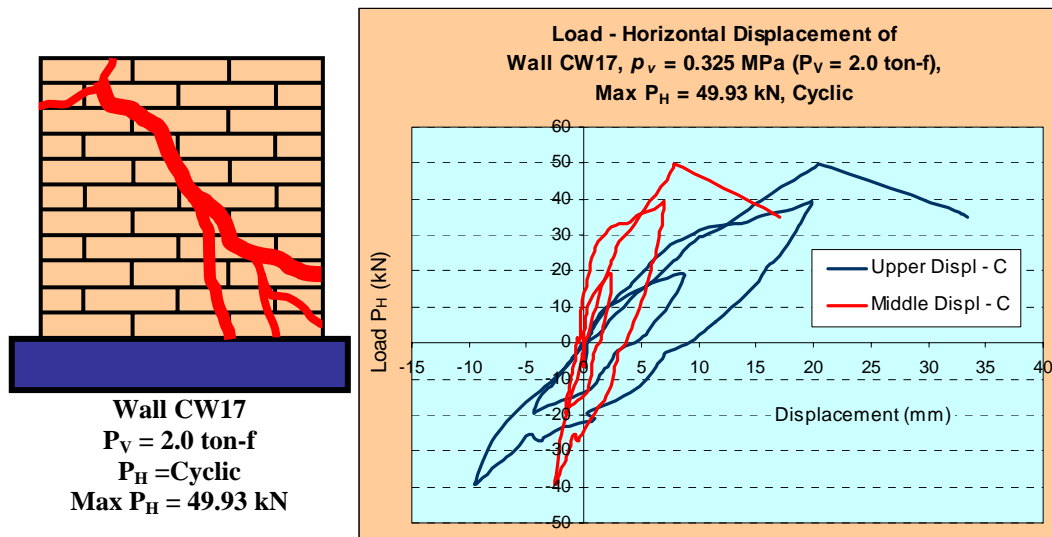


Figure 4.52 Failure pattern and load-displacement of wall CW17

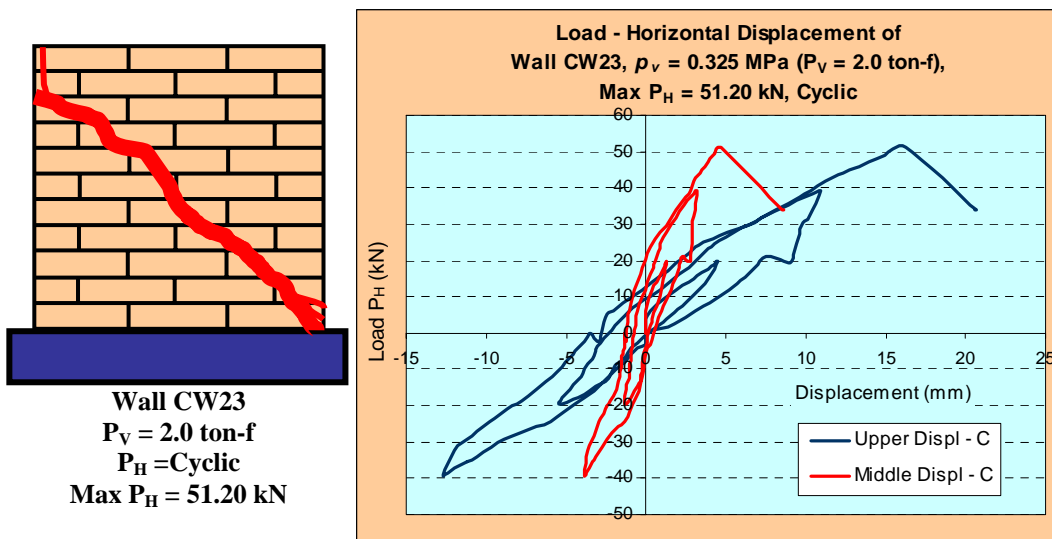


Figure 4.53 Failure pattern and load-displacement of wall CW23

#### 4.3.3.5 Walls CW under vertical pressure $p_v = 0.42 \text{ MPa}$ ( $P_V = 2.5 \text{ ton-f}$ )

Failure patterns and load-displacement responses of walls CW06 and CW04 are shown in Figures 4.54 and 4.55. Failure pattern of wall CW06 is a combination of slip and compression crush near bottom support and diagonal shear failure pattern in centre part. As seen in Figure 4.55, failure pattern of wall CW04 is in a form of a diagonal shear failure combined with spalling surface mortar part. Maximum capacity of wall in retaining lateral load was 113.30 kN and it collapsed in brittle failure mechanism. Wall CW18 was exposed to e cyclic load and collapsed in combination of compressive and shear diagonal failure patterns. Wall capacity in

retaining cyclic lateral load was 50% of that of the wall CW04. This wall has very low ductility, as shown in Figure 4.56

In Figures 4.57 and 4.58, a failure pattern of the wall CW24 is a combination of slip and diagonal shear failure pattern with brittle failure mechanism. Wall capacity in retaining lateral load is about 50% of that of wall CW04. No ductility was found in this experiment work and the wall CW24 was found to be the weaker than those under monotonic and repeated lateral loads.

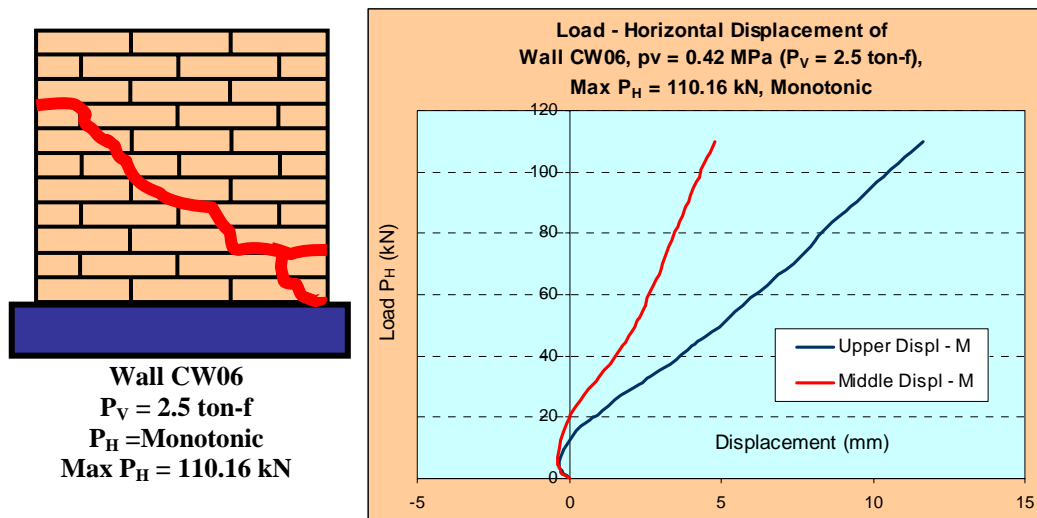


Figure 4.54 Failure pattern and load-displacement of wall CW06

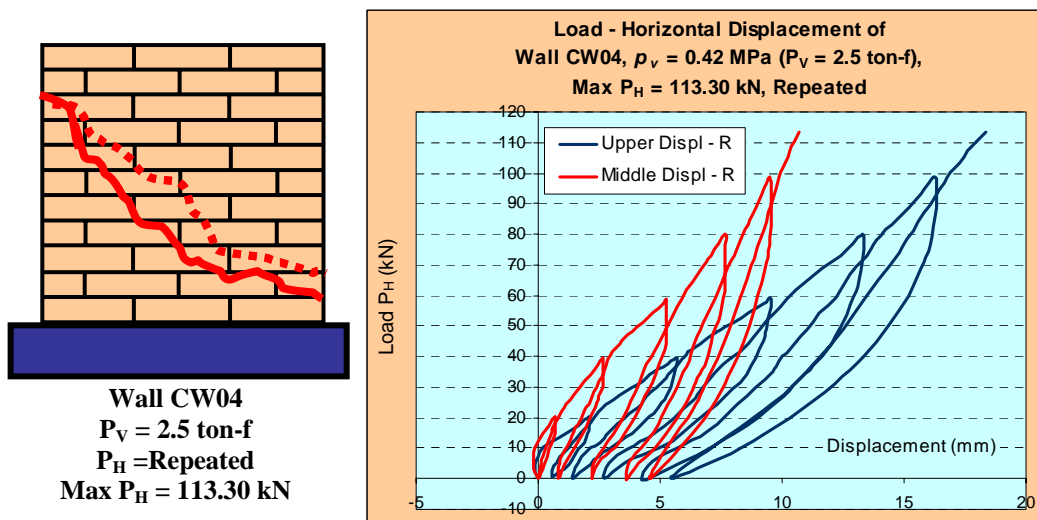


Figure 4.55 Failure pattern and load-displacement of wall CW04

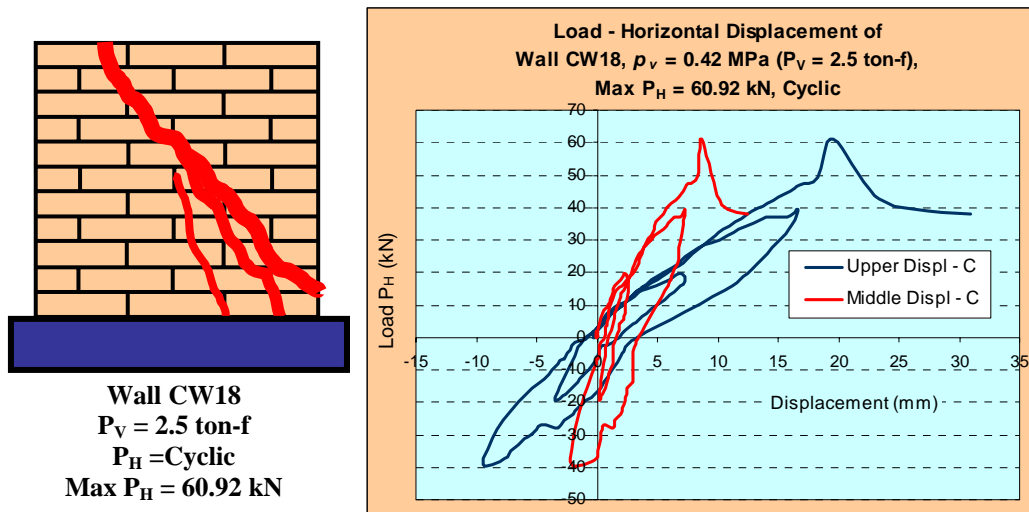


Figure 4.56 Failure pattern and load-displacement of wall CW18

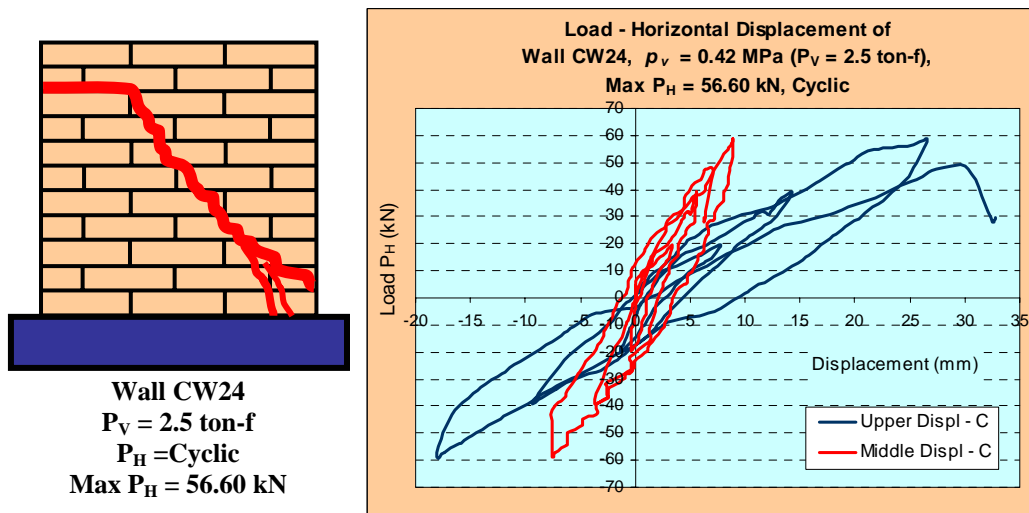


Figure 4.57 Failure pattern and load-displacement of wall CW24



Figure 4.58 Failure pattern of wall CW24



#### 4.3.4 Walls MWA

In this experimental work, walls MWA were tested under combination of compressive pressures of  $p_v = 0.165$  MPa, 0.245 MPa, 0.325 MPa, 0.42 MPa and monotonic, repeated and cyclic horizontal load. More detailed performances of walls MWA are described in the following sections.

##### 4.3.4.1 Walls MWA under vertical pressure $p_v = 0.165$ MPa ( $P_v = 1.0$ ton-f)

The responses of walls MWA01, MWA05 and MWA09 are shown in Figures 4.70, 4.71 and 4.72 respectively. Shear diagonal failure pattern happened in wall MWA01, while a combination of compressive and shear diagonal failure patterns are found in walls MWA05 and MWA09. Walls subjected to monotonic and repeated lateral loads were stronger than the wall under cyclic load. Capacity of wall MWA09 in retaining cyclic lateral load is 45% of that of the walls MWA01 or MWA05.

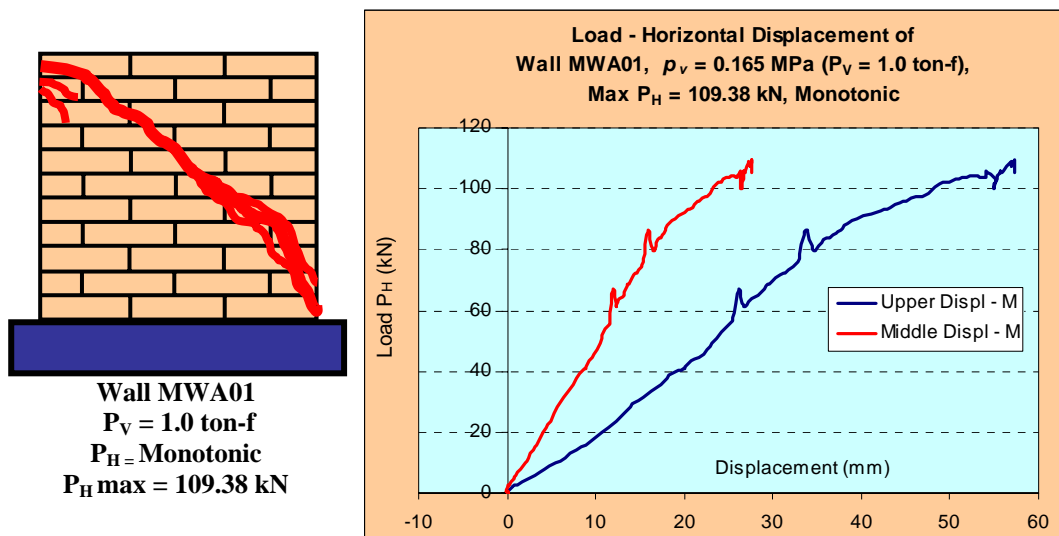


Figure 4.59 Failure pattern and load-displacement of wall MWA01

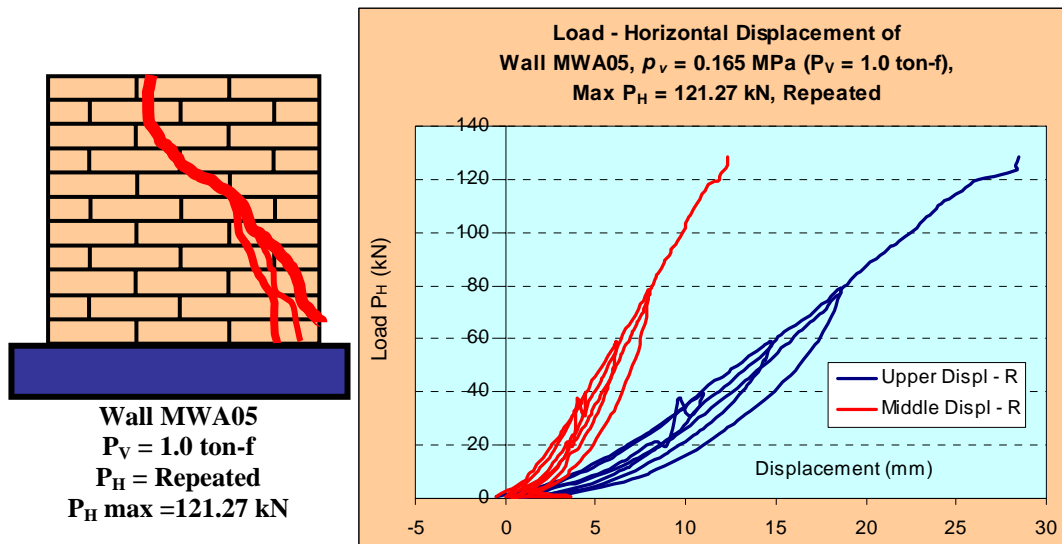


Figure 4.60 Failure pattern and load-displacement of wall MWA05

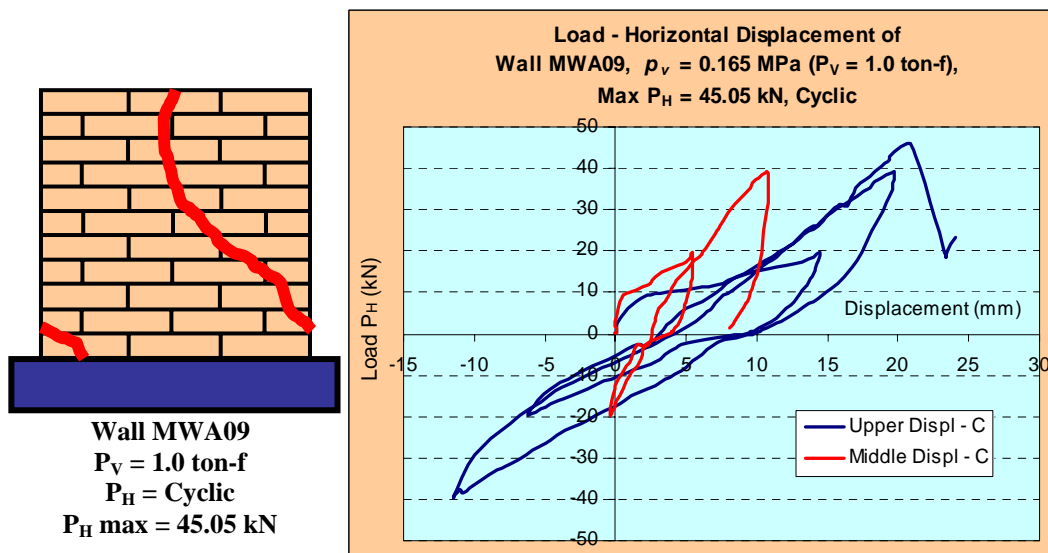


Figure 4.61 Failure pattern and load-displacement of wall MWA09

#### 4.3.4.2 Walls MWA under vertical pressure $p_v = 0.245 \text{ MPa}$ ( $P_V = 1.5 \text{ ton-f}$ )

In Figures 4.62 and 4.63, the responses of walls MWA02 and MWA06 look very similar. Both walls collapsed in brittle failure mechanism with diagonal shear failure pattern, with no ductility.

In Figure 4.64, it can be seen that wall MWA10 collapsed at local corner area near applied horizontal force and at the bottom support. The response of load-displacement is weaker than that of the walls MWA06 or MWA02, and the wall MWA10 collapsed in brittle failure mechanism with small ductility.

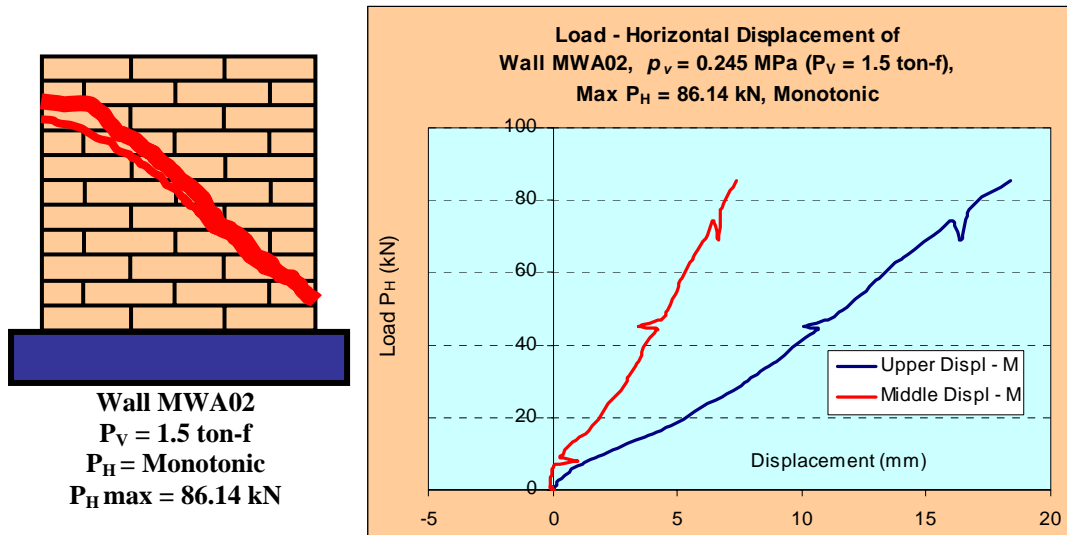


Figure 4.62 Failure pattern and load-displacement of wall MWA02

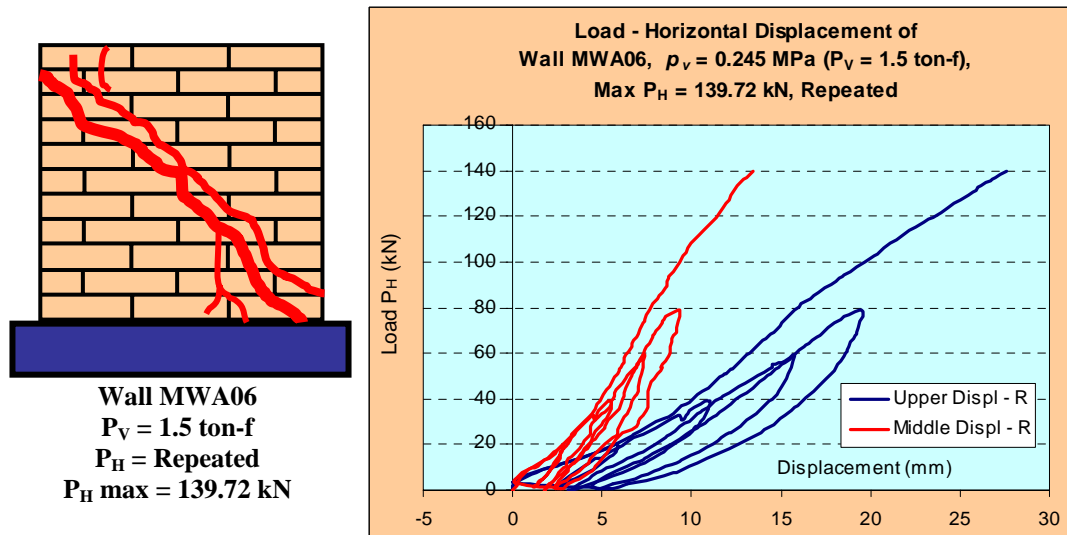


Figure 4.63 Failure pattern and load-displacement of wall MWA06

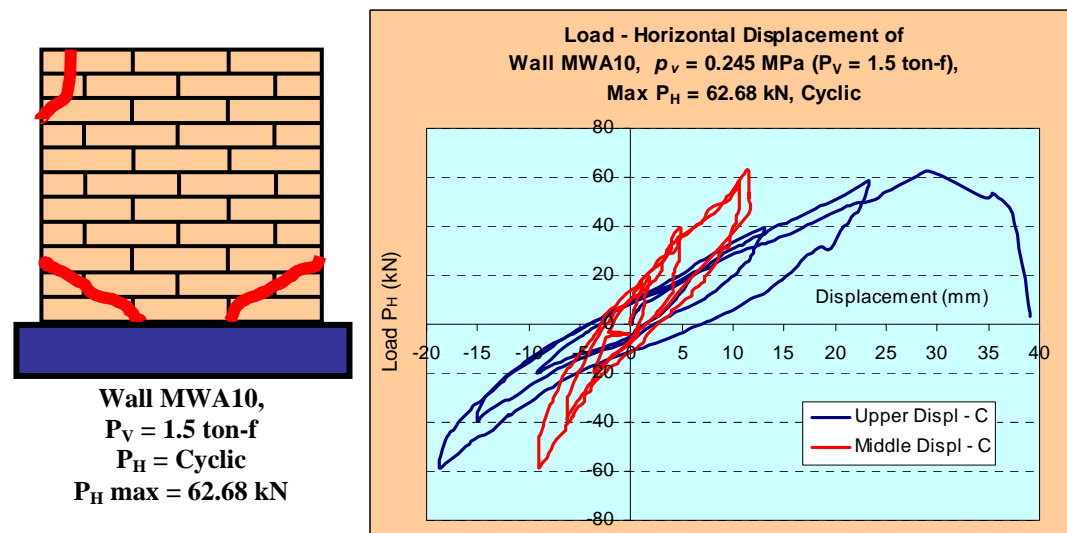


Figure 4.64 Failure pattern and load-displacement of wall MWA10

#### 4.3.4.3 Walls MWA under vertical pressure $p_v = 0.325$ MPa ( $P_v = 2.0$ ton-f)

Fully diagonal shear failure patterns happened in walls MWA03 and MWA07, with similar load-displacement response. No ductility responses were found during the experiments. Wall capacities in retaining lateral loads were 86.74 kN and 143.42 kN for walls MWA03 and MWA07 respectively, as shown in Figures 4.65 and 4.66. In Figure 4.67, failure pattern and load-displacement of wall MWA11 was affected by compressive pressure. Wall capacity in retaining lateral load was less than 50% of that of the wall MWA07.

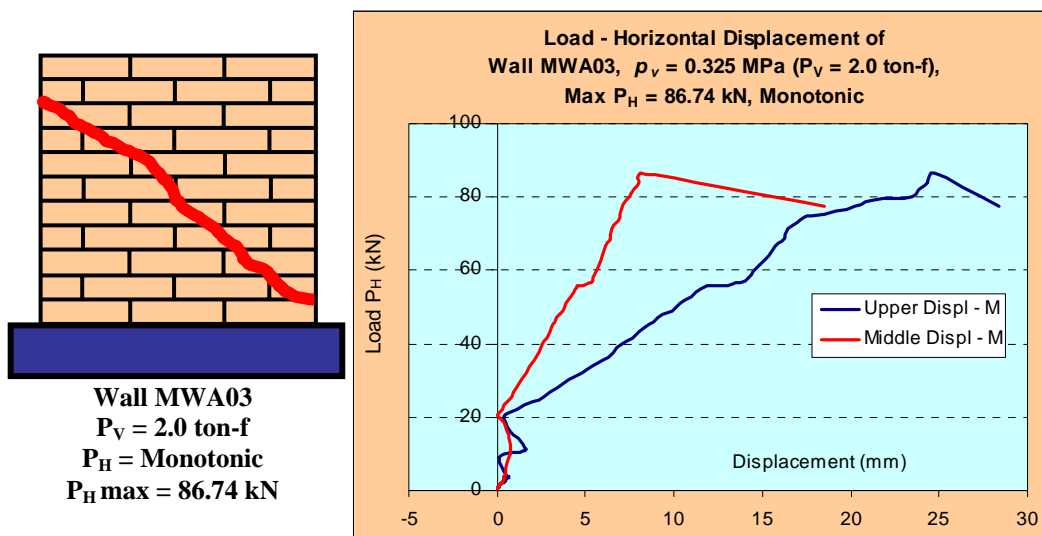


Figure 4.65 Failure pattern and load-displacement of wall MWA03

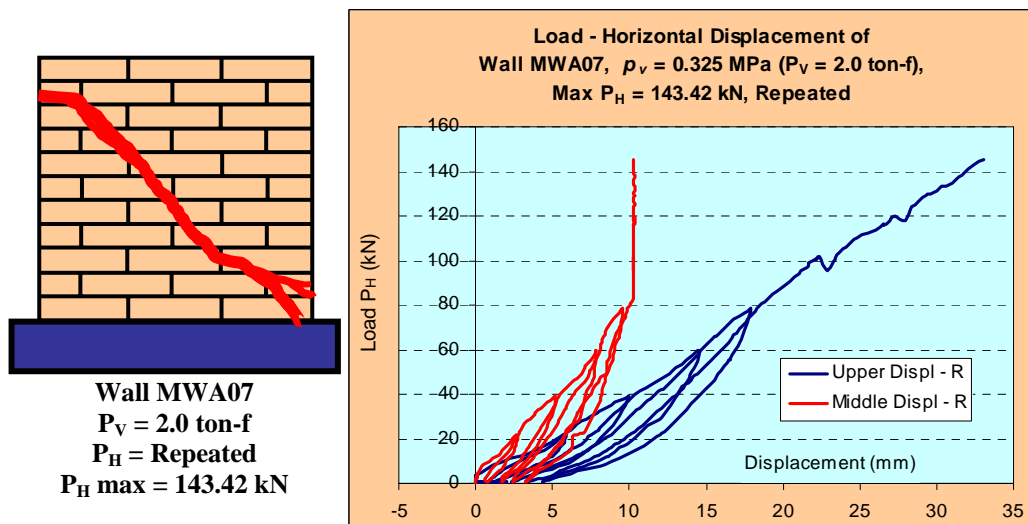


Figure 4.66 Failure pattern and load-displacement of wall MWA07

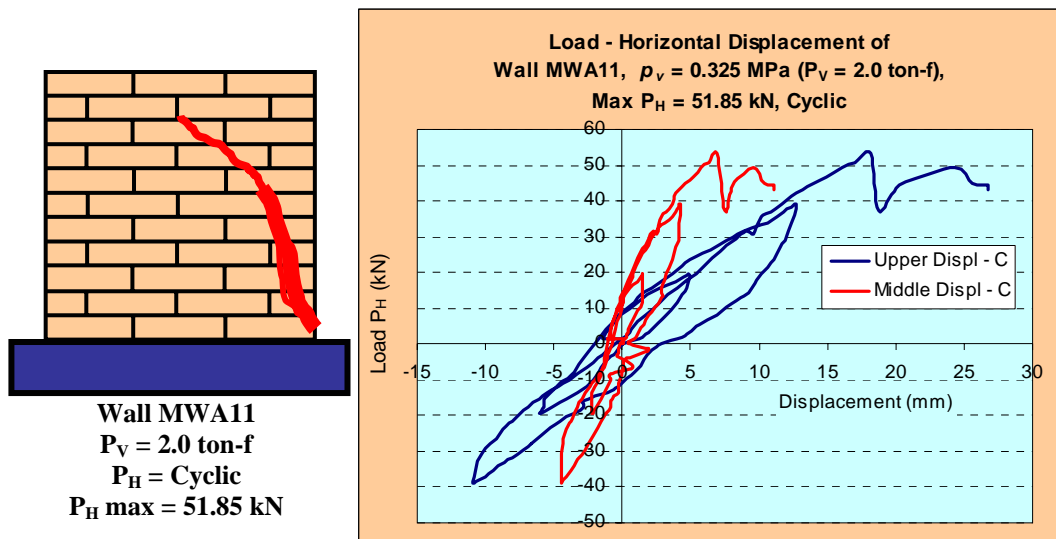


Figure 4.67 Failure pattern and load-displacement of wall MWA11

#### 4.3.4.4 Walls MWA under vertical pressure $p_v = 0.42 \text{ MPa}$ ( $P_V = 2.5 \text{ ton-f}$ )

In Figures 4.68, 4.69 and 4.71, compressive failures dominated the failure mechanisms of walls MWA04 and MWA12. In Figure 4.70, wall MW08 collapsed in shear diagonal failure pattern. Capacity of wall MWA12 in retaining cyclic lateral load was 50% of that of the wall MWA08. No ductility response was found in these experiments.

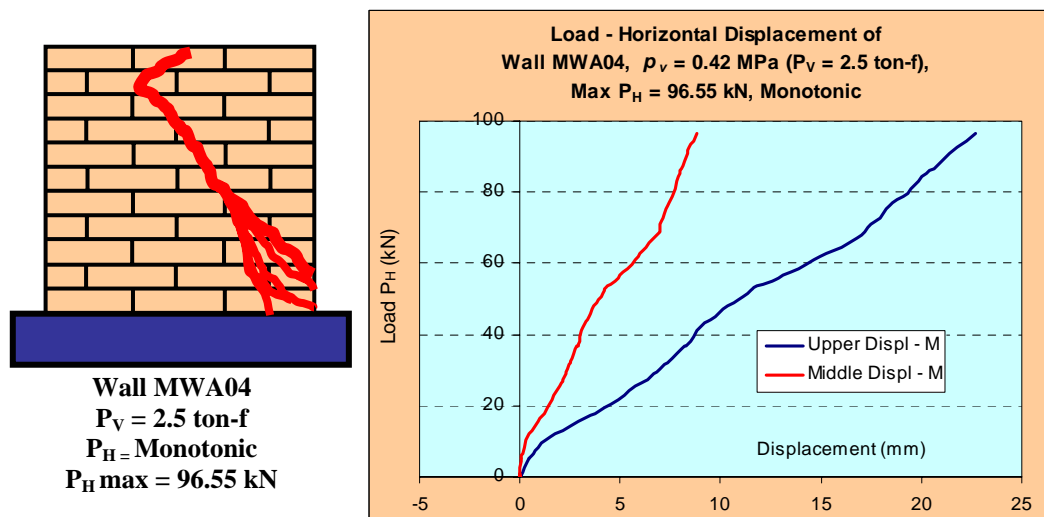


Figure 4.68 Failure pattern and load-displacement of wall MWA04



Figure 4.69 Failure pattern and load-displacement of wall MWA04

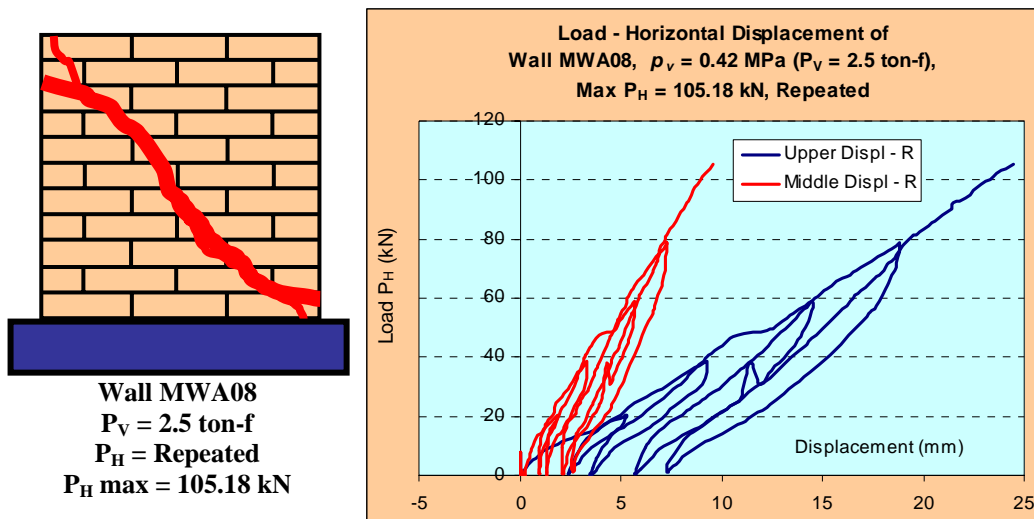


Figure 4.70 Failure pattern and load-displacement of wall MWA08

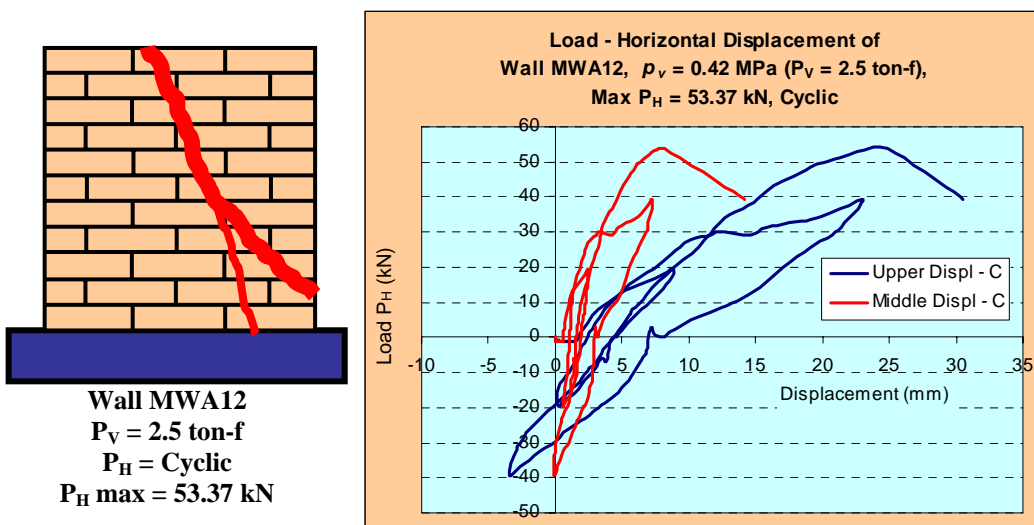


Figure 4.71 Failure pattern and load-displacement of wall MWA12

### 4.3.5 Walls CWA

Combination of vertical pressures of  $p_v = 0.165$  MPa, 0.245 MPa, 0.325 MPa, 0.42 MPa and monotonic, repeated and cyclic horizontal load were applied to walls CWA. All failure patterns and load-displacement responses of wall CWA are discussed in the following sentence.

#### 4.3.5.1 Walls CWA under vertical pressure $p_v = 0.165$ MPa ( $P_v = 1.0$ ton-f)

Walls CWA01, CWA05, CWA09 were tested under monotonic, repeated and cyclic lateral load respectively. Their failure patterns were diagonal shear failure patterns with brittle collapse mechanisms. Wall CWA09 tested under cyclic lateral load was the weakest among these three walls. Its capacity of retaining cyclic lateral load was 30 % of that of the walls CWA05 or CWA01.

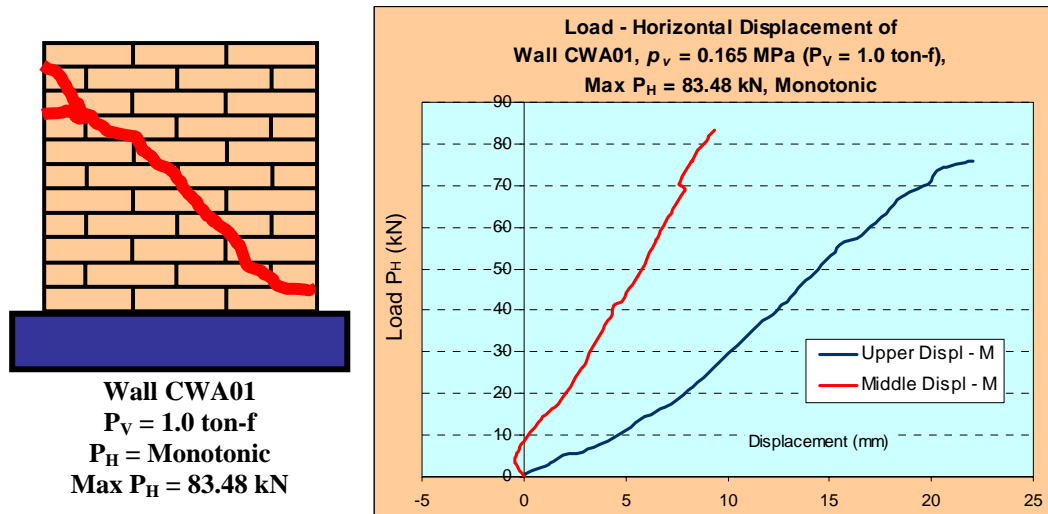


Figure 4.72 Failure pattern and load-displacement of wall CWA01

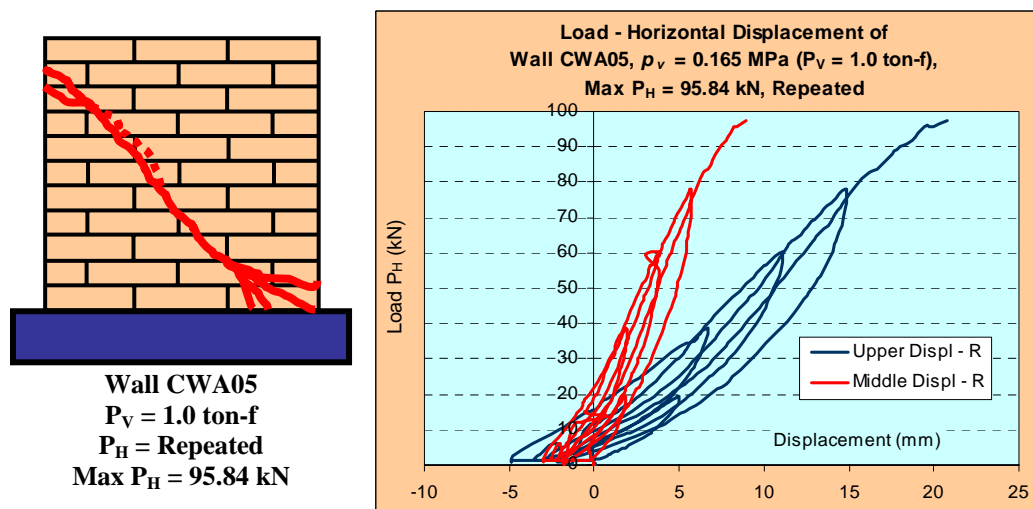


Figure 4.73 Failure pattern and load-displacement of wall CWA05

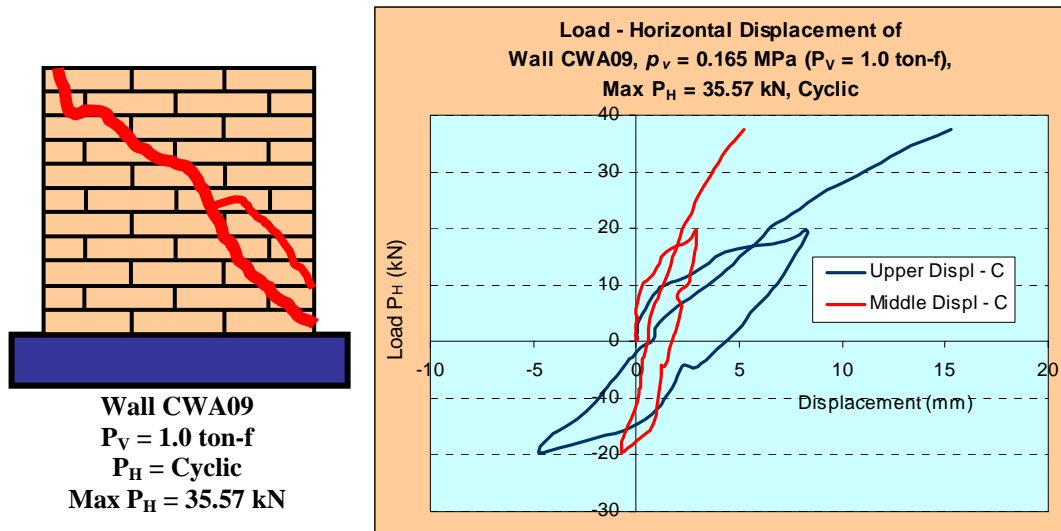


Figure 4.74 Failure pattern and load-displacement of wall CWA09

#### 4.3.5.2 Walls CWA under vertical pressure $p_v = 0.245 \text{ MPa}$ ( $P_V = 1.5 \text{ ton-f}$ )

Diagonal shear failure patterns happened to walls CWA02 and CWA06, as shown in Figures 4.75, 4.76 and 4.77. In wall CWA10 tested under cyclic lateral load, a combination of compressive and diagonal shear failure appeared. In this experiment, vertical compression load of  $p_v = 0.245 \text{ MPa}$  produced a high capacity of wall CWA10. This response is shown in Figure 4.78.

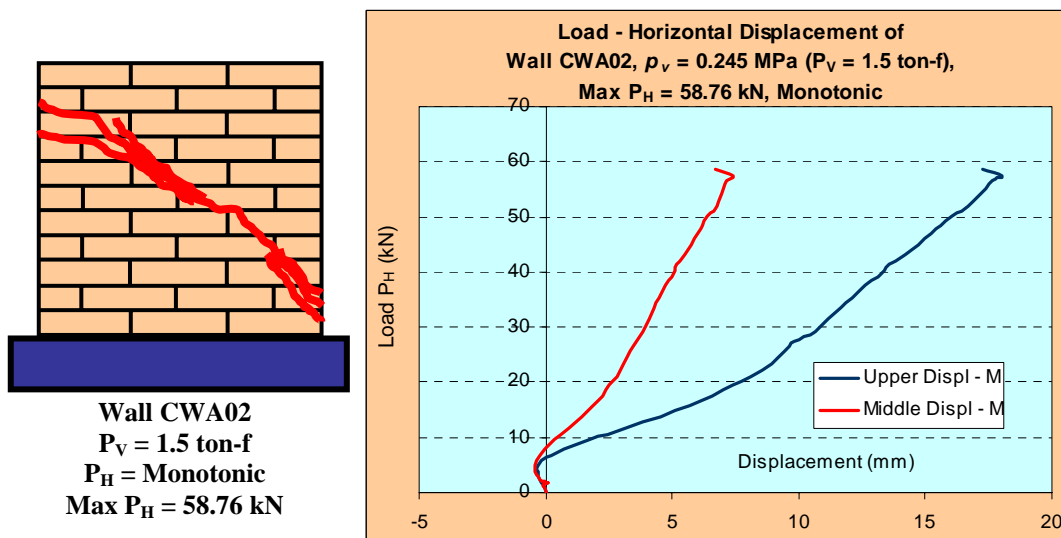


Figure 4.75 Failure pattern and load-displacement of wall CWA02





Figure 4.76 Failure pattern and load-displacement of wall CWA02

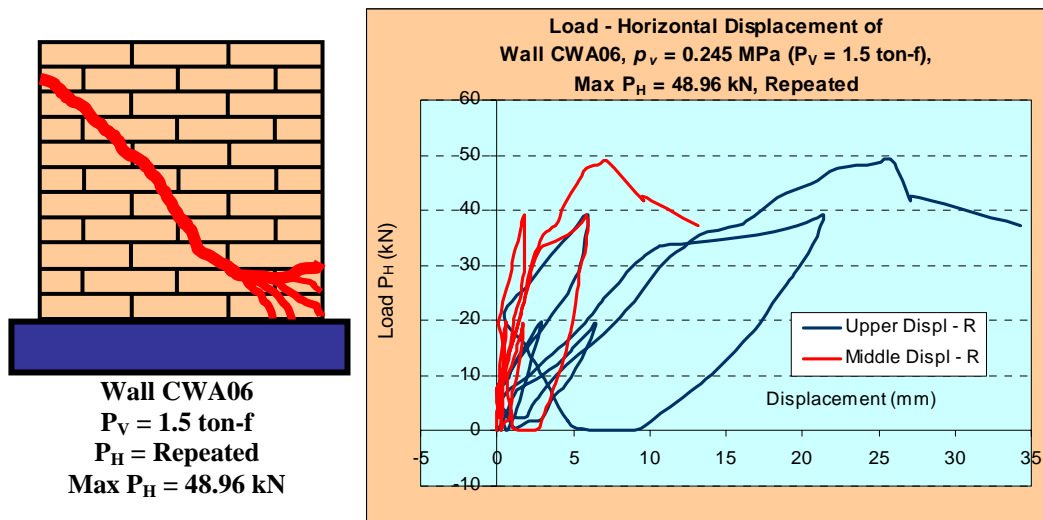


Figure 4.77 Failure pattern and load-displacement of wall CWA06

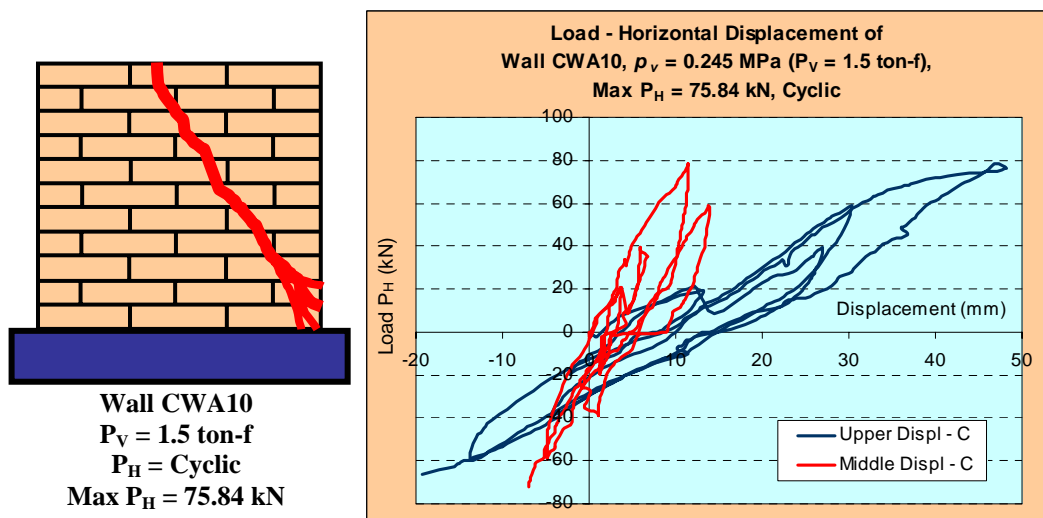


Figure 4.78 Failure pattern and load-displacement of wall CWA10

### 4.3.5.3 Walls CWA under vertical pressure $p_v = 0.325$ MPa ( $P_v = 2.0$ ton-f)

Applying the vertical pressure of 0.325 MPa, walls CWA03, CWA07 and CWA11 collapsed in diagonal shear failure patterns, without any ductility in gradual collapse mechanisms. Wall CWA11 demonstrated low capacity in retaining lateral cyclic load, less than 50% of that of the wall CWA07. All responses are shown in Figures 4.79, 4.80 and 4.81.

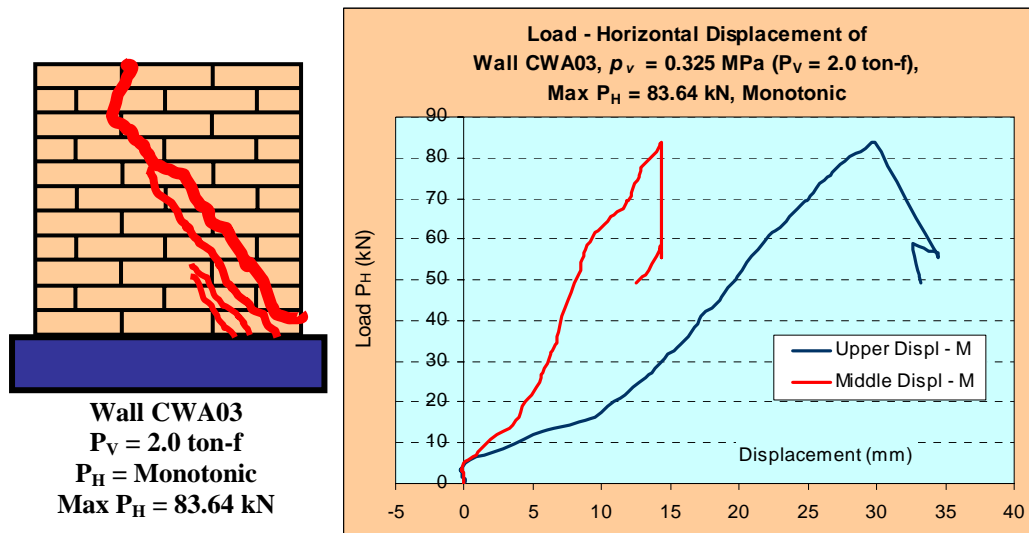


Figure 4.79 Failure pattern and load-displacement of wall CWA03

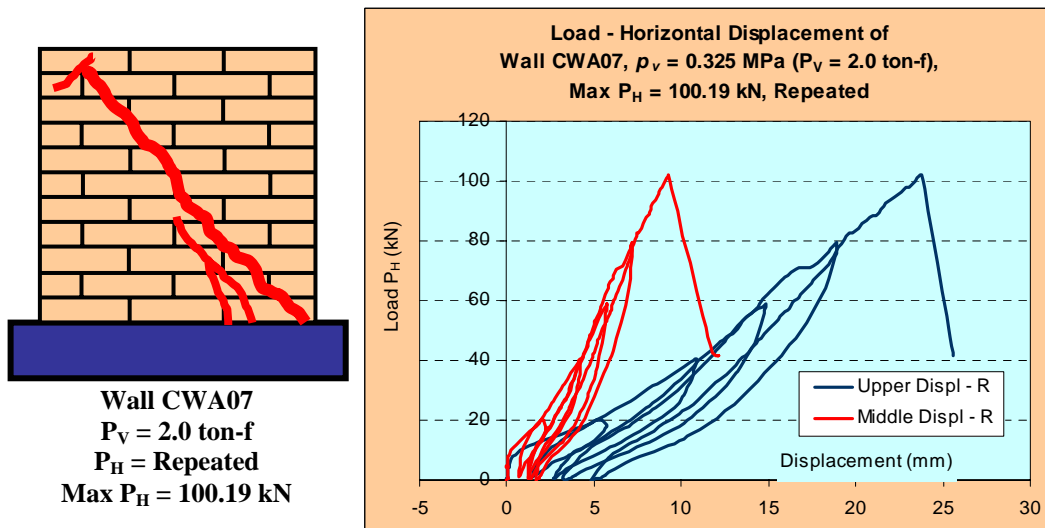


Figure 4.80 Failure pattern and load-displacement of wall CWA07

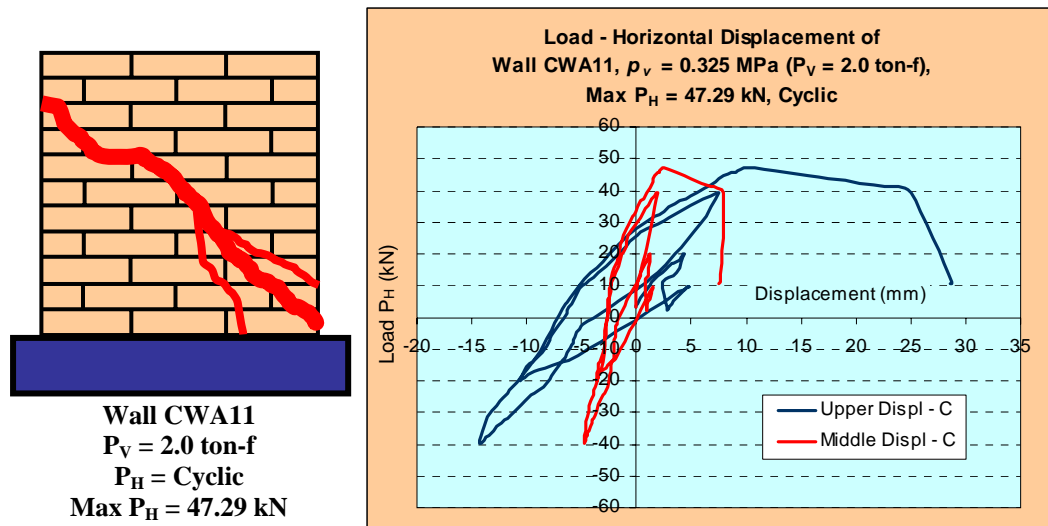


Figure 4.81 Failure pattern and load-displacement of wall CWA11

#### 4.3.5.4 Walls CWA under vertical pressure $p_v = 0.42 \text{ MPa}$ ( $P_V = 2.5 \text{ ton-f}$ )

As the pressure increased up to  $p_v = 0.42 \text{ MPa}$ , the responses of walls CWA04, CWA08 and CWA12 were similar to those of walls CWA under  $p_v = 0.325 \text{ MPa}$ . Most walls collapsed in diagonal shear failure, with no ductility and brittle failure mechanism, as shown in Figure 4.82, 4.83 and 4.84. The capacity of wall CWA12 in retaining cyclic lateral load is 60% of that of the walls under monotonic or repeated loads.

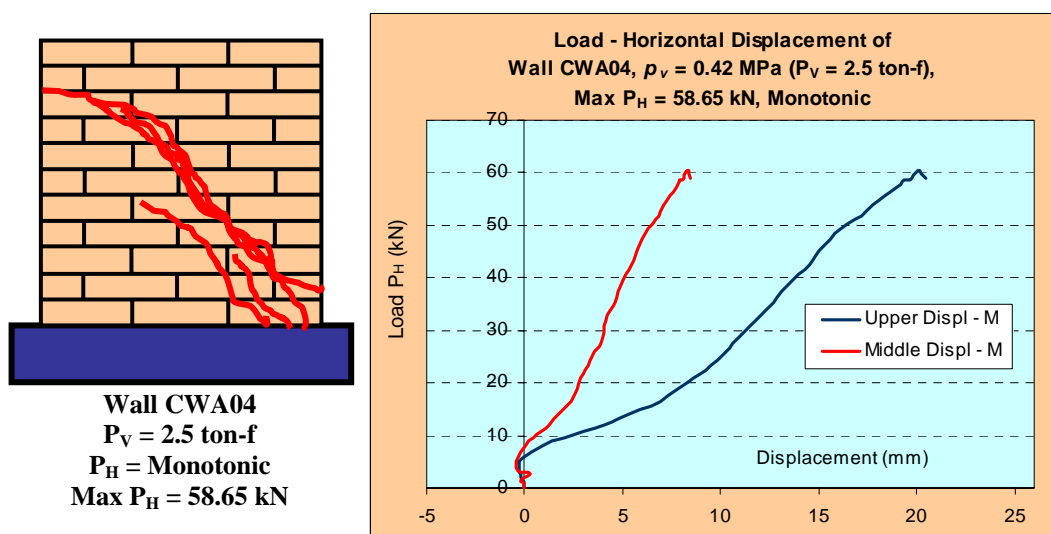


Figure 4.82 Failure pattern and load-displacement of wall CWA04

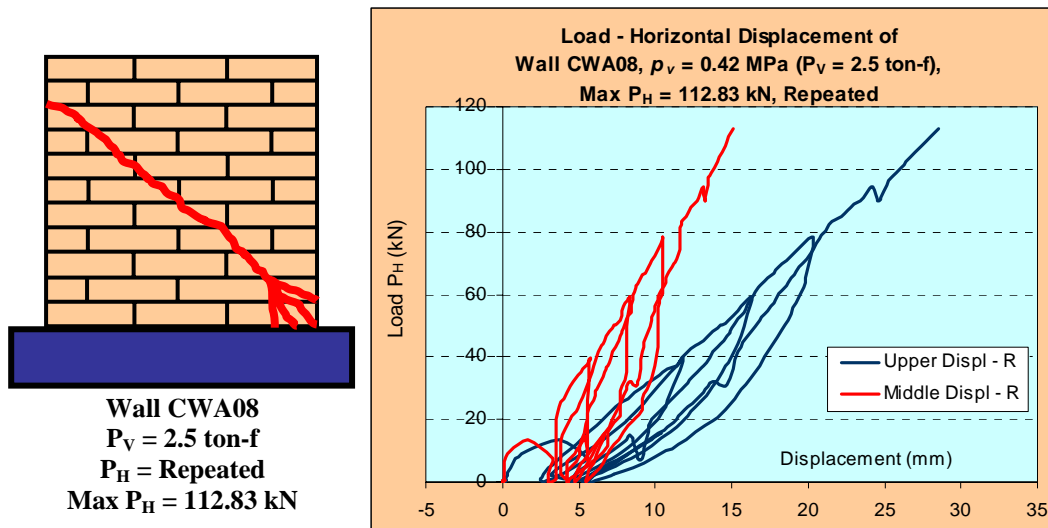


Figure 4.83 Failure pattern and load-displacement of wall CWA08

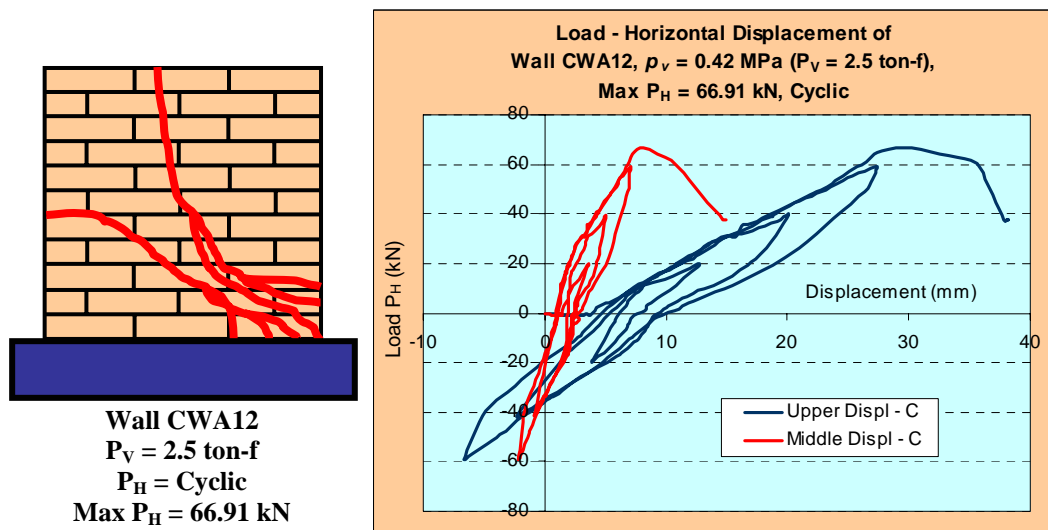


Figure 4.84 Failure pattern and load-displacement of wall CWA12

#### 4.3.6 Walls MWE

Extra walls MWE were tested under combination of vertical pressures of  $p_v = 0.08$  MPa, 0.165 MPa, 0.245 MPa, 0.325 MPa, 0.42 MPa and monotonic horizontal loads. In Figures 4.85 to 4.90, it can be seen that most failure patterns of walls MWE1, MWE2, MWE3, MWE4 and MWE5 were of diagonal shear failure mechanisms, with brittle collapse. As can be seen in Figure 4.85, wall MWE01 started to crack at  $P_H = 45.03$  ton-f. The crack initiated, the capacity of retaining lateral load decreased and the specimen experienced shear hardening that produced little ductility and then the wall collapsed in brittle failure mechanism.

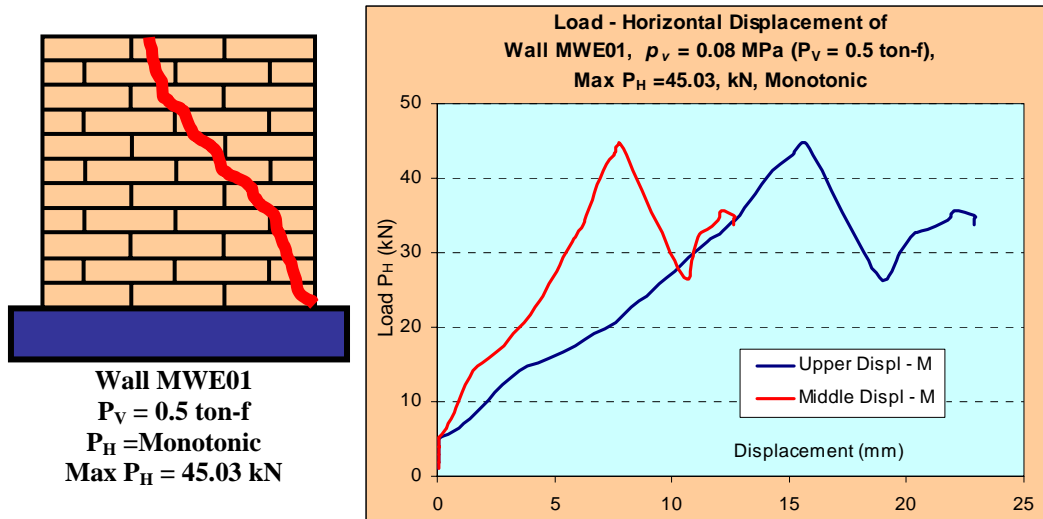


Figure 4.85 Failure pattern and load-displacement of wall MWE01

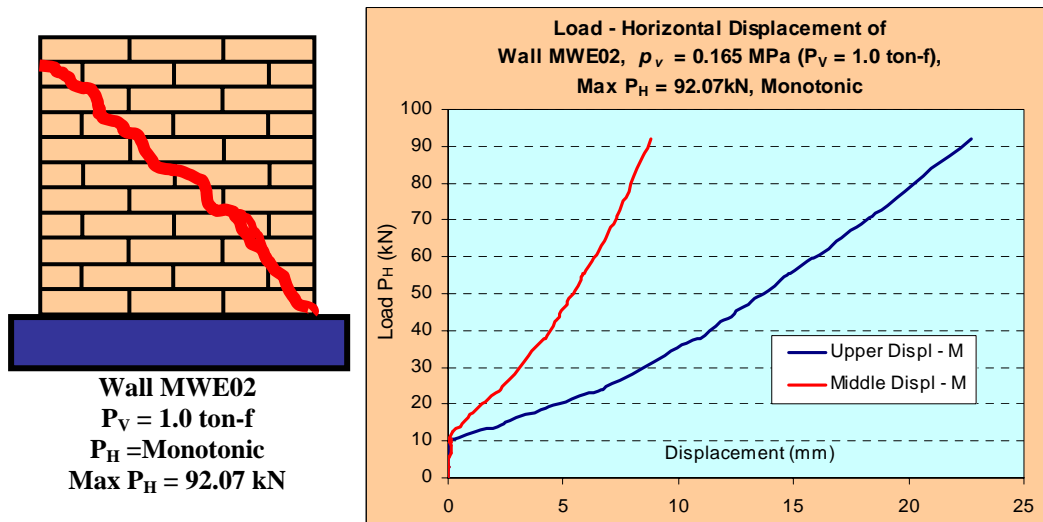


Figure 4.86 Failure pattern and load-displacement of wall MWE02

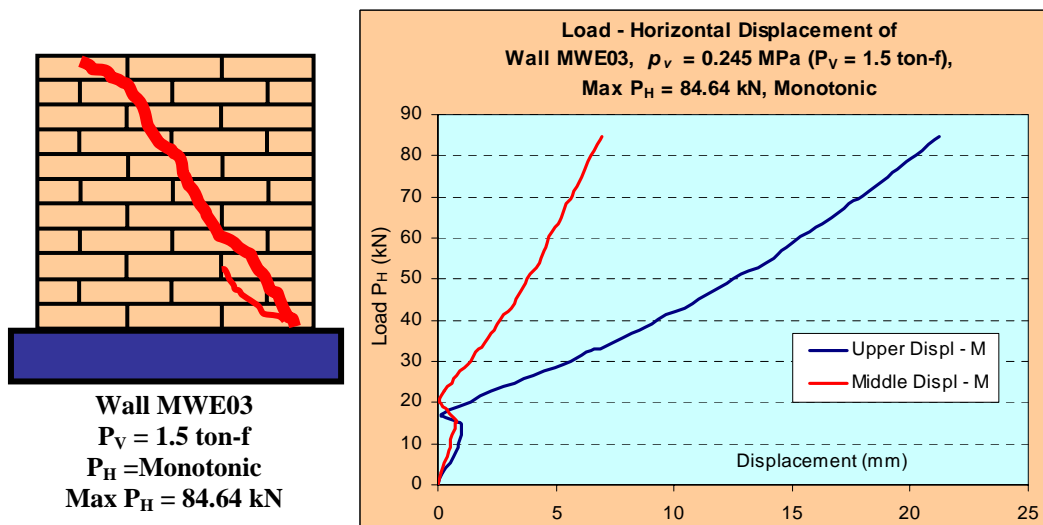


Figure 4.87 Failure pattern and load-displacement of wall MWE03



Figure 4.88 Failure pattern of wall MWE03

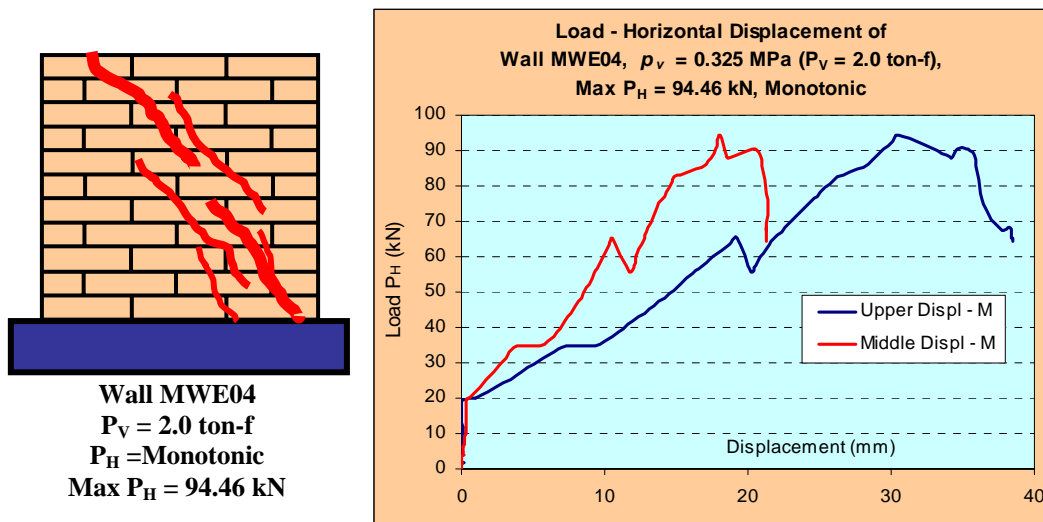


Figure 4.89 Failure pattern and load-displacement of wall MWE04

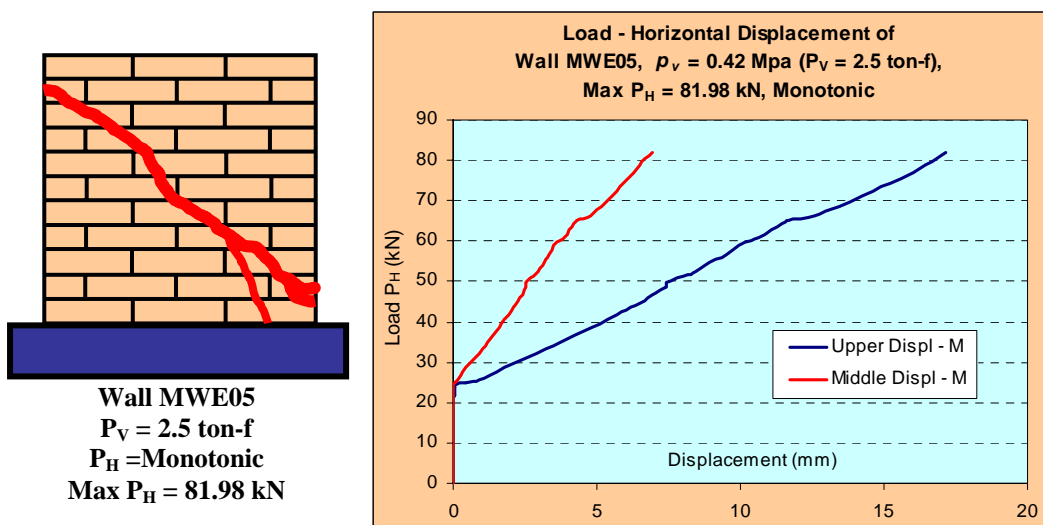


Figure 4.90 Failure pattern and load-displacement of wall MWE05



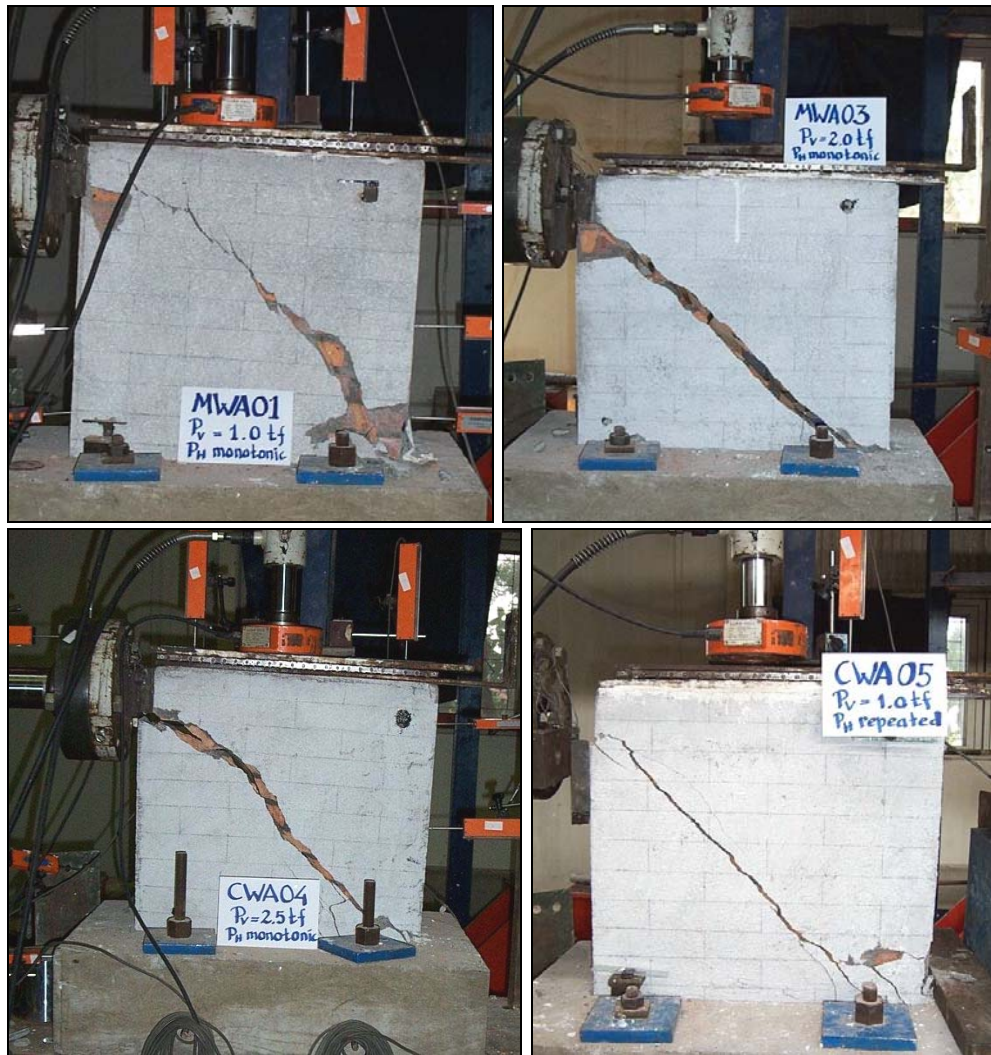


Figure 4.91 Failure pattern of walls MWA and CWA



Figure 4.92 Cross sections of failure patterns of single walls.

In Figure 4.91, it can be seen that the failure patterns of walls MWA and CWA were significantly affected by the presence of surface mortar type A. It is already known that the compressive strength of mortar type A is higher than that of the mortar type B. Wall diagonal cross sections after failure are shown in Figure 4.92. As can be seen in this picture, the wall with surface plaster collapsed in diagonal shear failure without slip. The bricks started to collapse as the crack in the surface plaster was initiated. This type of failure is considered as diagonal shear failure, predominantly caused by mortar. In this case, as a confinement system, mortar plaster type A exhibited a lower support capacity to the lateral load than that of mortar plaster type B. The use of mortar type A for plastering wall surface has not significantly improved the capacity of walls MWA and CWA in retaining lateral load.

#### 4.4 Wall capacity in retaining lateral load

Observing all wall responses described in Section 4.3, the capacity of wall panels in retaining lateral loads is recorded in Table 4.4 and graphically shown in Figure 4.93. The response of walls BW indicated that their capacities of retaining lateral load were mostly lower than those of walls MW and comforted walls CW. In general, walls MW increased their lateral capacity about 2 times compared to the walls BW and walls CW increased their lateral capacity about 1.5 times to the walls BW. It was also found that there was no significant advantages in choosing walls CW as oppose to the walls MW, since walls MW always exhibited better performance in retaining lateral load.

The result also indicated that all types of wall panels BW, MW and CW had a peak capacity in retaining lateral load as vertical pressure applied to the panels. The overall maximum capacity of wall panels in retaining lateral load were noticed under compressive pressure in the range of 0.245 MPa – 0.325 MPa. When the compressive pressure increased beyond 0.325 MPa ( $P_V = 2$  ton-f), wall panels became weaker in retaining lateral loads. This phenomenon was not found in all former research and it is affected by the individual quality of brick unit. Since the graphical representation of the capacity of wall panels in Figure 4.93 are not clearly visible, more detailed results are described in the following sub-section. The results are classified into  $P_H$  monotonic, repeated and cyclic loading



Table 4.4 Capacity of wall panels in retaining horizontal load (kN)

Wall type	Type of load	Compressive load (ton-f)					Notes:
		0.5	1.0	1.5	2.0	2.5	
		Compressive pressure (MPa)					
		0.08	0.165	0.245	0.325	0.42	
BW	Mon		74.38	81.89	83.34	54.05	Slip failure, small ductility
	Rep.		58.85	93.39	71.57	73.67	
	Cycl		47.38	24.32	50.91	46.99	
MW	Mon		176.78	136.95	145.09	109.18	Shear diagonal failure pattern, very small ductility
	Rep.	78.48	118.80	184.92	169.42	133.32	
	Cycl	41.49	52.19	50.71	45.71	46.89	
CW	Mon		126.15	122.52	121.30	110.16	
	Rep.	70.92	129.49	103.49	98.59	113.30	
	Cycl	37.27	45.22	35.41	49.93	60.92	
MWA	Mon		109.38	86.14	86.74	96.55	
	Rep.		121.27	139.72	143.42	105.18	
	Cycl		45.05	62.68	51.85	53.37	
CWA	Mon		83.48	62.19	93.31	85.65	
	Rep.		95.84	48.96	100.19	112.83	
	Cycl		35.57	75.84	47.29	66.91	
MWE	Mon	45.03	96.55	77.02	86.44	67.21	

Mon. = Monotonic, Rep. = Repeated, Cycl. = Cyclic (Total = 75 walls)

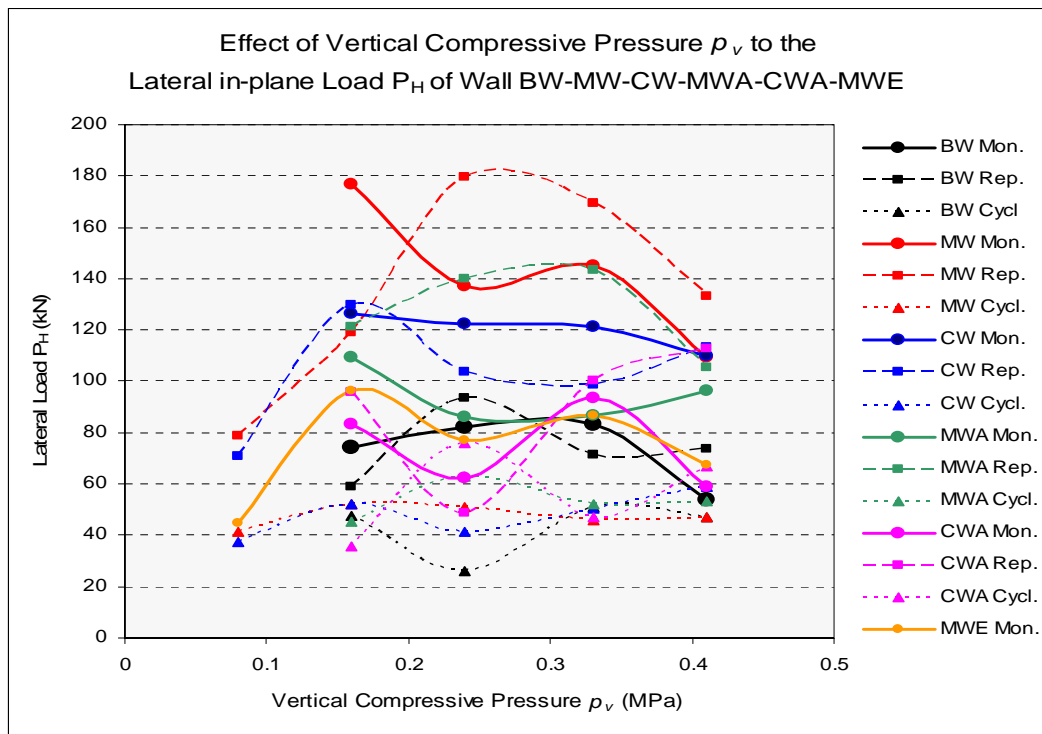


Figure 4.93 Capacity of wall panels in retaining lateral load

#### 4.4.1 Wall capacity under monotonic lateral load $P_H$

As can be seen in Table 4.5, the maximum capacity of walls MW, CW, MWA, MWE, in retaining lateral load was under the compressive pressure of 0.165 MPa, while the walls BW and CWA was under the compressive pressure of 0.325 MPa. Most trend lines as seen in Figure 4.49, showed a decrease in performance of maximum capacity of walls to retain monotonic lateral load. It means that increasing compressive pressure does not improve lateral capacity of walls. The strongest response was performed by wall MW.

Table 4.5 Capacity of wall panels in retaining horizontal monotonic loads (kN)

Type of wall	Compressive load (ton-f)				
	0.5	1.0	1.5	2.0	2.5
	Compressive pressure (MPa)				
	0.08	0.165	0.245	0.325	0.42
BW		74.38	81.89	83.34	54.05
MW		176.78	136.95	145.09	109.18
CW		126.15	122.52	121.3	110.16
MWA		109.38	86.14	86.74	96.55
CWA		83.48	62.19	93.31	85.65
MWE	45.03	96.55	77.02	86.44	67.21

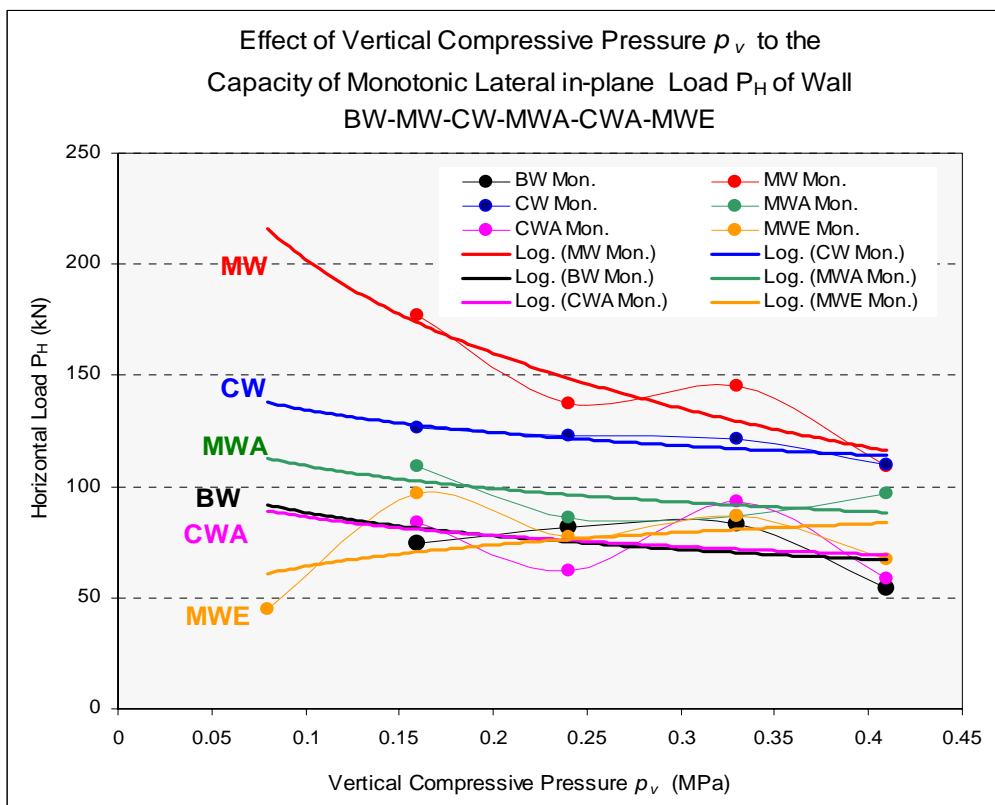


Figure 4.94 Capacity of wall panels in retaining monotonic lateral load

#### 4.4.2 Walls capacity under repeated lateral load $P_H$

From Table 4.6 and Figure 4.95, it can be seen that capacities of walls in retaining repeated lateral loads are similar to those under monotonic loads. Walls become weaker as compression load increased above 0.325 MPa. Overall, wall MW exhibited better performance than other walls.

Table 4.6 Capacity of wall panels in retaining horizontal repeated loads (kN)

Type of wall	Compressive load (ton-f)				
	0.5	1.0	1.5	2.0	2.5
	Compressive pressure (MPa)				
	0.08	0.165	0.245	0.325	0.42
BW		58.85	93.39	71.57 48.9	73.67
MW	78.48	118.8	184.92	169.42	133.32
CW	70.92	129.49	103.49	98.59	113.3
MWA		121.27	139.72	143.42	105.18
CWA		95.84	48.96	100.19	112.83

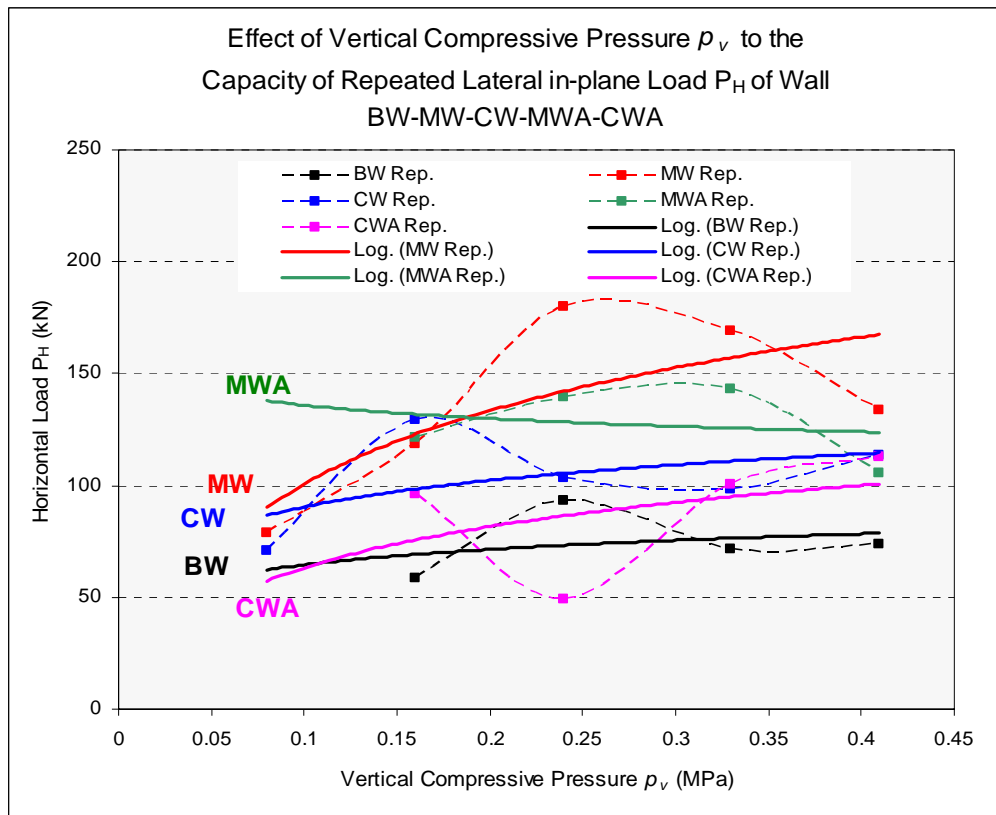


Figure 4.95 Capacity of wall panels in retaining repeated lateral load

### 4.4.3 Wall capacity under cyclic lateral load $P_H$

From Table 4.7 and Figure 4.96, the capacities of walls in retaining cyclic lateral loads are around 50% of the capacities of walls under repeated and monotonic lateral load. This affects the strength of masonry building in retaining earthquake loads, as the majority of earthquake loads can be modelled as cyclic lateral in-plane loads. Under a certain condition of a compressive pressure of 0.245 MPa, wall CWA showed a high capacity of retaining lateral load. However, the average performance of walls MW, MWA and CWA are better than that of wall BW.

Table 4.7 Capacity of wall panels in retaining horizontal repeated loads (kN)

Type of wall	Compressive load (ton-f)				
	0.5	1.0	1.5	2.0	2.5
	Compressive pressure (MPa)				
	0.08	0.165	0.245	0.325	0.42
BW		47.38	26	50.92	46.99
MW	41.49	52.19	50.71	45.71	46.89
CW	37.27	45.22	35.41	49.93	60.92
MWA		45.05	62.68	51.85	53.37
CWA		35.57	75.84	47.29	66.91

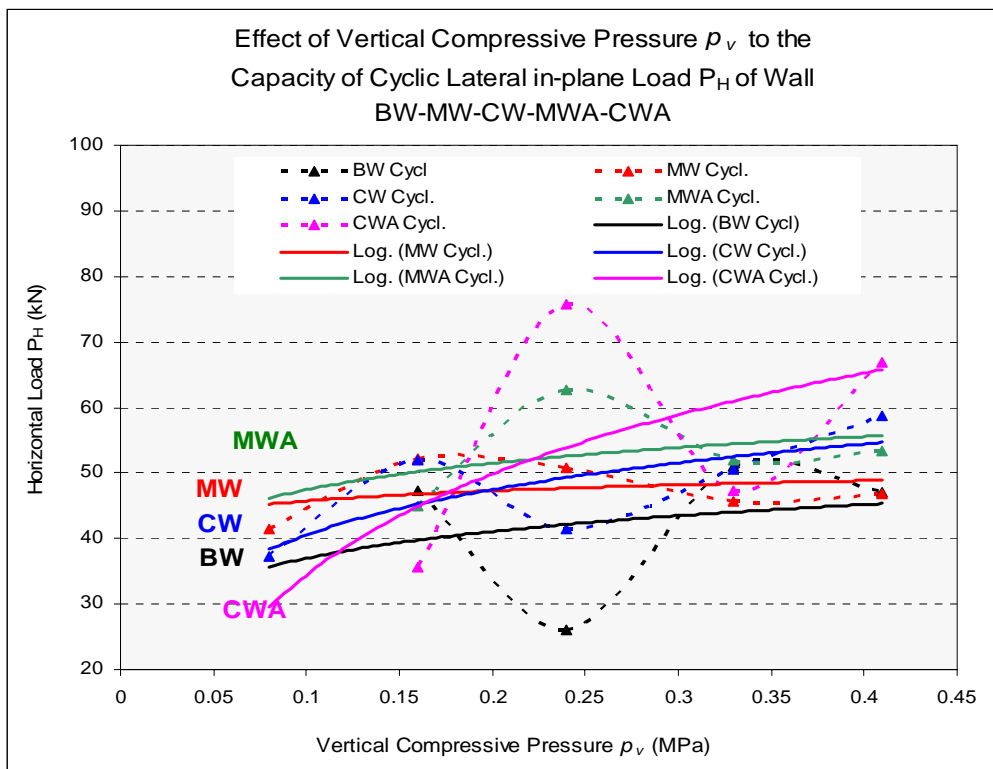


Figure 4.96 Capacity of wall panels in retaining cyclic lateral load

#### 4.4.4 Capacity of wall BW

The capacity of wall BW to retain lateral load is shown in Figures 4.97. The capacity of wall BW under monotonic load decreased with increasing compressive pressure. This was caused by slip failure occurring during the test. Bonding resistance between mortar and brick surface was low, when the compressive pressure was less than 2 MPa. Based on the outcomes from experimental stage 1, the stress strain performance of all type of brick masonry assemblages was still in a fissure closing region. The stress strain behaviour of brick assemblages was similar to that of soft rock or hard soil. By increasing compressive pressure, the capacity of wall BW to retain repeated lateral load, was increased. As lateral load decreased to zero, wall BW maintained its consolidation stage. As the load increased, the load-displacement response of wall panels became stronger. The presence of compressive stress significantly increased the capacity of wall BW to retain repeated lateral load. In general, the average capacity of wall BW to retain cyclic lateral load decreased by 50% compared to that of monotonic or repeated load.

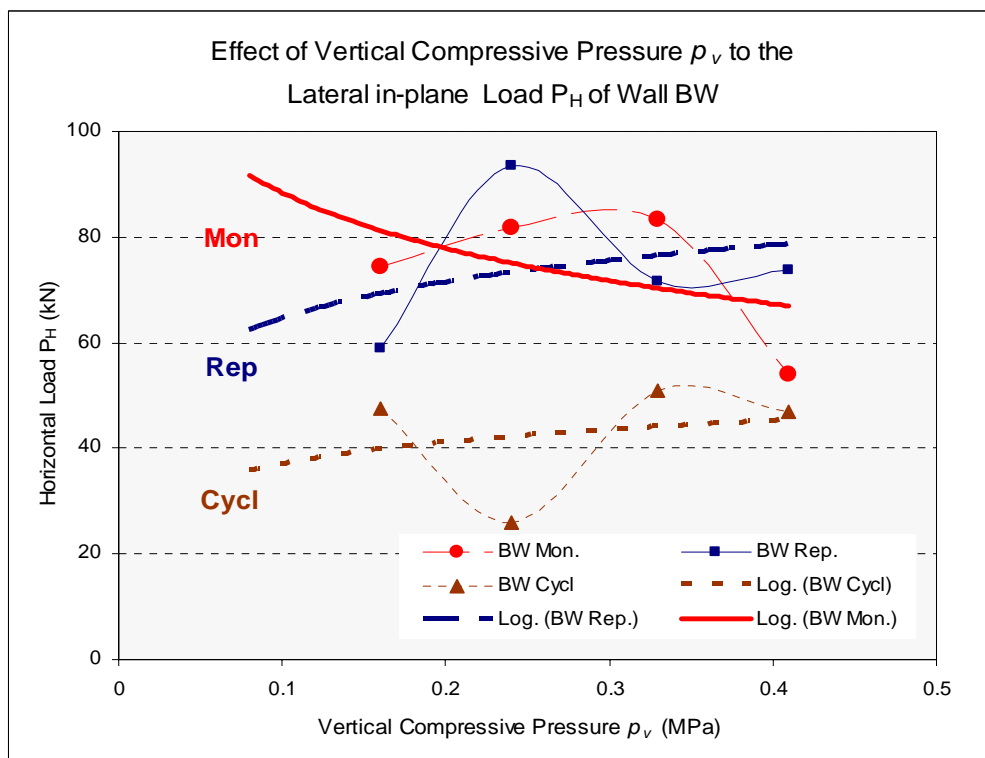


Figure 4.97 Maximum capacity of walls BW

#### 4.4.5 Capacity of walls MW and wall CW

Walls MW and CW exhibited a similar response and behaviour as did wall BW. As seen in Figures 4.98 and 4.99, the capacity of walls MW and CW to retain monotonic lateral loads decreased with increasing compressive pressure; but it increased in case of repeated lateral loads. The average capacity of these walls to retain cyclic loads decreased on average by 30% compare to that of monotonic and repeated load.

#### 4.4.6 Capacity of walls MWA and CWA

The graphs presenting the capacities of wall MWA and CWA are shown in Figures 4.100 and 4.101. As can be seen from these figures, these capacities are not similar. The capacity of wall MWA to retain repeated lateral load was about 15 to 20 % higher that to monotonic load. The increased capacity was caused by the presence of mortar type A over wall surface. Wall CWA exhibited a similar response to other walls, except for the wall MWA. The capacity of wall MWA to retained cyclic lateral load decreased by 40% to 60% compare to that of monotonic load. The same was observed for wall CWA. The use of mortar type A for strengthening of the wall surface did not have a significant effect on the masonry construction.

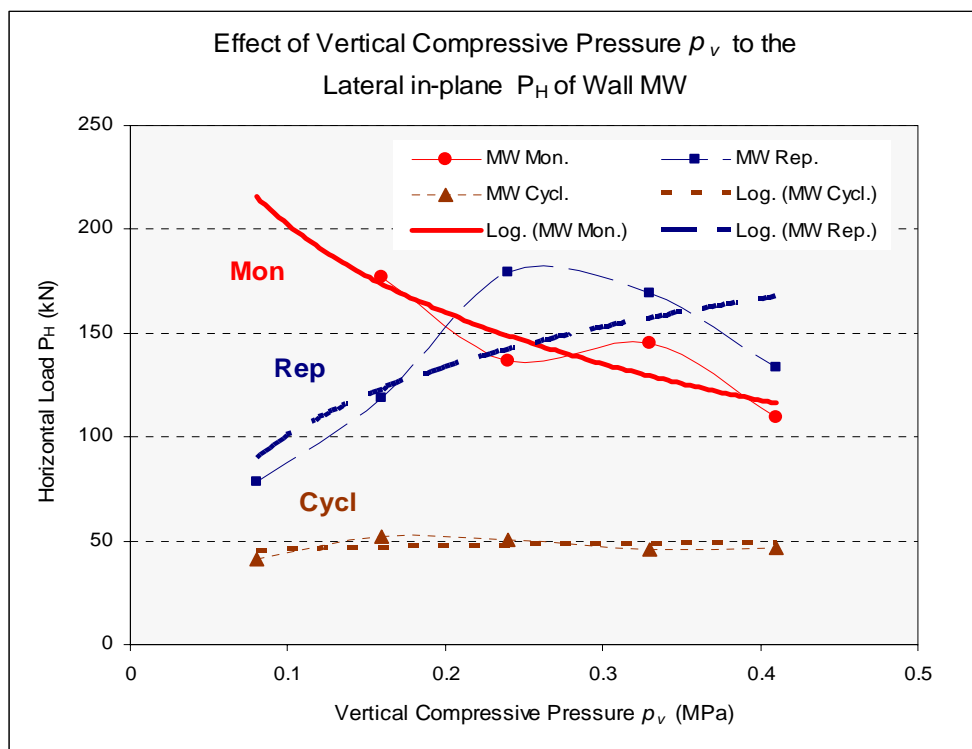


Figure 4.98 Maximum capacity of walls MW

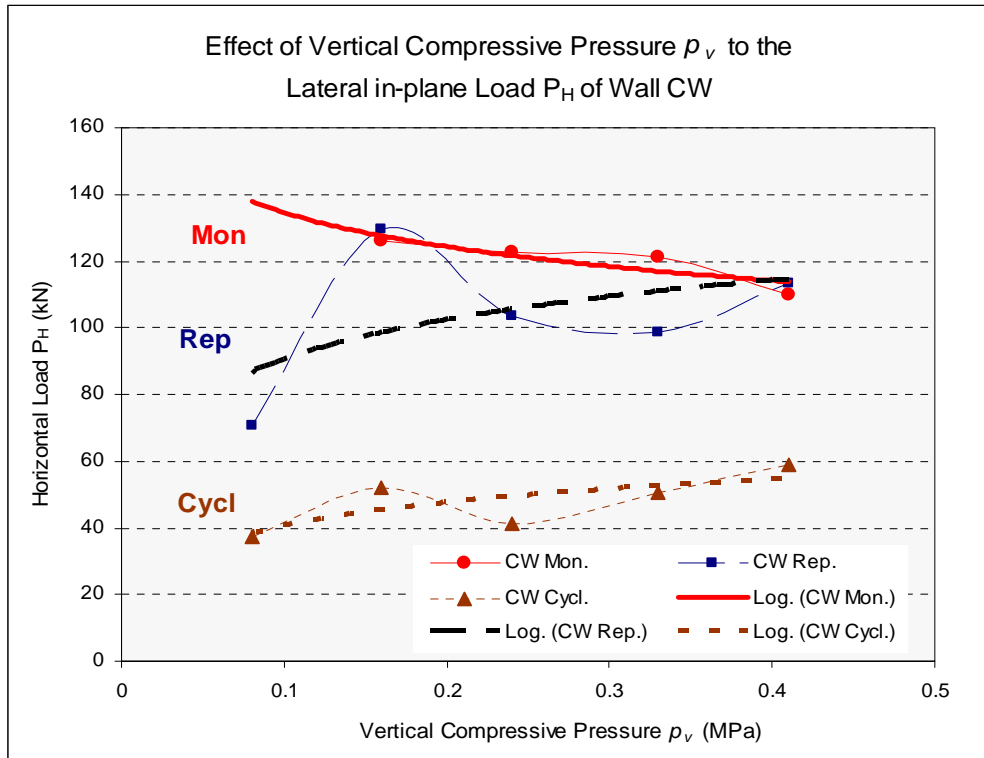


Figure 4.99 Maximum capacity of walls CW

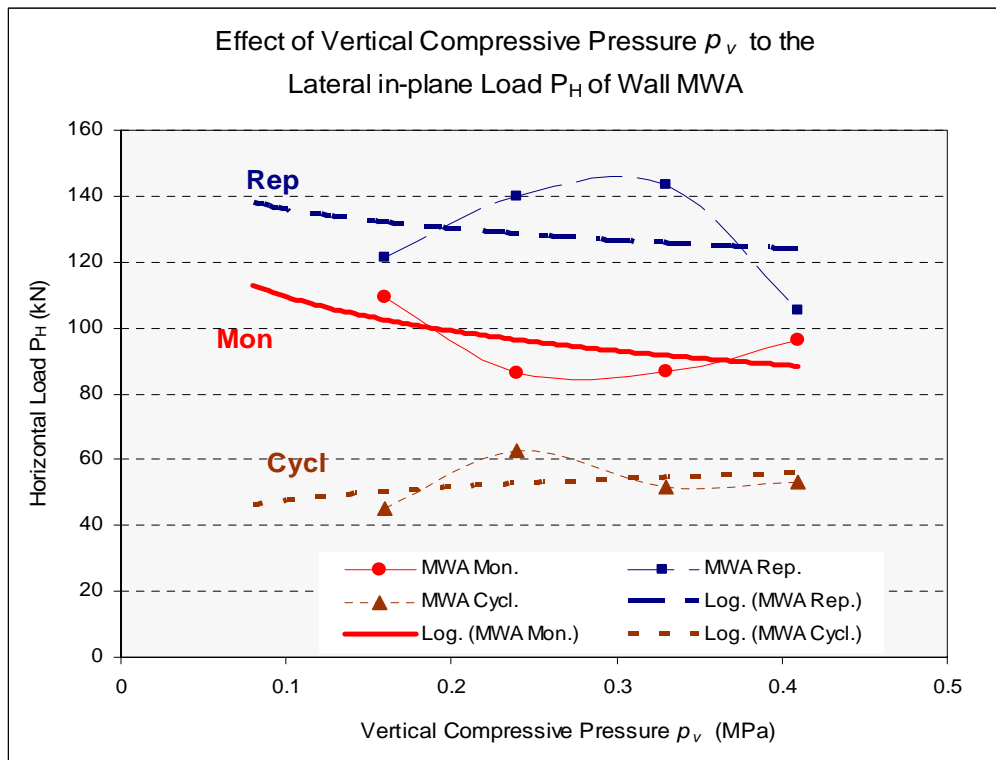


Figure 4.100 Maximum capacity of walls MWA

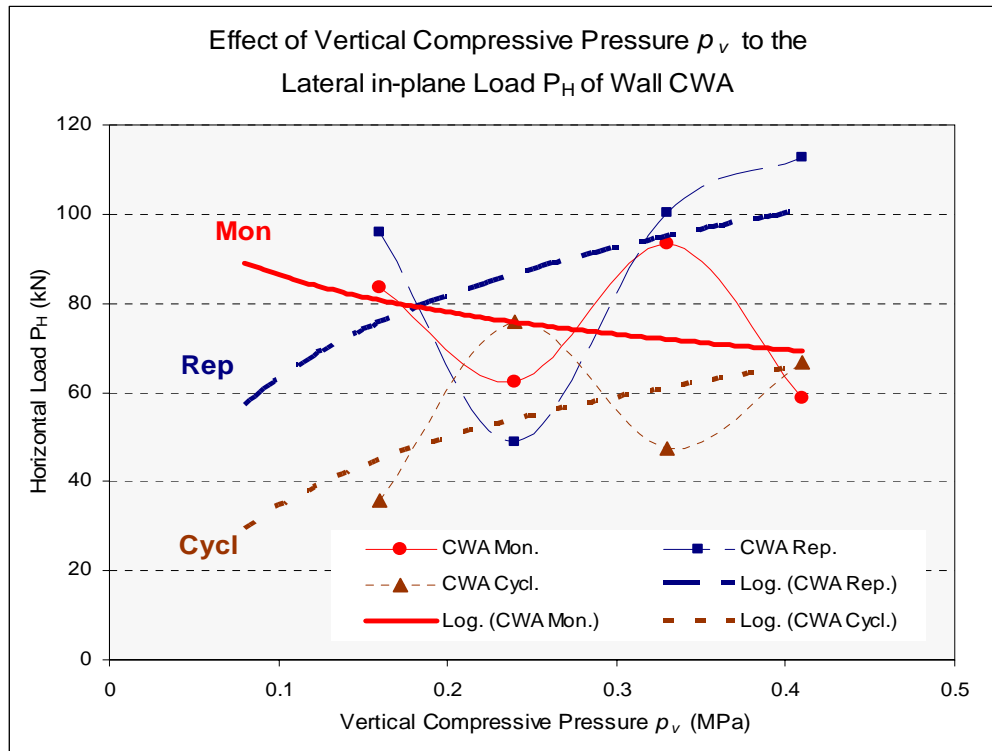


Figure 4.101 Maximum capacity of walls CWA

## 4.5 Lateral stiffness of wall panels under compression and monotonic lateral in-plane loads

The responses of wall panels to monotonic lateral loads based on compressive pressure parameter are discussed below. Taking a linear regression of response of each wall specimens, it can be seen that the values of the wall lateral stiffness were of a wide range from 2.41 to 8.79 kN/mm, depending on the type of walls and compression pressure acting on each wall. The detailed explanations of load displacement response of each wall based on types of walls are given in Section 4.5.1. The responses based on types of compressive vertical loads are explained in Section 4.5.2.

### 4.5.1 Load-displacement response to monotonic lateral loads based on types of walls

To evaluate the response of each group of wall panels, the curves were classified into 6 wall groups; the walls BW, MW, CW, MWA, CWA, and MWE separately. Based on the parameter of compression load applied on each of the wall specimen, the resulting applied compressive pressure is given in Table 4.1, Section 4.1.



#### 4.5.1.1 Walls BW

Load displacement responses of walls BW04, BW03, BW05, and BW21 are shown in Figure 4.102. The highest lateral stiffness was found in wall BW05 under compressive pressure  $p_v = 0.325$  MPa, and the lowest in wall BW21 under compressive pressure  $p_v = 0.42$  MPa. As the trends of load-horizontal displacement curves are similar and the curves are close to each other, it can be assumed that lateral stiffness of wall BWs are not significantly affected by the compressive pressure. The maximum stiffness occurred at compressive pressure ranging from 0.245 to 0.325 MPa, then the stiffness decreases as the pressure raised up to 0.42 MPa. Wall BW04 under compressive pressure of 0.165 MPa produced a lateral stiffness of 3.81 kN/mm, wall BW03 under the same compressive pressure produced a lateral stiffness of 3.51 kN/mm. Wall BW05 under compressive pressure of 0.245 MPa produced a lateral stiffness of 4.63 kN/mm, wall BW21 under compressive pressure of 0.42 MPa produced a lateral stiffness of 2.74 kN/mm. The average value of lateral stiffness of walls BW, irrespective of the compressive pressure parameter, is 3.67 kN/mm.

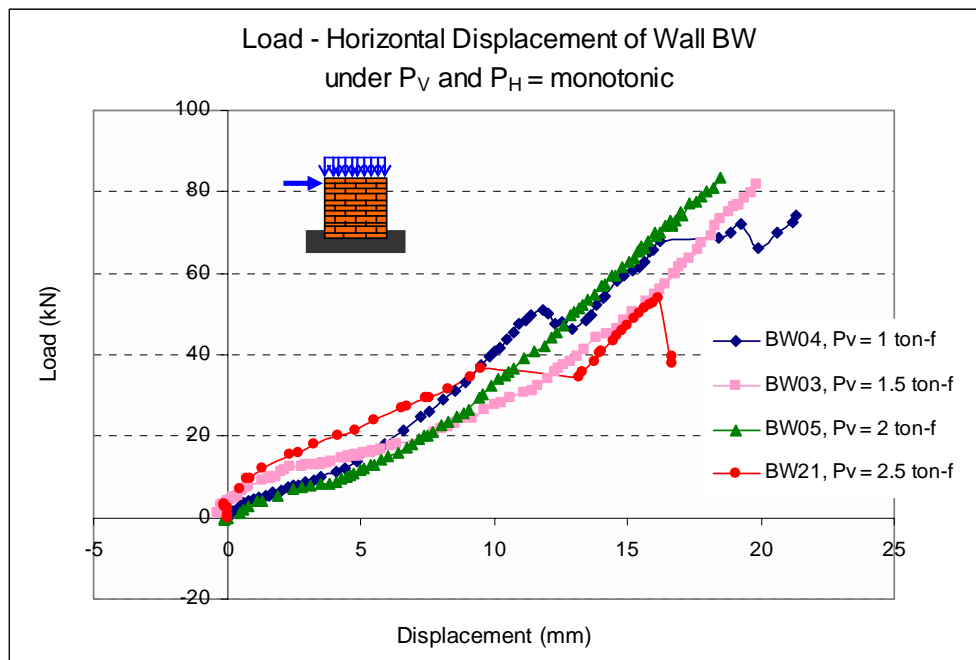


Figure 4.102 Load-displacement of walls BW under monotonic loads

#### 4.5.1.2 Walls MW and CW

When evaluating load-displacement responses of walls MW as illustrated in Figure 4.103, two groups of load-displacement curves are noticed. The compressive

pressures of 0.165 MPa, 0.245 MPa, 0.325 MPa and 0.42 MPa were applied to walls MW08, MW07, MW01 and MW 0.42 respectively and the resulting stiffness were 6,99 kN/mm, 6.08 kN/mm, 8.43 kN/mm and 8.79 kN/mm. Lateral stiffness of wall MW under compressive pressure less than 0.27 MPa was lower than that of wall MW under compressive pressure higher than 0.27 MPa.

Load-displacement responses of walls CW can also be categorised into two groups, curves with lower lateral stiffness for walls under compressive pressure less than 0.27 MPa and curves with higher lateral stiffness, as pressure increase above 0.27 MPa. The curves are shown in Figure 4.104. The lateral stiffness of wall CW07 under compressive pressure of 0.165 MPa was 5.60 kN/mm, of wall CW08 under compressive pressure of 0.245 MPa was 6.33 MPa, of wall CW01 under compressive pressure of 0.325 MPa was 8.55 kN/mm, and of wall CW06 under compressive pressure of 0.42 MPa was 8.70 kN/mm.

These results show that wall MW and CW became stiffer as the compressive stress increased. Both load-displacement curves shown in Figures 4.103 and 4.104 are similar, and produced stiffer slopes than the responses of other types of walls.

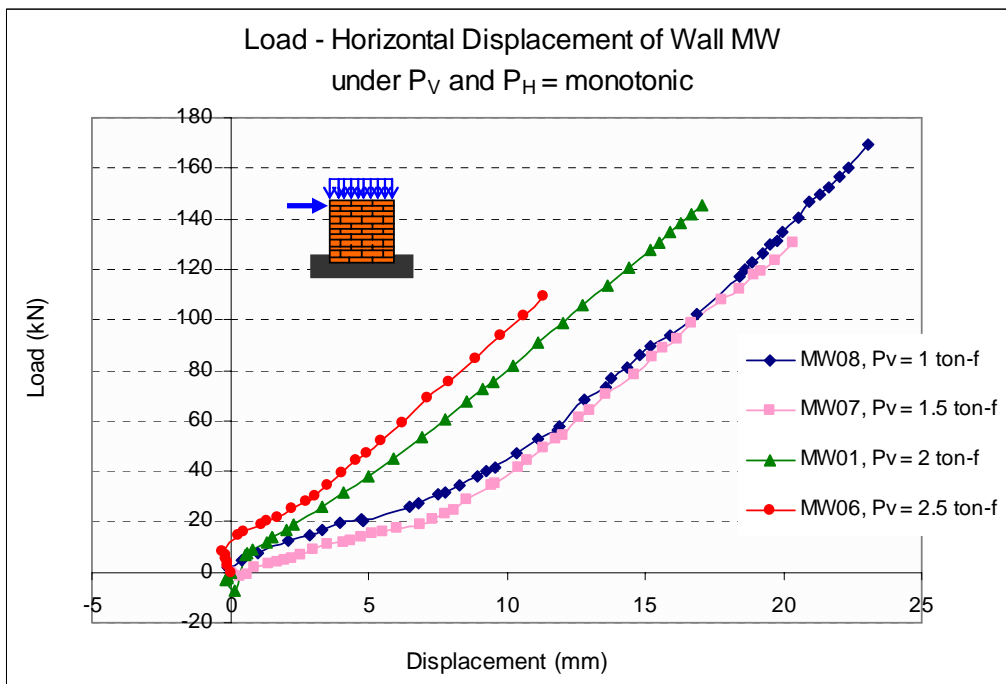


*Figure 4.103 Load-displacement of walls MW under monotonic loads*

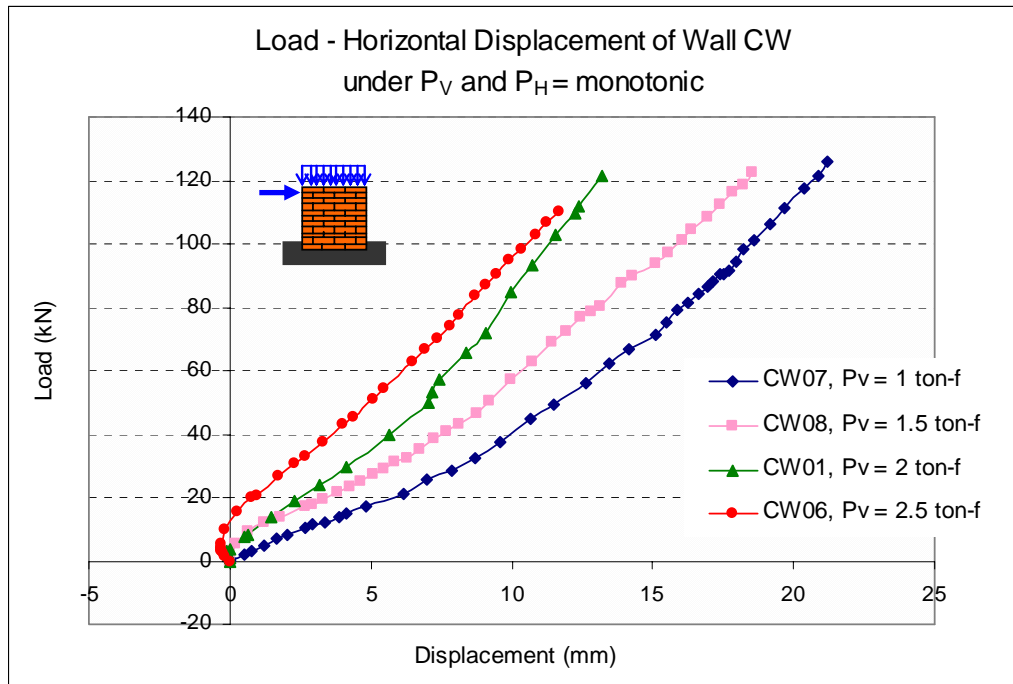


Figure 4.104 Load-displacement of walls CW under monotonic loads

#### 4.5.1.3 Walls MWA and CWA

The curves of load-horizontal displacement responses of walls MWA, CWA and MWE are very similar in their trends, as can be seen in Figures 4.105, 4.106 and 4.107. Walls MWA, CWA and MWE under compressive pressure less than 0.325 MPa are generally weaker than those under compression pressure greater than 0.325 MPa.

In Figure 4.105, it is shown that lateral stiffness of walls MWA according to  $P_V = 1$  ton-f, 1.5 ton-f, 2 ton-f, and 2.5 ton-f or compressive pressure of  $p_v = 0.165$  MPa, 0.245 MPa, 0.325 MPa, and 0.42 MPa are 2.34 kN/mm, 5.21 kN/mm, 3.56 kN/mm, and 4.12 kN/mm respectively.

As shown in Figure 4.106, the lateral stiffness of walls CWA according to  $P_V = 1$  ton-f, 1.5 ton-f, 2 ton-f, and 2.5 ton-f were 3.74 kN/mm, 2.94 kN/mm, 3.56 kN/mm, and 4.12 kN/mm respectively. As  $P_V$  increase above 2 ton-f, both walls MWA and CWA responded in the same way.

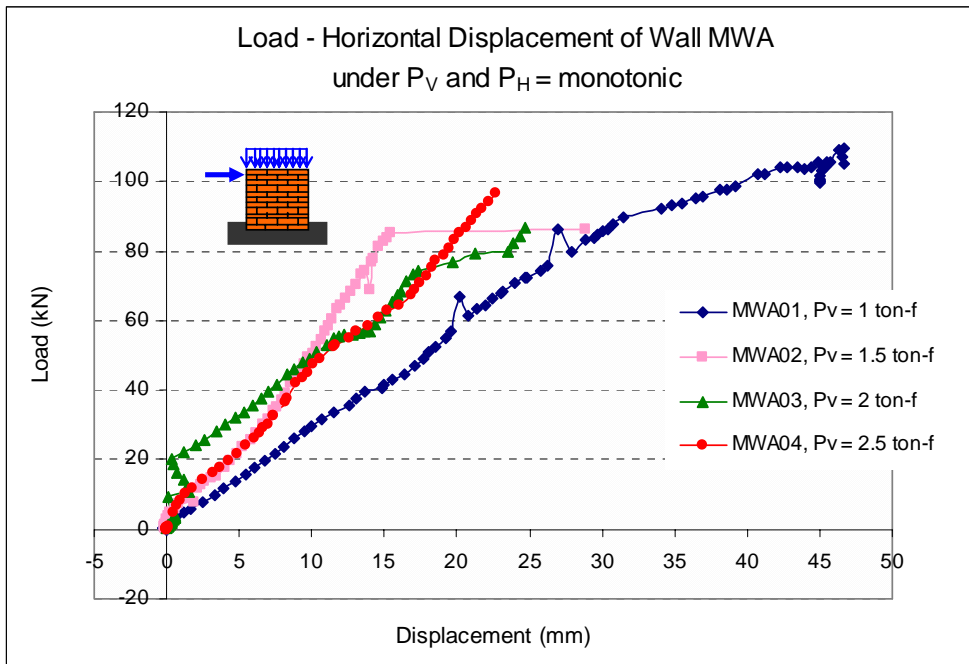


Figure 4.105 Load-displacement of walls MWA under monotonic loads

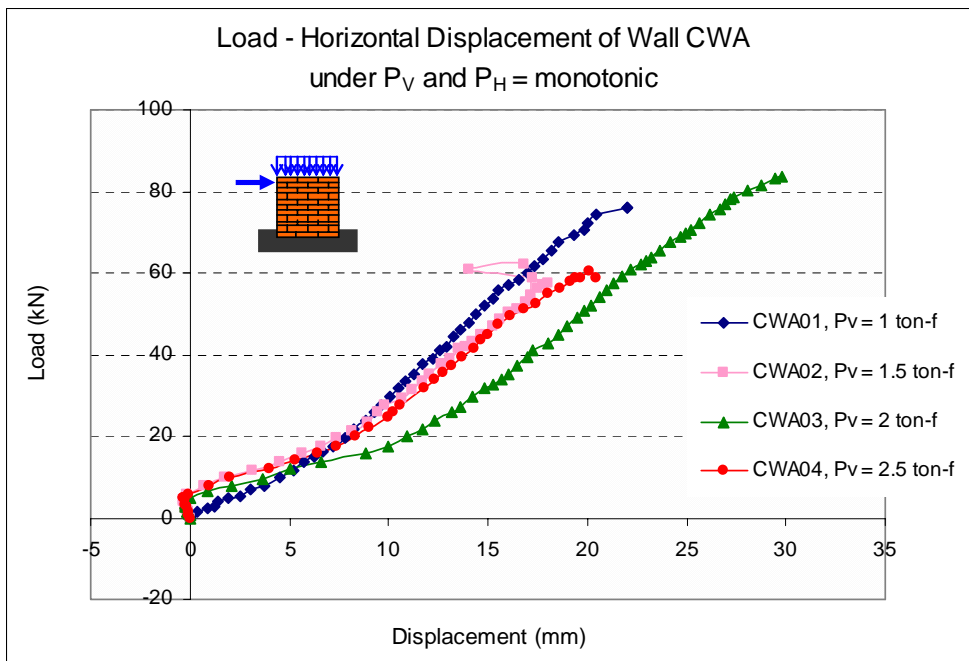


Figure 4.106 Load-displacement of walls CWA under monotonic loads

#### 4.5.1.4 Walls MWE

As seen in Figure 4.107, the lateral stiffness of walls MWE according to  $P_V = 0.5$  ton-f, 1 ton-f, 1.5 ton-f, 2 ton-f, and 2.5 ton-f were 2.34 kN/mm, 3.67 kN/mm, 3.17 kN/mm, 2.42 kN/mm, and 3.56 kN/mm. Wall MWE under  $P_V = 0.5$  ton-f was the weakest in retaining lateral load. The lateral stiffness of walls under lateral in-plane

loading is listed in Table 4.8 and graphically shown in Figures 4.108 and 4.109. According to Figure 4.109, the lateral stiffness of wall therefore can be classified into two different groups as shown in Table 4.9. First group is lateral stiffness of wall MW and CW, and second group is the stiffness of other wall types.

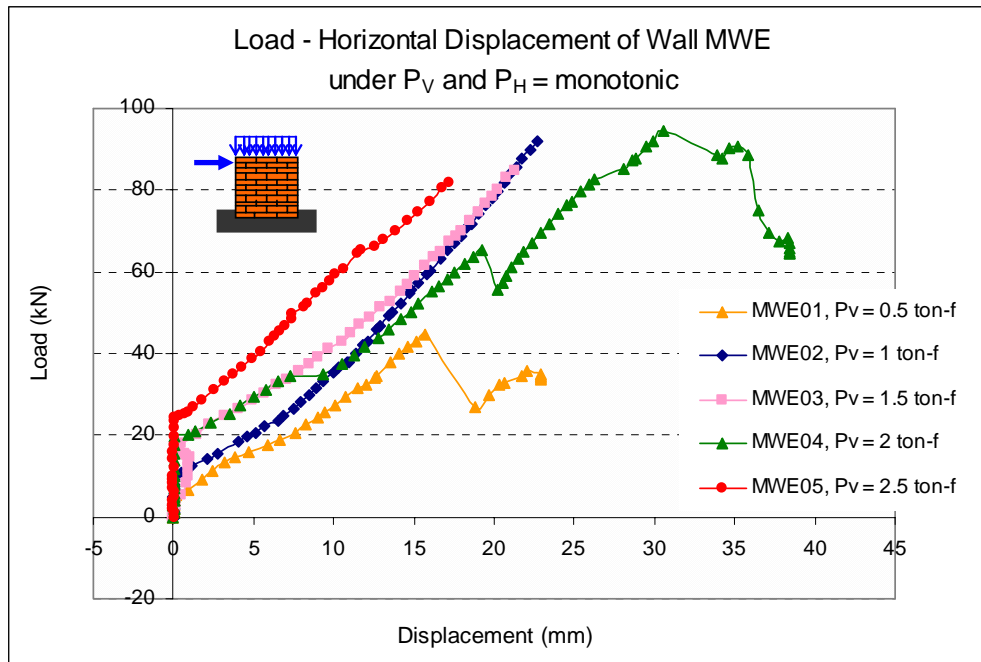


Figure 4.107 Load-displacement of walls MWE under monotonic loads

Table 4.8 Lateral stiffness of walls under different types of compressive pressures (kN/mm)

Wall	Compression Load $P_v$ (ton-f)			
	1	1.5	2	2.5
	Compressive Pressures $p_v$ (MPa)			
	0.165	0.245	0.325	0.42
Wall BW	3.81	3.51	4.63	2.74
Wall MW	6.99	6.08	8.43	8.79
Wall CW	5.60	6.33	8.55	8.70
Wall MWA	2.34	5.21	3.56	4.12
Wall CWA	3.74	2.94	3.56	4.12
Wall MWE	3.67	3.17	2.42	3.56

Table 4.9 Wall lateral stiffness

Wall Groups	Pressure	Lateral Stiffness
MW and CW	< 0.325 MPa	6 kN/mm
	≥ 0.325 MPa	8 kN/mm
BW, MWA, CWA, MWE	any	3 – 4 kN/mm

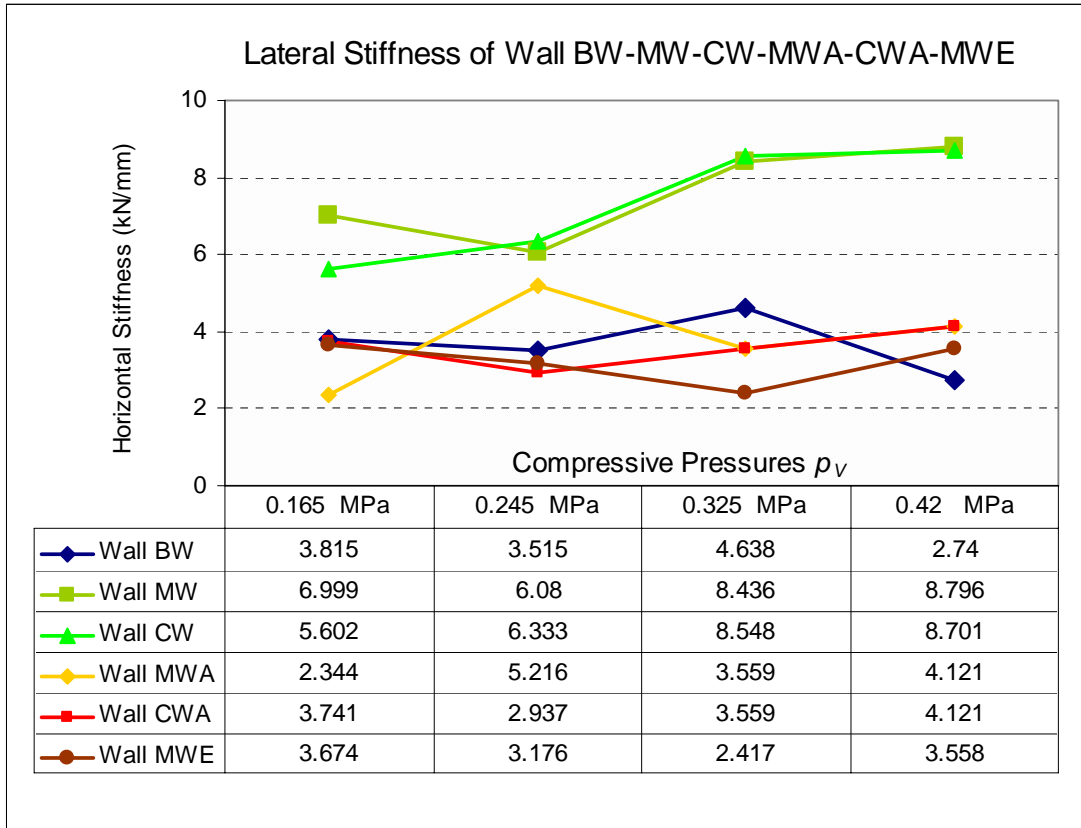


Figure 4.108 Lateral stiffness of walls

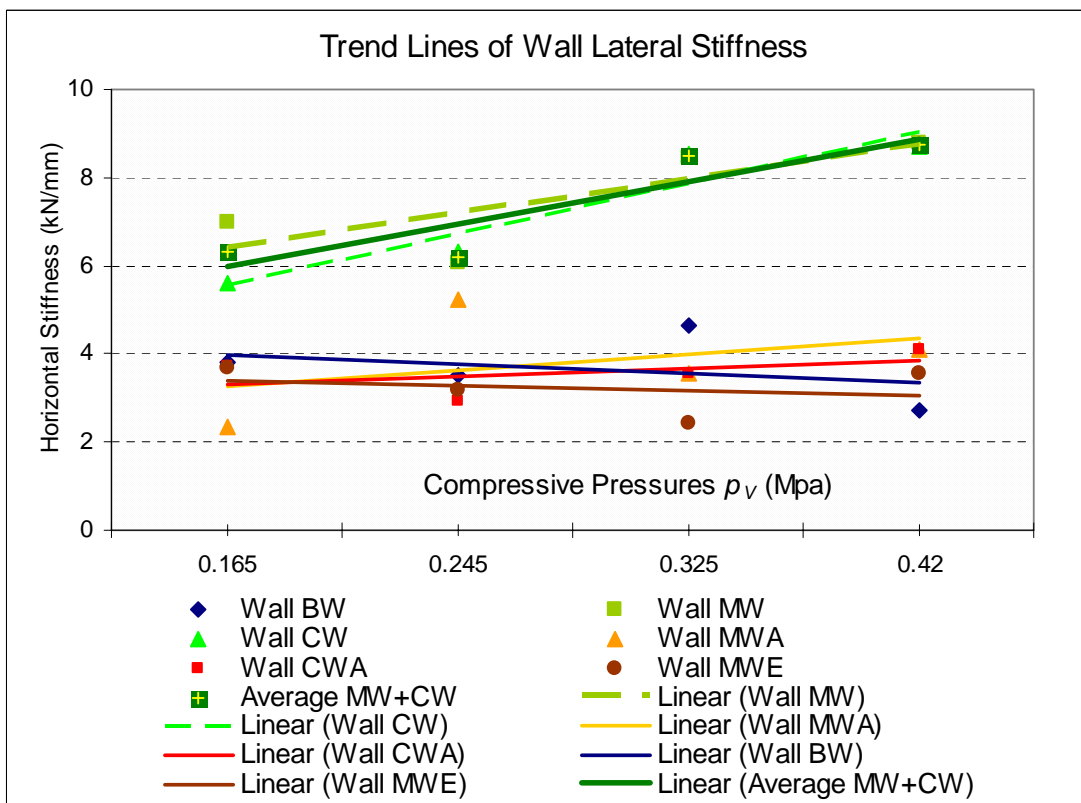


Figure 4.109 Generalised lateral stiffness of walls

#### 4.6 The principal stress of walls approaching failure

Based on the results from experimental work discussed in previous sections, it is important to determine the principal stress that caused the failure of wall panels. This analysis aims to determine the maximum tensile and shear stress that caused gradual crack and failure in wall panels. Referring to the load applied on wall panels, compressive pressure is considered to be compressive stress acting vertically in y direction. Shear stress caused by lateral in-plane load acted in positive direction, as detailed in Appendix A.

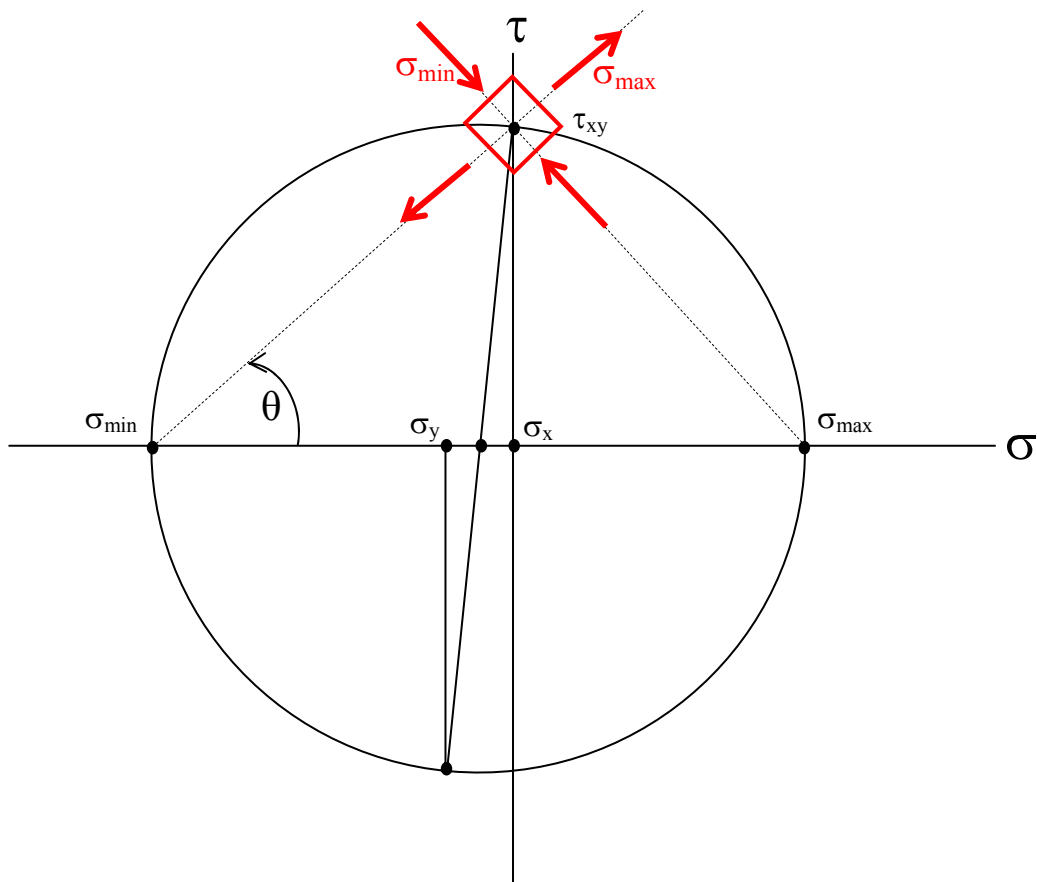


Figure 4.110 Mohr circle for principal stress

Referring to Figure 4.110, the maximum and minimum principal stress and the maximum shear stress occurred in wall specimens at maximum failure load. They are analysed by using the formula given below:

$$\sigma_{\max, \min} = \frac{\sigma_x + \sigma_y}{2} \pm \sqrt{\left(\frac{\sigma_x - \sigma_y}{2}\right)^2 + (\tau_{xy})^2}$$

$$\tau_{\max} = \frac{\sigma_x - \sigma_y}{2}$$

$$\tan 2\theta = \frac{2\tau_{xy}}{\sigma_x - \sigma_y}$$

Therefore, the inclination angle  $\theta$  is:

$$\theta = \frac{1}{2} \text{arc tan} \left( \frac{2\tau_{xy}}{\sigma_x - \sigma_y} \right)$$

where

- $\sigma_{\max}$  = maximum stress,
- $\sigma_{\min}$  = minimum stress,
- $\sigma_x$  = normal stress in the direction of x axis,
- $\sigma_y$  = normal stress in the direction of y axis,
- $\tau_{xy}$  = shear stress in xy plane,
- $\theta$  = angle of inclination

In this experiments, the average shear stress  $\tau_{xy}$  was taken as maximum horizontal load  $P_H/A$ ,  $\sigma_x = 0$  and  $\sigma_y = P_V/A$  where A is the cross section area of wall.

#### 4.6.1 Maximum shear stress of wall BW

From Figure 4.111, maximum shear stress of wall BW under monotonic and repeated lateral load is within a range of 1.2 to 1.5 MPa, and those of wall under cyclic load is between 0.7 to 0.9 MPa. It means that any wall BW experiencing cyclic load will collapse as shear force approaching 0.7 MPa.



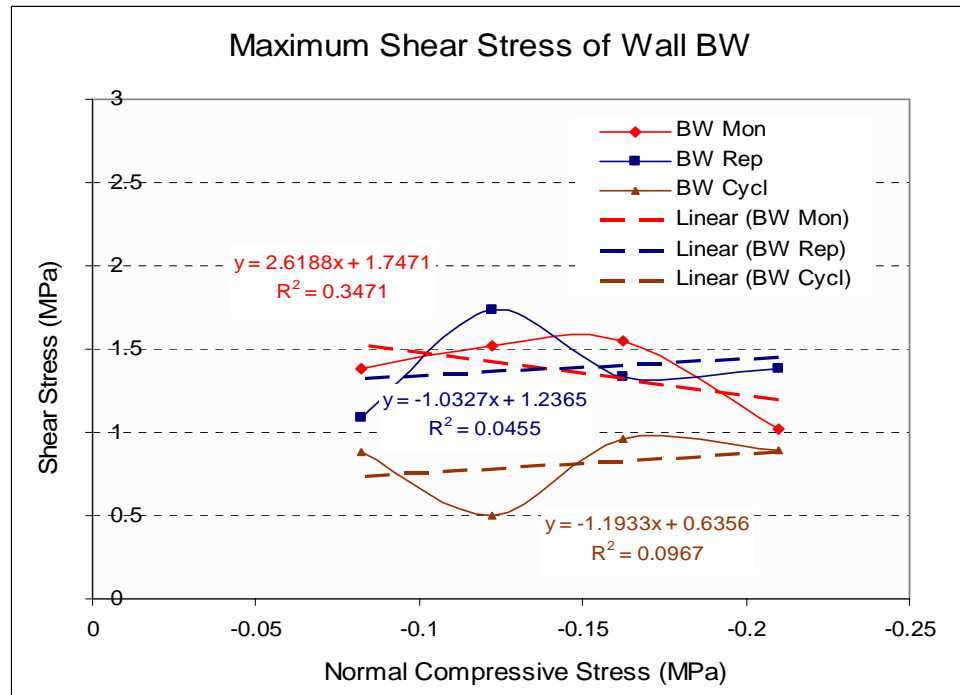


Figure 4.111 Maximum shear stress of walls BW

#### 4.6.2 Maximum shear stress of wall MW and CW

In Figures 4.112 and 4.113, the maximum shear stress of wall MW and CW under cyclic loads is within a range of 0.6 to 0.9 MPa. This range is nearly the same as that of wall BW. As seen in this frames, walls MW and CW will collapse under cyclic loads as shear force approaches 0.6 MPa.

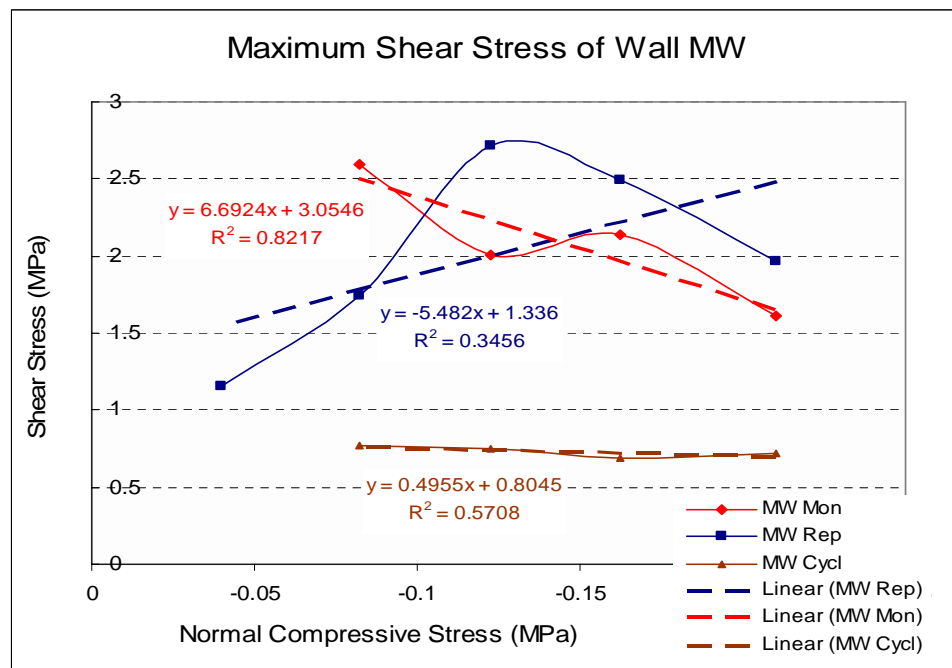


Figure 4.112 Maximum shear stress of walls MW

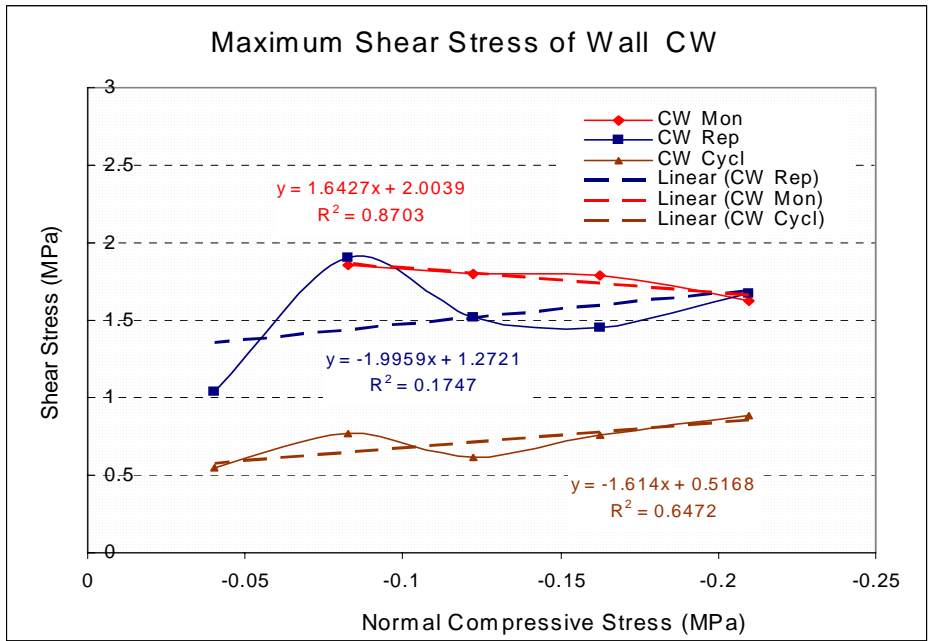


Figure 4.113 Maximum shear stress of walls CW

#### 4.6.3 Maximum shear stress of walls MWA and CWA

In Figures 4.114 and 4.115, the maximum shear stress of wall MWA and CWA under cyclic loads is within a range of 0.7 to 1.0 MPa. Similarly as in case of walls MW and CW, this range is also nearly the same as that of wall BW. Consequently, it can be concluded that walls MWA and CWA will collapse under cyclic loads as shear force approaches 0.7 MPa.

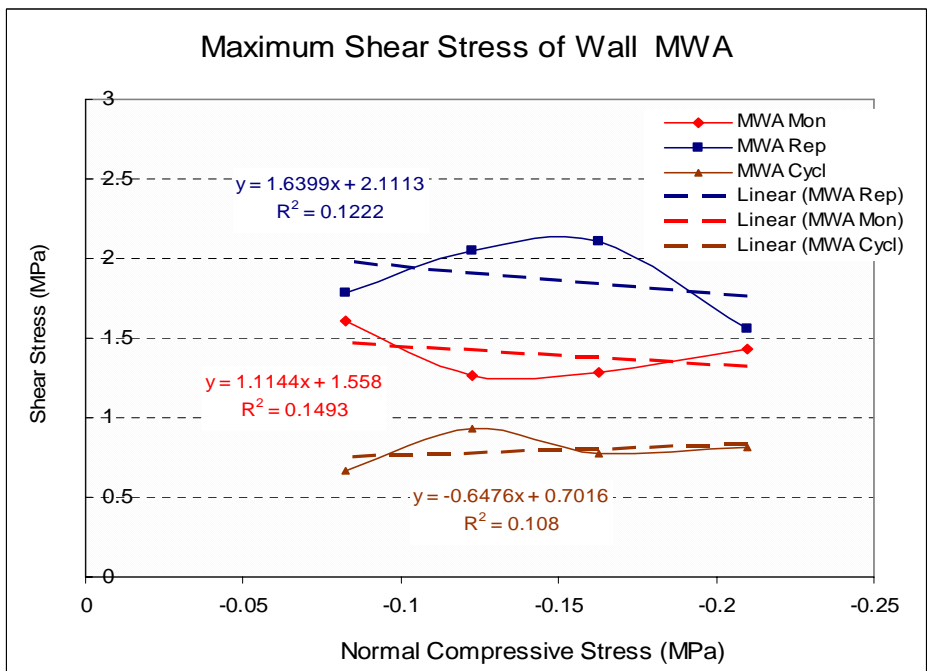


Figure 4.114 Maximum shear stress of walls MWA

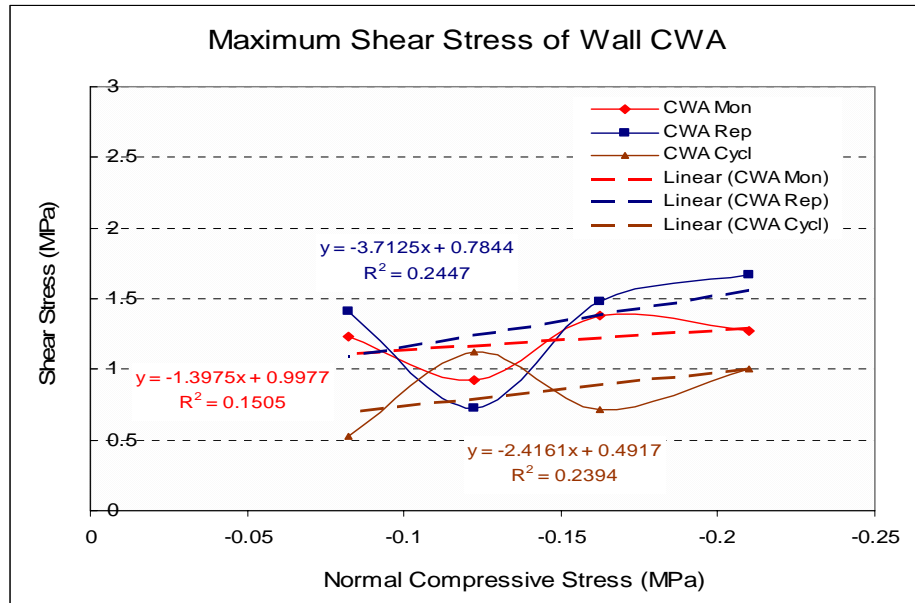


Figure 4.115 Maximum shear stress of walls CWA

#### 4.6.4 Maximum shear stress of wall MWE

In Figure 4.116, wall MWE was only tested under monotonic load. Since the maximum shear stress was noticed within a range of 1.0 to 1.2 MPa, therefore the critical shear stress under cyclic load can be approximated to 50% of wall capacity under monotonic load. This critical shear stress was within a range of 0.5 to 0.6 MPa. This wall MWE experienced the lowest capacity among the walls BW, MW, CW, MWA and CWA. The maximum critical stresses of walls BW, MW, CW, MWA, CWA as obtain by principal stress analysis are given in Table 4.10.

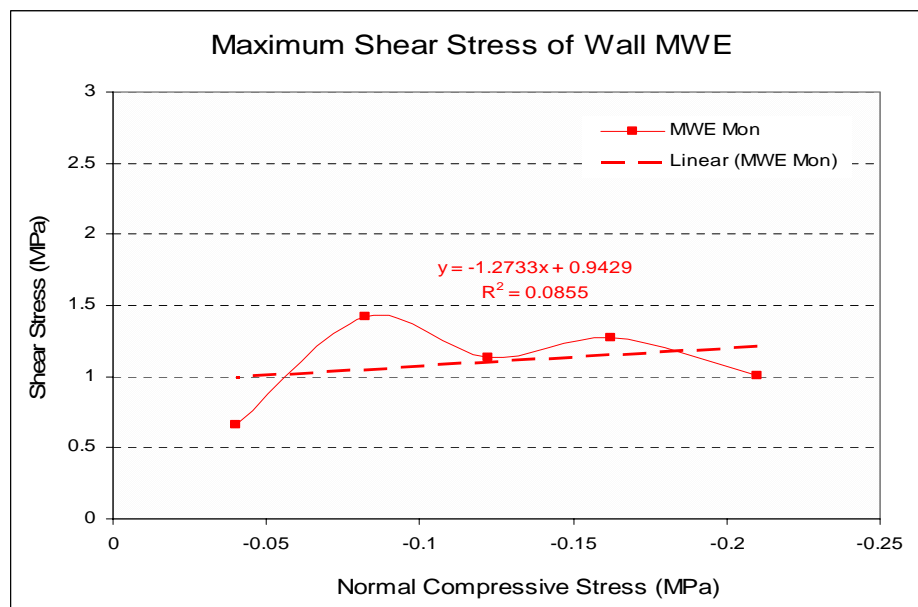


Figure 4.116 Maximum shear stress of walls MWE

Table 4.10 The principal stress of walls (MPa)

Wall	$\rho_v$	$\tau_{max}$			$\sigma_{max}$			$\sigma_{min}$		
		Mon	Rep	Cycl	Mon	Rep	Cycl	Mon	Rep	Cycl
BW	-0.165	1.2974	1.0104	0.9665	1.3799	1.0929	0.8815	-1.4624	-1.1754	-0.7965
	-0.245	1.3989	1.6113	0.6224	1.5214	1.7338	0.4974	-1.6439	-1.8563	-0.3724
	-0.325	1.3894	1.1728	1.1223	1.5519	1.3353	0.9573	-1.7144	-1.4978	-0.7923
	-0.42	0.8127	1.1703	1.1052	1.0227	1.3803	0.8952	-1.2327	-1.5903	-0.6852
MW	-0.08		1.1114			1.1514			-1.1914	
	-0.165	2.5109	1.6614	0.6872	2.5934	1.7439	0.7697	-2.6759	-1.8264	-0.8522
	-0.245	1.8893	2.5917	0.6311	2.0114	2.7142	0.7536	-2.1343	-2.8367	-0.8761
	-0.325	1.9711	2.327	0.5271	2.1336	2.4895	0.6896	-2.2961	-2.6520	-0.8522
CW	-0.42	1.4046	1.7561	0.5089	1.6146	1.9661	0.7189	-1.8246	-2.1761	-0.9289
	-0.08		1.0007	0.5079		1.0406	0.5479		-1.0807	-0.5879
	-0.165	1.7690	1.8180	0.6843	1.8515	1.9005	0.7668	-1.9341	-1.9830	-0.8493
	-0.245	1.6781	1.3999	0.4974	1.8006	1.5224	0.6199	-1.9232	-1.6449	-0.7424
MWA	-0.325	1.6235	1.2922	0.5965	1.7860	1.4547	0.759	-1.9485	-1.6172	-0.9215
	-0.42	1.4188	1.4645	0.6768	1.6288	1.6745	0.8868	-1.8388	-1.8845	-1.0968
	-0.165	1.5234	1.6976	0.5832	1.6059	1.7801	0.6657	-1.6884	-1.8626	-0.7482
	-0.245	1.1465	1.9298	0.8047	1.2690	2.0523	0.9272	-1.3915	-2.1748	-1.0497
CWA	-0.325	1.1197	1.9467	0.6149	1.2822	2.1092	0.7774	-1.4443	-2.2717	-0.9399
	-0.42	1.2212	1.3465	0.6002	1.4312	1.5565	0.8102	-1.6412	-1.7665	-1.0202
	-0.165	1.1443	1.3252	0.4455	1.2268	1.4077	0.528	-1.3093	-1.4902	-0.6105
	-0.245	0.7976	0.6058	0.9962	0.9201	0.7283	1.1188	-1.0426	-0.8508	-1.2413
MWE	-0.325	1.2153	1.3155	0.5497	1.3771	1.4780	0.7122	-1.5403	-1.6405	-0.8747
	-0.42	1.0633	1.4577	0.7933	1.2733	1.6677	1.0033	-1.4833	-1.8777	-1.2133
	-0.08	0.6215			0.6615			-0.7015		
	-0.165	1.3356			1.4182			-1.5006		
MWE	-0.245	1.0136			1.1359			-1.2585		
	-0.325	1.1153			1.2778			-1.4403		
MWE	-0.42	0.7976			1.0076			-1.2176		

## 4.7 Shear modulus of walls

Shear stress  $\tau$  is assumed to be uniformly distributed over the wall cross section area and it is equal to  $P_H/A$ . The angle of rotation of the wall measured during experiments noted as  $\gamma$ . This angle  $\gamma$  is equal to  $\sin \gamma$  and also equal to  $\tan \gamma$ , therefore the small deformation theory of solid mechanics was applied to analyse the shear strain of walls, which is equal to  $\gamma$  and it is taken as the ratio of horizontal displacement  $\Delta_2$  to  $h_2$  or  $\Delta_1$  to  $h_1$ . Test configuration is as seen in Figure 4.1. Shear strain of each wall type was taken from recorded horizontal displacement, divided by vertical distance between base support and the location of horizontal LVDT instrument. By taking the tangent of the shear stress versus shear strain curves, the shear modulus of wall can be obtained.

#### 4.7.1 Shear stress strain of walls BW

The shear stress strain behaviour of walls BW was similar and the response curves were close to each other. The effect of compressive pressure did not significantly change the shape of shear stress strain curves. Compared to the response of walls MW and CW, wall BW exhibited lower stiffness. The presence of surface mortar increased the wall stiffness, but did not improve wall ductility.

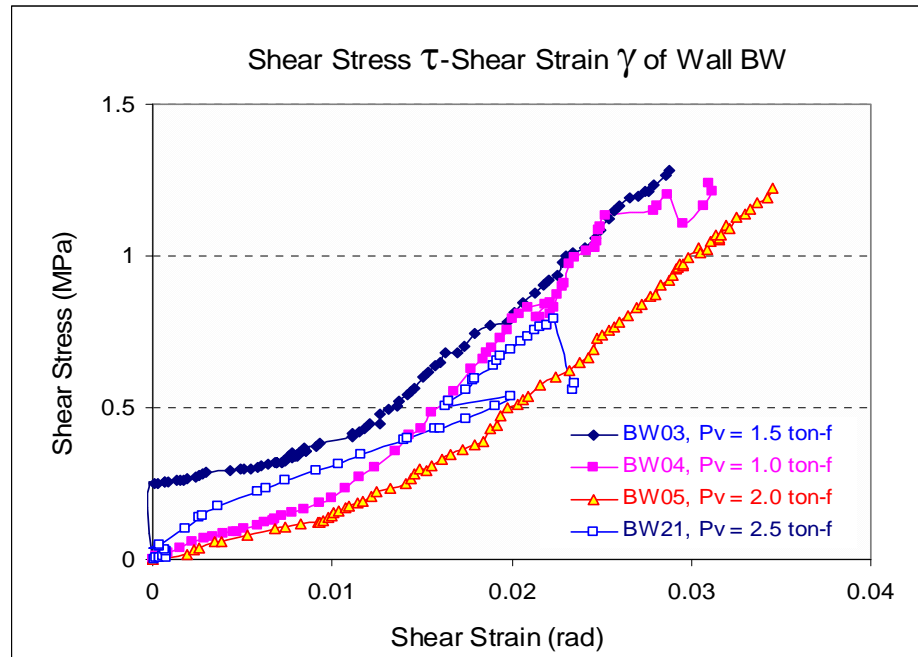


Figure 4.117 Shear stress - shear strain of walls BW

#### 4.7.2 Shear stress strain of walls MW and CW

The performances of shear stress strain curves of walls MW and CW are shown in Figures 4.118 and 4.119. Walls MW01 and MW08 produced a different curves compare to those of walls MW07 and MW08. As compressive pressure increased above 0.325 MPa, walls MW became stiffer. This phenomenon was also found in the response of walls CW. Walls CW were weaker than walls MW. This was caused by the non-homogeneity of mortar plaster and brick wall.

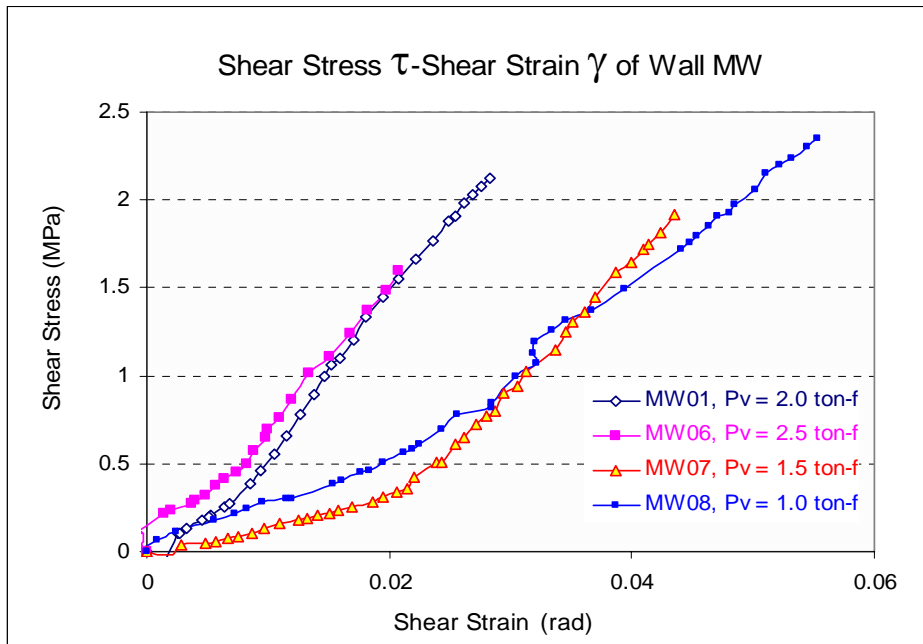


Figure 4.118 Shear stress - shear strain of walls MW

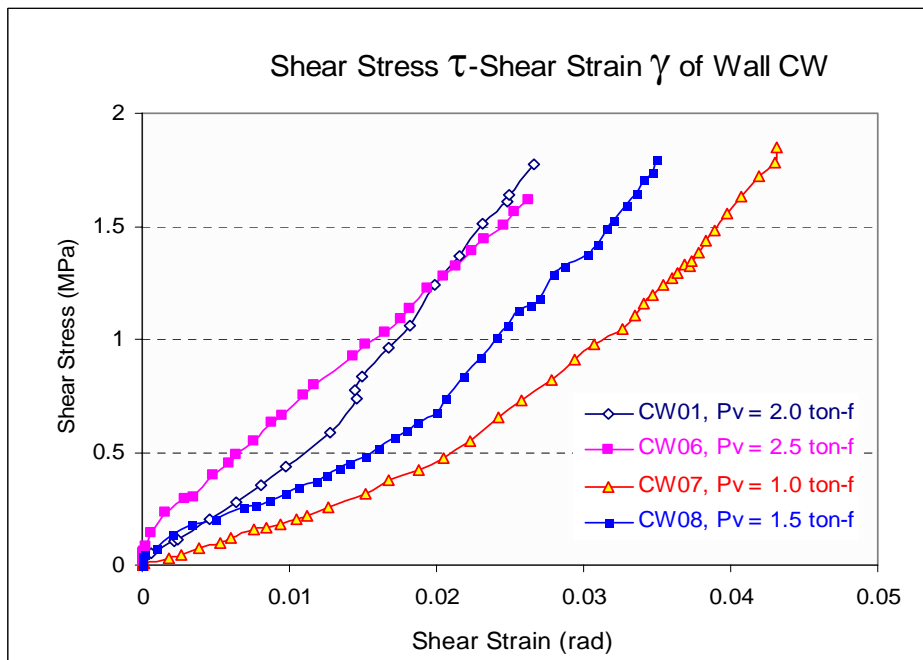


Figure 4.119 Shear stress - shear strain of walls CW

### 4.7.3 Shear stress strain of walls MWA and CWA

The shear stress strain curves of walls MWA and CWA are shown in Figures 4.120 and 4.121. Walls MWA01, MWA03 and MWA04 behaved in pattern similar to those of walls CWA. Walls CWA is weaker than walls MWA. It is caused by the non-homogeneity between mortar plaster and brick wall. The shear stress strain curves of walls CWA were not significantly affected by the presence of compressive pressure.

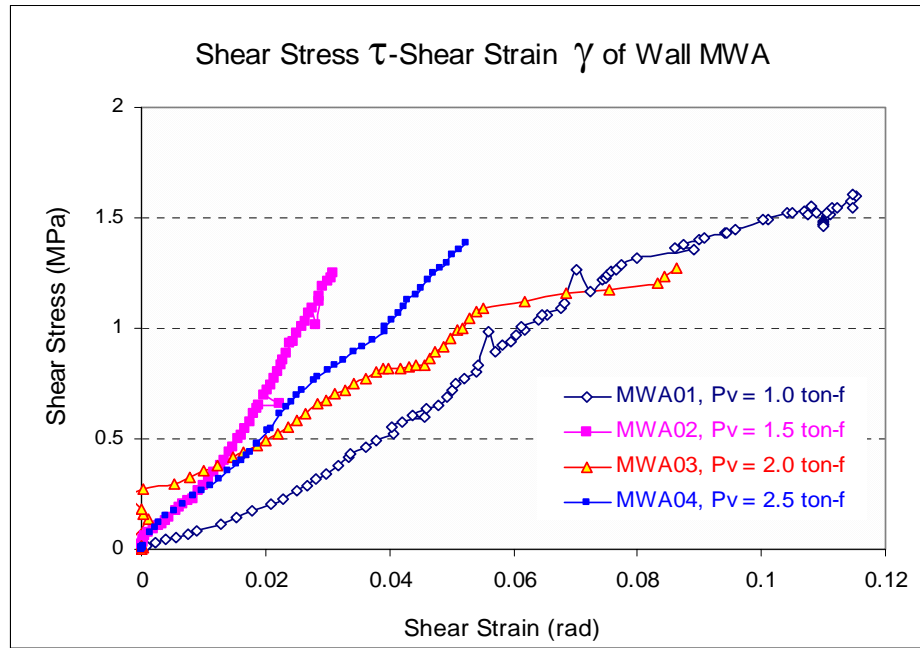


Figure 4.120 Shear stress - shear strain of walls MWA

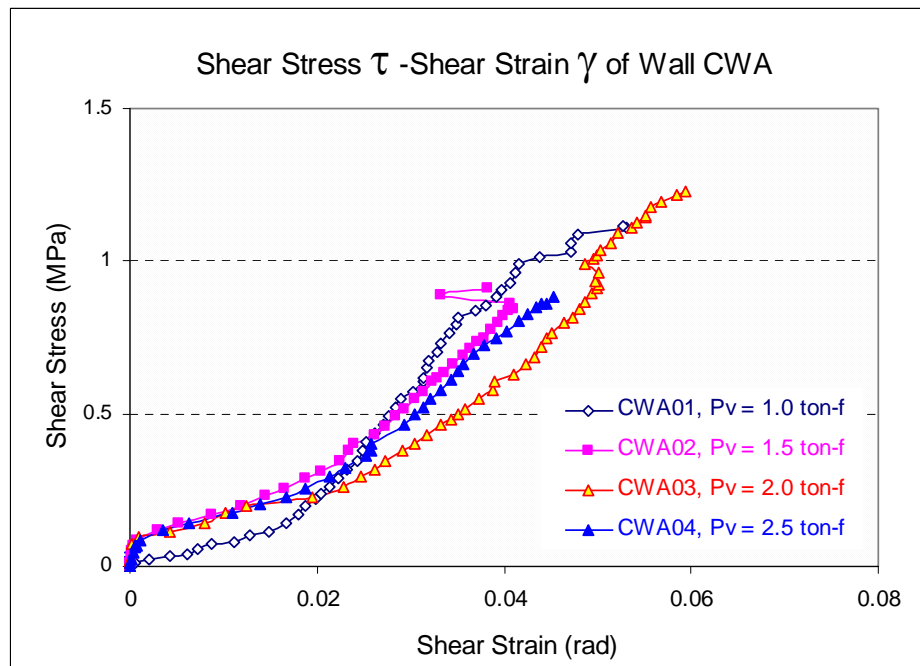


Figure 4.121 Shear stress - shear strain of walls CWA

#### 4.7.4 Shear stress strain of walls MWE

The responses of shear stress strain of walls MWE are shown in Figure 4.122. Wall MW01 collapsed under shear stress of 0.65 MPa. Overall, the average maximum shear stress which caused wall failure was 1.2 MPa

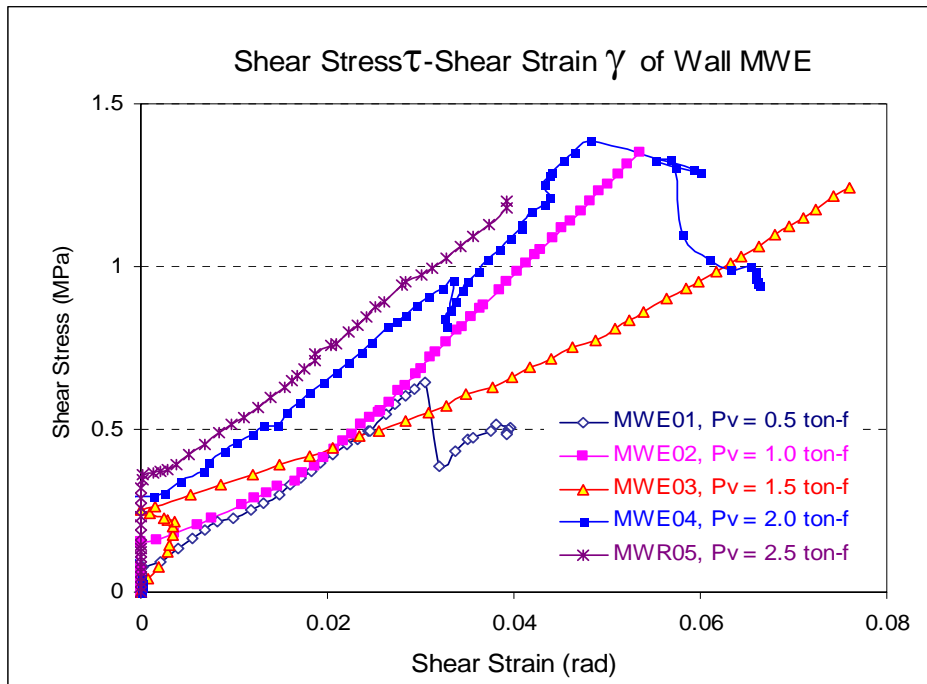


Figure 4.122 Shear stress - shear strain of walls MWE

#### 4.7.5 Shear modulus of wall panel

When evaluating shear stress strain behaviour of walls BW, MW, CW, MWA, CWA and MWE; shear modulus of each wall panel was determined by taking the value of tangential slope of linear trend lines of shear stress-strain curves as given in Table 4.11. Referring to the compressive pressure as parameter, the generalised shear modulus of walls is drawn in Figure 4.123. By using the statistical approach, the value of shear modulus was then regressed. The increase of compressive pressure in wall BW decreased the value of shear modulus. The opposite trends were observed for walls MW and CW. The presence of mortar plaster in walls MW and CW improved the value of shear modulus. The response of walls MWA, CWA and MWE was weaker than that of walls MW, CW and BW. Overall, wall BW was weaker than walls MW and CW.

Based on the above results, the value of shear modulus of each type of wall was determined by taking the average value of shear modulus, while ignoring the parameter of compressive stress as the compressive stress was in a range within fissure closing stage. The best characteristic performance was exhibited by wall CW. The average values of shear modulus of wall panels are given in Table 4.12.



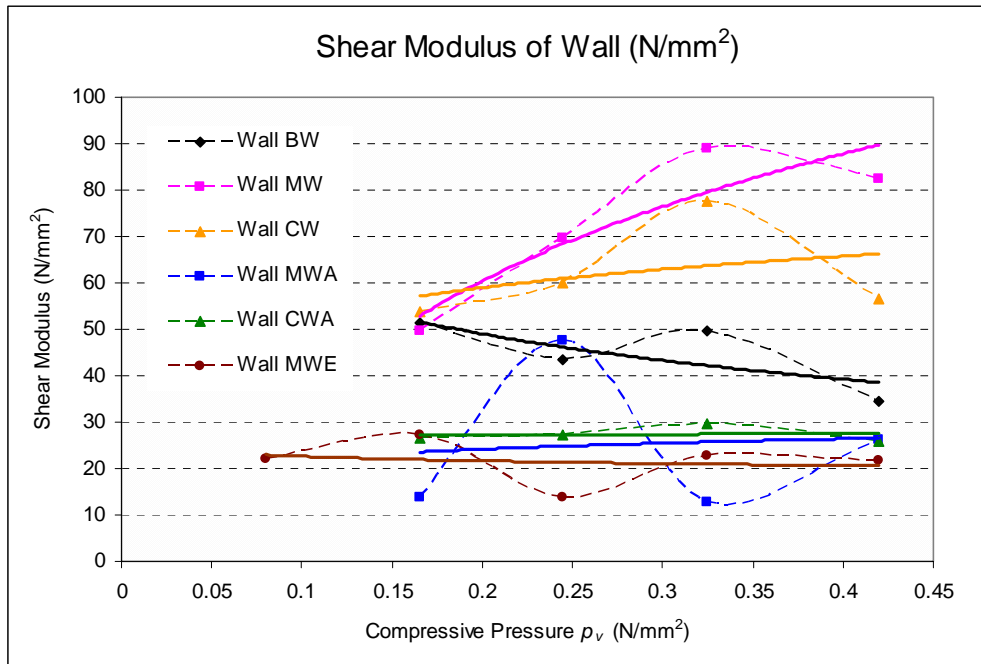


Figure 4.123 Shear modulus of walls BW, MW, CW, MWA, CWA, MWE

Table 4.11 Trend-line equations of shear modulus

Wall	Pressure (MPa)	Curves	Precision	Shear Modulus G (MPa)
BW04	0.165	$y = 51.21x - 0.283$	$R^2 = 0.948$	51.21
BW03	0.245	$y = 43.51x - 0.020$	$R^2 = 0.985$	43.51
BW05	0.325	$y = 49.54x - 0.499$	$R^2 = 0.997$	49.54
BW21	0.420	$y = 34.35x - 0.057$	$R^2 = 0.698$	34.35
MW08	0.165	$y = 49.55x - 0.440$	$R^2 = 0.991$	49.55
MW07	0.245	$y = 69.64x - 1.146$	$R^2 = 0.995$	69.64
MW01	0.325	$y = 89.02x - 0.338$	$R^2 = 0.996$	89.02
MW06	0.420	$y = 82.42x - 0.128$	$R^2 = 0.996$	82.42
CW07	0.165	$y = 53.82x - 0.627$	$R^2 = 0.979$	53.82
CW08	0.245	$y = 60.01x - 0.408$	$R^2 = 0.984$	60.01
CW01	0.325	$y = 77.58x - 0.317$	$R^2 = 0.991$	77.58
CW06	0.420	$y = 56.58x + 0.120$	$R^2 = 0.999$	56.58
MWA01	0.165	$y = 13.93x + 0.061$	$R^2 = 0.944$	13.92
MWA02	0.245	$y = 47.74x - 0.243$	$R^2 = 0.984$	47.74
MWA03	0.325	$y = 12.66x + 0.281$	$R^2 = 0.954$	12.66
MWA04	0.420	$y = 26.36x - 0.002$	$R^2 = 0.996$	26.36
CWA01	0.165	$y = 28.65x - 0.276$	$R^2 = 0.949$	26.65
CWA02	0.245	$y = 27.32x - 0.259$	$R^2 = 0.911$	27.32
CWA03	0.325	$y = 29.63x - 0.522$	$R^2 = 0.969$	29.63
CWA04	0.420	$y = 25.89x - 0.278$	$R^2 = 0.996$	25.89
MWE01	0.080	$y = 22.09x - 0.032$	$R^2 = 0.996$	22.09
MWE02	0.165	$y = 27.38x - 0.124$	$R^2 = 0.997$	27.38
MWE03	0.245	$y = 13.68x + 0.148$	$R^2 = 0.988$	13.68
MWE04	0.325	$y = 22.93x + 0.198$	$R^2 = 0.975$	22.93
MWE05	0.420	$y = 21.74x + 0.315$	$R^2 = 0.996$	21.74

Table 4.12 The average value of shear modulus of walls

Wall	Coding	Pressure (MPa)	Shear Modulus G (MPa)	Average (MPa)
BW	BW04	0.165	51.21	44.65
	BW03	0.245	43.51	
	BW05	0.325	49.54	
	BW21	0.42	34.35	
MW	MW08	0.165	49.55	72.66
	MW07	0.245	69.64	
	MW01	0.325	89.02	
	MW06	0.42	82.42	
CW	CW07	0.165	53.82	62
	CW08	0.245	60.01	
	CW01	0.325	77.58	
	CW06	0.42	56.58	
MWA	MWA01	0.165	13.92	25.17
	MWA02	0.245	47.74	
	MWA03	0.325	12.66	
	MWA04	0.42	26.36	
CWA	CWA01	0.165	26.65	27.37
	CWA02	0.245	27.32	
	CWA03	0.325	29.63	
	CWA04	0.42	25.89	
MWE	MWE01	0.08	22.09	21.52
	MWE02	0.165	27.38	
	MWE03	0.245	13.68	
	MWE04	0.325	22.93	
	MWE05	0.42	21.74	

#### 4.8 Application of results to prototype walls

All the above results presented the behaviour of wall specimens having the dimensions 600 mm x 600 mm x 90 mm for wall BW and 600 mm x 600 mm x 110 mm for the other wall models - MW, CW, MWA, CWA, and MWE. To convert the capacity of specimen to a prototype wall, similarity theory can be applied. This model is categorised as a complete similarity model as the modulus of elasticity of material for model and prototype are identical. The scale factor of the modulus of elasticity is  $S_E = 1$ . For complete similarity of the structural behaviour of the model and prototype, including the inelastic effect of cracking and yielding, a dimensional analysis will give scale factors shown in Table 4.13, column 4. If it is assumed that the stresses caused by the self-weight of the structure are not significant, as usually the case with most masonry buildings, the scale factors given in Table 4.13, column

5 will be adequate for modelling masonry structures. (Harris and Sabnis, 1999). Analyses of the model results are presented in Chapter 5.

*Table 4.13 Summary of Scale Factors for Masonry*

Group	Quantity	Dimension	Static Loading	
			True Model	Practical True Model
(1)	(2)	(3)	(4)	(5)
Loading	Concentrated load	F	$S_{\sigma}S_L^2$	$S_L^2$
	Line load	$FL^{-1}$	$S_{\sigma}S_L$	$S_L$
	Pressure	$FL^{-2}$	$S_{\sigma}$	1
	Moment	FL	$S_{\sigma}S_L^3$	$S_L^3$
Geometry	Linear dimension	L	$S_L$	$S_L$
	Displacement	L	$S_L$	$S_L$
	Angular displacement	1	1	1
	Area	$L^2$	$S_L$	$S_L$
Material properties	Masonry unit stress	$FL^{-2}$	$S_{\sigma}$	1
	Masonry unit strain	1	1	1
	Elasticity Modulus of masonry	$FL^{-2}$	$S_{\sigma}$	1
	Masonry unit Poisson's ratio	1	1	1
	Specific weight	$FL^{-3}$	$S_{\sigma}/S_L$	$1/S_L$
	Mortar stress	$FL^{-2}$	$S_{\sigma}$	1
	Mortar strain	1	1	1
	Elasticity Modulus of mortar	$FL^{-2}$	$S_{\sigma}$	1
Mortar Poisson's ratio	1	1	1	

## 4.9 Conclusion

- **Failure crack pattern**

Observing the crack failure pattern occurred in walls BW, MW, CW, MWA, CWA, and MWE, it was noticed that wall BW experienced slip failure pattern as compressive pressure decreased below 0.325 MPa. Bond shear strength between mortar and brick surface did not properly retain shear stress produced by applied lateral load. Diagonal failure pattern occurred while the wall panel was tested under  $p_v = 0.325$  MPa, combined with repeated and cyclic  $P_H$ . Under monotonic and repeated loads, as compressive stress approached 0.42 MPa, the connection between

mortar and brick surface was considerably compact, therefore the shear diagonal failure pattern occurred in overall walls. Wall BW under compressive pressure of 0.42 MPa and cyclic lateral load exhibited crushing failure types, where the compressive pressure significantly affected the failure type of this wall.

Walls MW and CW exhibited shear diagonal failure pattern for most specimens and some of them were affected by crushing failure. These walls experienced brittle failure mechanism, where gradual crack propagated in diagonal direction and was significantly affected by the presence of surface mortar plaster. Walls MWA and CWA also exhibited similar failure mechanisms to those of walls MW and CW, but spalling failure was the mostly occurring type of failure, caused by the differential strength of mortar A and mortar B.

- **Wall capacity**

Observing the capacity of wall to retain lateral load, it can be concluded that wall MW had the highest capacity amongst all the walls examined. All types of the walls showed a low capacity in retaining lateral cyclic loads, which was as low as 50% of those to the repeated and monotonic loads. The capacities of walls MW and CW to retain repeated lateral load were greater than those of walls BW, CWA, MWA and MWE.

- **Lateral stiffness of walls**

In general the lateral stiffness of wall BW, MW, CW, MWA, CWA and CWE recorded from the experimental works, can be categorised into two groups. First group was represented by wall MW and CW, which provided two values of lateral stiffness. As compressive pressure was less than 0.325 MPa, lateral stiffness is taken as 6kN/mm and as compressive pressure was higher or equal to 0.325 MPa, lateral stiffness was 8 kN/mm. In the second group, the lateral stiffness of walls BW, MW, CWA and MWE for any compressive pressure was within a range of 3 – 4 kN/mm.

- **Maximum shear stress**

Observing the maximum shear stress from principal stress analysis, it was noticed that the value of critical shear stress for all types of walls that causing failure under

cyclic load was within a range of 0.5 to 1.0 MPa. Walls MWE and BW were weaker compared to walls MW, CW, MWA and CWA.

- **Shear modulus**

Based on the results from the above analysis, the average shear modulus of wall BW was 44.65 MPa, of wall MW was 72.66 MPa, of wall CW was 62 MPa, of wall MWA was 25.17 MPa, of wall CWA was 27.37 MPa and of wall MWE was 21.52 MPa. Wall MW produced the highest shear modulus, whereas wall MWE produced the lowest value. These values of shear modulus were further used to develop a simplified formula for diagonal spring stiffness, described in the Chapter 5.

#### 4.10 Further application

The outcomes of the investigation reported in this chapter provided useful information for a contribution to the development of guidelines on masonry construction for houses and low-rise buildings in Indonesia. Since the performance characteristics of walls MW were much better than those of other walls, all MW was selected to be used in construction site. There is no significant benefit of using wall CW, compared to wall MW. Wall MWA and CWA are considerably weak. Wall BW needs to be constructed properly to reach its compactness condition. Using non-standard sand may decrease the general capacity of wall, as exhibited by wall MWE.



## Chapter 5. Contribution to the Indonesian Guidelines for Un-reinforced Brick Masonry Houses and Low Rise Buildings

---

### 5.1 Introduction

As load bearing structures, masonry buildings are considered to be adequately strong in retaining gravity load. In Indonesia, especially in villages or rural areas, masonry houses and buildings are mostly constructed without following the proper design regulations. Furthermore the main functions of masonry walls are considered to be subdivision of space, thermal insulation, and weather protection, rarely are they considered to be important components that provide structure and retain load.

Clay brick masonry is relatively cheap building material from which external wall finishes of very good and acceptable appearance are produced. The basic advantage of masonry construction is that it uses the same element to perform a variety of functions, and the construction work is flexible in terms of building layout.

In the present time brick construction for multi storey buildings is no longer used and in being replaced by steel or reinforced concrete framed structures. However, in contribution of houses and simple low-rise buildings, brick masonry structures still dominate. Based on the general structural systems, building structures are divided into two parts, the lower part, called sub structure and the upper part called upper structure. Sub structure is a part that is located under the ground surface and is called foundation. The upper structure is a part that consists of roof, wall, beams and columns or frames. For ordinary houses, the main parts of structural systems are roofs, ceilings, house frames, walls and foundations.

Based on the research outcomes from experiments performed on 75 wall specimens loaded under compression and increasing lateral in-plane forces, it was concluded that it is necessary to develop technical guidelines for design and construction of low strength clay brick masonry houses and low rise buildings in Indonesia.

## 5.2 The characteristics of clay brick masonry

In order to develop an applicable design guideline for non engineered and simple masonry houses in Indonesia and as determined by evaluation in this thesis, the physical and mechanical characteristics of clay bricks to be considered are given in Table 5.1 and 5.2.

*Table 0.1 Physical characteristics of Cikarang clay bricks*

Length	190 ± 2.5 mm
Width	90 ± 1.5 mm
Thickness	46 ± 1.5 mm
Density	1.69 ± 0.04 gram/mm <sup>3</sup>
Water Absorption	0.00214 ± 0.0007 (gram/mm <sup>2</sup> )/minute

*Table 0.2 Mechanical characteristics of Cikarang clay bricks*

Design development	Mechanical characteristics of clay bricks	
Experimental results (Indonesian – Cikarang clay brick)	Compressive strength	12 MPa
	Modulus of rupture	1.7 – 3.0 MPa
	Modulus of elasticity:	
	- $f_b' \leq 2 \text{ MPa}$	10 $f_b'$
- $f_b' > 2 \text{ MPa}$	45 $f_b'$	

## 5.3 Simplified design approach for unreinforced masonry structures

To develop a design guideline based on the result from experimental work, the generalised axial, shear, flexural and lateral stiffness of wall panels of different sizes is determined.



### 5.3.1 Estimation of load applied to the structures

According to the general structural wall, all clay brick walls are gravity load bearing structures. The roof usually rests directly on the walls without any special connection. All gravity loads are transferred to the shallow stone footing. In order to resist lateral forces caused by earthquake, columns and tie beams are constructed as interconnection at the corner of the walls. The uniformly distributed structural weight of walls of 4 m high is assumed to be approximately equal to 10 kN/m, as drawn in Figure 5.1.

The estimation of structural loading can therefore be determined as follows:

Total weight of half part of the building is  $10 \text{ m} \times 10 \text{ kN/m} = 100 \text{ kN}$ .

Earthquake shear force is assumed to be equal to  $0.1 \times 100 \text{ kN} =$

$$10 \text{ kN} = 10000 \text{ N.}$$

The compressive pressure retained by wall =  $10000 \text{ N}/(1000 \times 95) \text{ mm}^2 =$

$$0.11 \text{ N/mm}^2 \text{ or } 0.11 \text{ MPa.}$$

Based on this estimation, the value of modulus of elasticity and shear modulus to be used in this simplified design approach are taken from the result of experimental tests on wall panels under the compressive pressure of 0.165 MPa.

According to a model of wall panel from experimental test and considering a structural design purpose, the generalised capacity of wall panel to retain an applied in-plane lateral load should be determined. Based on the result from Chapter 4, the capacities of the walls in retaining lateral cyclic loading under any type of compressive pressure is 50 kN. Therefore, the maximum earthquake shear force in seismically active regions is assumed to be less or equal to  $50 \text{ kN}/0.6 \text{ m} = 83.33 \text{ kN}$  per one meter length of the wall.

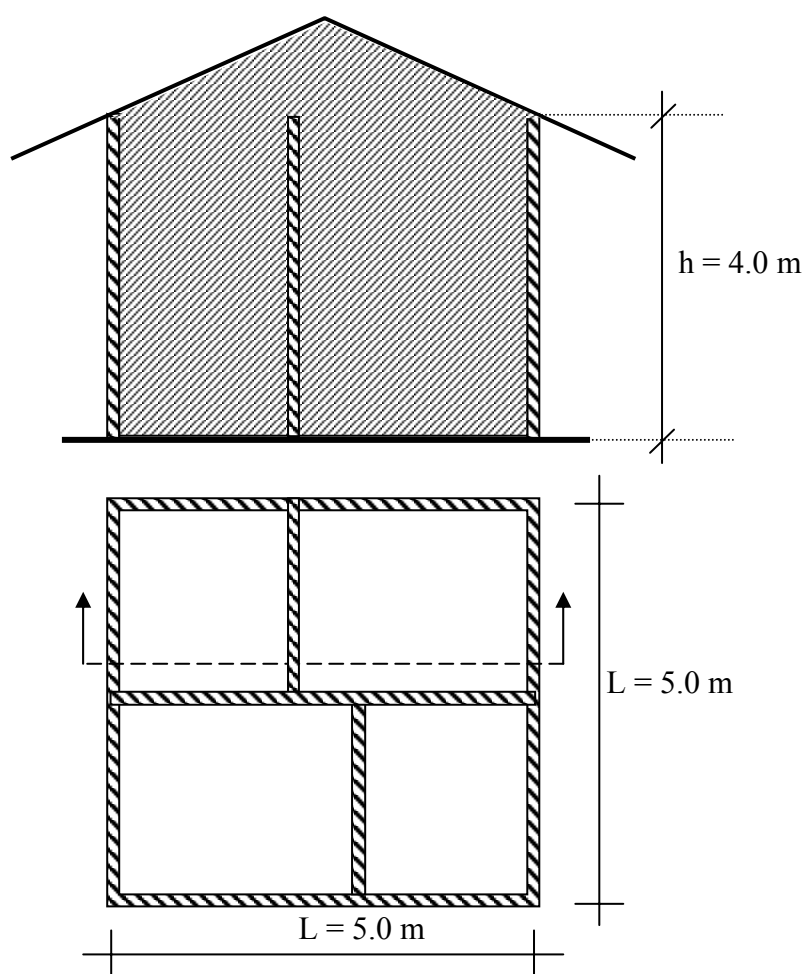


*Figure 0.1 A simple structural layout of rural masonry house*

### 5.3.2 Axial stiffness of wall panels

The axial stiffness of wall panels was derived by observing the experimental result from Chapter 3. The formula for axial stiffness is:

$$k_{wv} = \frac{EA}{h}$$

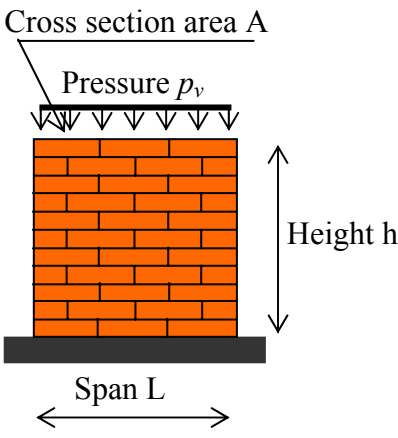
Where

- E = the modulus of elasticity of wall panel in MPa
- A = cross section area in mm<sup>2</sup>
- h = height of the wall in mm

As the axial stiffness of walls was observed from 600 mm x 600 mm x 110 mm wall panels, therefore the axial stiffness of wall panels with span size of 2.0 to 5.0 m and height size of 2.0 to 5.0 m are given in Table 5.3 and graphically shown in Figures

5.17 to 5.22. Some additional graphs of axial stiffness based on the height of wall panels are given in Appendix B.

Table 0.3 Axial stiffness of wall panels



The diagram illustrates a brick wall panel with a cross-section area  $A$ , subjected to a uniform vertical pressure  $p_v$ . The wall has a height  $h$  and a span  $L$ . The wall is shown as a brickwork structure on a foundation.

Axial Stiffness of Walls (kN/mm)					
Wall	$L/h$	200	300	400	500
BW	200	133.95	200.92	267.89	334.87
	300	89.30	133.95	178.60	223.25
	400	66.97	100.46	133.95	167.43
	500	53.58	80.37	107.16	133.95
MW	200	135.40	203.10	270.80	338.50
	300	90.27	135.40	180.53	225.67
	400	67.70	101.55	135.40	169.25
	500	54.16	81.24	108.32	135.40
CW	200	58.32	87.48	116.64	145.80
	300	38.88	58.32	77.76	97.20
	400	29.16	43.74	58.32	72.90
	500	23.33	34.99	46.66	58.32
MWA	200	44.75	67.13	89.51	111.88
	300	29.84	44.75	59.67	74.59
	400	22.38	33.57	44.75	55.94
	500	17.90	26.85	35.80	44.75
CWA	200	46.11	69.17	92.23	115.29
	300	30.74	46.11	61.49	76.86
	400	23.06	34.59	46.11	57.64
	500	18.45	27.67	36.89	46.11
MWE	200	45.43	68.15	90.87	113.58
	300	30.29	45.43	60.58	75.72
	400	22.72	34.08	45.43	56.79
	500	18.17	27.26	36.35	45.43

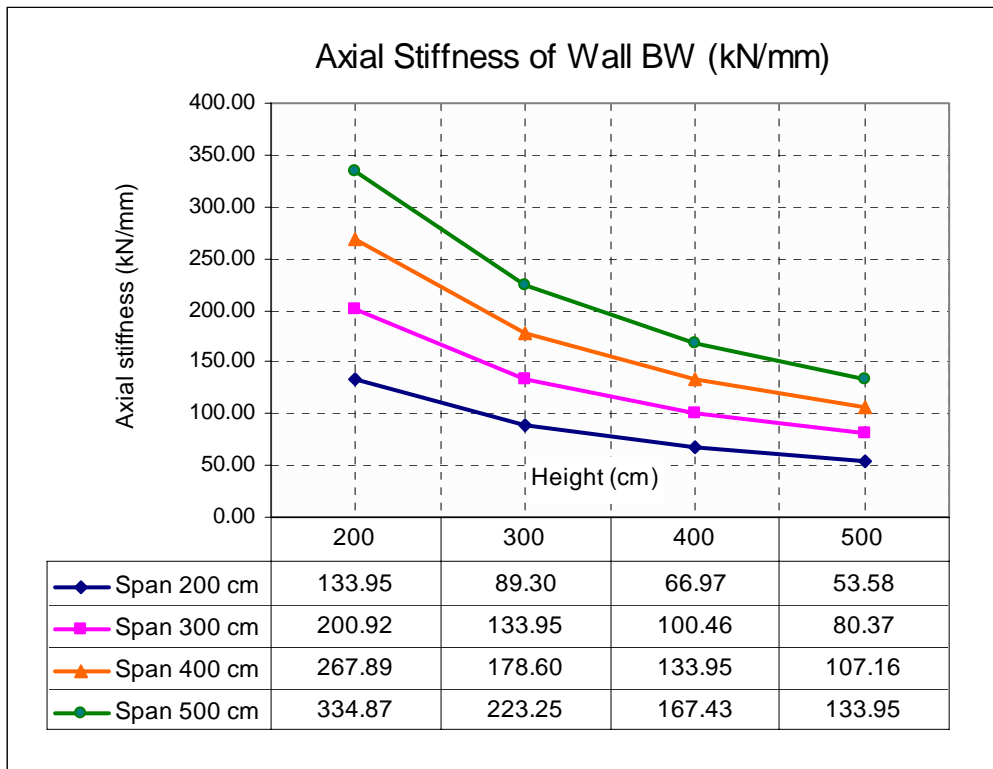


Figure 0.2 Axial stiffness of wall BW

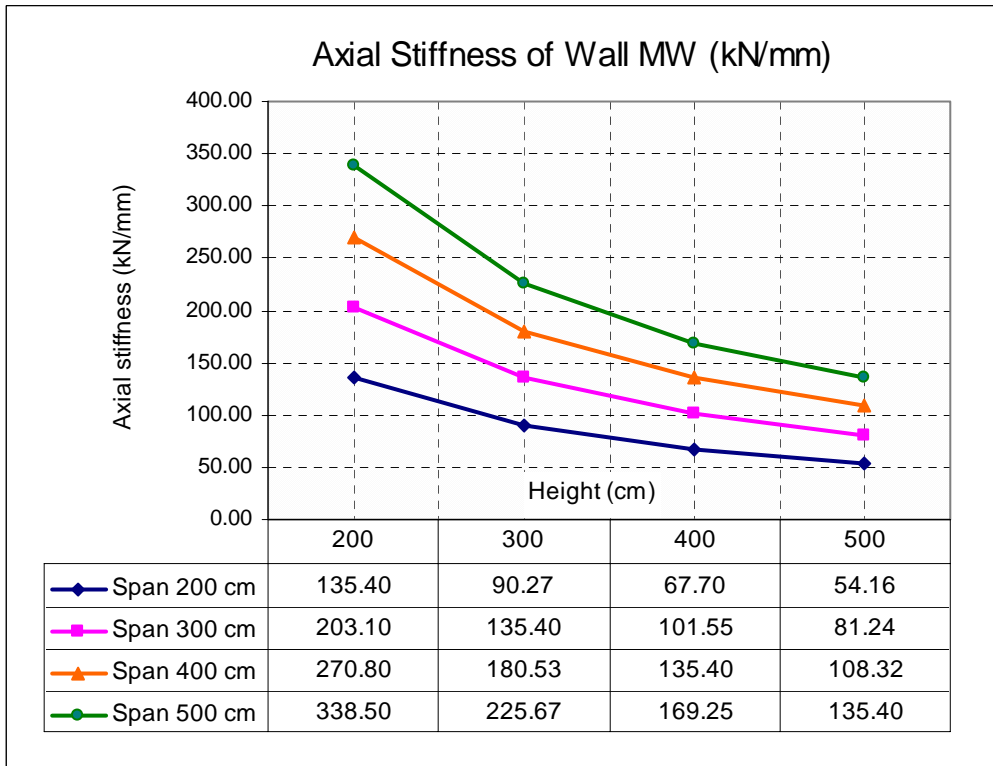


Figure 0.3 Axial stiffness of wall MW

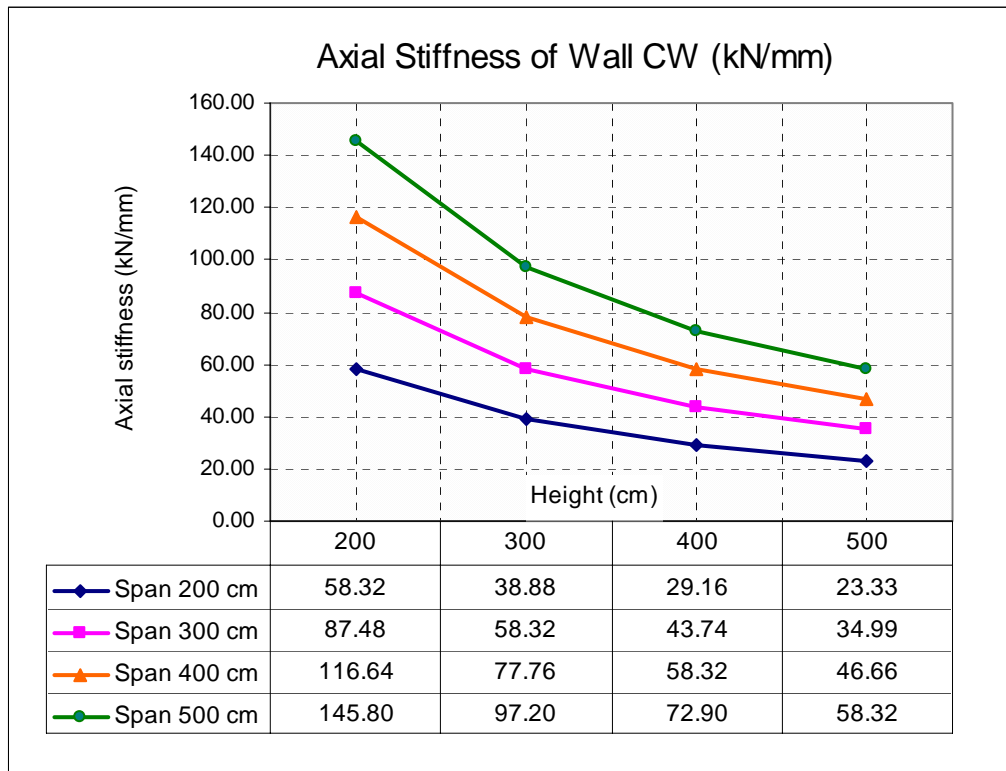


Figure 0.4 Axial stiffness of wall CW

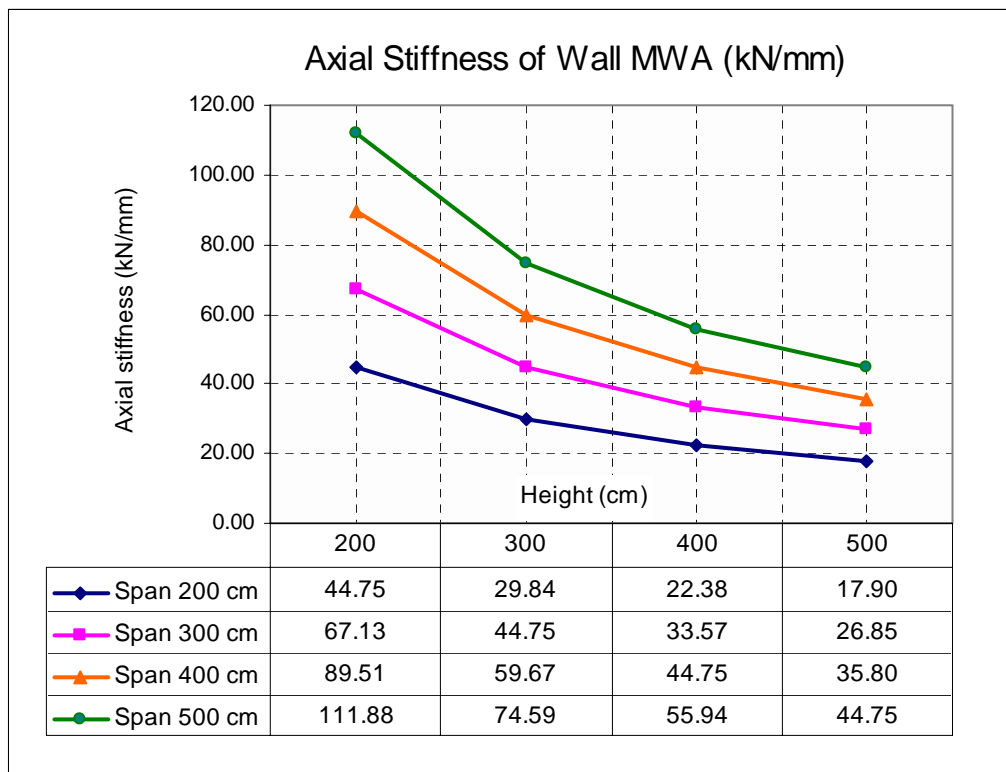


Figure 0.5 Axial stiffness of wall MWA

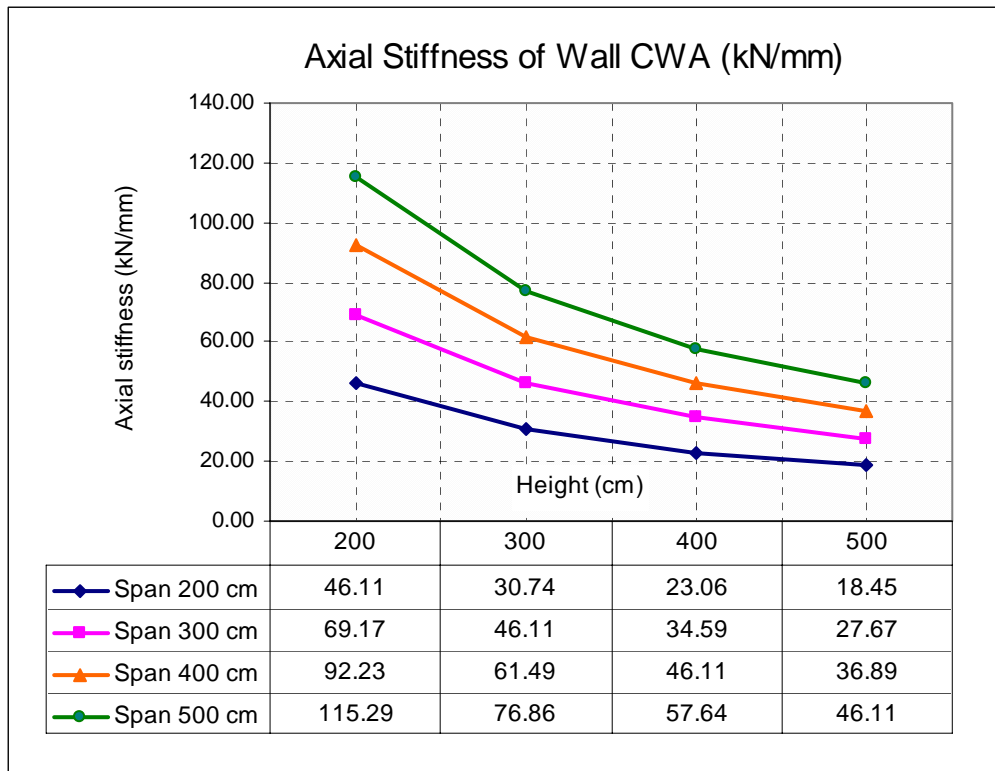


Figure 0.6 Axial stiffness of wall CWA

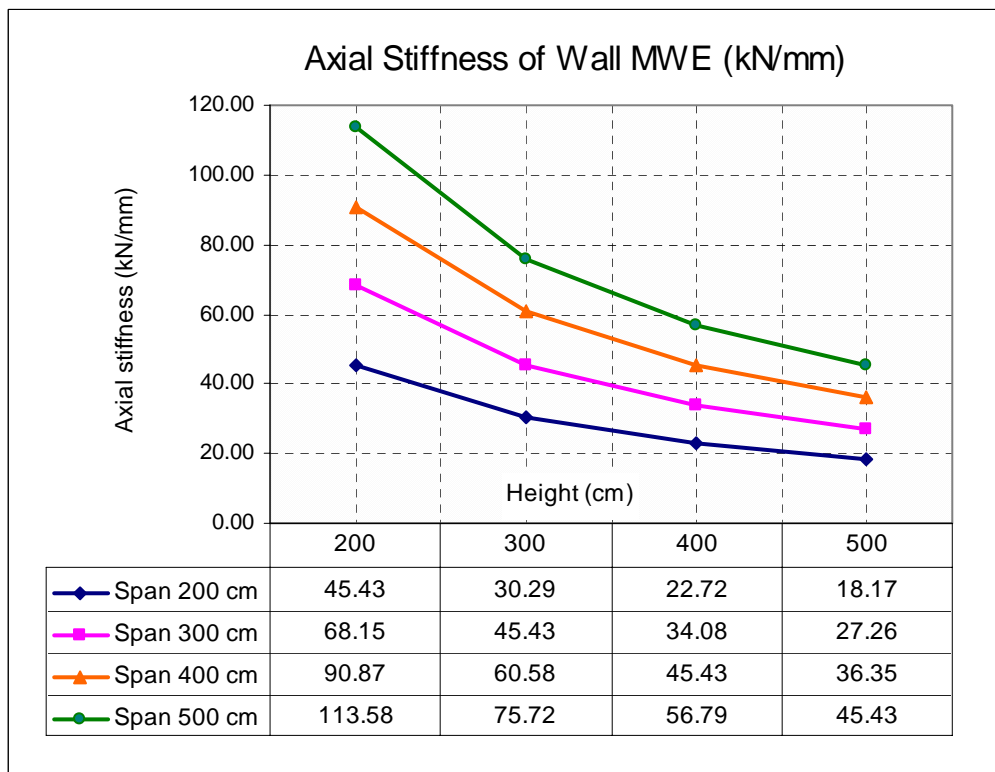


Figure 0.7 Axial stiffness of wall MWE

### 5.3.3 The generalised lateral stiffness of walls

The lateral stiffness of walls are analysed and derived based on the data collected from the test as drawn in Figure 5.8. From these experimental results, the generalised lateral stiffness of the walls are affected by the shear stiffness caused by lateral in-plane load and the flexural stiffness caused by bending moment and they are combined together in series action.

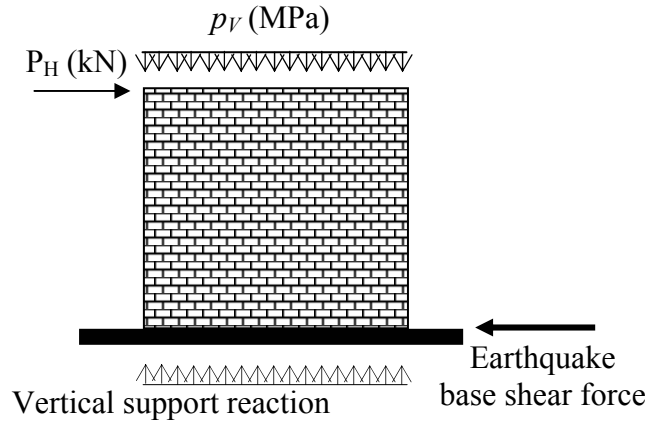


Figure 0.8 Wall panel under compressive pressure and lateral load

Therefore, the lateral stiffness of the walls is formulated as:

$$\frac{1}{k_{WH}} = \frac{1}{k_{WQ}} + \frac{1}{k_{WM}}$$

The shear stiffness is:

$$k_{WQ} = \frac{P_H}{\Delta_H},$$

$$k_{WQ} = \frac{P_H/A}{\Delta_H/A} = \frac{\tau_{ave}}{\Delta_H/A} = \tau_{ave} \frac{A}{\Delta_H} = \tau_{ave} \frac{A/h}{\Delta_H/h},$$

as

$$\Delta_H/h = \gamma,$$

therefore,

$$k_{wQ} = \frac{\tau_{ave}}{\gamma} \times \frac{A}{h}$$

and

$$k_{wQ} = \psi G \times \frac{A}{h}.$$

For a rectangular cross section,  $\psi$  is equal to 1.50.

The flexural stiffness caused by the bending moment is formulated as:

$$k_{wM} = \frac{3EI}{h^3} = 3E \times \frac{1}{12} \times \frac{L^3 t}{h^3} = \frac{Et}{4} \left( \frac{L}{h} \right)^3,$$

$$k_{wM} = \frac{Et}{4} \left( \frac{L}{h} \right)^3.$$

Where,

- $A$  = cross section area of walls in  $\text{mm}^2$ ,
- $E$  = modulus of elasticity of wall in  $\text{N/mm}^2$ ,
- $G$  = shear modulus in  $\text{N/mm}^2$ ,
- $H$  = height of walls in mm,
- $k_{wH}$  = lateral stiffness of wall in  $\text{N/mm}$  or  $\text{kN/mm}$ ,
- $k_{wM}$  = flexural stiffness of wall in  $\text{N/mm}$  or  $\text{kN/mm}$ ,
- $k_{wQ}$  = shear stiffness of wall in  $\text{N/mm}$  or  $\text{kN/mm}$ ,
- $P_H$  = lateral load or horizontal force in  $\text{kN}$  or  $\text{ton-f}$ ,
- $t$  = thickness of wall in mm,
- $\gamma$  = angle of wall rotation as shear strain in radiant,
- $\Delta_H$  = horizontal displacement in mm,
- $\tau_{ave}$  = average shear stress in  $\text{N/mm}^2$ ,
- $\psi$  = coefficient of maximum shear stress.



The ratio of shear cross section area to the height of the wall panels according to the type of span and type of height are given in Figures 5.9 and 5.10 respectively and are also listed in Table 5.4.

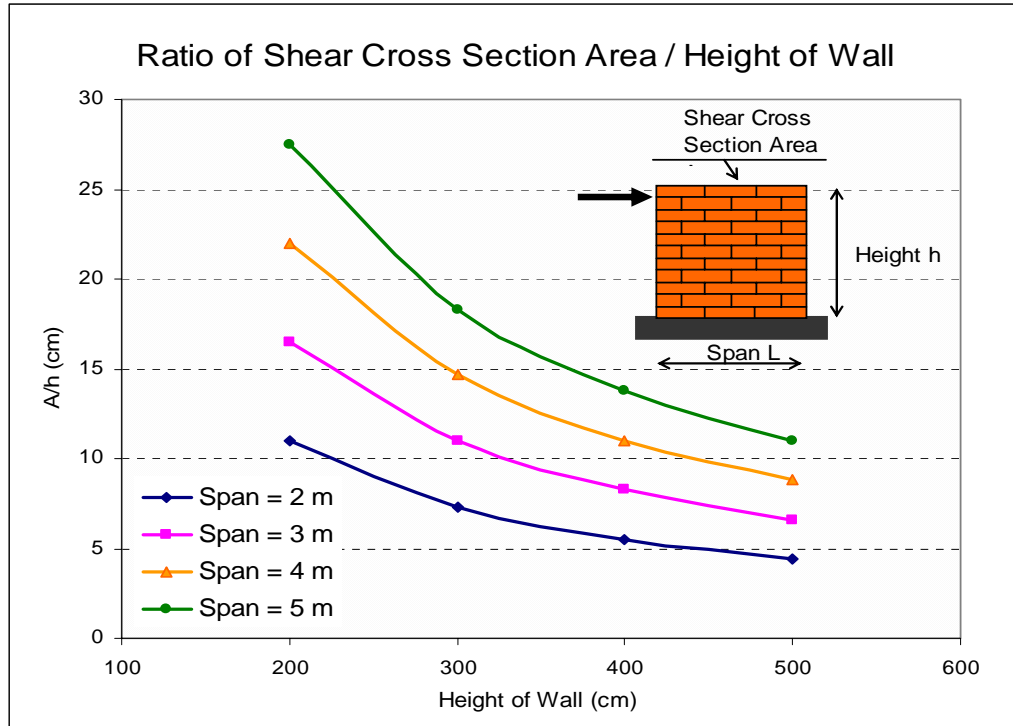


Figure 0.9 Ratio of cross section area to the height of the walls, based on span size

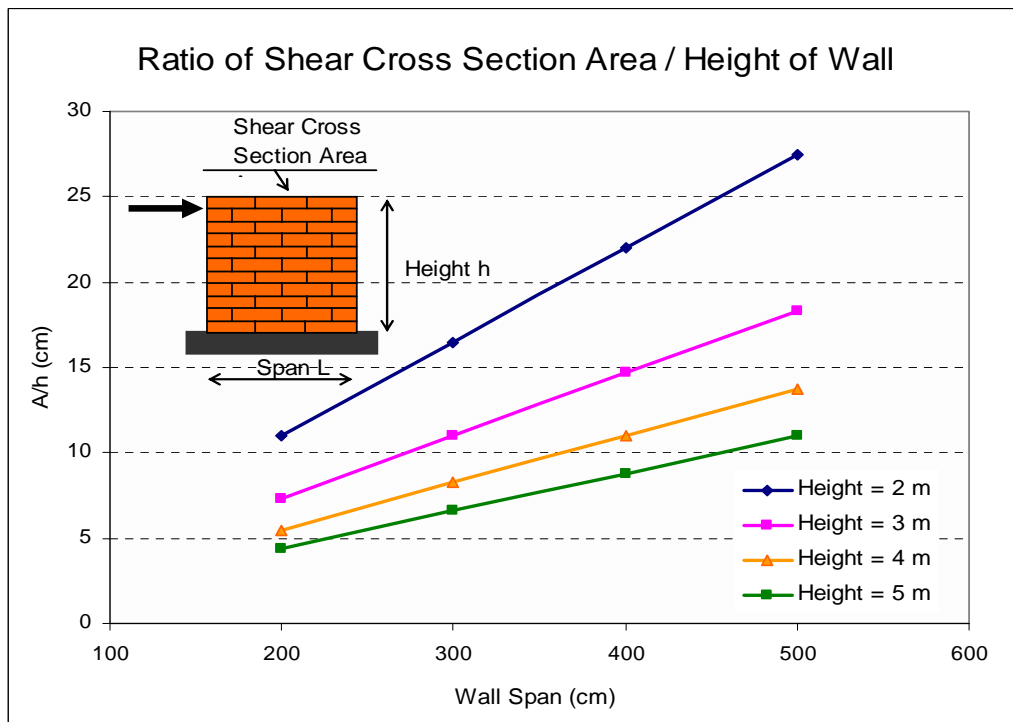


Figure 0.10 Ratio of cross section area to the height of the walls, based on height size

Table 0.4 The ratio of shear cross section area to the height of wall panels

The ratio of shear cross section area to the height of wall panels A/h (mm)				
Wall Span (cm)	200	300	400	500
Thickness (cm)	11	11	11	11
Cross section area A (cm <sup>2</sup> )	2200	3300	4400	5500
Height h (cm)				
200	110	165	220	275
300	73.3	110	146.7	183.3
400	55	82.5	110	137.5
500	44	66	88	110

Table 0.5 The average value of shear modulus of wall panels

Type of Wall	Average Shear Modulus (N/mm <sup>2</sup> )
BW	44.65
MW	72.66
CW	62.00
MWA	25.17
CWA	27.37
MWE	21.52

By observing the ratio of A/h, as given in Table 5.4 and considering the shear modulus of wall G based on types of walls, as given in Table 5.5, the shear stiffness of walls BW, MW, CW, MWA, CWA and MWE can be determined as  $k_{wQ}$ :

$$k_{wQ} = 1.5 G \times \frac{A}{h}$$

where G is given in N/mm<sup>2</sup>, and A/h is recorded in mm. The flexural stiffness also determined as:

$$k_{wM} = \frac{Et}{4} \left( \frac{L}{h} \right)^3$$

And the lateral stiffness of walls is equal to:

$$k_{wH} = \frac{k_{wM} \times k_{wQ}}{k_{wM} + k_{wQ}}$$

In designing simple masonry buildings, the shear stiffness, the flexural stiffness and the lateral stiffness of the walls are taken from Table 5.6, 5.7 and 5.8 respectively. The graphical representation of the shear stiffness, the flexural stiffness and the

lateral stiffness of the walls under examination is shown in Figures 5.11 to 5.28. Some additional graphs of shear and flexural stiffness of walls are given in Appendix B.

Table 0.6 Shear stiffness of walls

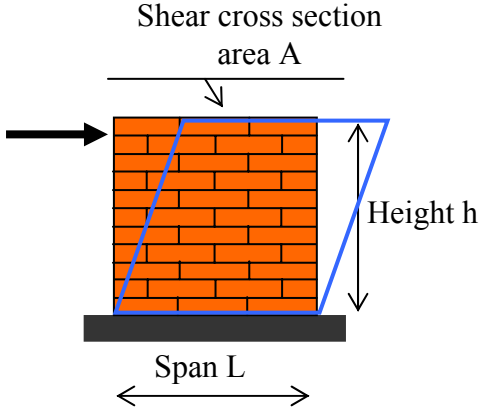
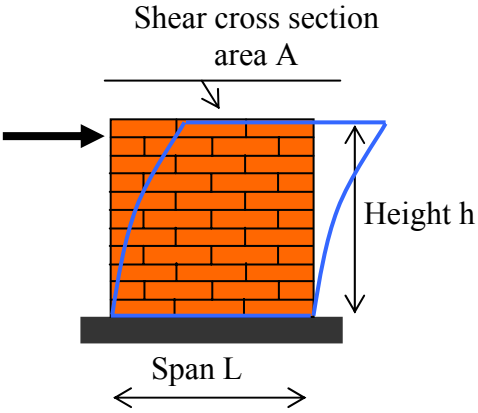
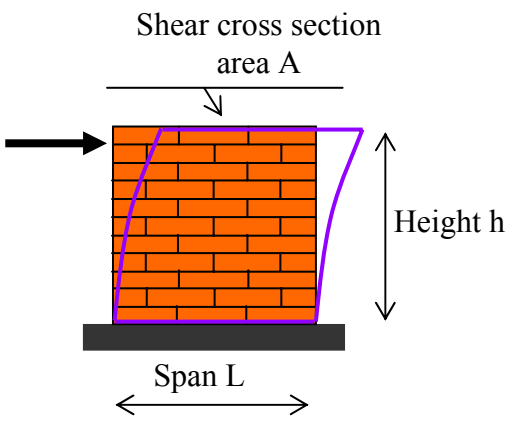
					
Shear Stiffness of Walls (kN/mm)					
Wall	L(cm) H (cm)	200	300	400	500
BW	200	6.03	9.04	12.06	15.07
	300	4.02	6.03	8.04	10.05
	400	3.01	4.52	6.03	7.53
	500	2.41	3.62	4.82	6.03
MW	200	11.99	17.98	23.98	29.97
	300	7.99	11.99	15.99	19.98
	400	5.99	8.99	11.99	14.99
	500	4.80	7.19	9.59	11.99
CW	200	10.23	15.35	20.46	25.58
	300	6.82	10.23	13.64	17.05
	400	5.12	7.67	10.23	12.79
	500	4.09	6.14	8.18	10.23
MWA	200	4.15	6.23	8.31	10.38
	300	2.77	4.15	5.54	6.92
	400	2.08	3.11	4.15	5.19
	500	1.66	2.49	3.32	4.15
CWA	200	4.52	6.77	9.03	11.29
	300	3.01	4.52	6.02	7.53
	400	2.26	3.39	4.52	5.65
	500	1.81	2.71	3.61	4.52
MWE	200	3.55	5.33	7.10	8.88
	300	2.37	3.55	4.73	5.92
	400	1.78	2.66	3.55	4.44
	500	1.42	2.13	2.84	3.55

Table 0.7 Flexural stiffness of walls



Flexural stiffness of walls (kN/mm)					
Wall	L(cm) \ H (cm)	200	300	400	500
	BW	200	33.48	113.00	267.84
300		9.92	33.48	79.36	155.00
400		4.19	14.12	33.48	65.39
500		2.14	7.23	17.14	33.48
MW	200	33.85	114.25	270.82	528.95
	300	10.03	33.85	80.24	156.72
	400	4.23	14.28	33.85	66.12
	500	2.17	7.31	17.33	33.85
CW	200	14.58	49.19	116.60	227.73
	300	4.32	14.58	34.55	67.48
	400	1.82	6.15	14.58	28.47
	500	0.93	3.15	7.46	14.58
MWA	200	11.17	37.68	89.32	174.45
	300	3.31	11.17	26.47	51.69
	400	1.40	4.71	11.17	21.81
	500	0.71	2.41	5.72	11.17
CWA	200	11.52	38.89	92.18	180.04
	300	3.41	11.52	27.31	53.34
	400	1.44	4.86	11.52	22.50
	500	0.74	2.49	5.90	11.52
MWE	200	11.33	38.24	90.64	177.03
	300	3.36	11.33	26.86	52.45
	400	1.42	4.78	11.33	22.13
	500	0.73	2.45	5.80	11.33

Table 0.8 Lateral stiffness of walls



Lateral stiffness of walls (kN/mm)					
Wall	L(cm) H (cm)	200	300	400	500
BW	200	5.11	8.37	11.54	14.65
	300	2.86	5.11	7.30	9.43
	400	1.75	3.42	5.11	6.76
	500	1.13	2.41	3.76	5.11
MW	200	8.85	15.54	22.03	28.36
	300	4.45	8.85	13.33	17.72
	400	2.48	5.52	8.85	12.22
	500	1.49	3.63	6.17	8.85
CW	200	6.01	11.70	17.41	22.99
	300	2.64	6.01	9.78	13.61
	400	1.34	3.41	6.01	8.82
	500	0.76	2.08	3.90	6.01
MWA	200	3.03	5.35	7.60	9.80
	300	1.51	3.03	4.58	6.10
	400	0.83	1.87	3.03	4.19
	500	0.50	1.23	2.10	3.03
CWA	200	3.24	5.77	8.23	10.62
	300	1.60	3.24	4.93	6.60
	400	0.88	2.00	3.24	4.51
	500	0.52	1.30	2.24	3.24
MWE	200	2.70	4.68	6.59	8.45
	300	1.39	2.70	4.02	5.32
	400	0.79	1.71	2.70	3.70
	500	0.48	1.14	1.91	2.70

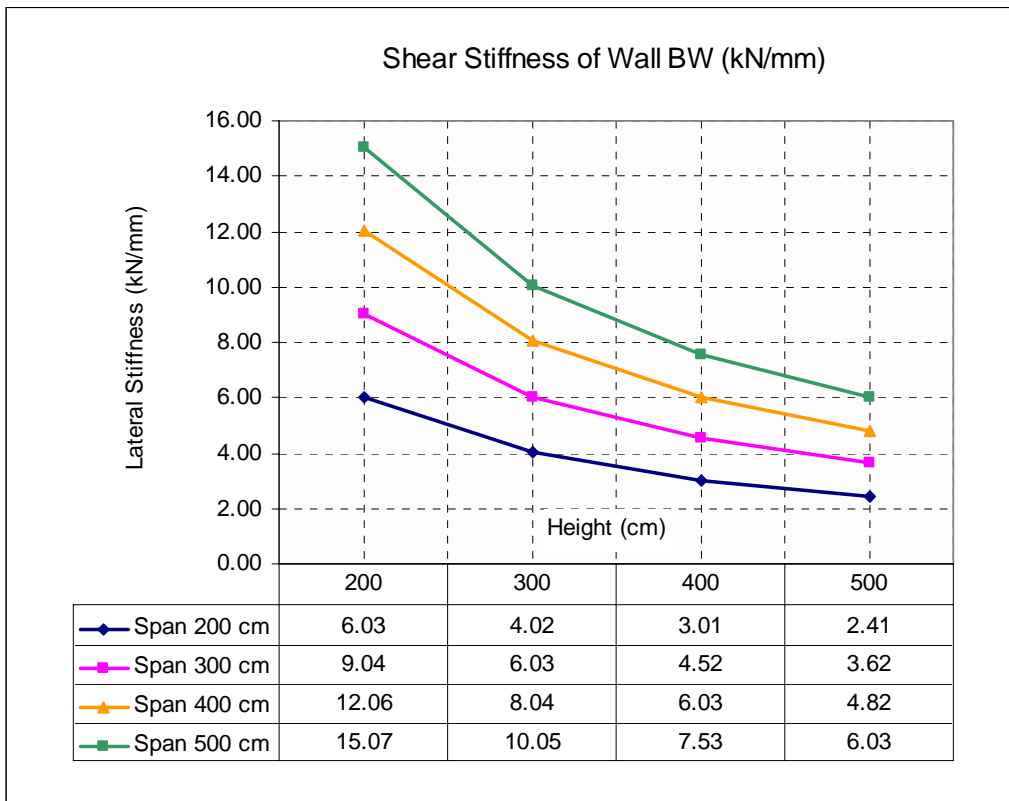


Figure 0.11 Shear stiffness of wall BW

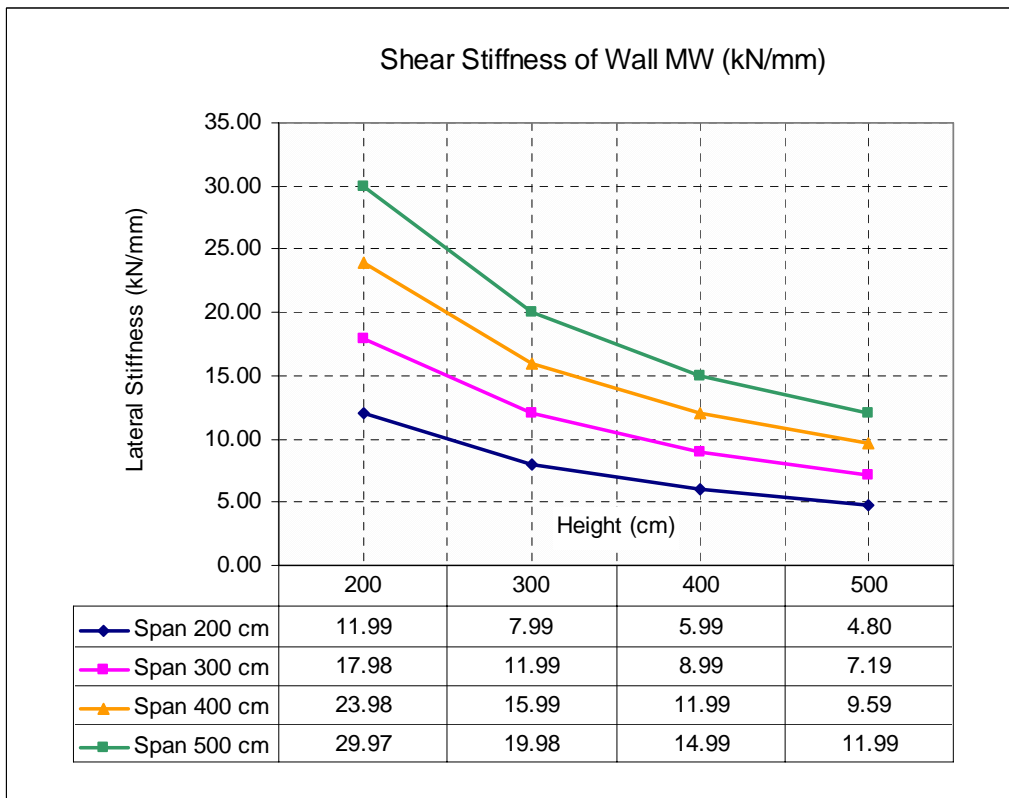


Figure 0.12 Shear stiffness of wall MW

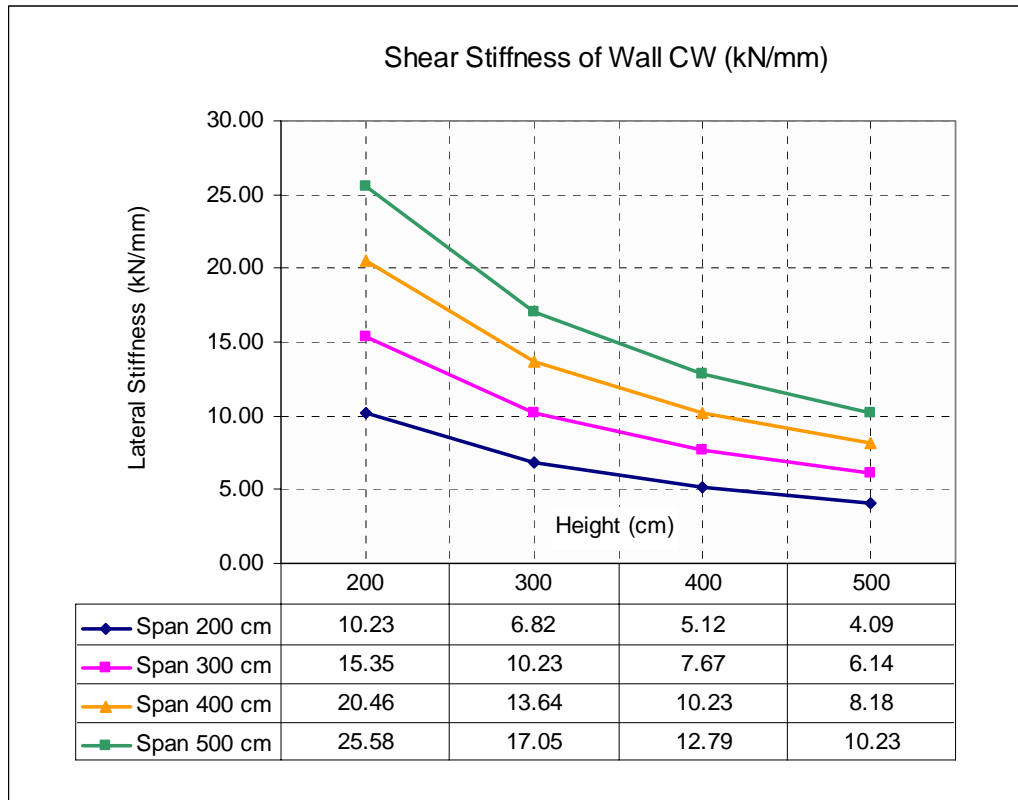


Figure 0.13 Shear stiffness of wall CW

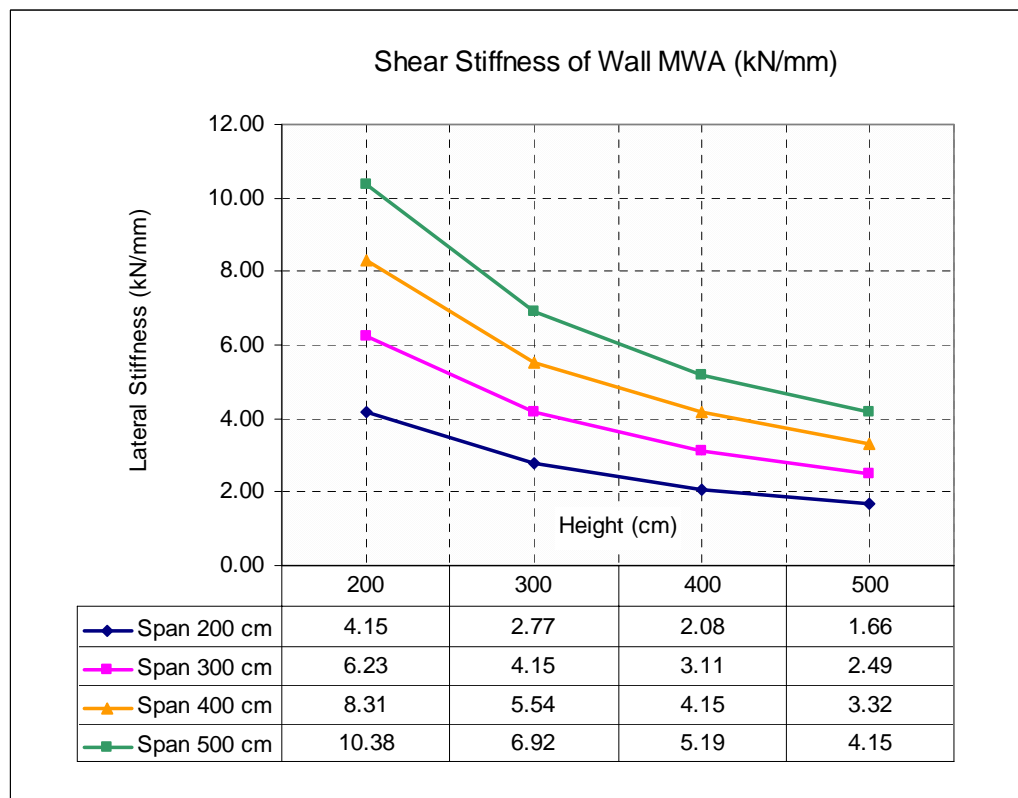


Figure 0.14 Shear stiffness of wall MWA

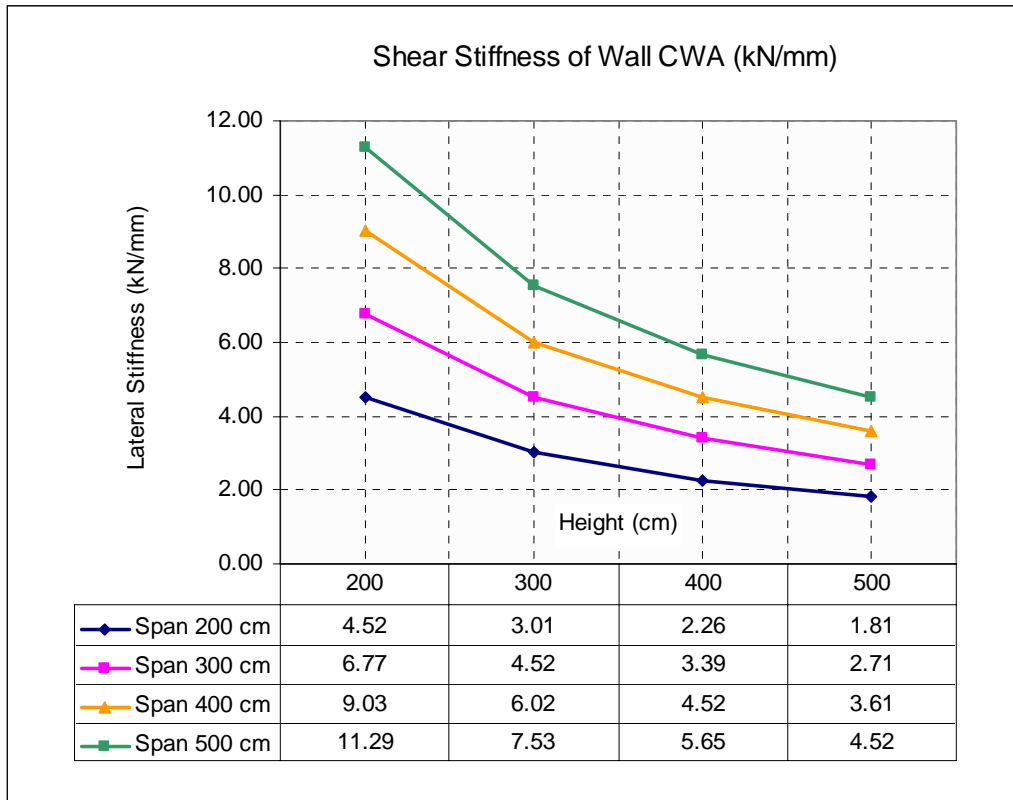


Figure 0.15 Shear stiffness of wall CWA

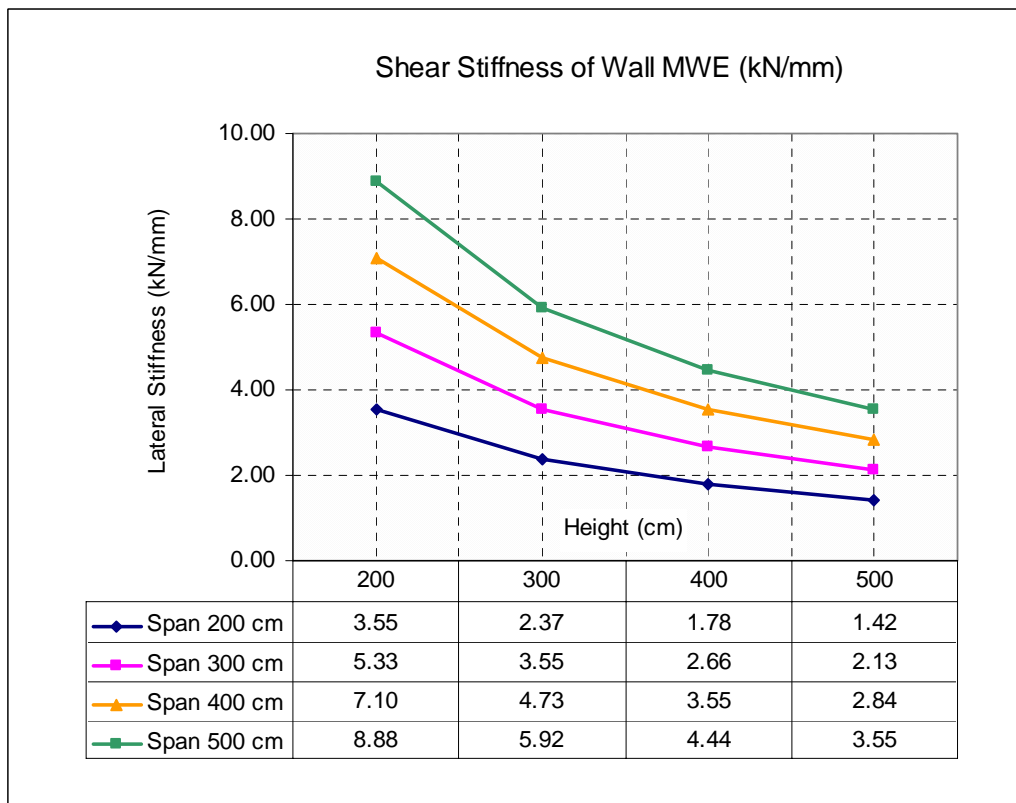


Figure 0.16 Shear stiffness of wall MWE



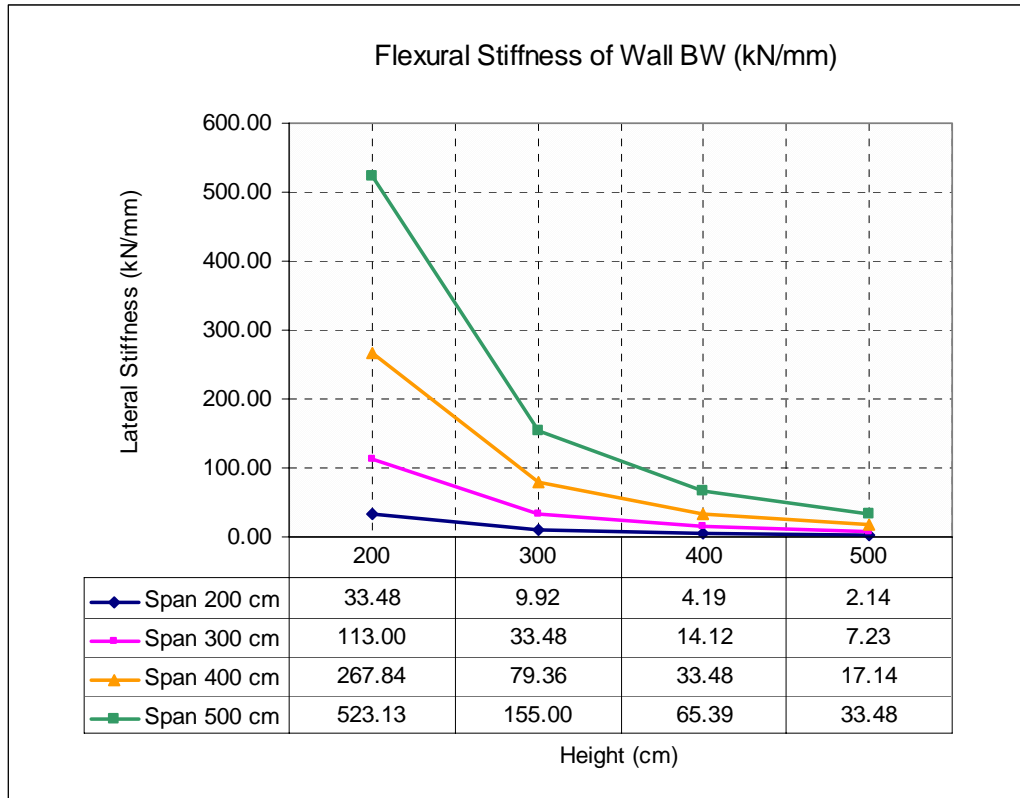


Figure 0.17 Flexural stiffness of wall BW

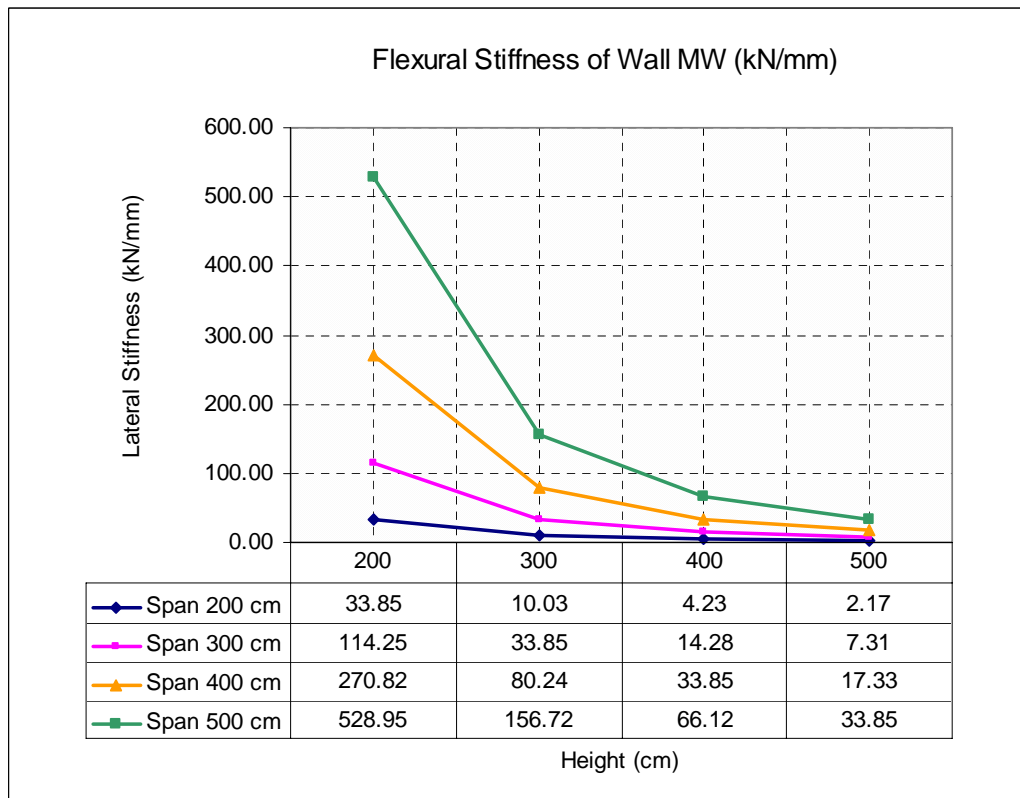


Figure 0.18 Flexural stiffness of wall MW

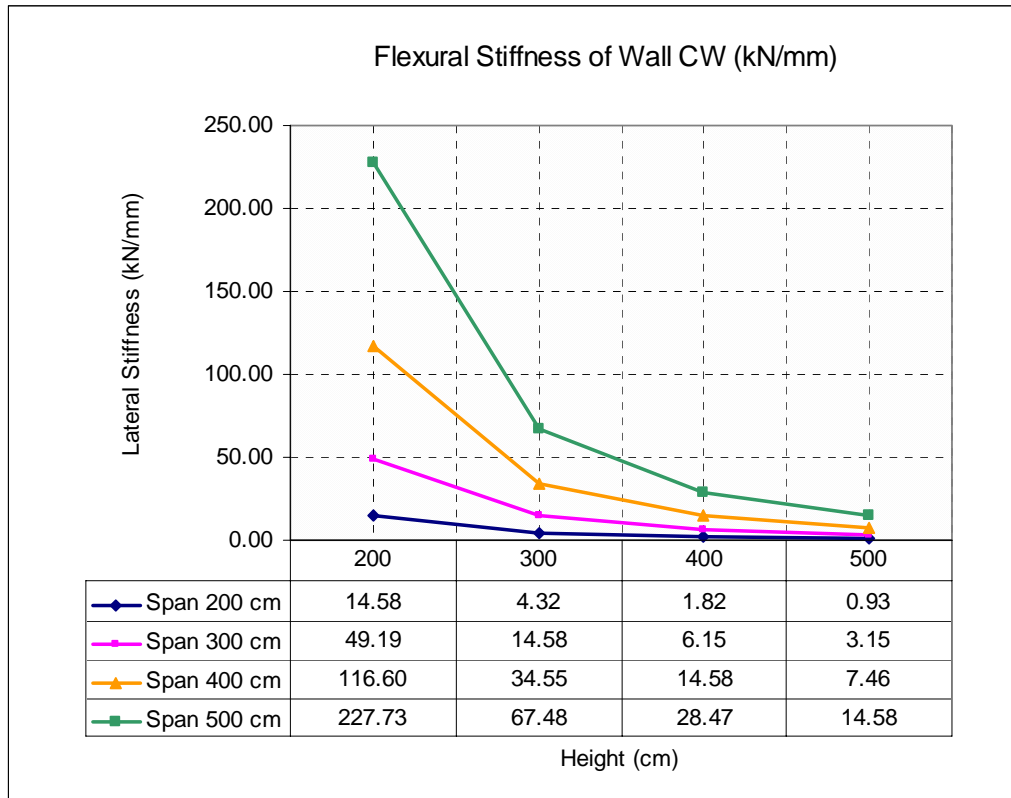


Figure 0.19 Flexural stiffness of wall CW

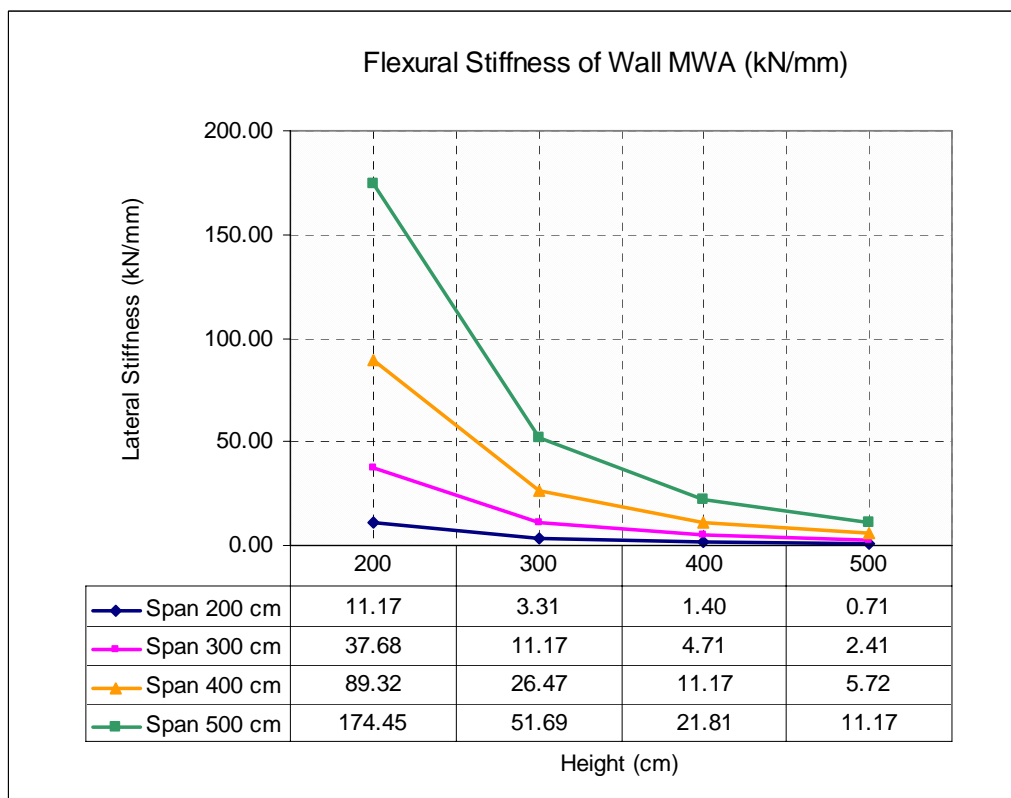


Figure 0.20 Flexural stiffness of wall MWA

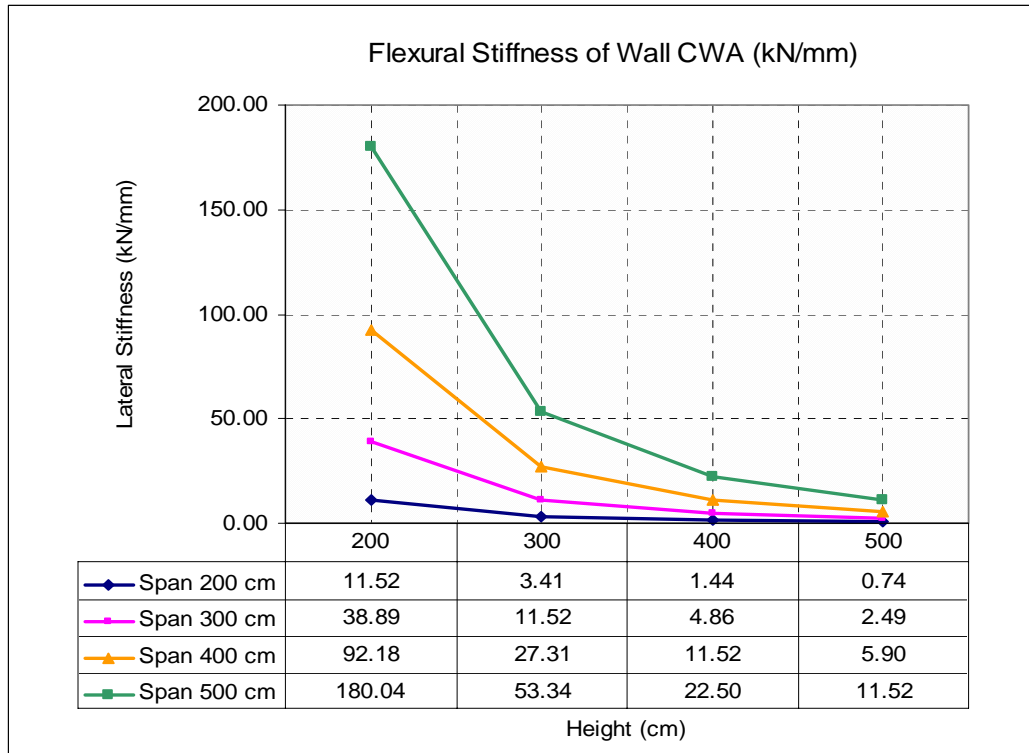


Figure 0.21 Flexural stiffness of wall CWA

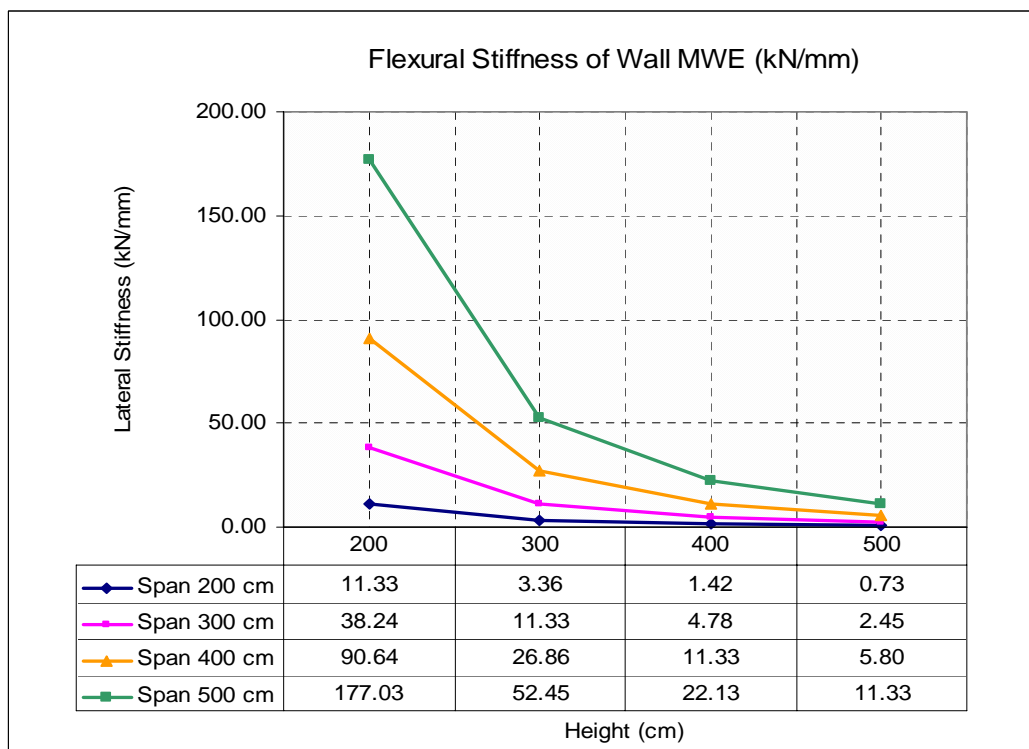


Figure 0.22 Flexural stiffness of wall MWE

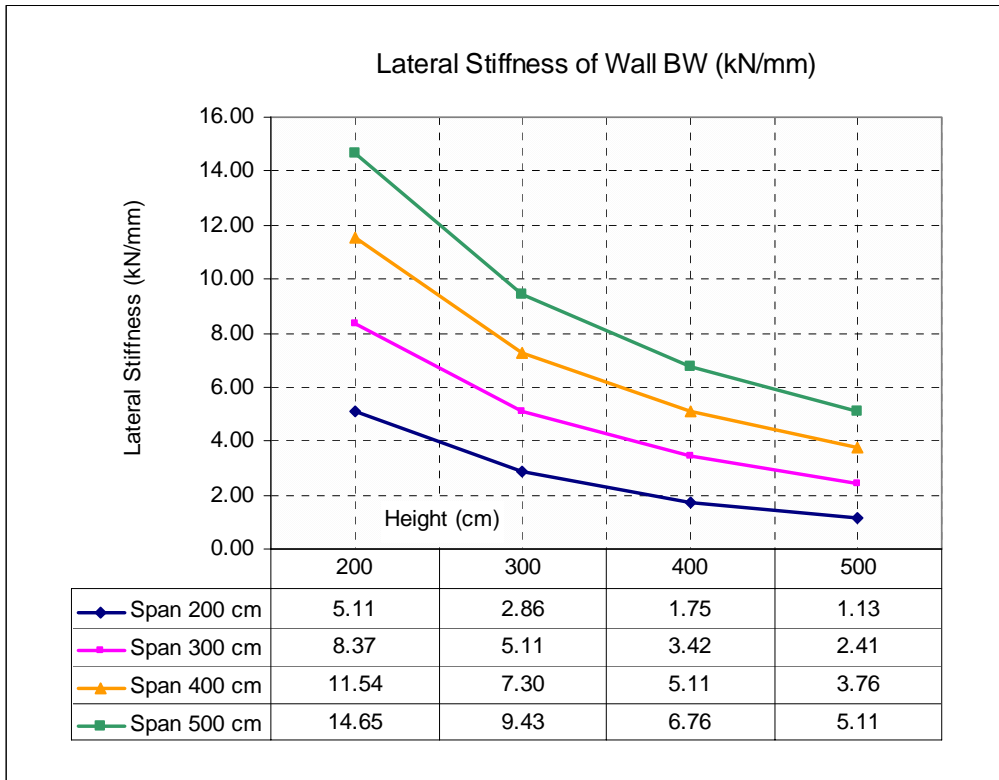


Figure 0.23 Lateral stiffness of wall BW

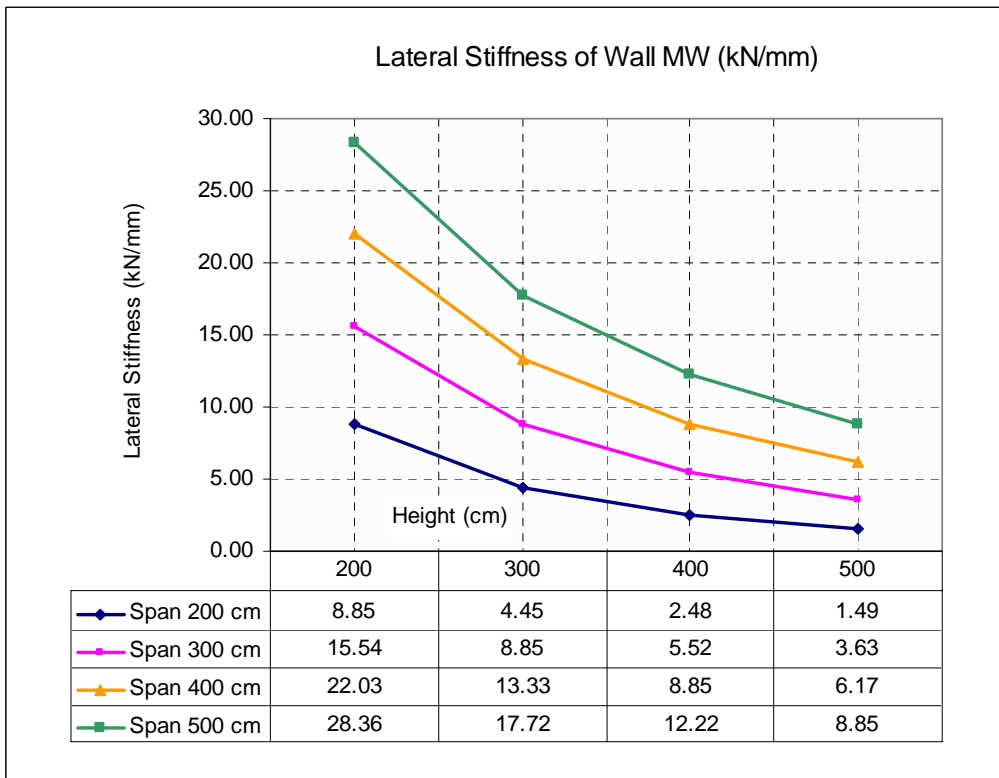


Figure 0.24 Lateral stiffness of wall MW

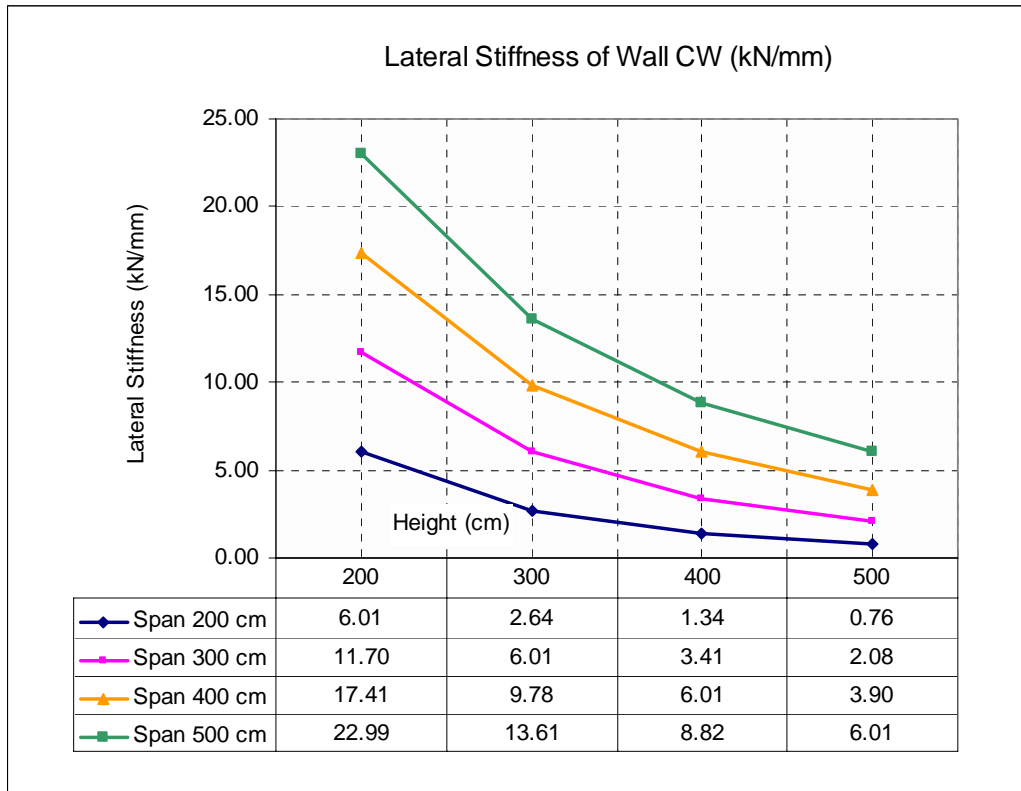


Figure 0.25 Lateral stiffness of wall CW

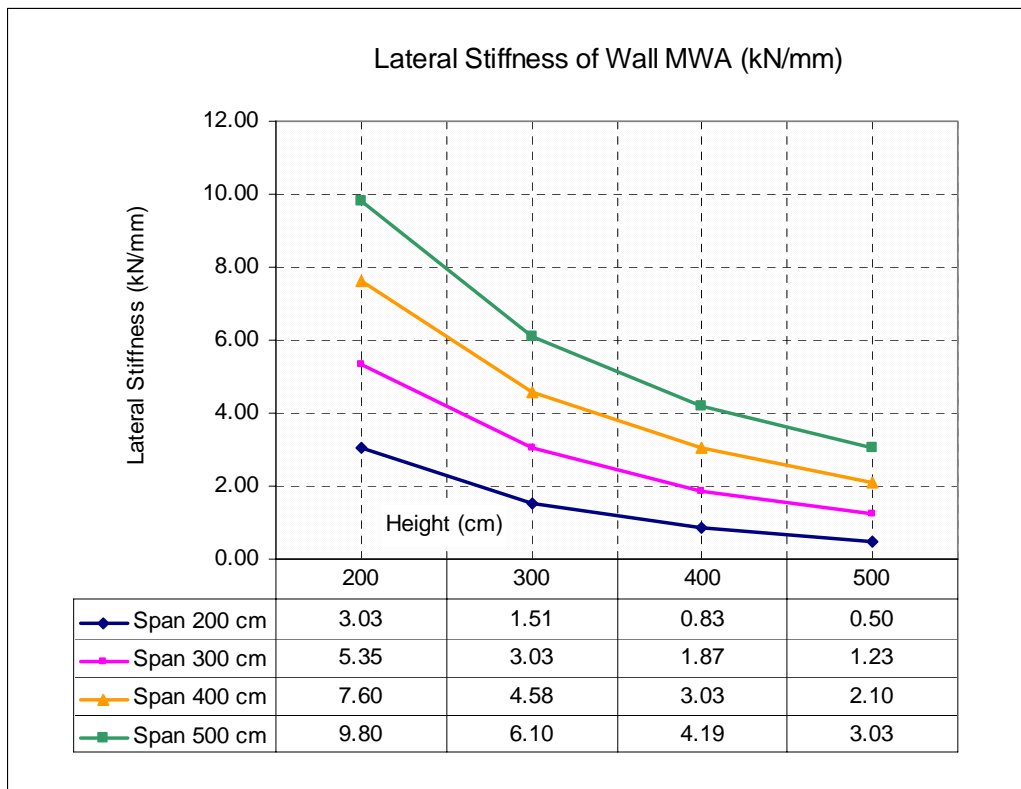


Figure 0.26 Lateral stiffness of wall MWA

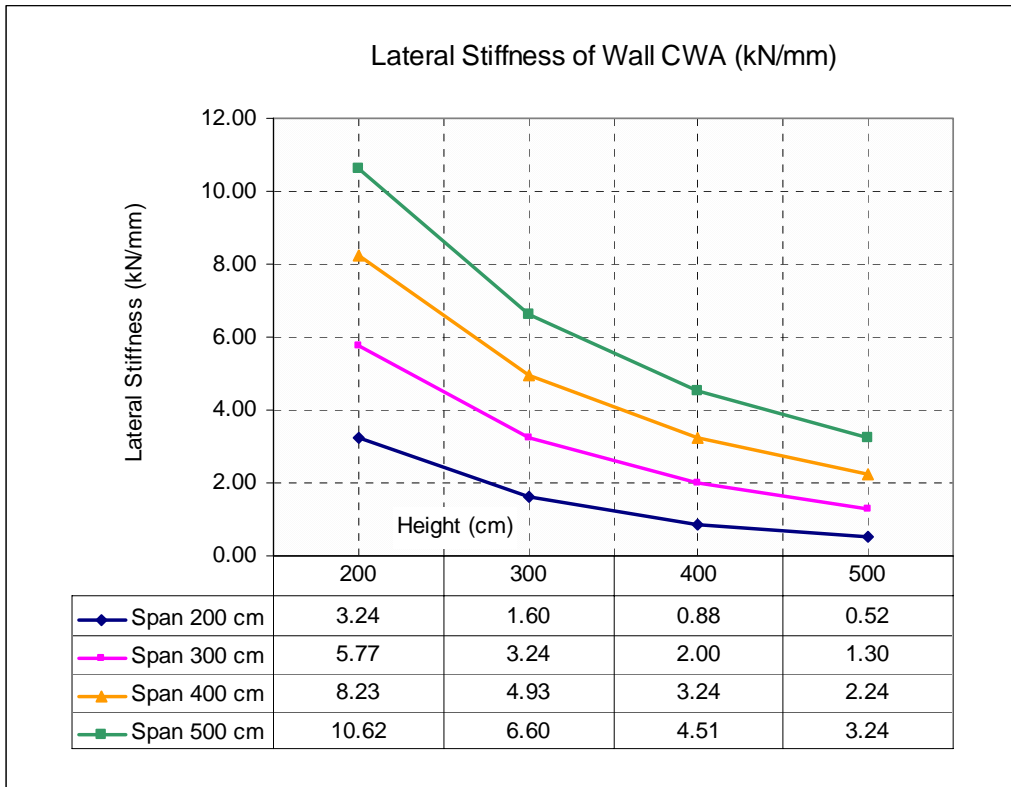


Figure 0.27 Lateral stiffness of wall CWA

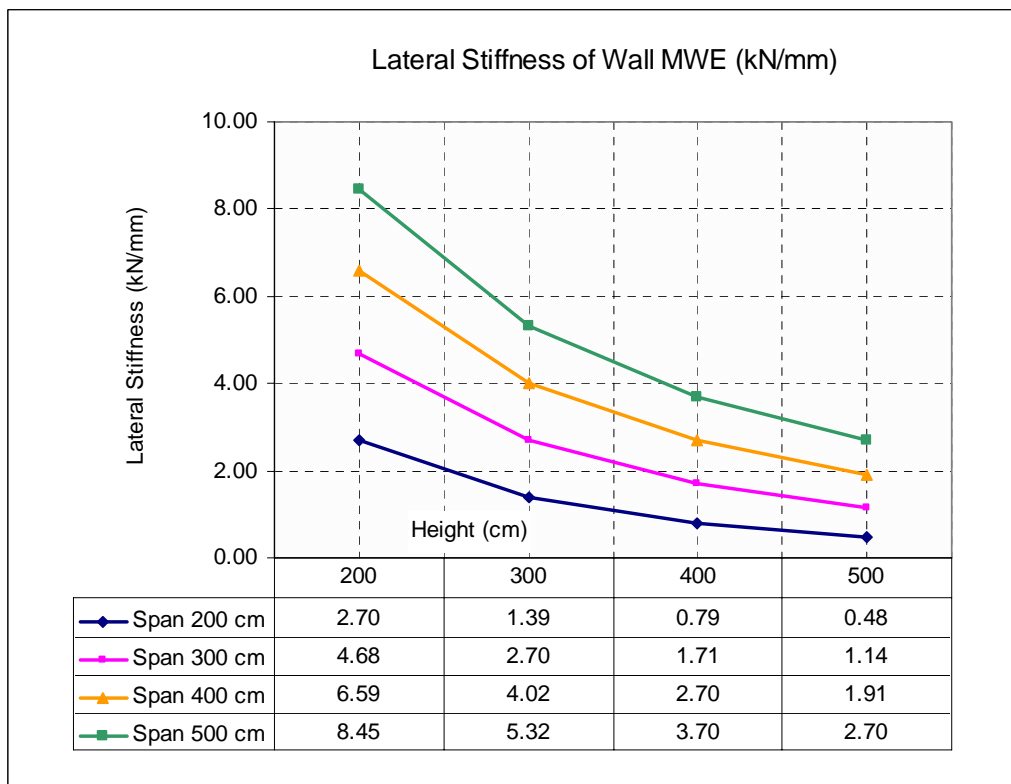


Figure 0.28 Lateral stiffness of wall MWE

### 5.3.4 Stiffness verification using dimensional analysis

Using the results from experimental testing on wall specimens, the stiffness of prototype wall can be determined using dimensional analysis with similarity theorem (Harris and Sabnis, 1999). As the shear or compressive cross sectional area is equal to

$$A = t \times L$$

the scale factor of area  $S_A$  will be equal to

$$S_A = S_t \times S_L$$

Since the prototype has the same thickness as the model, therefore  $S_t = 1$  and  $S_A = S_L$ . The scale factor of height is  $S_h$ . Knowing that the prototype has the same material properties as the model, the scale factor for the modulus of elasticity  $S_E$  and the shear modulus  $S_G$  are both equal to 1. The axial stiffness  $k_{WV}$ , shear stiffness  $k_{WQ}$  and flexural stiffness  $k_{WM}$  are therefore equal to:

$$k_{WV} = E \times (A/h) = S_E \times (S_L / S_h) = Et (1 \times S_L/S_h) = Et \times (S_L/S_h)$$

$$k_{WQ} = 1.5 G \times (A/h) = 1.5 S_G \times (S_L \times S_h) = Gt (1.5 \times 1 \times S_L/S_h) = 1.5 Gt \times (S_L/S_h)$$

$$k_{WM} = \frac{1}{4} E \times t (L/h)^3 = \frac{1}{4} S_E \times S_t (S_L/S_h)^3 = \frac{1}{4} Et \times 1 \times 1 (S_L/S_h)^3 = \frac{1}{4} Et \times (S_L/S_h)^3$$

Based on the above equations, the scale factors of the length and the height of the wall are given in Table 5.9 and the stiffness of walls BW, MW, CW, MWA, CWA, MWE are also shown in Tables 5.10, 5.11, 5.12, 5.13, 5.14 and 5.15 respectively.

Table 0.9 Scale factor for length and height of walls

$S_h$	$(S_L/S_h)$				$(S_L/S_h)^3$			
	$S_L$				$S_L$			
	3.333	5	6.667	8.333	3.333	5	6.667	8.333
3.333	1.00	1.50	2.00	2.50	1	3.38	8	15.63
5	0.67	1.00	1.33	1.67	0.3	1	2.37	4.63
6.667	0.50	0.75	1.00	1.25	0.12	0.42	1	1.95
8.333	0.40	0.60	0.80	1.00	0.06	0.22	0.51	1

Comparing all the results given in Tables 5.3, 5.6 and 5.7 with those in Tables 5.10, 5.11, 5.12, 5.13, 5.14, and 5.15; it is evident, that results evaluated based on the dimensional analysis using similarity theorem and experimental investigations agree well with those obtained from the analysis.

*Table 0.10 Stiffness of wall BW based on dimensional analysis*

Wall	BW			
Length (cm)	200	300	400	500
Height (cm)	Axial Stiffness kN/mm			
200	133.92	200.90	267.84	334.82
300	89.27	133.92	178.54	223.19
400	66.95	100.43	133.90	167.38
500	53.56	80.36	107.13	133.92
	Shear Stiffness kN/mm			
200	6.03	9.04	12.06	15.07
300	4.02	6.03	8.04	10.05
400	3.01	4.52	6.03	7.53
500	2.41	3.62	4.82	6.03
	Flexural Stiffness kN/mm			
200	33.48	113.03	267.84	523.22
300	9.92	33.48	79.34	154.98
400	4.18	14.12	33.46	65.37
500	2.14	7.23	17.14	33.48

*Table 0.11 Stiffness of wall MW based on dimensional analysis*

Wall	MW			
Length (cm)	200	300	400	500
Height (cm)	Axial Stiffness kN/mm			
200	135.41	203.14	270.82	338.55
300	90.26	135.41	180.53	225.67
400	67.69	101.55	135.39	169.25
500	54.16	81.25	108.32	135.41
	Shear Stiffness kN/mm			
200	11.99	17.99	23.98	29.97
300	7.99	11.99	15.98	19.98
400	5.99	8.99	11.99	14.98
500	4.80	7.19	9.59	11.99
	Flexural Stiffness kN/mm			
200	33.85	114.29	270.82	529.04
300	10.03	33.85	80.22	156.71
400	4.23	14.28	33.84	66.10
500	2.17	7.31	17.33	33.85



*Table 0.12 Stiffness of wall CW based on dimensional analysis*

Wall	CW			
Length (cm)	200	300	400	500
Height (cm)	Axial Stiffness kN/mm			
200	58.30	87.46	116.60	145.76
300	38.86	58.30	77.73	97.16
400	29.15	43.72	58.29	72.87
500	23.32	34.98	46.64	58.30
	Shear Stiffness kN/mm			
200	10.23	15.35	20.46	25.58
300	6.82	10.23	13.64	17.05
400	5.11	7.67	10.23	12.79
500	4.09	6.14	8.18	10.23
	Flexural Stiffness kN/mm			
200	14.58	49.21	116.60	227.78
300	4.32	14.58	34.54	67.47
400	1.82	6.15	14.57	28.46
500	0.93	3.15	7.46	14.58

*Table 0.13 Stiffness of wall MWA based on dimensional analysis*

Wall	MWA			
Length (cm)	200	300	400	500
Height (cm)	Axial Stiffness kN/mm			
200	44.66	67.00	89.32	111.66
300	29.77	44.66	59.54	74.43
400	22.33	33.49	44.65	55.82
500	17.86	26.80	35.73	44.66
	Shear Stiffness kN/mm			
200	4.15	6.23	8.31	10.38
300	2.77	4.15	5.54	6.92
400	2.08	3.11	4.15	5.19
500	1.66	2.49	3.32	4.15
	Flexural Stiffness kN/mm			
200	11.17	37.69	89.32	174.48
300	3.31	11.17	26.46	51.68
400	1.39	4.71	11.16	21.80
500	0.71	2.41	5.72	11.17

*Table 0.14 Stiffness of wall CWA based on dimensional analysis*

Wall	CWA			
Length (cm)	200	300	400	500
Height (cm)	Axial Stiffness kN/mm			
200	46.09	69.14	92.18	115.23
300	30.72	46.09	61.45	76.81
400	23.04	34.57	46.08	57.61
500	18.43	27.66	36.87	46.09
	Shear Stiffness kN/mm			
200	4.52	6.77	9.03	11.29
300	3.01	4.52	6.02	7.53
400	2.26	3.39	4.52	5.64
500	1.81	2.71	3.61	4.52
	Flexural Stiffness kN/mm			
200	11.52	38.90	92.18	180.07
300	3.41	11.52	27.30	53.34
400	1.44	4.86	11.52	22.50
500	0.74	2.49	5.90	11.52

*Table 0.15 Stiffness of wall MWE based on dimensional analysis*

Wall	MWE			
Length (cm)	200	300	400	500
Height (cm)	Axial Stiffness kN/mm			
200	45.32	67.99	90.64	113.31
300	30.21	45.32	60.42	75.53
400	22.66	33.99	45.31	56.64
500	18.13	27.19	36.25	45.32
	Shear Stiffness kN/mm			
200	3.55	5.33	7.10	8.88
300	2.37	3.55	4.73	5.92
400	1.78	2.66	3.55	4.44
500	1.42	2.13	2.84	3.55
	Flexural Stiffness kN/mm			
200	11.33	38.25	90.64	177.06
300	3.36	11.33	26.85	52.45
400	1.42	4.78	11.32	22.12
500	0.72	2.45	5.80	11.33

## 5.4 Simplified model for diagonal stiffness of wall panels

To include wall panels into the analysis of structural frames, it is necessary to obtain the stiffness of walls in diagonal direction. This is achieved through diagonal spring model, which is developed using simplified method. A configuration of this model is shown in Figure 5.23. As the diagonal displacement of spring  $\Delta_D$  is equal to 1 unity, the diagonal force  $P_D$  is considered to be the wall diagonal spring stiffness  $k_{WD}$ .

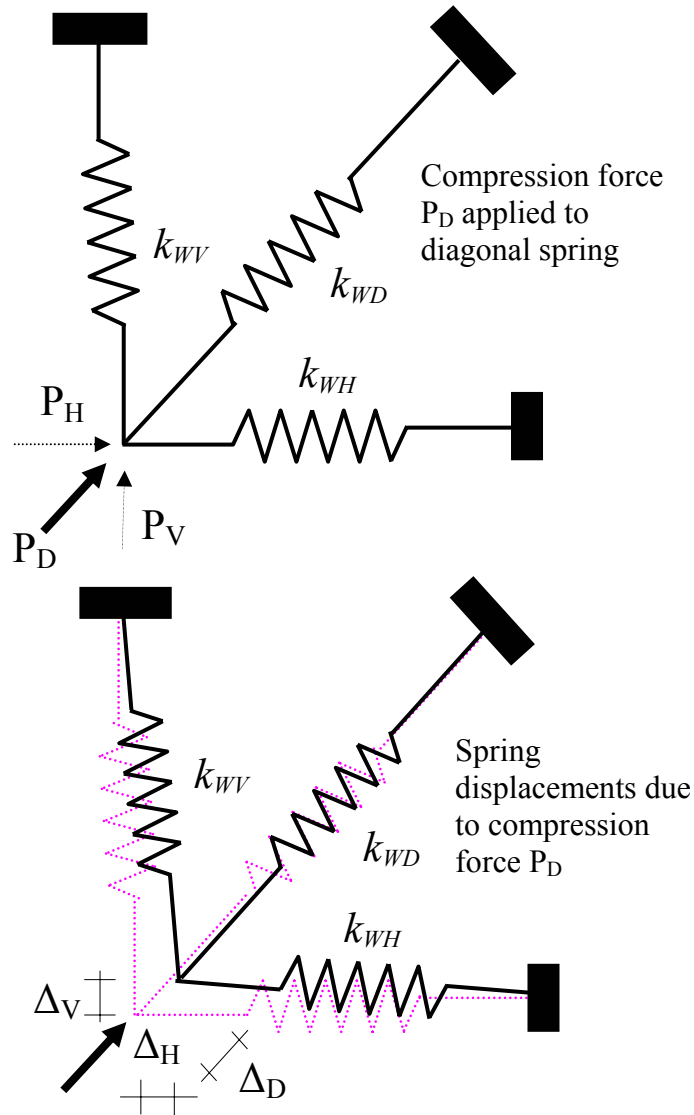


Figure 0.29 Spring model for determining the diagonal stiffness of walls

In this simplified rheology model and neglecting the damping factor of walls, wall diagonal stiffness  $k_{WD}$  can be determined by considering the equilibrium condition of force  $P_D$ , where  $k_{WH}$  and  $k_{WV}$  are wall lateral stiffness and wall axial stiffness taken

from Tables 5.5 and 5.11. As  $P_D$  is compression force acting in diagonal spring direction, the horizontal and vertical component of  $P_D$  are  $P_H$  and  $P_V$  respectively:

$$P_D^2 = P_V^2 + P_H^2 ,$$

$$k_{WD}^2 \Delta_D^2 = k_{WV}^2 \Delta_V^2 + k_{WH}^2 \Delta_H^2 ,$$

$$k_{WD} \Delta_D = \Delta_H \sqrt{k_{WV}^2 \left( \frac{\Delta_V}{\Delta_H} \right)^2 + k_{WH}^2} .$$

Since  $\frac{\Delta_V}{h}$  and  $\frac{\Delta_H}{h}$  are maximum allowable axial strain and shear strain, therefore

$\frac{\Delta_V}{\Delta_H}$  is equal to  $\frac{\varepsilon}{\gamma}$  and  $\left( \frac{\Delta_V}{\Delta_H} \right)^2$  is equal to  $\left( \frac{\varepsilon}{\gamma} \right)^2$ . According to the experimental

results, maximum allowable axial strain  $\varepsilon$  and shear strain  $\gamma$  for walls BW, MW, CW

and for walls MWA, CWA, MWE including the ratio of  $\frac{\varepsilon}{\gamma}$  and  $\left( \frac{\varepsilon}{\gamma} \right)^2$  are recorded

in Table 5.13.

According to the above approximation, the formula for diagonal stiffness will be equal to

$$k_{WD} = \frac{\Delta_H}{\Delta_D} \sqrt{k_{WV}^2 \left( \frac{\Delta_V}{\Delta_H} \right)^2 + k_{WH}^2} .$$

Based upon a small deformation theory of solid mechanics for small element of wall;

and taking  $\Delta_D$  to be equal to unity, therefore  $\Delta_H$  is equal to  $\cos (45^\circ)$  and  $\frac{\Delta_H}{\Delta_D}$  can be

simplified to be equal to 0.71.

Table 0.16 The ratio of axial strain to shear strain of walls

Wall	$\varepsilon$	$\gamma$	$\frac{\varepsilon}{\gamma}$	$\left(\frac{\varepsilon}{\gamma}\right)^2$
BW	0.004	0.02	0.2	0.04
MW	0.004	0.02	0.2	0.04
CW	0.004	0.02	0.2	0.04
MWA	0.006	0.04	0.15	0.025
CWA	0.006	0.04	0.15	0.025
MWE	0.006	0.04	0.15	0.025

By using this simplified approach; therefore, the generalised formula for diagonal stiffness of wall is:

$$k_{WD} = 0.71 \sqrt{0.04 k_{wV}^2 + k_{wH}^2} \dots\dots \text{for wall BW, MW, CW.}$$

$$k_{WD} = 0.71 \sqrt{0.025 k_{wV}^2 + k_{wH}^2} \dots\dots \text{for wall MWA, CWA, MWE.}$$

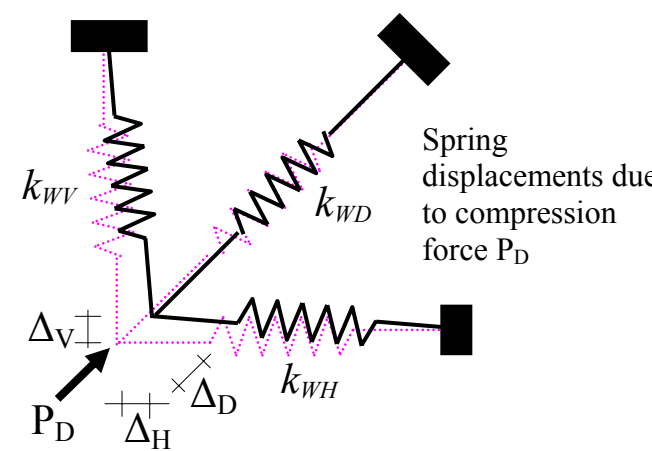
From those two derived formulas, the expression for a formula to be used in modeling diagonal stiffness in structural analysis of brick masonry wall is:

$$k_{WD} = 0.71 \sqrt{c_w \times k_{wV}^2 + k_{wH}^2} .$$

where,  $c_w$  is non dimensional strain coefficient of wall, it is equal to 0.04 for walls BW, MW, CW and 0.025 for walls MWA, CWA and MWE.

From the derived formula stated above, the diagonal stiffness of the walls is given in Table 5.10. The graphical representation of the diagonal stiffness of each type of wall is shown in Figures 5.30 to 5.35. Some additional graphs of the diagonal stiffness of the walls based on the height of wall panels are given in Appendix B.

Table 0.17 Diagonal stiffness of walls



Diagonal stiffness of walls (kN/mm)

Wall	L(cm)		200	300	400	500
	H (cm)					
BW	200		19.36	29.14	38.91	48.68
	300		12.84	19.36	25.88	32.40
	400		9.59	14.47	19.36	24.25
	500		7.65	11.54	15.45	19.36
MW	200		20.23	30.88	41.51	52.12
	300		13.20	20.23	27.33	34.43
	400		9.77	14.94	20.23	25.55
	500		7.76	11.82	15.99	20.23
CW	200		9.32	14.94	20.67	26.37
	300		5.83	9.32	13.04	16.85
	400		4.25	6.67	9.32	12.10
	500		3.36	5.18	7.18	9.32
MWA	200		5.46	8.44	11.41	14.36
	300		3.52	5.46	7.45	9.43
	400		2.58	4.00	5.46	6.95
	500		2.04	3.14	4.29	5.46
CWA	200		5.67	8.78	11.89	14.98
	300		3.63	5.67	7.74	9.82
	400		2.66	4.13	5.67	7.22
	500		2.10	3.24	4.44	5.67
MWE	200		5.45	8.34	11.22	14.09
	300		3.54	5.45	7.38	9.30
	400		2.61	4.01	5.45	6.89
	500		2.07	3.17	4.30	5.45

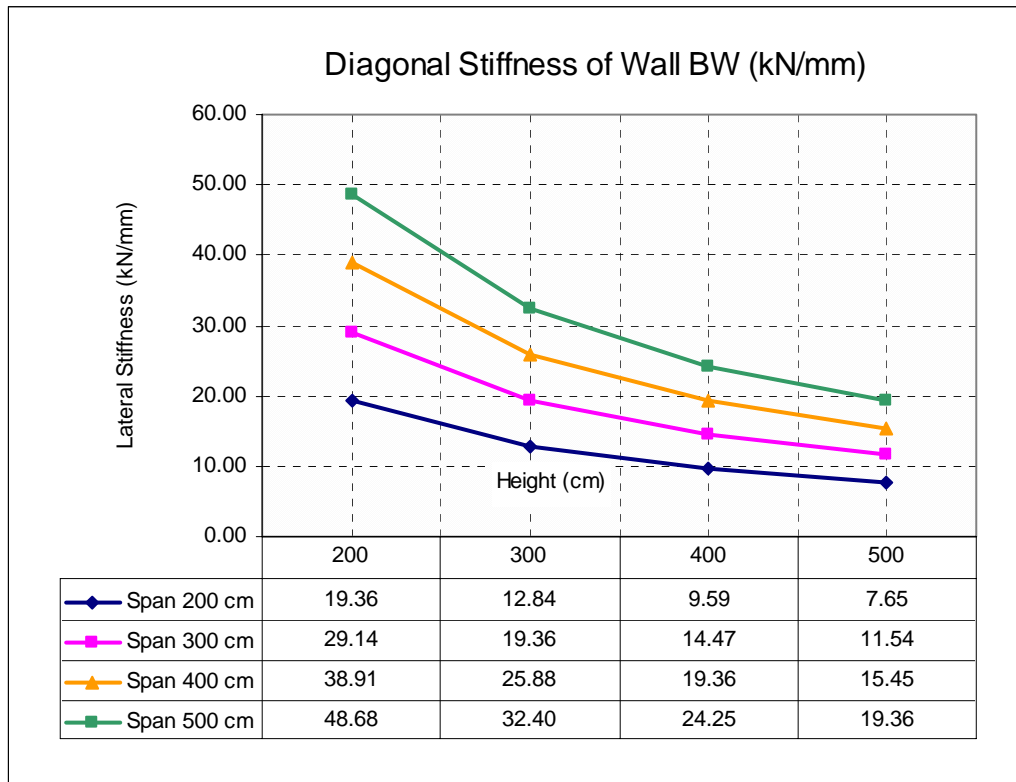


Figure 0.30 Diagonal stiffness of wall BW

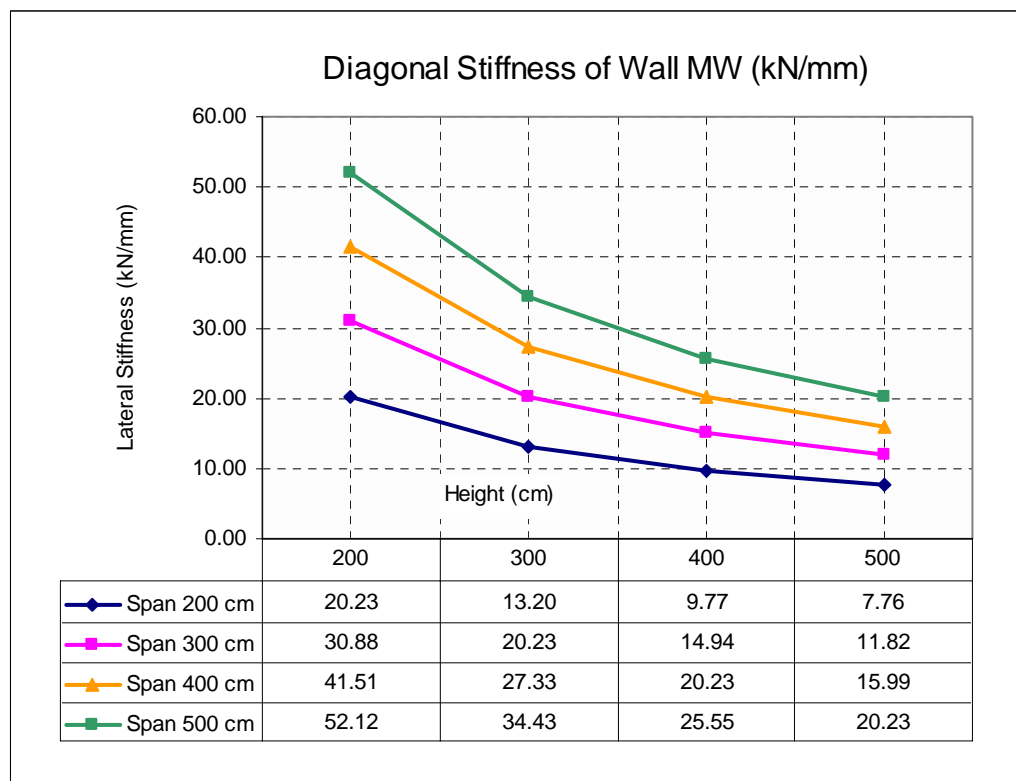


Figure 0.31 Diagonal stiffness of wall MW

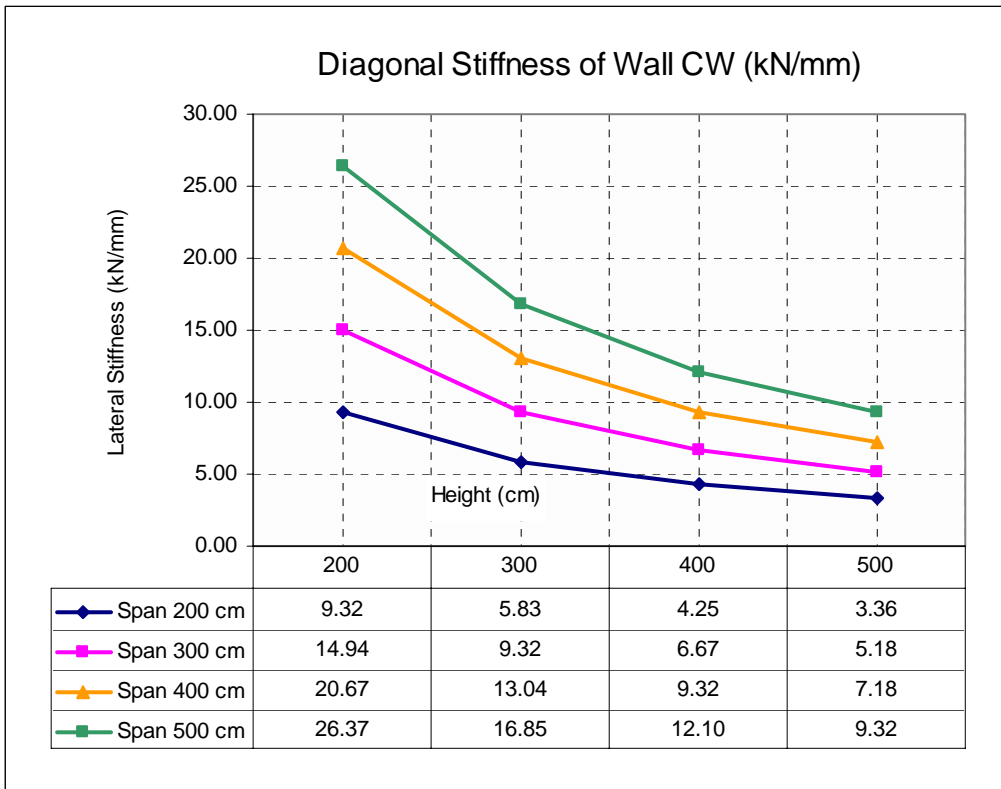


Figure 0.32 Diagonal stiffness of wall CW

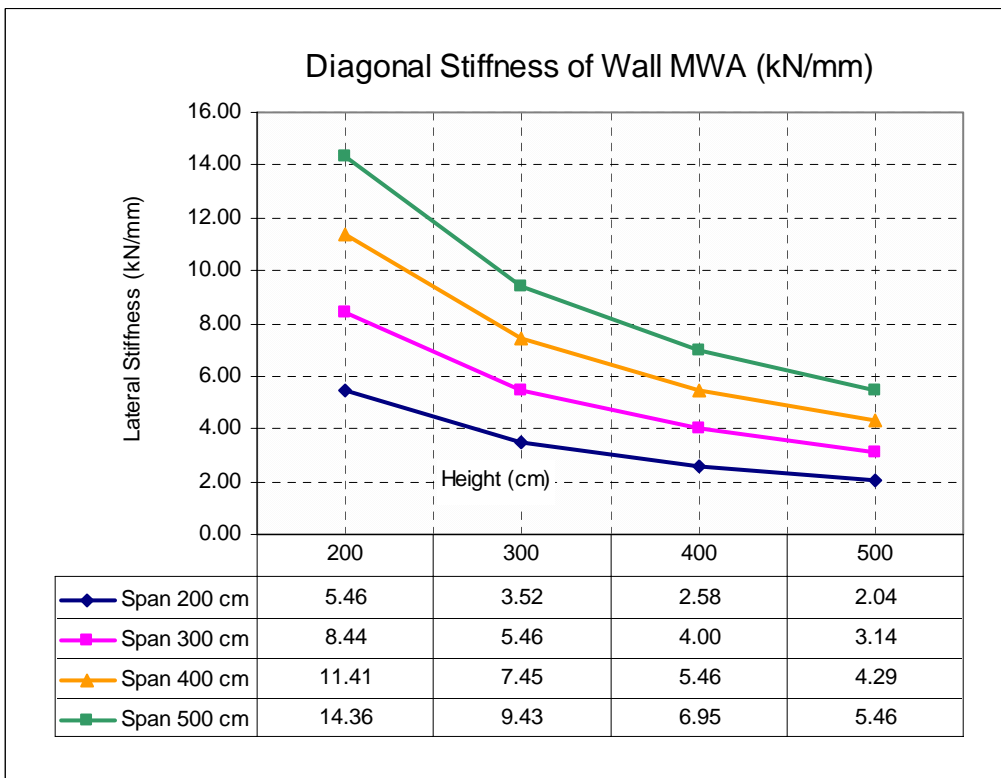


Figure 0.33 Diagonal stiffness of wall MWA



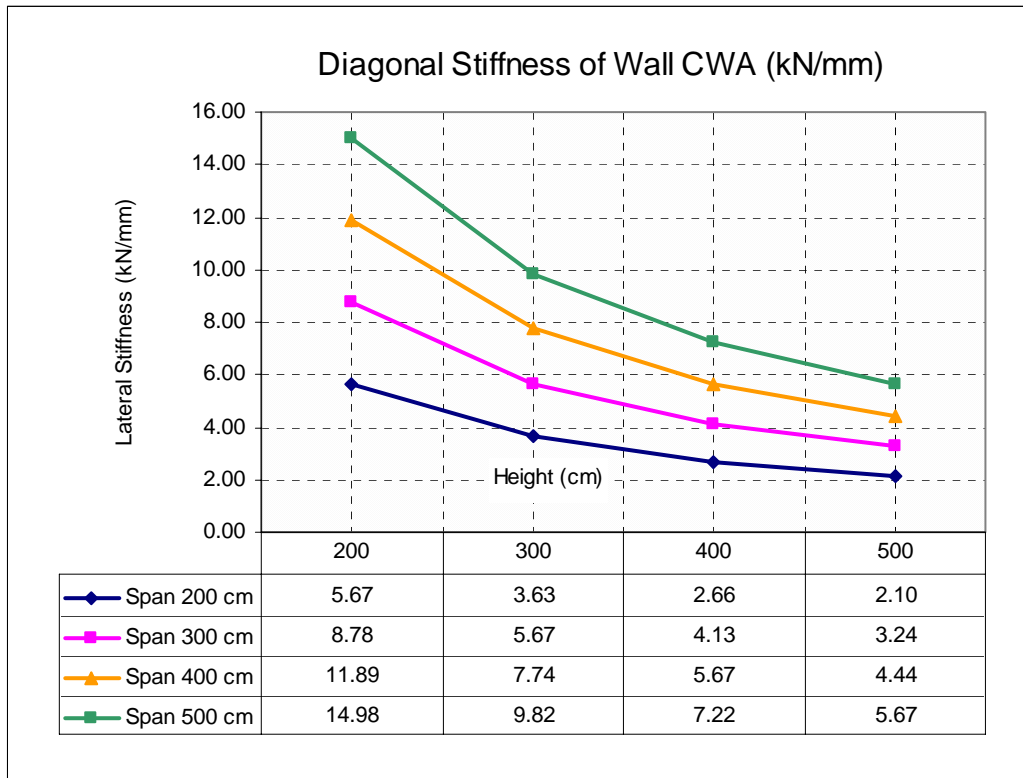


Figure 0.34 Diagonal stiffness of wall CWA

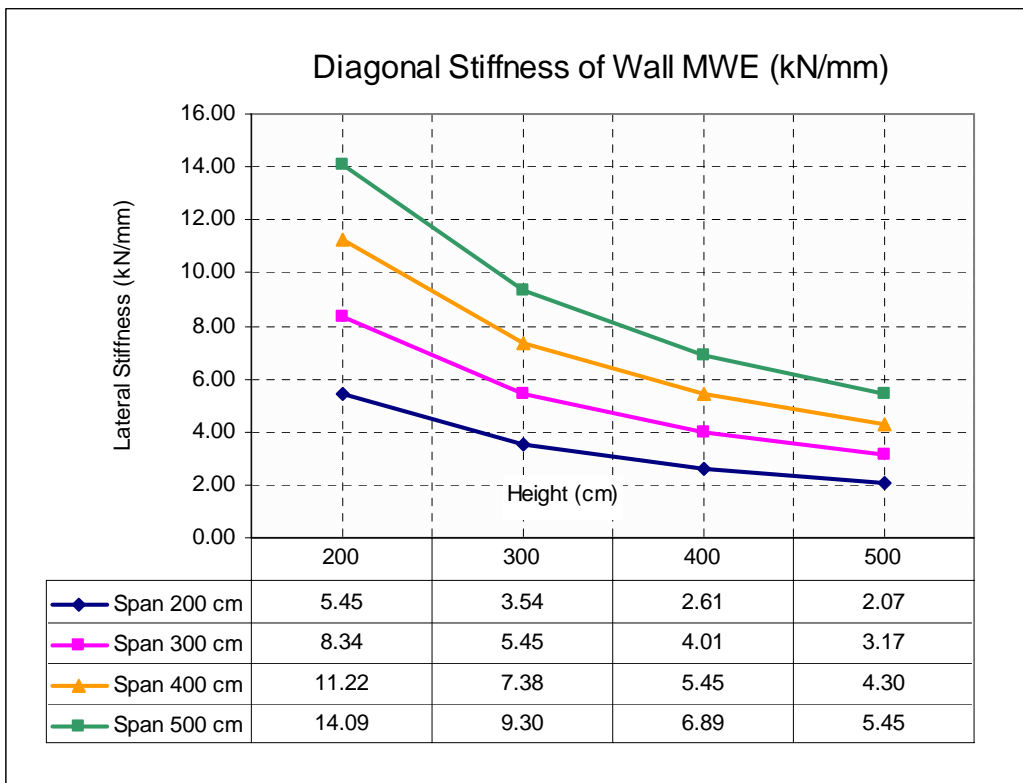


Figure 0.35 Diagonal stiffness of wall MWE

## 5.5 Wall capacity based on Indonesian seismic zones

According to SNI-1726-2002, the magnitude of base shear force of building can be determined by using the following formula:

$$V = \frac{C_i I W_t}{R}$$

where  $V$  is base shear force acting on a house or low-rise building structures,  $C_i$  is the coefficient of earthquake response, based on the Indonesian Earthquake Response Spectrum, as explained in Chapter 2, Sub-section 2.6.5. Coefficient of building importance  $I$ , for houses and low-rise buildings is taken as 1.0.  $W_t$  is the total weight of building. For simple ordinary houses, the total weight of structure is assumed to be equal to 100 kN and  $R$  is the coefficient of earthquake reduction factor taken as 1.6.

By observing the results from the tests, the average capacity of walls BW, MW, CW, MWA, CWA and CWE to resist lateral in-plane loads were determined and given in Table 5.18. The static equivalent lateral earthquake loads  $V$  based on six seismic regions are given in Table 5.19.

*Table 0.18 Capacity of 1 meter wall to retain base static shear force*

Wall	Capacity of wall to retain base static shear force (kN)	Capacity of wall to retain base cyclic shear force – 30% of static capacity (kN).
BW	99	29.7
MW	160	48.0
CW	136	40.8
MWA	55	16.5
CWA	59	17.7
MWE	48	14.4

*Table 0.19 Static equivalent lateral earthquake load  $V$  (kN) for wall of 1 meter length*

Static Equivalent Lateral Earthquake Load (kN) based on SNI-1726-2002 Assuming $W_t = 10$ kN/m			
Seismic Zone	Type of Soil		
	Soft	Moderate	Hard
1	1.25	0.81	0.63
2	3.13	2.38	1.88
3	4.69	3.44	2.81
4	5.31	4.38	3.75
5	5.63	5.00	4.38
6	5.93	5.63	5.19

Since the masonry houses are generally weak in retaining cyclic loads, to construct masonry houses with safe structure, it can be assumed that cyclic load applied on the structures is multiplied by a load safety factor. In general, the capacity of wall to retain cyclic lateral load is 30 – 50 % of that of monotonic load. Based on these experimental results, the load safety factor can be approximated as the inverse of percentage of decreasing wall capacity, therefore it is assumed to be taken as 2 – 3. Based on this determination, the dynamic equivalent earthquake loads are as given in Table 5.30.

*Table 0.20 Dynamic earthquake load (kN)*

Dynamic earthquake load (kN/m) based on SNI-1726-2002 (3× of static equivalent earthquake load)			
Seismic Zone	Type of Soil		
	Soft	Moderate	Hard
1	3.75	2.43	1.89
2	9.39	7.14	5.64
3	14.07	10.32	8.43
4	15.93	13.14	11.25
5	16.89	15.00	13.14
6	17.802	16.89	15.57

Observing Table 5.8 and 5.9, therefore the masonry houses constructed by using walls BW, MW, CW, MWA, CWA and MWE are theoretically safe to be built in

seismic zones as detailed in Table 5.21, and are to be recommended to the development of guidelines.

*Table 0.21 Type of wall that can be built in Indonesian seismic zone*

Dynamic equivalent earthquake load (kN/m) based on SNI-1726-2002			
Seismic Zone	Type of soil		
	Soft	Moderate	Hard
6	BW, MW, CW	BW, MW, CW, MWA, CWA	
5	BW, MW, CW, MWA	BW, MW, CW, MWA, CWA	
4	BW, MW, CW, MWA, CWA	BW, MW, CW, MWA, CWA, MWE	
3	BW, MW, CW, MWA, CWA, MWE		
2	BW, MW, CW, MWA, CWA, MWE		
1	BW, MW, CW, MWA, CWA, MWE		

## 5.6 Conclusion

The summary of the main contributions to the development of guidelines, as detailed in this chapter is as follows:

- **Lateral stiffness**

To maintain good performance in lateral stiffness, it is recommended to install a tie beam with the maximum of panel height of 3.00 m. As the height of wall increase, the lateral stiffness decrease. The generalized lateral stiffness is derived from the experiments on square wall panels. The lateral stiffness of wall BW, MW, CW, MWA, CWA, and MWE are 4.95 kN/mm, 8.03 kN/mm, 6.82 kN/mm, 2.27 kN/mm, 2.97 kN/mm and 2.42 kN/mm respectively.

- **Diagonal stiffness**

The diagonal stiffness for structural analysis is expressed in a formula:

$$k_{WD} = 0.71 \sqrt{c_w \times k_{WV}^2 + k_{WH}^2}$$

where,  $k_{wd}$ ,  $k_{wv}$  and  $k_{wh}$  are diagonal, axial and lateral stiffness of walls respectively;  $c_w$  is strain coefficient of wall and it is equal to 0.04 for wall BW, MW and CW and 0.025 for walls MWA, CWA and MWE.

- The permission for construction of houses and low-rise buildings in six seismic zones in Indonesia should be informed in the design guideline. It is presented in Tables 5.22, 5.24 and 5.25.

*Table 0.22 The permissible construction of houses and low-rise buildings on soft soil*

Seismic zones Wall	1	2	3	4	5	6
BW	yes	yes	yes	yes	yes	yes
MW	yes	yes	yes	yes	yes	yes
CW	yes	yes	yes	yes	yes	yes
MWA	yes	yes	yes	yes	yes	no
CWA	yes	yes	yes	yes	no	no
MWE	yes	yes	yes	no	no	no

*Table 0.23 The permissible construction of houses and low-rise buildings on moderate soil*

Seismic zones Wall	1	2	3	4	5	6
BW	yes	yes	yes	yes	yes	yes
MW	yes	yes	yes	yes	yes	yes
CW	yes	yes	yes	yes	yes	yes
MWA	yes	yes	yes	yes	yes	yes
CWA	yes	yes	yes	yes	yes	yes
MWE	yes	yes	yes	yes	yes	no

*Table 0.24 The permissible construction of houses and low-rise buildings on hard soil*

Seismic zones Wall	1	2	3	4	5	6
BW	yes	yes	yes	yes	yes	yes
MW	yes	yes	yes	yes	yes	yes
CW	yes	yes	yes	yes	yes	yes
MWA	yes	yes	yes	yes	yes	yes
CWA	yes	yes	yes	yes	yes	yes
MWE	yes	yes	yes	yes	yes	no

## Chapter 6. Conclusion

---

This chapter presents the discussion and conclusions from the research findings presented in this thesis. The recommendations and suggestions for further research work are also proposed.

The main and additional findings of this thesis are:

- Main findings:
  - Plastering wall surface using mortar type A (1:3), does not improve the lateral load response of the walls.
  - Plastering wall surface using mortar type B (1:4), improves the stiffness of mortared and combed wall by 1.5 – 2.0 times of that of brick walls; however, it does not improve the ductility.
  - Vertical pressure applied to the wall specimens increased the lateral load carrying capacity of the walls under repeated loads, but not under cyclic and monotonic loads. Walls under repeated loads experienced a relaxation of the stress-strain responses during unloaded stages.
  - A formula for diagonal stiffness of wall panels was developed.
  - Guidelines for construction of houses and low-rise buildings based on type of soil and seismic zones in Indonesia were proposed.
  
- Additional findings:
  - The capacity of wall under cyclic loads is 50% less than that under monotonic and repeated lateral in-plane loads.
  - Fissure closing stage of brick assemblages, columns and walls appears in stress-strain response when the compressive stress is less than or equal to 2.0 MPa.
  - All walls collapsed in brittle failure mechanism, without the presence of ductility.

Masonry houses and low-rise buildings in Indonesia are poorly constructed without following design guidelines and proper engineering supervision. However, in majority of villages, cities, the non-engineered and semi-engineered houses and buildings are constructed using comforted mortar wall, as it is assumed to be the strongest structure.

From the study on the comparative responses of un-reinforced masonry brick walls, with and without mortar confinement or surface plaster, the physical and mechanical behaviour of these types of walls were determined. The result from these 2 stages of experimental work were summarised into three categories:

1. The compressive strength and stress-strain behaviour of brick assemblages, columns and walls.
2. The load-displacement response and lateral stiffness of wall under applied lateral in-plane loads in monotonic, repeated and cyclic pattern, and
3. The simplified formula for diagonal stiffness of walls.

The physical characteristics of Cikarang clay bricks were determined based on the size of bricks, the density, the water absorption, the compressive strength and the modulus of rupture. The average size of bricks is 46 mm × 90 mm × 190 mm, the density is 1.69 gram/cm<sup>3</sup>, the water absorption is 0.036 mm/sec, the compressive strength is 12.0 MPa, and the modulus of rupture is 3.0 MPa.

The overall stress-strain response of brick assemblages, masonry columns and masonry walls were graphically shown in bilinear curves, which had a gentle slope when the compressive stress was below or equal to 2 MPa. As the compressive stress increased above 2 MPa, the slope of stress-strain curves became steeper. It can be concluded that all types of Cikarang-Indonesian clay brick assemblages remain in a fissure closing stage as the compressive pressure is below or equal to 2 MPa. This type of stress-strain behaviour containing fissure closing stage is not found in any other research work.

Wall panels tested under compression and cyclic lateral in-plane loads, produced the average maximum capacity of 50% of those tested under compression and monotonic or lateral in-plane loads. The angle of rotation of wall noted as  $\gamma$ , measured as the



ratio of horizontal displacement to the original height of wall, observed from the experimental results was very small. Consequently, the lateral stiffness of walls can be linearly approximated. From this simple analytical approach, the formula for diagonal stiffness of clay brick wall was determined. It was also recorded that the presence of surface mortar plaster as wall confinement system increased the stiffness of wall, but did not affect to the improvement of wall ductility.

By observing the capacities of walls in retaining lateral loads, the requirement for construction of houses and low-rise buildings in six seismic zones in Indonesia is obtained. It is proposed that these requirements are included in the design guidelines. A recommendation for the construction of masonry houses based on the experimental study of the research presented in this thesis, are:

- Mortared wall MWE should not be constructed on soft soil in seismic zones 4 and 5, and should not be constructed on moderate and hard soil in seismic zones 6.
- Comforted wall CWA should not be constructed on soft soil in seismic zones 5 and 6.
- Mortared wall MWA should not be constructed on soft soil in seismic zones 6.

#### **Further application.**

According to the presented findings, a further experimental and analytical research is necessary in the area of mechanics of masonry using clay or other bricks found in the different regions in Indonesia. There is an urgent need for the development of guidelines referring to the certain seismic regions, especially for places in high seismic risk zone. It is very important that a clear and understandable structural detailing procedure, which applicable to a certain region is published nationally and made known among the regional building constructors and civil engineering technical workers.

The outcomes of the investigation reported in this thesis provided useful information for a contribution to the development of guidelines on masonry construction for houses and low-rise buildings in Indonesia. Since the performance characteristics of

mortared wall MW were much better than those of other walls, mortared wall MW was recommended to be used in construction site. Compared to mortared wall MW, there is no significant benefit in using comforted wall CW. Mortared and comforted walls MWA and CWA were considerably weak. Brick wall BW needs to be constructed properly to reach its compactness condition. Using non-standard sand may decrease the general capacity of the wall, as exhibited by mortared wall MWE.

In conclusion, the most important findings of the research reported in this thesis are the formula for diagonal stiffness of walls and the statement of recommendation for construction of brick masonry houses in Indonesia.

It is crucial that the findings from this research be considered and implemented into the policy for the development of guidelines for brick masonry houses and low-rise buildings in Indonesia.

## References

---

- Abrams, D. P. "Effect of mortar Shrinkage on In-Plane Stresses in Clay Brickwork." *The Masonry Structures*, 77-84, 1995
- Abrams, D. P. "Effect of Scale and Loading Rate with Test of Concrete and Masonry Structures." *Earthquake Spectra*, 12, 13-28, 1996
- Adreaus, U. "Failure Criteria for Masonry Panels under In-Plane Loading." *Journal of Structural Engineering*, 122(1) 37-46, 1996
- AlShebani, M. M., and Sinha, S. N. "Effect of Panel Height on the Cyclic Behaviour of Brick Masonry." 5th Australasian Brick Masonry Conference, Gladstone, Queensland, Australia, 1-11, 1998
- AlShebani, M. M., and Sinha, S. N. "Stress-Strain Characteristics of Brick Masonry under Uniaxial Cyclic Loading." *Journal of Structural Engineering*, ASCE, 125(9), 600-604, 1999
- Al-Shebani, M. M., and Sinha, B. P. "Stress-Strain Characteristics of brick Masonry under Cyclic Biaxial Compression." *Journal of Structural Engineering*, ASCE, 126(9), 1004-1007, 2000
- Anand, S. C., and Young, D. T. (1982). "Finite Element Model for Composite Masonry." *Journal of Structural Engineering*, , vol. 108, pp. 2637-2651, 1982.,
- Anand, S. S., and Yalamanchili, K. K. "Three-Dimensional Failure Analysis of Composite Masonry Walls." *Journal of Structural Engineering*, 122(9), 1031-1039, 1996
- Andreas J. Kappos, A.J., Penelis, G.G, and Christos G. Drakopoulos,C.G., "Evaluation of Simplified Models for Lateral Load Analysis of Unreinforced Masonry Buildings. ", *Journal of Structural Engineering*, 128(7), 890-897, 2002
- Andreaus, U. (1996). "Failure Criteria for Masonry Panels under In-Plane Loading." *Journal of Structural Engineering*, 122(1), 37-46, 1996
- Anthoine, A., Magonette, G., and Magenes, G. "Shear compression testing and analysis of brick masonry walls." 10th European Conference on Earthquake Engineering, 1657-1662, 1995
- Anthoine, A. (1997). "Homogenization of Periodic Masonry: Plane Stress, Generalize Plane Strain or 3D Modelling ?" *Communication in Numerical Methods in Engineering*, 13, 319-326, 1997

- Atkinson, R. H., Amadei, B. P., Saeb, S., and Sture, S. "Response of Masonry Bed Joints in Direct Shear." *Journal of Structural Engineering*, 115(9), 2276-2296, 1989
- Asteris, P.G. and Syrmakezis, C.A., "Strength of Unreinforced Masonry Walls under Concentrations Compression Loads." *Practice Periodical on Structural Design and Construction*, 10(2),133-140, 2005
- AS 3700-2001 Australian Standard for Masonry Structures, 2001
- Basoenondo, E. A., Giles, R. S., Thambiratnam, D. P., and Purnomo, H. "Response of Unreinforced Brick Masonry Wall Structures to Lateral Loads." *International Conference on Structural Engineering, Mechanics and Computation*, Cape Town, South Africa, 419-425, 2001
- BS 5628-2, Code of practice for the use of masonry, Part 2: Structural use of reinforced and prestressed masonry.
- Bati, S. B., Ranocchiai, G., and Rovero, L. "Suitability of Micromechanical Model for Elastic Analysis of Masonry." *Journal of Engineering Mechanics*, 125(8), 922-929, 1999
- Biolzi, L. "Evaluation of Compressive Strength of Masonry Walls by Limit Analysis." *Journal of Structural Engineering*, 114(10), 2179 – 2189, 1988
- Chukwunenyne, A. and Hamid, A. "Compression Behavior of Concrete Masonry Prisms." *Journal of Structural Engineering*, vol. 112(3), 605 - 613, 1986.
- CIPTA KARYA, Lampiran Surat Keputusan Direktur Jenderal Cipta Karya, Departemen PU, Nomer: 111/KPTS/CK/1993, Tanggal 28 September 1993 Tentang: Pedoman Pembangunan Bangunan Tahan Gempa, Bagian E: Bangunan Tembok Bata.
- Dhanasekar, M., Kleeman, P. W., and Page, A. W. "Biaxial Stress-Strain Relations for Brick Masonry." *Journal of Structural Engineering*, 111(5), 1085 – 1100, 1985
- Dhanasekar, M., Page, A. W., and Kleeman, P. W. "The Failure of Brick Masonry Under Biaxial Stresses." *Proceeding of Institutions in Civil Engineers*, Part 2, 79(6), 295-313, 1985
- El-Sakhawy, N.R., Abdel Raof, H., Gouhar, A., (2002), "Shearing Behavior of Joints in Load-Bearing Masonry Wall." *Journal of Materials in Civil Engineering*, 14(2), 145-150, 2002
- Fahmi, E. H., and Ghoneim, T. G. M. "Behavior of Concrete Block Masonry Prism under Axial Compression." *Canadian Journal of Civil Engineering*, 22, 898 – 915, 1995

- Ghazali, M. Z., and Riddington, J. R. "Simple test method for masonry shear strength." *Proceeding of Institutions in Civil Engineers, Part 2*, 85(9), 567-574, 1988
- Giles, R. S., Thambiratnam, D. P., and Bullen, F. "An investigation into the behaviour of masonry walls subjected to lateral in-plane loading." *Bachelor in Civil Engineering, Queensland University of Technology, Brisbane, QLD, Australia*, (2001)
- Grimm, C.T., and Tucker, L. R. "Flexural Strength of Masonry Prisms versus Wall Panels." *Journal of Structural Engineering*, 111(9), 2021-2032, 1985
- Grimm, C. T. "Clay Brick Masonry Weight Variation." *Journal of Architectural Engineering*, 2(4), 135-137, 1996
- Goodman, R. "Introduction to Rock Mechanics." John Wiley, New York, 1989
- Hamid, A. A., and Chukwunenye, A. O. "Compression Behavior of Concrete Masonry Prisms." *Journal of Structural Engineering*, 112(3), 605 – 613, 1986
- Hamid, A. A., and Drysdale, R. G. "Proposed Failure Criteria for Concrete Block Masonry under Biaxial Stresses." *Journal of the Structural Division*, 107(8), 1675-1687, 1981
- Haris, H.G. and Sabnis, G.M. "Structural Modelling and Experimental Techniques, 2<sup>nd</sup> ed. ", CRC Press LLC, 1999
- Khalaf, F. M. "Blockwork Masonry Compressed in Two Orthogonal Directions." *Journal of Structural Engineering*, 123(5), 591-596, 1997
- Köksal, H.O., Karakoc, C. and Yildirim, H., (2005), "Compression Behavior and Failure Mechanisms of Concrete Masonry Prisms." *Journal of Materials in Civil Engineering*, 17(1), 107-115, 2005
- La Mendola, L. (1997). "Influence of Nonlinear Constitutive Law on Masonry Pier Stability." *Journal of Structural Engineering*, 123(10), 1303-1311.
- La Mendola, L., and Papia, M. (1993). "Stability of masonry piers under their own weight and eccentric load." *Journal of Structural Engineering*, 119(6), 1678-1693.
- La Mendola, L., Papia, M., and Zingone, G. "Stability of Masonry Walls Subjected to Seismic Transverse Forces." *Journal of Structural Engineering*, 121(11), 1581-1587, 1995
- Lafuente, M., Genatios, C., and Lorrain, M. "Analytical studies of masonry walls subjected to monotonic lateral loads." *10th European Conference on Earthquake Engineering*, 1751-1756, 1995

- Lourenco, P.B. and Ramos, L.F. "Characterization of Cyclic Behavior of Dry Masonry Joints." *Journal of Structural Engineering*, 130(5)779-786, 2004
- Lu, M., Schultz, A.E., and Stolarski, H.K. "Analysis of the Influence of Tensile Strength on the Stability of Eccentrically Compressed Slender Unreinforced Masonry Walls under Lateral Loads." *Journal of Structural Engineering*, 130(6), 921-933, 2004
- Madan, A., Reinhorn, A. M., Mander, J. B., and Valles, R. E. "Modeling of Masonry Infill Panels for Structural Analysis." *Journal of Structural Engineering*, ASCE, 123(No. 10, October 1997), 1295 – 1302, 1997
- Magenes, G., and Calvi, G. M. "Shaking Table Test of Brick Masonry Walls." 10th European Conference on Earthquake Engineering, Madrid, Spain, 1995
- Magenes, G., and Calvi, G. M. "In-plane Seismic Response of Brick Masonry Walls." *Earthquake Engineering and Structural Dynamics*, 26, 1091 – 1112, 1997
- Mc Nary, W. S., and Abrams, D. P. "Mechanics of Masonry in Compression." *Journal of Structural Engineering*, 111(4), 857 – 870, 1985
- Mehrabi, A. B., and Shing, P. B. (1997). "Finite Element Modeling of Masonry-Infilled RC Frames." *Journal of Structural Engineering*, 123(5), 604-613, 1997
- Mohamed A. H. Abdel-Halim, Samer A. Barakat. "Cyclic Performance of Concrete-Backed Stone Masonry Walls." *Journal of Structural Engineering*, 129(5), 596-605, 2003
- Mojsilovic, N., and Marti, P. "Strength of Masonry Subjected to Combined Actions." *ACI Structural Journal*, 94(6), 633-642, 1997
- Naraine, K., and Sinha, S. "Behavior of Brick Masonry under Cyclic Compressive Loading." *Journal of Structural Engineering*, 115(6), 1432-1445, 1989
- Naraine, K., and Sinha, S. "Loading and Unloading Stress-Strain Curves for Brick Masonry." *Journal of Structural Engineering*, 115(10), 2631-2644, 1989
- Naraine, K., and Sinha, S. "Cyclic Behavior of Brick Masonry under Biaxial Compression." *Journal of Structural Engineering*, 117(5), 1336-1355, 1991
- Naraine, K., and Sinha, S. "Stress-Strain Curves for Brick Masonry in Biaxial Compression." *Journal of Structural Engineering*, 118(6), 1451-1461, 1992
- Nary, W. S. M., and Abrams, D. P. "Mechanics of Masonry in Compression." *Journal of Structural Engineering*, ASCE, 111(4), 857 – 870, 1985
- Page, A. W. "A biaxial failure criterion for brick masonry in the tension-tension range." *The International Journal of Masonry Construction*, 1(1), 26-29, 1980

- Page, A. W. "An Experimental Investigation of the Biaxial Strength of Brick Masonry." 6th International Brick Masonry Conference, Roma, Italy, 3-15, 1982
- Page, A. W. "Strength of brick masonry under biaxial tension-compression." The International Journal of Masonry Construction, 3(1), 26-31, 1983
- Riddington, J. R., and Ghazali, M. Z. "Hypothesis for shear failure in masonry." Proceeding of Institutions in Civil Engineers, Part 2, 89(March), 89-102, 1990
- Riddington, J. R., and Jukes, P. "A masonry joint shear strength test method." Proceeding of Institution in Civil Engineers Structures & Buildings, 104(8), 267-274., 1994
- Roca, P., Molins, C. and Marí, A. R. "Strength Capacity of Masonry Wall Structures by the Equivalent Frame Method." Journal of Structural Engineering, 131(10), 1601-1610, 2005
- Romano, F., Ganduscio, S., and Zingone, G. "Cracked Nonlinear Masonry Stability under Vertical and Lateral Load." Journal of Structural Engineering, 119, 69-87, 1993.
- Romano, F., Ganduscio, S., and Zingone, G. "Analysis of masonry walls subjected to cyclic shear." 10th European Conference on Earthquake Engineering, 1675-1680, 1995
- Sarangapani, G, Venkatarama Reddy, B. V. and Jagadish, K. S. "Brick-Mortar Bond and Masonry Compressive Strength." Journal of Materials in Civil Engineering, 17(2), 229-237, 2005
- Shing, P. B., Noland, J. L., Klamerus, E., and Spaeh, H. (1989). "Inelastic Behavior of Concrete Masonry Shear Walls." Journal of Structural Engineering, 115(4), 2204-2225, 1989
- Shing, P. B., Schuller, M., and Hoskere, V. S. "In-Plane Resistance of Reinforced Masonry Shear Walls." Journal of Structural Engineering, 116(3), 619 - 640, 1990
- Shing, P. B., Schuller, M., Hoskere, V. S., and Carter, E. "Flexural and shear Response of Reinforced Masonry Walls." ACI Structural Journal, 87(6), 646-656, 1990
- Shrive, N. G., and Sayed-Ahmed, E. Y. "Design recommendations for hollow concrete masonry walls subject to concentrated loads, based on a test program." Canadian Journal of Civil Engineering, 24, 380-391, 1997
- Sinha, B. P., Ng, C. L., and Pedreschi, R. F. "Failure Criterion and Behavior of Brickwork in Biaxial Bending." Journal of Materials in Civil Engineering, 9(2), 70-75, 1997

- Sinha, B. P., and Pedreschi, R. "*Compressive strength and some elastic properties of brickwork.*" *The International Journal of Masonry Construction*, 19-25, 1983
- Sinha, S.N. and AlShebani, M.M. "*Effect of Panel Height on the Cyclic Behaviour of Brick Masonry.*" Gladstone, Queensland, Australia, 1998.
- SNI 15 1328-1989 Bata Merah Pejal, Syarat Penerimaan ( Term of acceptance )
- SNI 15-3758-1995 Semen Aduk Mortar Pasangan (Masonry Mortar)
- SNI 03-4164-1996 Metode Pengujian Kuat Tekan Dinding Pasangan Bata Merah
- SNI 15-2094-2000 Bata Merah Untuk Bahan Bangunan , Mutu dan Cara Uji
- SNI 03-6825-2002 Metode Pengujian Kekuatan Tekan Mortar Semen Portland untuk Pekerjaan Sipil
- SNI – 1726-2002 Standar Perencanaan Ketahanan Gempa Untuk Struktur Bnagunan Gedung
- Subramaniam, K. V. L., and Sinha, S. N. "*Analytical Model for Cyclic Compressive Behavior of Brick Masonry.*" *ACI Structural Journal*, 92(May - June), 288 – 294, 1995
- Syrmakezis, C. A., and Asteris, P. G. "*Masonry Failure Criterion under Biaxial Stress State.*" *Journal of Materials in Civil Engineering*, 13(1), 58-64, 2001
- Tomazevic, M., and Klemenc, I. "*Seismic Behaviour of Confined Masonry Walls.*" *Earthquake Engineering and Structural Dynamics*, 26, 1059 – 1071, 1997
- Tomazevic, M., and Klemenc, I. "*Verification of Seismic Resistance of Confined Masonry Buildings.*" *Earthquake Engineering and Structural Dynamics*, 26, 1073-1088, 1997
- Tomazevic, M., and Lutman, M. "*Simulation of seismic behaviour of reinforced masonry walls by laboratory testing.*" 10th International Brick and Block Masonry Conference, Calgary, Canada, 293-302,1994
- Tomazevic, M., Lutman, M., and Petkovic, L. "*Seismic Behaviour of Masonry Walls: Experimental Simulation.*" *Journal of Structural Engineering*, 122(9), 1040-1047, 1996
- Venkatarama Reddy, B.V. and Gupta, A. "*Tensile Bond Strength of Soil-Cement Block Masonry Couplets using Cement-Soil Mortars.*" *Journal of Materials in Civil Engineering*, 18(1), 36-45, 2006
- Venkatarama Reddy, B.V. and Gupta, A. "*Strength and Elastic Properties of Stabilized Mud Block Masonry using Cement-Soil Mortars.*" *Journal of Materials in Civil Engineering*, 18(3), 472-476, 2006



- Venkatarama Reddy, B.V., Lal, R., and Nanjunda Rao, K. S. "*Enhancing Bond Strength and Characteristics of Soil-Cement Block Masonry.*" *Journal of Materials in Civil Engineering*, 19(2), 164-172, 2007
- Yi, T., Moon, F.L., Kahn, L.F. "Analyses of a Two-Story Unreinforced Masonry Building ." *Journal of Structural Engineering*, 132(5), 653-662, 2006
- Zarnic, R. "*Modelling of response of masonry in-filled frames.*" 10th European Conference on Earthquake Engineering, 1481-1486, 1995
- Zhuge, Y., Yang, Y., Thambiratnam, D. P., and Corderoy, H. J. B. "*On the Behaviour of Brick Masonry Structures Under Lateral Loads.*" 13th Australasian Conference on the Mechanics of Structures and Materials, University of Wollongong, Australia, 1993
- Zhuge, Y., Thambiratnam, D., and Corderoy, J. "*Experimental Testing of Masonry Walls Under In-Plane Cyclic Loads.*" 10th International Brick and Block Masonry Conference, Calgary, Alberta, Canada, 1994
- Zhuge, Y., Corderoy, J., and Thambiratnam, D. P. "*Numerical Modelling Of Unreinforced Masonry Shear Walls.*" 14<sup>th</sup> Australasian Conference on the Mechanics of Structures and Materials, Tasmania, Australia, 1995
- Zhuge, Y., Corderoy, J., and Thambiratnam, D. P. "*Behavior of Unreinforced Brick Masonry Under Lateral Load (Cyclic) Loading.*" *The Masonry Society Journal*, 55-62, 1996
- Zhuge, Y., Thambiratnam, D. P., and Corderoy, J. "*Parametric studies on the dynamic characteristics of unreinforced masonry.*" *The Mechanics of Structures and Materials*, 1997.
- Zhuge, Y., and Thambiratnam, D. "*Nonlinear Dynamics Analysis of Unreinforced Masonry.*" *Journal of Structural Engineering*, 124(3), 270 – 277, 1998
- Zughe, Y. "*Experimental study on partially reinforced clay block masonry under simulated earthquake load.*" 6th Australasian Masonry Conference, Adelaide, South Australia, 413-420, 2001

## Appendix A

Data for compressive and shear stress of walls BW				
BW Monotonic				
BW Repeated				
BW Cyclic				

Data for compressive and shear stress of walls MW			
MW Monotonic			
MW Repeated			
MW Cyclic			

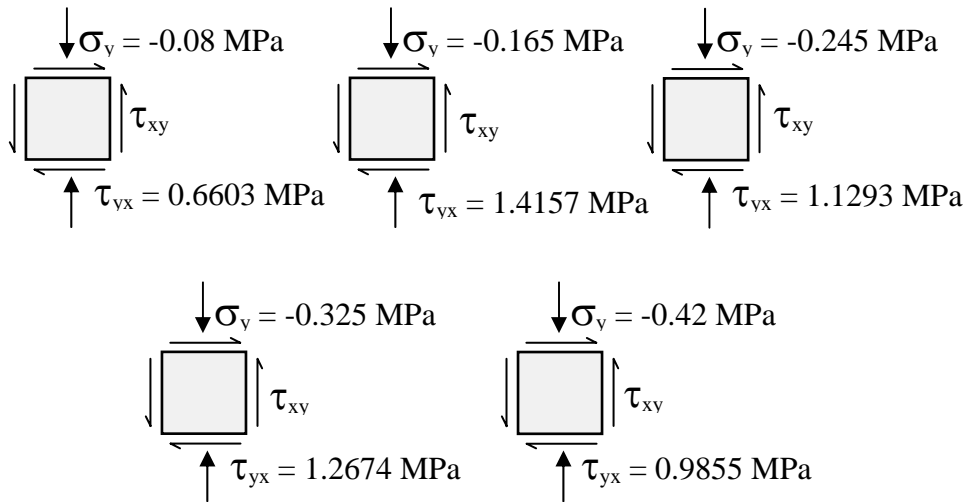
Data for compressive and shear stress of walls CW			
CW Monotonic			
<p><math>\downarrow \sigma_v = -0.165 \text{ MPa}</math>  <math>\uparrow \tau_{vx} = 1.8497 \text{ MPa}</math></p>	<p><math>\downarrow \sigma_v = -0.245 \text{ MPa}</math>  <math>\uparrow \tau_{vx} = 1.7965 \text{ MPa}</math></p>	<p><math>\downarrow \sigma_v = -0.325 \text{ MPa}</math>  <math>\uparrow \tau_{vx} = 1.7786 \text{ MPa}</math></p>	<p><math>\downarrow \sigma_v = -0.42 \text{ MPa}</math>  <math>\uparrow \tau_{vx} = 1.6152 \text{ MPa}</math></p>
CW Repeated			
<p><math>\downarrow \sigma_v = -0.08 \text{ MPa}</math>  <math>\uparrow \tau_{vx} = 1.0399 \text{ MPa}</math></p>	<p><math>\downarrow \sigma_v = -0.165 \text{ MPa}</math>  <math>\uparrow \tau_{vx} = 1.8987 \text{ MPa}</math></p>	<p><math>\downarrow \sigma_v = -0.245 \text{ MPa}</math>  <math>\uparrow \tau_{vx} = 1.5174 \text{ MPa}</math></p>	
	<p><math>\downarrow \sigma_v = -0.325 \text{ MPa}</math>  <math>\uparrow \tau_{vx} = 1.4456 \text{ MPa}</math></p>	<p><math>\downarrow \sigma_v = -0.42 \text{ MPa}</math>  <math>\uparrow \tau_{vx} = 1.6613 \text{ MPa}</math></p>	
CW Cyclic			
<p><math>\downarrow \sigma_v = -0.08 \text{ MPa}</math>  <math>\uparrow \tau_{vx} = 0.5465 \text{ MPa}</math></p>	<p><math>\downarrow \sigma_v = -0.165 \text{ MPa}</math>  <math>\uparrow \tau_{vx} = 0.7623 \text{ MPa}</math></p>	<p><math>\downarrow \sigma_v = -0.245 \text{ MPa}</math>  <math>\uparrow \tau_{vx} = 0.6077 \text{ MPa}</math></p>	
	<p><math>\downarrow \sigma_v = -0.325 \text{ MPa}</math>  <math>\uparrow \tau_{vx} = 0.7414 \text{ MPa}</math></p>	<p><math>\downarrow \sigma_v = -0.42 \text{ MPa}</math>  <math>\uparrow \tau_{vx} = 0.8616 \text{ MPa}</math></p>	

Data for compressive and shear stress of walls MWA				
MWA Monotonic				
MWA Repeated				
MWA Cyclic				

Data for compressive and shear stress of walls CWA				
CWA Monotonic				
CWA Repeated				
CWA Cyclic				

**Data for compressive and shear stress of walls MWE**

**MWE Monotonic**



## Appendix B

The axial, shear, flexural and lateral stiffness of walls, based on height of panels

